GeoE.171.007

Summary report of resources mapping and characterization

HotLime Deliverable 2.0

including descriptive reports on the case studies T2.1 – T2.10 (= Deliverable D2.1 – D2.10)

2020-01-24

HotLime Deliverable # / WP / due month	D 2.0 / WP2 / M18
Revised M36 version for publication	2020-07-07
Dissemination Level	Public
Partner / Person in charge	LGRB / Isabel Rupf
This deliverable describes the results of HotLime's WP2 Mapping and Characterization of 11 case study areas. It consists of a synopsis highlighting and comparing the generic findings of all case study areas envisaged for publication e.g. as HotLime's Mid-term Report, and descriptive reports on each individual case study, designated to underpin the spatial products of prospective geothermal reservoirs foreseen for upload to EGDI, thus forming an essential part of the hyperlinked HotLime knowledge base. Due to HotLime's synergetic and iterative implementation process this report partly addresses also topics at the interface to WP3 "Play and Prospect Evaluation".	

This document is part of a project that has received funding by the European Union's Horizon 2020 research and innovation programme, grant agreement number 731166.

Imprint

Collator and editor: Isabel Rupf (LGRB), WP2 Lead
Author of chapters 1 to 4.0: Gerold Diepolder (LfU), reviewed by Brian McConnell (GSI)
Compilation, technical editing and layout of figures 1 to 3: Sabine Schmidbauer (LfU)
Author(s) of chapters 4.1 to 4.10 as stated in the subheadline of the chapters

Recommended citing:

Rupf, I., Diepolder, G.W. & HotLime Team (2020): Summary report of resources mapping and characterization, including descriptive reports on the case studies T2.1 - T2.10. - HotLime Deliverable 2.0: 130 pp. https://repository.europe-geology.eu/egdidocs/hotlime/hotlime_deliverable_20.pdf

Disclaimer

List of abbreviations and acronyms repetedly used in the text

D#	Deliverable #
EGDI	European Geological Data Infrastructure
FAIR	Findable, Accessible, Interoperable, Re-usable (data)
GSO	Geological Survey Organization
LOD	Linked Open Data https://de.wikipedia.org/wiki/Linked_Open_Data
M	Month (of GeoERA implementation)
Ma	Million years
MUSE	GeoERA GeoEnergy Project “Managing Urban Shallow Geothermal Energy”
NAFB	North Alpine Foreland Basin (aka Molasse Basin)
SKOS	Simple Knowledge Organization System https://en.wikipedia.org/wiki/Simple_Knowledge_Organization_System
SRP	(GeoERA) Scientific Research Project
T#	Task number
URI	Uniform Resource Identifier https://en.wikipedia.org/wiki/Uniform_Resource_Identifier
WP	(HotLime) Work package

Contents

1. Executive Summary

The objective of HotLime is the mapping, characterization, estimation, comparison and prospect ranking of hydrothermal plays in deep carbonate rocks from different target areas across Europe in order to identify their structural control/s for de-risking these challenging geothermal plays.

HotLime's investigations are geared towards outcomes serving planners and decision- makers to focus further research for site selection on the most promising areas. HotLime's case studies in mapping and characterization of the key national/regional carbonate basins, and the evaluation of their geothermal capacity, result in a variety of multidimensional spatial information, the associated feature data and methodological approaches (knowledge base, reports) that are foreseen to be disseminated via GeoERA's central information repository and dissemination portal, the European Geological Data Infrastructure (EGDI). In addition, based on the Simple Knowledge Organization System (SKOS) within the Linked Open Data Semantic Web, the HotLime Knowledge Base will provide controlled vocabularies, glossaries, reports and underpinning information hyperlinked to HotLime's spatial information, following the 'FAIR Guiding Principles for scientific data management and stewardship' (https://doi.org/10.1038/sdata.2016.18).

2. Introduction

This document presents the results of HotLime's WP2 Mapping and Characterization of 11 case study areas. The document consists of a synopsis highlighting and comparing the generic findings of the general characterization of the key national/regional carbonate basins, the case study areas (chapter 3). This chapter is envisaged for publication e.g. as HotLime's Mid-term Report. In addition, the document presents descriptions of each individual case study (chapter 4) designed to underpin the spatial products of the prospective geothermal reservoirs, intended for upload to EGDI to form an essential part of the hyperlinked HotLime knowledgebase.
Although this document describes (and depicts examples of) HotLime's principal outcomes, i.e. various spatial representations relevant for geothermal base assessment, the requirements and specifications for the storage, visualization and query of these spatial outcomes as well as the associated explanatory information such as the HotLime's knowledge base, are not subject of this WP2 summary report. These issues are addressed in detail in HotLime's D5.2.1 submitted 2019-12-31.
Due to HotLime not being a purely sequential, but rather a synergetic and iterative, implementation process, this report also partly addresses topics at the interface to HotLime's WP3 "Play and Prospect Evaluation".

2.1 Objective and scope of work carried out

The objective of HotLime is to apply established methods for characterization and estimation of hydrothermal resources in different geological settings rather than to conduct cutting-edge research. The key challenge is to do so in case studies of disparate levels of knowledge, data coverage and available information and to apply uniform methods for comparison and prospect ranking. On one hand, this inevitably means generalizing and reducing methods of resource base assessments and comparison to the lowest common denominator. On the other hand, this serves the revision of methods and their range of applicability and helps to share knowledge and experience.

The principal objective of HotLime's WP2 Mapping and Characterization has been specific regional mapping and modeling studies for characterization of deep carbonate rock suites and specifying parameters relevant to geothermal potential assessment, thereby testing the essential requirement for any successful geothermal development, the presence of a reservoir of sufficient thickness with an adequate reservoir quality. To this end, mapping and characterization following a general workflow has been carried out in 11 case studies on key national/regional carbonate settings, each with a special focus on specific issues identified in these hydrothermal plays. The case study areas across Europe are roughly outlined and compared in chapter 3 and are described in more specific detail in chapter 4.

2.2 Description of work carried out

WP2 was implemented by the GSO(s) in charge of the respective areas, but progressed in parallel between M1 and M18 allowing all HotLime partners to exchange experience on the various step of the workflow, to track all necessary adaptions and improvements ascertained in any study area, and to compare and draw pan-European conclusions by analogy among the partners. This inter-partner communication and knowledge exchange for best practice was bolstered by two hands-on workshops, (1) on seismic interpretation and (2) on temperature modelling, the latter jointly with the GeoERA SRP MUSE, held at the Croatian GSO in Zagreb in M7.

The following parameters, considered crucial for an assessment of the prospectivity of any proposed geothermal development, are the minimum requirement that has been tested for all case study areas investigated within the project:

- The presence of a reservoir
- Outlines of that reservoir (lateral extent and possible compartmentalisation)
- Depth and gross thickness distribution of the reservoir (geometries of base and top)
- Permeability of the reservoir (qualitative, specifically considering areas of enhanced permeability due to faulting and/or facies distribution), thus special focus on
- Principle faults intersecting the reservoir
- Temperature distribution assessment of the reservoir
- Basic characteristics of groundwater (total dissolved solids, in terms of proneness to scaling)

A major challenge in mapping and characterization of rock formations at great depths is the availability of data with an adequate distribution and resolution to address the geological situation properly. Legal requirements on data privacy imposing data access restrictions on some of HotLime's partners exacerbate the problem of data paucity. Only few partners could make full use of mature databases from extensive hydrocarbon exploration campaigns. Thus, the geothermal resource assessment carried out in HotLime faces the problem of high degrees of uncertainties for both subsurface geometries and petrophysical property data.

The type and quantity of baseline data available determined not only the mode of data preparation and starting point of capturing the subsurface geometries in depth or time domain, but also controlled the entire procedure of mapping and model building throughout WP2. Even though an overarching general workflow for data preparation, (seismic) interpretation, time-depth conversion and the entire mapping and modelling cascade was set up for both points of departure – starting in time domain vs. starting in depth domain – we learned that there is no universal best practice applicable to all geological regions or project settings. With scarce baseline data, mapping and modelling was driven by geological concepts and implicit knowledge guided by the modeler and the software's algorithms. In contrast, when baseline data are sufficiently available and expert knowledge is on hand, explicit modeling was the means of choice. In practice, both extremes and all facets in between could occur in the same investigation area.

For instance, most parts of the central Molasse Basin realm are well covered by seismic records in its deeper parts, numerous but scattered downhole data from hydrocarbon and geothermal exploration and production campaigns, information from geological and structural maps in its shallower parts, as well as legacy 3D geological models combining all this information in sub-areas. The modelling workflow overview for the western part of the Molasse Basin case study area (#1 in figure 1), shall serve as an example for elucidation of a sophisticated model building procedure adjusted to the regional data background.

- Data preparation
  - quality check and selection of downhole data, earmarking model units by well markers,
  - reprocessing and digitization (where not pre-existing), interpretation of seismic lines,
  - generation and iterative improvement of velocity model for time-depth conversion (calibration with check shots, alignment of seismic reflectors and well markers, etc.),
- Modelling in depth domain based on outcrop (map features) and well data,
- Modelling in time domain based on seismic interpretation and well data converted into time domain (deeper part of the modelling area) and time-depth conversion of the modelled objects
- Integration and adaptation of the 3D geological model to faults and horizons from the seismic interpretation in the depth domain
- Consistency and plausibility checks

However, as discussed, the best practice workflows for mapping and modelling in the different case study areas varies widely, pursuant to the data situation. The data background and the mapping and modelling procedures based thereon are described in more detail in chapter 4.

As with the data for capture of the subsurface geometries, HotLime's case study areas feature an extremely disparate data situation for temperature distribution estimation, one of the crucial parameters for any geothermal base assessments. Accordingly, methods for data preparation and regionalization (mapping and modelling) of the temperature distribution – within or at least at the top surface of the hydrothermal reservoir(s) under consideration – vary considerably. Only a few partners could make use of pre-existing sophisticated 3D-temperature models for at least subareas of the case study. Most partners had to extrapolate sparse borehole temperature measurements or just geothermal gradients derived from various sources.
As one of the parameters mandatory for all case study areas, derivation of temperature maps, i.e. the temperature distribution at the top surface of the reservoirs under consideration, is collated in chapter 3.

Chapter 3 also collates the other mandatory minimum achievements of WP2 required for geothermal base assessment as presently carried out in HotLime's WP3 "Play and Prospect Evaluation":

- Depth and geometry (volume) of the reservoir
- Fault distribution pattern (also as areas of secondarily enhanced permeability and so higher production favorability leading to a reduced exploitation risk)
- Temperature of the reservoir (broad-brush average or depth serialized)

3. Publishable Summary of Results

This chapter summarizes the work of HotLime's WP2 and collates its results in a uniform and comparable manner. It is intended as a stand-alone summary for publishing. As such, naturally, it includes some reiteration of the previous chapters and does not feature a numeration of the sub-chapters. It also includes a list of references cited.

HotLime – Mapping and Assessment of Geothermal Plays in Deep Carbonate Rocks – summary of mapping and generic characteristics of 11 case studies

Rationale

Despite its significant potential to provide low carbon and dispatchable energy, geothermal energy has remained underdeveloped compared to other renewable energies except in a few particularly suitable regions situated on top of magmatic hot spots. In 2017, it accounted for only 3.0 % of the EU total primary renewable energy production (EUROSTAT 2019). The main reason for the discrepancy between its potential and the lagging development of geothermal resources is the high up-front costs of drilling and risks related to geological uncertainties.

Considered on a worldwide scale, carbonate rocks are regarded as the most prevalent geothermal aquifers of low-enthalpy systems (GOLDSCHEIDER et al. 2010). However, such low-enthalpy hydrothermal systems harbor a particular exploitation risk as they require drilling to great depths to reach suitably elevated temperatures. Such depths can result in a decreased fluid flow due to the decreased primary porosity and permeability caused by mechanical compaction – deep carbonate bedrock commonly is perceived as 'tight'. Accordingly, apart from a few areas where viability of hydrothermal heat and power generation has been proved, most deep carbonate bedrock across Europe has received relatively little attention. In order to de-risk geothermal exploration in deep carbonate rocks it is crucial to improve our understanding of generic geological conditions that determine the distribution and technical recoverability of their potential resources, specifically the possible groundwater yield controlled by fracture conduits and karstification.

The objective of HotLime is to apply established methods for characterization and estimation to hydrothermal resources in different geological settings rather than to conduct cutting-edge research. The key challenge is to do so in case studies of disparate levels of knowledge, data coverage and available information and to apply uniform methods for comparison and prospect ranking. On one hand, this inevitably means generalizing and reducing methods of resource base assessments and comparison to the lowest common denominator. On the other hand, this serves the revision of methods and their range of applicability and helps to share knowledge and experience, thus complying with the spirit of transnational collaboration as fostered by the EU.

Objective and focus of mapping and characterization

The basic requirement for any successful geothermal development is the presence of a reservoir of sufficient thickness with an adequate reservoir quality.

The objective of HotLime's WP2 "Mapping and Characterization" for all areas under consideration was to collate, revise and harmonize all existing geological data, from downhole data and geophysical surveys, to fill the gaps in between pre-existing spatial information, to merge it into one holistic overall picture and (re-)model the geometry and structural inventory of the reservoir. These revised geometries serve as the input for parameterization with respect to facies and temperature distribution.

Actual mapping, characterization and comparison of geological situations, and the structural inventory of the deep carbonate hydrothermal plays was implemented in 11 different target areas across Europe from

July 2018 to December 2019, aimed at identification of the generic structural controls of geothermal plays in deep carbonate rocks.

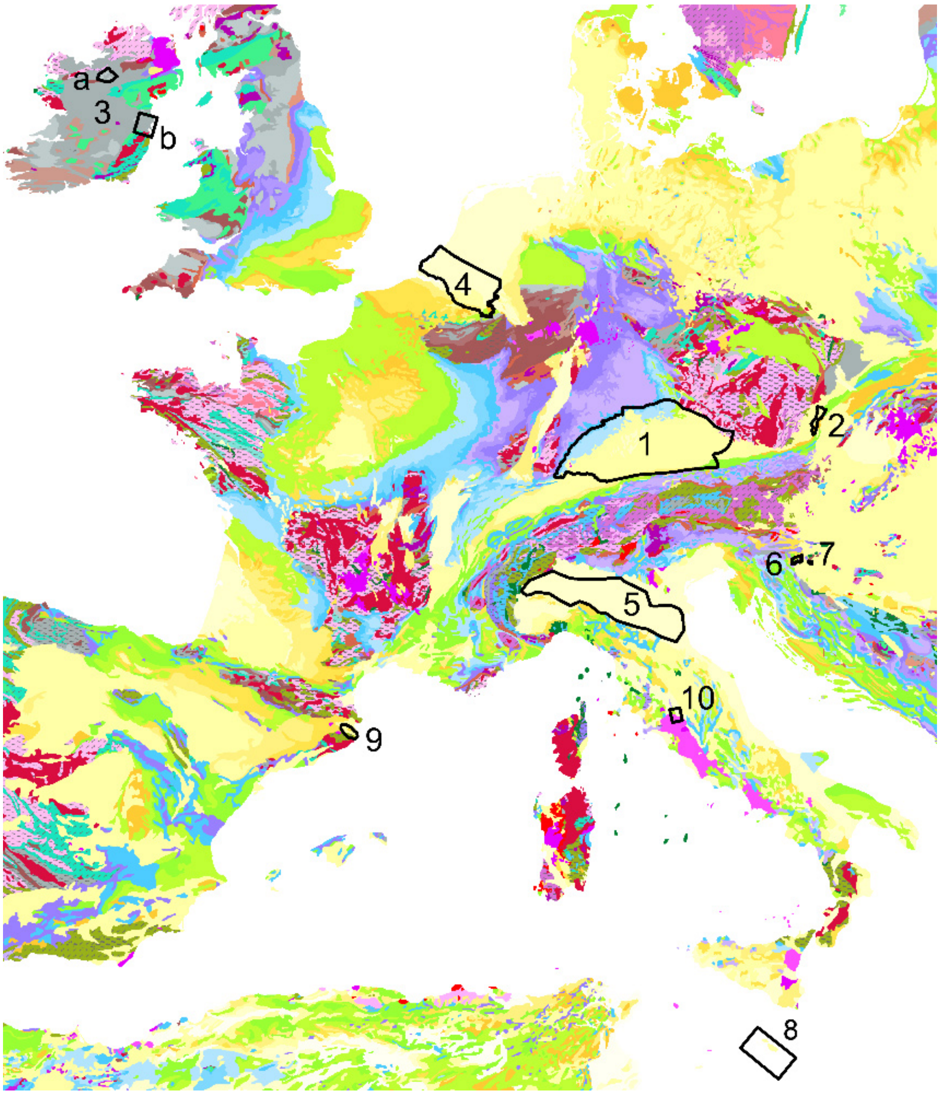

Figure 1: Location of HotLime's case study areas plotted on the 1:5m-scale International Geological Map of Europe – IGME5000 (ASCH 2005). The map omits offshore geology for clearer territory contours. (From DIEPOLDER et al. 2020, updated)

***#1**: Upper Jurassic and Middle Triassic carbonates in the central part of the North Alpine Molasse Basin (DE/AT)*
***#2**: Upper Jurassic carbonates in the Molasse Basin-Carpathian Foredeep transition zone (AT/CZ)*
***#3**: Carboniferous carbonates in (**a**) Lough Allen Basin and (**b**) Dublin Basin (IE)*
***#4**: Dinantian carbonates at the flanks of the London-Brabant Massif (NL/BE)*
***#5**: Upper Triassic to Lower Cretaceous carbonates of the Po Basin (IT)*
***#6**: Triassic carbonates of the Krško-Brežice sub-basin (SI)*
***#7**: Miocene and Triassic carbonates of Zagreb hydrothermal field (HR)*
***#8**: Triassic carbonates of the Pantelleria-Linosa-Malta rift complex (MT)*
***#9**: Eocene carbonates of the Empordà Basin (ES)*
***#10**: Triassic carbonates of Tuscan, Umbria and Marche nappes in the Umbria Trough (IT)*

The size of the case study areas varies from 54 km^2 to 47,700 km^2, and all encompass at least one hydrothermal carbonate horizon of proven but not yet quantified geothermal potential. All plays under consideration – except #6, #7 and #10 – are blind systems with no hydrothermal manifestation or measurable anomaly at the surface. According to the play type concept (MOECK 2014) most case studies are Conduction Dominated Systems that can be assigned to the Orogenic Belt (CD-2) Play Type (# 1, 2, 5, 6, 7, 9, 10) or the Intracratonic Basin (CD-1) Play Type (# 3, 4), except for #8 which appears to be a Convection Dominated – Extensional Domain (CV-3) Play Type.

Upfront Geothermal resource assessment, as implemented in HotLime, faces the problem of high degrees of uncertainties for both subsurface geometries and petro-physical property data: A major challenge in mapping and characterization of rock formations at great depths is the availability of data with an adequate distribution and resolution to address the geological situation properly. Legal requirements on data privacy imposing data access restrictions on some of HotLime's partners exacerbate the problem of data paucity, as not all partners could make full use of mature databases from extensive hydrocarbon exploration campaigns. However, sharing of knowledge and exchange of experience among HotLime's 15 partners helped to mitigate the lack of hard data through comparison of the geological situation and its evolution, and conclusions by analogy conveyed to less thoroughly documented areas.

Mapping – capture of subsurface geometries

Recent simulations for geothermal reservoir assessment (e.g. WELLMANN et al. 2011) illustrate that small uncertainties in the geological structure can have significant impact on geothermal resource estimations. Accordingly, special emphasis in HotLime's capture of the subsurface structure was placed on the mapping of the reservoir geometries, the structural inventory and the geological framework of all case study areas, applying state of the art 3D geological modeling methods at most partners. Varying among the partners in abundance and significance, the baseline data for HotLime's case studies beyond conceptual models have comprised scattered and clustered downhole data, various geophysical surveys, specifically seismic sections, geological maps and, rarely, legacy 3D models of subareas. As many data sets required for mapping the deep subsurface are classified, access restrictions required that all mapping and model building had to be implemented at the jurisdictional regional or national GSO. Consequently, the capture of subsurface geometries was conducted with different pre-existing proprietary software packages. Data sets of derived and re-interpreted data, however, were shared among partners for cross-border harmonization in transnational study areas (#1, #2, #4). Even though an overarching general workflow for data preparation, (seismic) interpretation, time-depth conversion and the entire mapping and modelling cascade was set up, we learned that there is no universal best practice applicable to all geological regions or project settings. With scarce baseline data, mapping and modelling was driven by geological concepts and implicit knowledge guided by the modeler and the software's algorithms. In contrast, when baseline data are sufficiently available and expert knowledge is on hand, explicit modeling was the means of choice. In practice, both extremes and all facets in between could occur in the same investigation area. In all cases, the geologists' expertise focused and controlled the capture of subsurface geometries through the mapping and modelling. Mapping outcomes, in turn, fed back into the conceptual models of the geological evolution of the target area, incrementally improving the understanding of the geological setup and the reservoir formation in space and time.

Throughout the entire mapping procedure, from seismic interpretation through to model consistency checks, a special focus was the fault and fracture network intersecting the target horizons. Such discontinuities not only define the possible compartmentalization of reservoirs and seal integrity, first and foremost they represent damage zones usually of higher permeability, thus conduits for hydrothermal fluids, and hence are the prime target for hydrothermal exploration in deep carbonate rocks.

Spatial representations (in 2D or 3D), revealing the principal geological setup for subsequent geothermal base assessment, are the prime outcomes of mapping and characterization. Figure 2 provides a comparative overview of the reservoir geometries, the structural features and the geological setting of HotLime's target horizons highlighted in the standardised colors of the International Chronostratigraphic Chart.

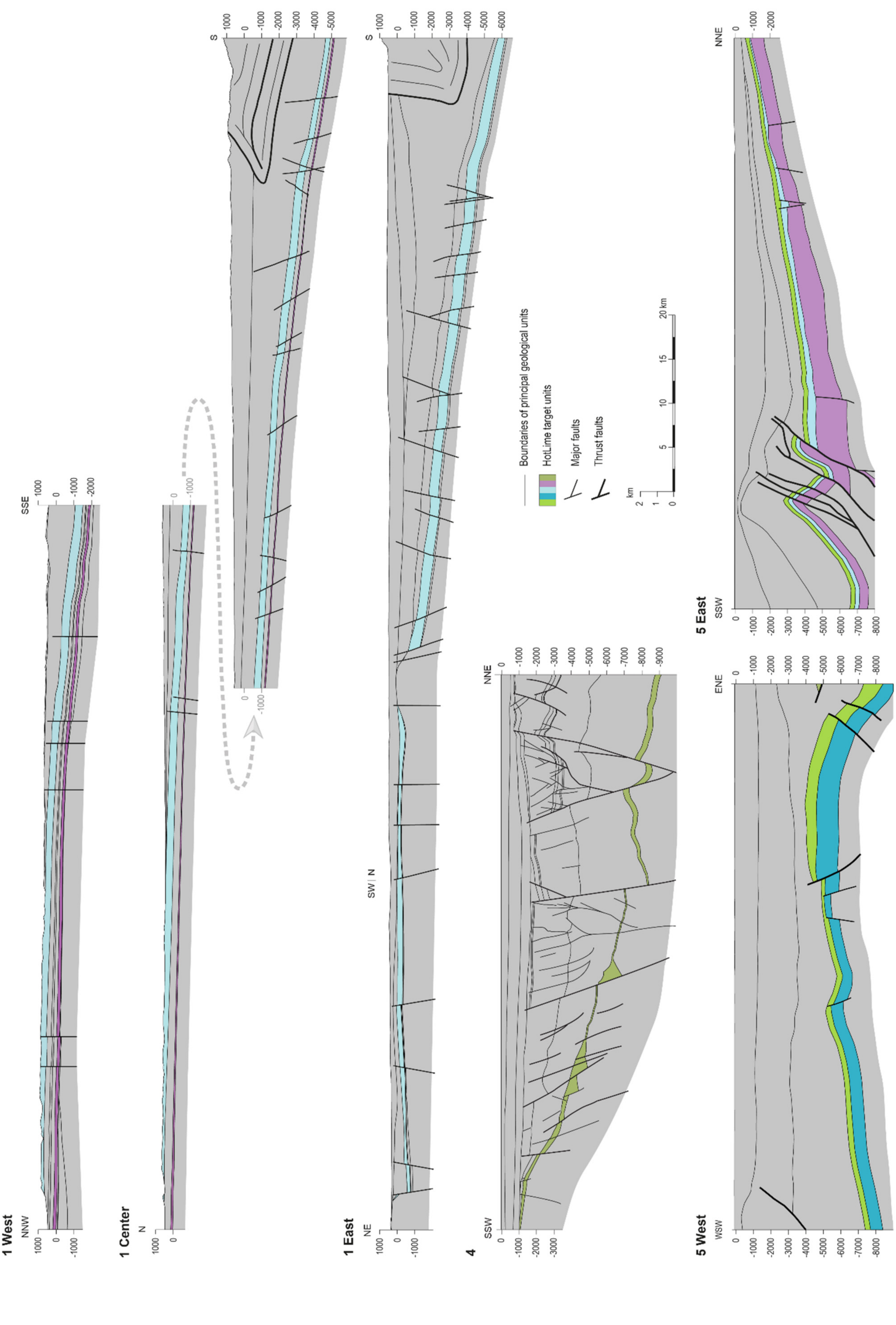
1 West
1 Center
1 East
4
5 West
5 East
Boundaries of principal geological units
HotLime target units
Major faults
Thrust faults

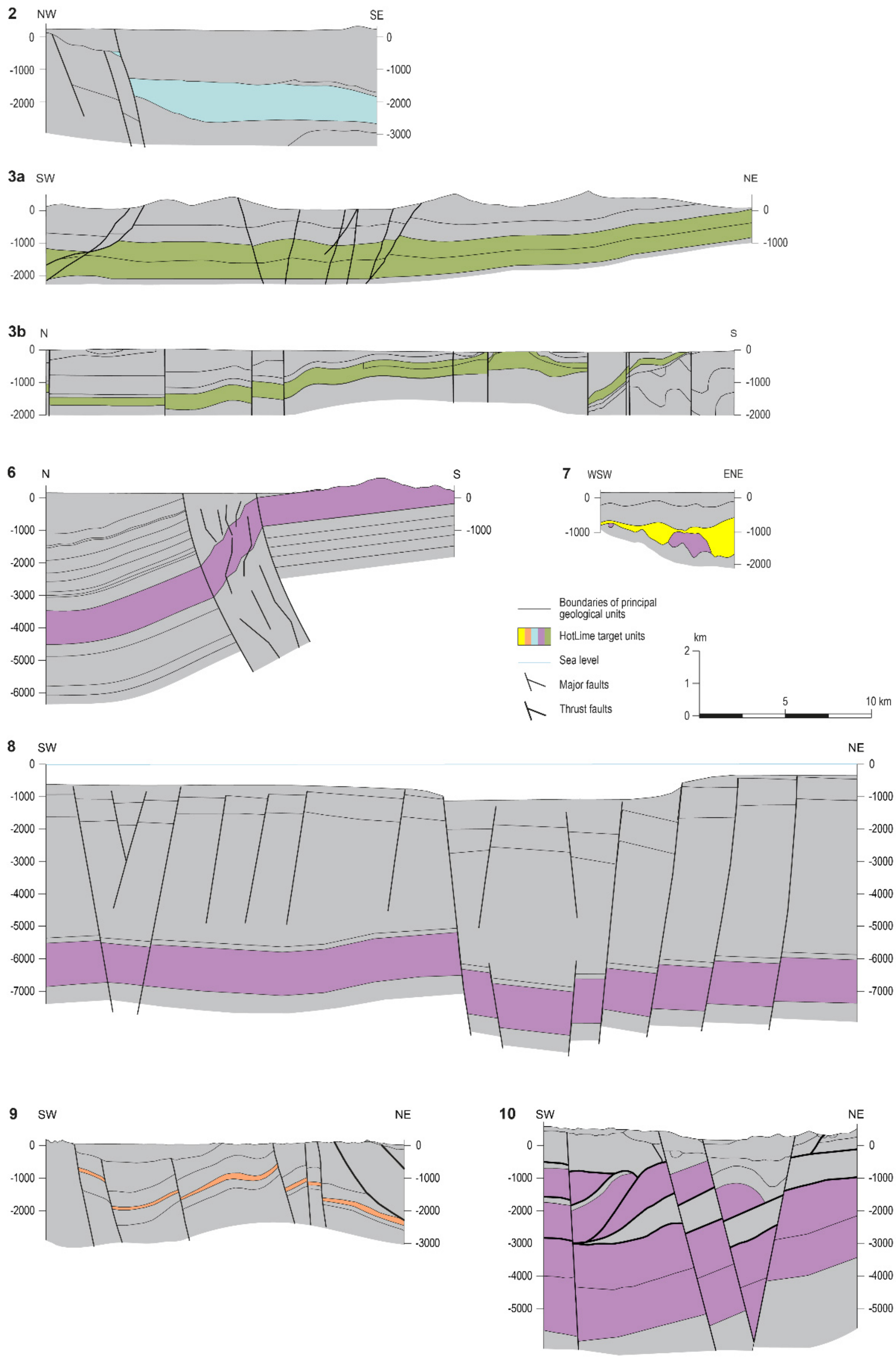

Figure 2 (cont'd from previous page): Comparison of HotLime's case study areas in geological sections. The investigated carbonate reservoirs are highlighted using the color codes of the ICS International Chronostratigraphic Chart (http://www.stratigraphy.org). Vertical exaggeration of all cross-sections is 2x, and, within the same plate, they are depicted at the same scale – but note the different scales of the plates. For section numberings refer to the map in figure 1, for the location of the cross-sections see the trace lines in figure 3.

Characterization – capture of petro-physical properties

Unlike systems in porous rocks, carbonate plays are highly heterogeneous and anisotropic with respect to rock properties. Their groundwater yield, a crucial factor for any hydrothermal development, depends only to a minor degree on the primary rock porosity (matrix permeability), but predominantly is controlled by fault, fracture and karst conduits. The quality of 'regular' carbonate reservoirs with respect to their hydrothermal potential, therefore, is governed by the fracture and fault network as well as the degree of dolomitization and karstification, which in turn are widely controlled by the facies type. Mapping these dominant factors at depth is particularly challenging because downhole data coverage increasingly dwindles with increasing depth of the aquifer. The only parameter that can be reliably assessed on a larger scale and at the forefront of exploration, before drillings are carried out, is fracture density. Due to the brittle characteristic of carbonates – dolostones more than limestones – the highest density of discontinuities generally is found in the core and damage zones along faults, which can be clearly identified in reflection seismic. For example, even at great depth beneath a thick overburden, DUSSEL et al. (2016) determined mechanically altered, permeable zones with a width of 50-150 m along main faults. BAUER et al. (2016) describe permeable zones of intensely fractured, uncemented rock up to hundreds of meters wide along faults in karstified carbonates. From this perspective, faults are the most reliable targets in geothermal prospectivity screening of the deep carbonate rocks. Many successful drillings for geothermal installations in carbonate reservoirs, specifically in the Molasse Basin, have proved this approach. However, recent failures of ultra-deep explorations (> 5,500 m) show that it is not inherently propitious at great depth where compaction by the high load of overburden seems to be a widespread process. Hence, faults and fault zones as mapped in HotLime's case study areas are considered indications rather than evidence for planar structures of higher groundwater yield and require verification through further investigations.

In contrast, facies and dolomitic domains – reef facies, reef debris and dolostones feature a higher secondary porosity than basin facies limestones – can be reliably detected only after drilling and seismic well log correlation (MOECK et al. 2015), or can be assessed from high-resolution 3D-seismics, usually available only for project size areas in advanced development stages. Consequently, these indicators for increased rock permeability, and thus higher groundwater potential, could be regionalized and mapped in very few (sub-)areas only, where distribution density of downhole information was deemed adequate. Extrapolation of subcrop facies distribution and paleo-geographic maps – usually available at large scales only – harbor an uncertainty that is too high for any scientifically sound statement. However, ongoing work in "Play and Prospect Evaluation" might reveal further generic controls that could help to tackle this issue.

Temperature Modelling

As with geological information for mapping and characterization, available temperature data for the HotLime case study areas are disparate with respect to distribution density and quality. Measurements collected for temperature modelling predominantly stem from downhole data of (legacy) hydrocarbon E&P campaigns, mostly taken as Bottom Hole Temperatures (BHT) and corrected using established weighting classifications (e.g. ZSCHOCKE 2005, RÜHAAK et al. 2010), or rarely from drill stem tests (DST). Only in the Molasse Basin (#1) are a significant number of temperature measurements from recent geothermal E&P available. The areal coverage of preexisting temperature models or temperature distribution maps for HotLime's target horizons in the different case study areas varies from full coverage to nil. Area-wide subsurface temperature information is available for #4 down to 6 km depth (BONTÉ et al. 2012) and for the top of the Upper Jurassic hydrothermal aquifer in #1 (AGEMAR & TRIBBENSEE 2014). The top of Middle Triassic of #1 (GeoMol TEAM 2015) is partially covered, and the top of the Upper Triassic to Lower Cretaceous sequence of the Po Basin (#5) has been extended and upgraded within HotLime. For most of the case study areas only few temperature measurements exist, in many cases too far apart for reliable interpolations.

As an area-wide temperature distribution is a crucial pre-requisite for all geothermal resource base assessments, regionalized geothermal gradients derived from downhole data (borehole logs) and literature values of heat flow density were used to fill the voids in areas where no reliable interpolation of measured values could be performed. To this end, isolated temperature gradient derivations, assumed to be representative for a certain area, have been used to extrapolate the temperature distribution depending on the depth of the top of the reservoir, applying the basic equation: $T_r = T_0 + gradT * Z$ (where T_0 is the mean annual surface temperature; gradT is the geothermal gradient and Z is the depth of the top surface of the target horizon). However, such generalization neglects the non-linearity of geothermal gradients and must be considered a first-order approximation only.

In some smaller case study areas lacking hard data, as in sub-areas of larger case studies, this approach of regionalization of geothermal gradients has been applied for the entire distribution of the reservoir top surface. Even so, some of the temperature distribution maps collated in figure 3 show "no data" sub-areas for realms where the data situation is considered inappropriate even for an educated guess pursuant to this approximation.

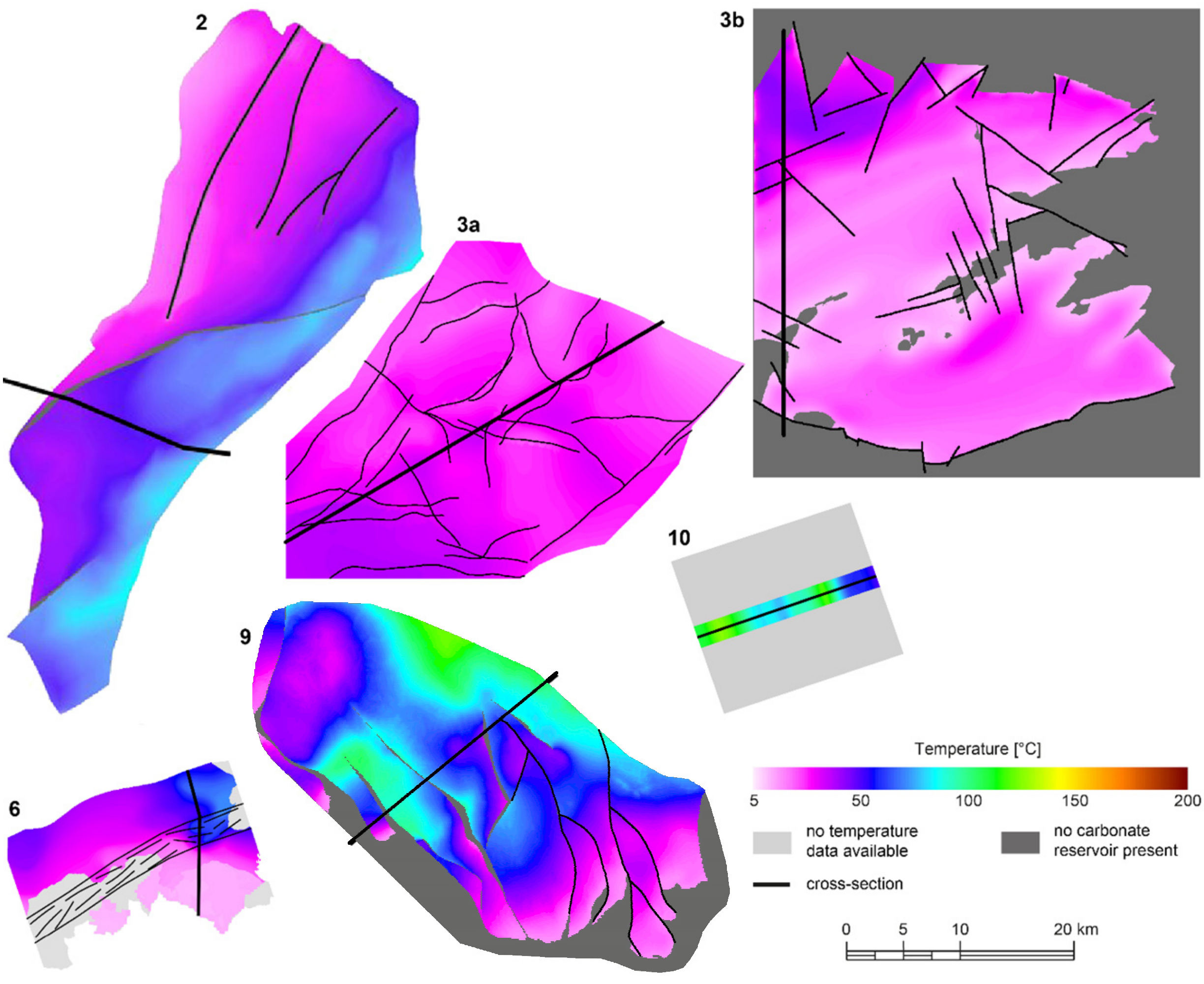

Figure 3 (cont'd next page): Case examples of temperature distribution calculated/assessed for the top of HotLime's target carbonate reservoirs. Also showing no reservoir realms, narrow linear "no reservoir present" zones are mostly due to dip-slip offsets at faults. For area numberings refer to the map in figure 1. The trace lines of cross-sections correspond with the geological sections depicted in figure 2.

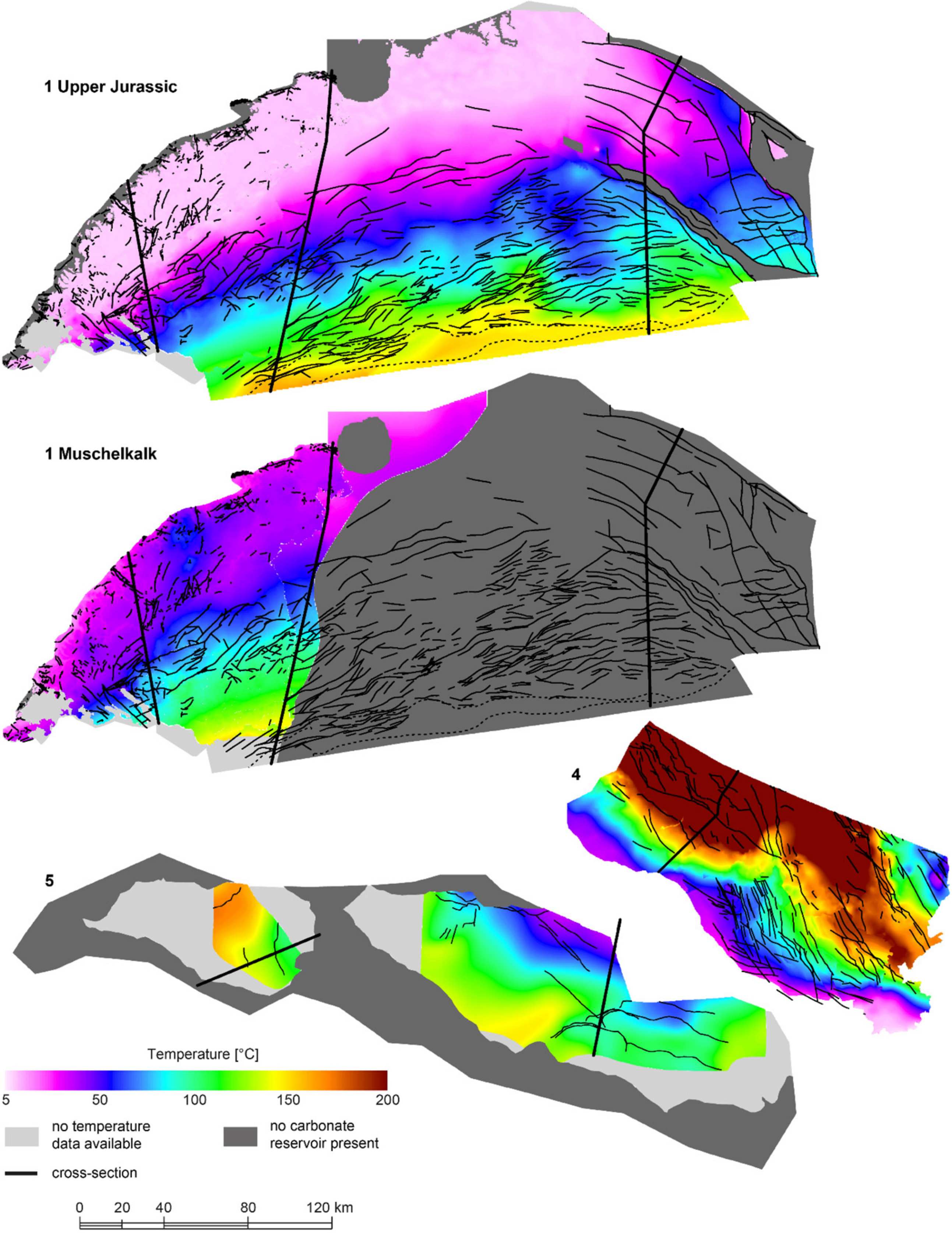
1 Upper Jurassic
1 Muschelkalk
4
5
Temperature [°C]
5
50
100
150
200
no temperature data available
no carbonate reservoir present
cross-section
0
20
40
80
120 km

Regionalized geothermal gradients are also used to estimate temperatures at the base of the considered reservoirs, usually far below the deepest BHT value measured. Particularly in reservoirs featuring a gross thickness of more than 200 m, the increase of temperature with depth within the target layers has a significant effect on the geothermal resource base assessment. Accordingly, such large-thickness reservoirs are dealt with as layered incremental intervals in the ongoing geothermal base assessment using the "Heat-in-Place" method of MUFFLER & CATALDI (1978) and applying both the deterministic as well as (optionally) the probabilistic approach of GARG & COMBS (2015), see DIEPOLDER et al. (2020) for details.

As demonstrated by some initial reliable tests, this present stage of the capture of the subsurface setup and temperature distribution gives good reasons to expect a sufficiently detailed knowledge of the reservoir geometries necessary for a sound geothermal resource base assessment, considering the volume of the reservoir, the temperature, the specific heat capacity of the rocks, and areas of increased porosity along the damage zone of faults.
For that purpose, additional parameterization, validation, and refinement within HotLime's "Play and Prospect Evaluation" presently is being carried out and modelling these parameters might reveal further generic controls of the geothermal prospectivity. Feedback thus may further improve knowledge about, and spatial products of, HotLime's case study areas until they are eventually uploaded to the GeoERA Information Platform (EGDI) in 2021, supplemented by LOD SKOS based controlled vocabularies (glossaries) on the displayed features and a knowledge base on the scientific background, methods and use limitations.

Acknowledgement

The achievements described are not only to a high degree owed to the candid share of knowledge and expertise among HotLime's partners and associated institutions but also due to the valuable inputs of HotLime's External Experts and Advisory Board: Leibniz Institute for Applied Geophysics (INGA MOECK & THORSTEN AGEMAR), British Geological Survey (CORINNA ABESSER), swisstopo (CHRISTIAN MINING), and Geothermal-Alliance Bavaria (MARKUS LOEWER & ANAHI MOLAR-CRUZ)

References

AGEMAR, T. & TRIBBENSEE, K. (2018): GeotIS-Verbundmodell des Top-Malm im Bereich des Vorlandbeckens der Alpen. – *ZDGG - German Journal of Geology* **169**: 335-341. https://doi.org/10.1127/zdgg/2018/0126 [2019-12-05]

ASCH, K. (2005): IGME 5000: the 1:5 Million International Geological Map of Europe and Adjacent Areas, Federal Institute for Geosciences and Natural Resources (BGR), Hannover. https://services.bgr.de/geologie/igme5000 [2019-07-18]

BAUER, H., SCHRÖCKENFUCHS, T.C. & DECKER, K. (2016): Hydrogeological properties of fault zones in a karstified carbonate aquifer (Northern Calcareous Alps, Austria). – *Hydrogeology Journal* **24**: 1147-1170. https://doi.org/10.1007/s10040-016-1388-9 [2020-01-10]

BONTÉ, D., VAN WEES, J.-D. & VERWEIJ, J.M. (2012): Subsurface temperatures of the onshore Netherlands: new temperature dataset and modelling. – *Netherlands Journal of Geosciences* **91**: 491-515. https://doi.org/10.1017/S0016774600000354 [2020-01-09]

DIEPOLDER, G.W., BOROVIĆ, S., HERMS, I. & HOTLIME TEAM (2020): HotLime – Mapping and Assessment of Geothermal Plays in Deep Carbonate Rocks. – *Proceedings,* **16040**, World Geothermal Congress, Reykjavik, Iceland. [accepted]

DUSSEL, M., LÜSCHEN, E., THOMAS, R., AGEMAR, T., FRITZER, T., SIEBLITZ, S., HUBER, B., BIRNER, J. & SCHULZ, R. (2016): Forecast for thermal water use from Upper Jurassic carbonates in the Munich region (South German Molasse Basin). – *Geothermics* **60**: 13-30. https://doi.org/10.1016/j.geothermics.2015.10.010 [2019-12-05]

EUROSTAT (European Statistical Office): Renewable energy statistic, *Statistics Explained*. https://ec.europa.eu/eurostat/ statistics-explained/pdfscache/7177.pdf [2019-11-17]

GARG, S.G. & COMBS, J. (2015): A reformulation of USGS volumetric "heat in place" resource estimation method. – *Geothermics* **55**: 150–158. http://dx.doi.org/10.1016/j.geothermics.2015.02.004

GEOMOL TEAM (2015): GeoMol – Assessing subsurface potentials of the Alpine Foreland Basins for sustainable planning and use of natural resources, *Project Report*, 188 pp. (Augsburg, Bayerisches Landesamt für Umwelt); www.geomol.eu/report [2019-11-15] and map viewer http://www.geomol.eu/mapviewer/ [2019-11-15]

GOLDSCHEIDER, N., MÁDL-SZŐNYI, J., ERŐSS, A. & SCHILL, E. (2010): Review: thermal water resources in carbonate rock aquifers. – *Hydrogeology Journal* **18**: 1303–1318

MOECK, I.S. (2014): Catalog of geothermal play types based on geologic controls. – *Renewable and Sustainable Energy Reviews* **37**, 867-882. http://dx.doi.org/10.1016/j.rser.2014.05.032 [2019-12-05]

MOECK, I.S., UHLIG, S., LOSKE, B., JENTSCH, A., FERREIRO MÄHLMANN, R. & HILD, S. (2015): Fossil multiphase normal faults – prime targets for geothermal drilling in the Bavarian Molasse Basin? – *Proceedings,* **11044**, World Geothermal Congress, Melbourne, Australia. https://www.geothermal-energy.org/pdf/IGAstandard/WGC/2015/11044.pdf [2019-12-11]

MUFFLER, L.J.P. & CATALDI, R. (1978): Methods for Regional Assessment of Geothermal Resources. – *Geothermics* **7**: 53-89. https://doi.org/10.1016/0375-6505(78)90002-0 [2019-12-05]

RÜHAAK, W., RATH, V. & CLAUSER, C. (2010): Detecting thermal anomalies within the Molasse Basin, southern Germany. – *Hydrogeology Journal* **18**: 1897-1915. https://doi.org/10.1007/s10040-010-0676-z [2020-01-09]

WELLMANN, J.F., REID, L.B., HOROWITZ, F.G. & REGENAUER-LIEB, K. (2011): Geothermal Resource Assessment: Combining Uncertainty Evaluation and Geothermal Simulation. – *Conference Paper*, AAPG/SPE/ SEG Hedberg Conference "Enhanced Geothermal Systems"; Napa, CA. https://www.researchgate.net/publication/237197648 [2019-11-28]

ZSCHOCKE, A. (2005): Correction of non-equilibrated temperature logs and implications for geothermal investigations. - *J. geophys. Eng.* **2**: 364–371

4. HotLime's case study areas

The following sections 4.1 to 4.10 present descriptive reports on each case study, designed to accompany and underpin the spatial products of prospective geothermal reservoirs compiled for each test case area. Intended for upload to the documents repository of EGDI (after possible upgrade due to additional or modified findings of the ongoing WPs 3 and 4) then hyperlinked to the related spatial representations of the case study area, they provide more detailed information beyond the products common to all case study areas as described and uniformly depicted for direct comparison in chapter 3. These individual reports also include information in addition to the minimum achievements defined in HotLime's project proposal and partly address topics at the interface to WP3 "Play and Prospect Evaluation". Following a template for common structuring but considered the intellectual property of the HotLime partners in charge, as represented by the authors stated, these reports are harmonized with respect to the layout only, and no content-wise editing has been implemented by the WP2 editorial team.

4.1 Central North Alpine Foreland Basin (DE/AT) – T2.1

Alica de Witt, Isabel Rupf, Edgar Nitsch & Carolin Tetzel (LGRB), Gerold Diepolder & Stephan Sieblitz (LfU), and Clemens Porpazcy (GBA)

4.1.1 Inducement and Objectives

The North Alpine Foreland Basin (NAFB) also known as Molasse Basin, stretching over more than 1000 km along the northern fringes of Alpine Mountain Belt, from Grenoble in France to almost Vienna in Austria, features highly productive aquifers at depth. Especially in the NAFB's middle part, these aquifers host enormous utilizable hydrothermal resources, considered holding the highest geothermal potential in Central Europe (Paschen et al. 2003, GeoMol Team 2015). Solely exploited for balneological use until the 1990s, the utilization of hydrothermal aquifers have become increasingly important for heat and energy generation over the last two decades, specifically in the NAFB's central and eastern parts and focusing on densely populated areas with a high heat demand. Within the territories of Baden-Württemberg, Bavaria and Upper Austria, at present, more than 40 geothermal installations exploit the thermal water for balneology, district heating, power generation or mixed uses, the ones longest in operation running trouble-free for more than 2 decades. However, recent throwbacks in exploring new sites, especially in the deeper, with respect to temperature most favorable parts of the basin, revealed that the generic controls of groundwater yield are not yet fully understood and need a profound and unbiased revision underpinned by the comparison with other carbonate reservoirs. On the other hand, the increasing use of the thermal aquifers requires an overall geothermal base assessment and balance beyond the side-specific prognoses, on a supra-regional scale.

The essential requirement for any successful geothermal development is the presence of a reservoir of sufficient thickness with an adequate reservoir quality. However, large-scale geothermal resource assessment faces the problem of high degrees of uncertainties for both subsurface geometries and petro-physical property data. Recent simulations for geothermal reservoir assessment (e.g. Wellmann et al. 2011) illustrate that small uncertainties in the geological structure can have significant impact on geothermal resource estimations. Correspondingly, applying state of the art 3D geological modeling methods, special emphasis was placed on mapping of reservoir geometries, the structural inventory and facies distribution, as well as the geological framework.

Objective for the implementation of the HotLime Task 2.1 was to revise, harmonize and merge all pre-existing 3D-geomodels of sub-areas, to fill in the gaps in between, to enlarge the areal coverage by the shallow part of the reservoir and the subcrop of the aquifers, and to re-model the geometry and structural inventory of the reservoir in a refined cross-border model exploiting all available downhole data and geophysical surveys. The revised geometries serve as the input for parameterization with respect to facies and temperature distribution.

4.1.2 Study area and geological setting

The Central Molasse Basin case study covers the central parts of the North Alpine Foreland Basin and the adjacent Swabian-Franconian Alb within the territories of Baden-Württemberg, Bavaria and westernmost Upper Austria (south of the Bohemian Massif). The case study area sprawls 400 km in W-E direction with a maximum N-S extend of 170 km, covering overall roughly 47,700 km^2, about 13,000 km^2 on Baden-Württemberg territory, 33,300 km^2 in Bavaria, and 1,400 km^2 on Austrian territory.

Regional geological setting

Situated immediately north of the Alpine-Carpathian Orogen, the NAFB is an asymmetric orogenic foreland basin filled with Tertiary deposits and resting on a footwall of south dipping Mesozoic sediments and a Paleozoic crystalline basement. To the northwest of the NAFB, the Tertiary basin fill pinches out and the Mesozoic sedimentary sequence crops out in the South German Scarplands, featuring the 15 Ma old Ries and Steinheim asteroid impact craters in its central part (Figure 4.1.1).

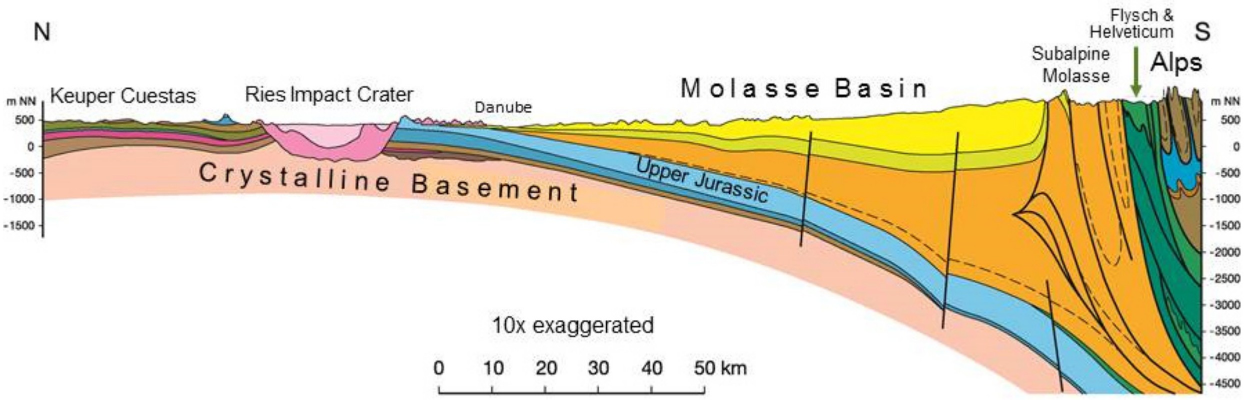

Figure.4.1.1: Geological cross-section approximately along the Baden-Württemberg–Bavaria border, intersecting the southern South German Cuesta Region, the Swabian-Franconian Alb – here almost completely made up of the Ries Crater impactites and crater lake sediments, the Alpine Foreland and the Pre-Alps (from DIEPOLDER et al. 2019, modified after DOPPLER et al. 2004)

The Alpine-Carpathian Orogen evolved from the collision of the Adriatic and European plates during Cretaceous and Tertiary. Along the forefront of the emerging orogenic belt, a large-scale downwarping of the European plate resulted in a foreland basin that gradually expanded to the north. The Basin was progressively filled with up to 5 km thick Tertiary 'Molasse' sediments eroded from the emerging Alps. These were deposited in alternating shallow marine to limnic-fluviatile environments from late Eocene to Miocene times with some Miocene volcanics in the west. Close to the Alpine Front (the northern border of the Alpine nappes) the southern rim of the NAFB was partly thrusted and folded by late Alpine compression during the Tertiary. Since Pliocene times (latest Tertiary) the NAFB was gradually uplifted and eroded, and the present landscape on top of the former Molasse Basin was shaped by several phases of Pleistocene glaciation.

The Jurassic and Triassic sedimentary sequences beneath the Molasse deposits host two hydrothermal aquifers, which are situated at great depth to the south. These are, mostly immediately below the base of the Tertiary, karstified carbonate rocks of the Upper Jurassic and, several hundred meters deeper but only present in the western part, intensely jointed middle-Triassic Muschelkalk carbonates.

Below the Triassic, Late Paleozoic deposits are predominatly present in troughs in the western part of the T2.1 area (Figure 4.1.2). Only few and small remnants occur in Bavaria and on Austrian territoryine the very southeast of the T2.1 area (FREUDENBERGER 1996). Mostly, the Triassic sediments directly rest upon Paleozoic crystalline rocks of the Variscan Basement.

Geological framework of the main carbonate reservoir(s)

The bedrock strata within the Central Molasse Basin study area can be subdivided into three principal sequences of Paleozoic, Mesozoic, and Cenozoic age, respectively.

Variscan Basement and Permo-Carboniferous sediments:

The oldest rocks in the subsurface of the NAFB are plutonic and medium- to high-grade metamorphic rocks of the Variscan Basement. They formed during the Middle to Late Paleozoic (Devonian to Carboniferous) Variscan (or Hercynian) orogeny that affected large parts of Central Europe. During Late Carboniferous and Permian times, eroded debris from this Orogen was locally deposited in small teconic troughs as an “intra-orogenic Molasse”. These clastic sediments are only known few boreholes of the NAFB area, present almost solely in the western part of the case study area (cf. Figures 4.1.1 and 4.1.2).

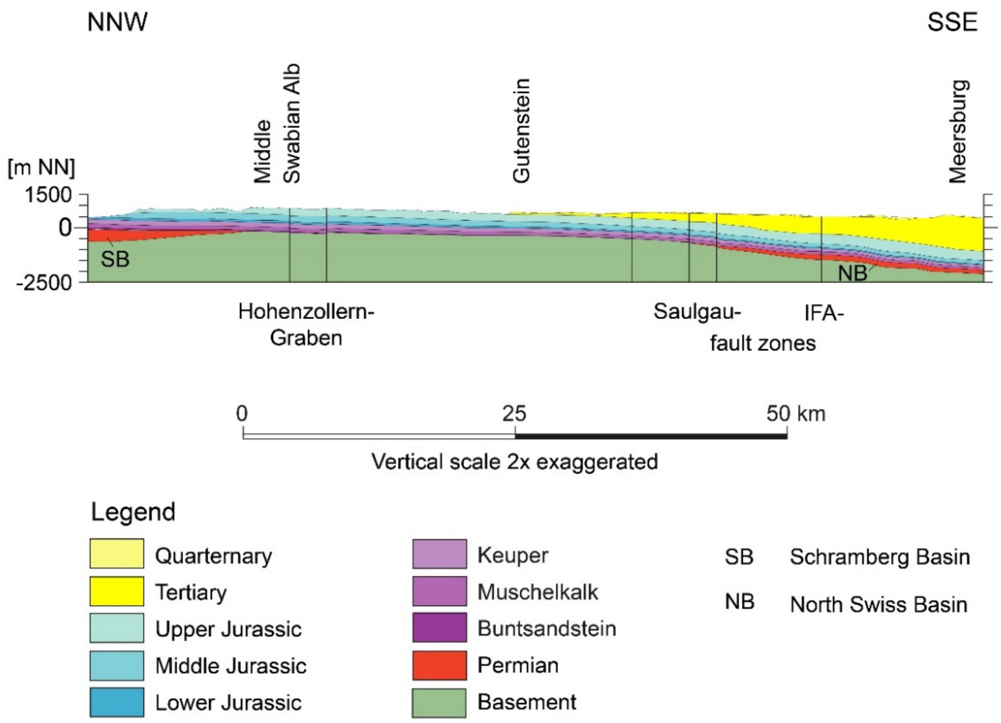

Figure.4.1.2: Geological cross-section approximately across the Baden-Württemberg part of the T2.1 case study area depicting the gently south dipping Mesozoic units overlying the Variscan Basement and Permo-Carboniferous sediments confined to troughs respectively basins.

Mesozoic units:
Resting unconformably upon the crystalline basement and the Permo-Carboniferous sediments, Triassic and Jurassic represent an intracontinental platform sequence of well-consolidated sediments. Continental depositional environments dominate the Triassic (tripartite) period, red beds (Buntsandstein, only present in the northwest of the NAFB subsurface), followed by marine carbonates and evaporites (Muschelkalk – representing the lower reservoir rock in the southwest of the case study area and pinching out to the east), capped by a series of terrestrial mud- and sandstones (Keuper, resting immediately on the Paleozoic basement in the east).
During the Jurassic, the progressive onlap of the Mesozoic sediments further to the southeast continued, successively flooding most of the former highlands forming shallow seas. In the Late Jurassic, the entire realm of the later Molasse Basin, from Savoy to Austria, was part of a tropical shallow shelf sea structured in various sedimentary environments (facies realms) like reefs and other bioherms, lagoons and basins. At the end of the Jurassic, the marine regression towards the Tethys Ocean in the south resulted in emergence of large parts of these carbonate platforms – only in the area around and south of today's Munich the deposition continued to the Early Cretaceous (Purbeck). The Upper Jurassic deposition left behind an up to 600 m thick carbonate rock sequence, subject to deep weathering and karstification under humid conditions during Cretaceous and early Tertiary times. This created considerable secondary permeability in the carbonates and made the Upper Jurassic (Malm) the most prominent reservoir of the Central North Alpine Foreland Basin – and thus the prime target of the T2.1 case study.
Deposition continued in the Tethys Ocean, resulting in sedimentary sequences that subsequently were detached and incorporated into the Alpine thrusts (Helveticum in Figure 4.1.1). Several regional scale marine transgressions during the Late Cretaceous deposited successions of littoral to shallow marine sediments in the east of the NAFB (and in the Swiss southwestern segment of it, outside the project area). Such Cretaceous deposits, directly overlying the Upper Jurassic karst relief and hydraulically connected to it in certain areas, occur in the Braunau Trough and Wasserburg Subbasin (MEYER 1996), on either side of the Landshut-Neuötting Crystalline Rise , known as Central Swell on Austrian territory.

Stratigraphic subunits and lithology of the reservoir rock suites

The most important subdivision of the Upper Jurassic in the project area is one of lateral facies change. To the north, most of the Upper Jurassic succession consists of partly karstified limestones of low organic content (Swabian facies), acting as the main aquifer in the Mesozoic cover. In the westernmost part of the project area, the lower part of the Upper Jurassic can be distinguished as Argovian Facies referring to a more biostromal lithology compared to the east. In parts of the Lake Constance area, the Swabian facies grades towards the South into bituminous limestones with intercalated marls. This Helvetian facies, also known in outcrop from the Helvetian Nappes in Switzerland, is poorly karstified and thus of little interest here.

Cenozoic units
A pronounced unconformity marks the boundary between the Mesozoic and the Molasse Basin fill, a sedimentary sequence up to 5,000 m thick. The basin's internal structure is typical for asymmetrical foreland basins with a basin axis parallel to the orogenic front and continuously migrating towards the foreland:
North of the Subalpine Molasse (also known as Folded, Imbricated, or Allochthonous Molasse) (cf. Figure 4.1.1), which is running from Switzerland south of Lake Constance to the Bavarian and Austrian parts of

the project area (and not present in Baden-Württemberg; Fig. 4.1.2), it consists of gently southward-dipping strata that thin out to the north and lap progressively onto the Mesozoic rocks of the foreland. The oldest Molasse deposits, mostly Eocene in age, only occur in the deep subsurface of Austria and Bavaria. Most of the basin fill is made of Oligocene and Miocene deposits, in which two sedimentary megacycles can be distinguished, both beginning with a marine transgression and ending with regression evidenced by the deposition of terrestrial fluvial and lacustrine sediments. The sedimentary sequence of the basin fill is traditionally divided into six lithostratigraphic units reflecting the evolving paleo-environmental conditions: these are the Lower Marine Molasse (UMM), Lower Brackish-water Molasse (UBM), and Lower Freshwater Molasse (USM) in the lower cycle, the Upper Marine Molasse (OMM), Upper Brackish-water Molasse (OBM), and Upper Freshwater Molasse (OSM) in the second cycle. As the changes in depositional environment did not affect the entire basin equally and simultaneously a Western Molasse and an Eastern Molasse can be distinguished, interfingering in the Bavarian part of the Basin. Figure 4.1.3 depicts a snap-shot of the continuously changing, complex depositional environment distribution in the central NAFB during Late Egerian (earliest Miocene, approximately 22 Ma ago). Sandstones and subordinate carbonates of the Lower and Upper Marine Molasse may also form local hydrothermal aquifers if at sufficient depth, but are not considered in HotLime.

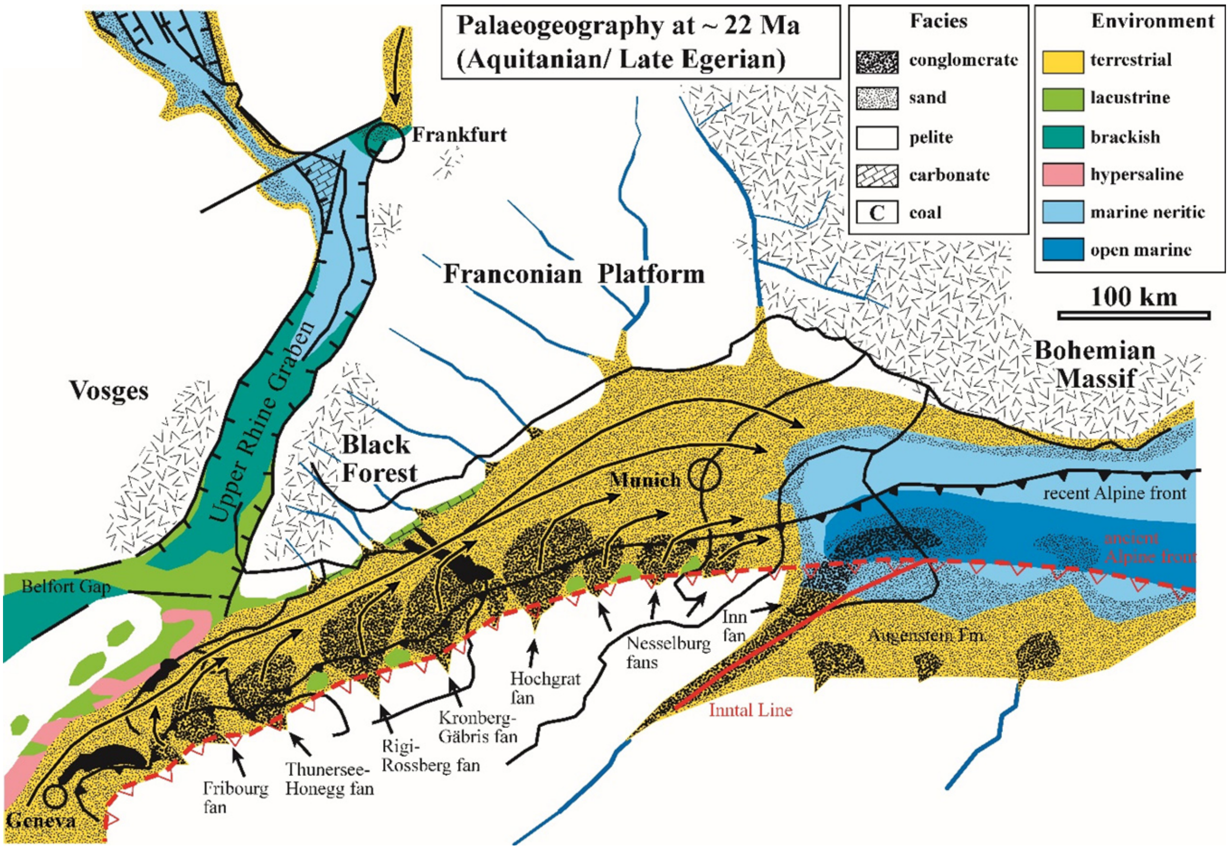

Figure 4.1.3: Sketch map of depositional environment distribution in the Northern Alpine Foreland Basin and connected depressions during Late Egerian, approximately 22 Ma ago (from KUHLEMANN & KEMPF 2008, slightly modified). The strong radial sediment supply through large gravel fans out of the emerging Alpine front caused pronounced disparities in the marine–terrestrial transition specifically in the western Molasse Basin.

Discontinuous Quaternary deposits are common to all regions of the pilot area, mainly as fluvial valley fills and lake deposits of varying thickness and composition. Pleistocene glacial and glacio-fluviatile deposits are also widespread, especially in the southern areas close to the Alps.

Tectonic setting

The central part of the South German Molasse Basin is characterized by predominantly N to NW dipping antithetic and subordinately S to SE dipping synthetic normal faults related to flexure-like strain of the foreland basin. Faults, often arranged as trains of concave and convex fault segments, predominantly trend SW-NE to W-E, subparallel to the basin's centerline and the Alpine Thrust Front, forming lineaments several tens of kilometers long and featuring throws of commonly some tens of meters, rarely as much as 100–200 m. One example for a SE-NW and SW-NE striking extension fault system is the Saulgau main fault zone.

Close to the Landshut-Neuötting crystalline rise the faults' strike is deflected subparallel to the counterfort of the northward Alpine thrust. The blind, roughly NW-SE (Hercynian strike) trending, tilted basement fault block of the Landshut-Neuötting crystalline rise continues into Austrian territory, there called Central Swell (Zentrale Schwellenzone). It represents the marked dividing line towards the Lower Bavaria Molasse Basin, featuring a different tectonic regime and fault pattern. Here, syn- and antithetic normal faults run subparallel to the Bohemian Massif, the counterfort of the Alpine thrust. These roughly Hercynian trending, in part conjugate faults partly result from reactivation of Permo-Carboniferous lineaments and subdivide the Lower Bavarian Molasse Basin into sub-basins and troughs (Figure 4.1.7).

The southern boundary of the Alpine Foreland Molasse towards the Subalpine (aka Folded or Imbricate) Molasse is formed by a commonly ENE-WSW trending steeply S dipping reverse fault, laterally displaced by few sinistral transverse faults which represent the sheared-off northernmost flanks of the synclines resulting from the compressional stress of the Alpine northward thrust. In the western part of Bavaria (Allgäu), where the Folded or Imbricate Molasse merges into a tectonic wedge forming triangle zones (Figure 4.1.4), the north dipping leg at the crest of the blind, protruding wedge represents the southern boundary of the Foreland Molasse.

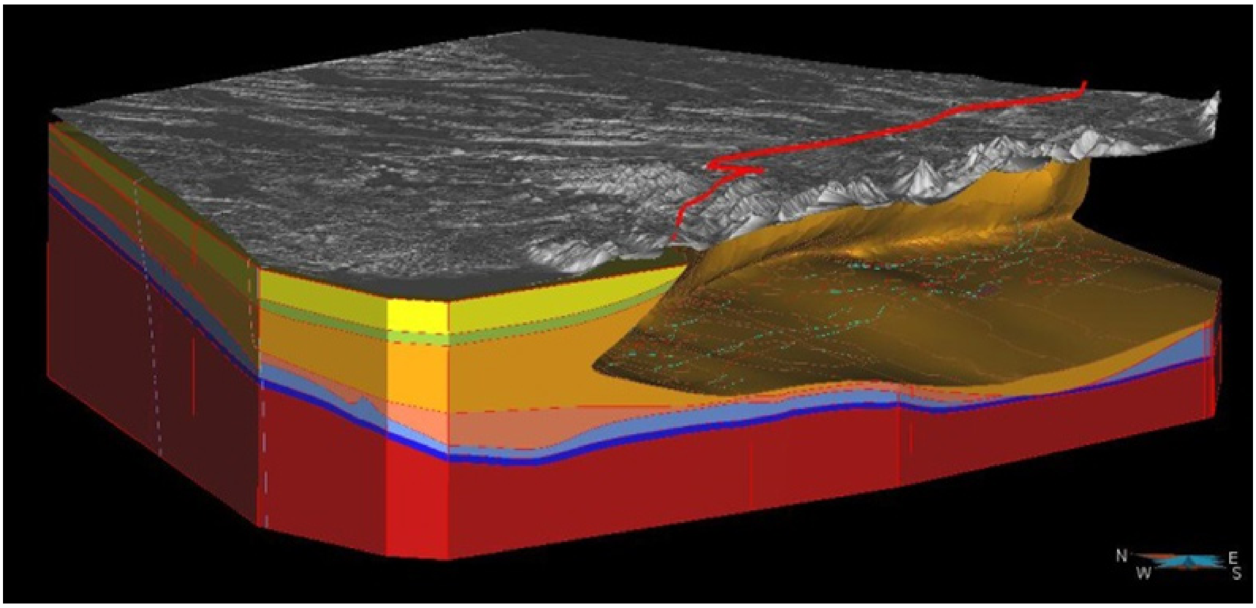

Figure 4.1.4: "Area of interest" tile of a preliminary 3D model of the southern boundary of the Molasse Basin in the western part of Bavaria (Allgäu). Molasse infill deposits are depicted in yellowish hues, Upper Jurassic in light blue, Middle and Lower Jurassic in dark blue, and the Crystalline Basement in red. The ochre-colored wedge marks the boundary of the blind, protruding triangle zone the Subalpine Molasse in front of the Alpine orogenic front. The red line represents the trace of the north-dipping wedge limp projected onto the terrain surface, displaced by a sinistral transverse fault. This cut-out of the preliminary 3D model also exemplifies an artefact caused by internal consistent but contextual inconsistent well markers (weirdly corrugated top of Upper Jurassic at front left) corrected on model quality assessment.

Faults and fault zones in the Upper Jurassic carbonates, and Muschelkalk alike, are the prime targets for any groundwater exploration and productions drilling, for drinking water supply as well as for hydrothermal utilization. The structural inventory at least of major fault systems, thus, was a primary target of 3D geological modelling of the T2.1 case study area.

3D Geological Modelling

A major challenge in 3D modelling of basin structures that reach down to more than 5 km, is the availability of data with an adequate distribution and resolution to address issues properly. Principal fundamental data for the T2.1 case study 3D geological model have been seismic data, scattered and clustered deep downhole data – both originating primarily from the 1960s to 1980s hydro-carbon exploration and production, and secondarily from the investigations for geothermal installations that commenced in the 1990s – and contour line drawings, all held together by the conceptual model of the Molasse Basin evolution. The use of different baseline data originating from multiple sources and various dates of origin imperatively required data harmonization from the very beginning of the model building workflow starting with the selection and preparation of the input data. Applying consistent methods and common parameters for model preparation and fault assessment, the integration of data in time domain and information in depth domain imposed particular requirements on the velocity models employed and the modelling workflow that requires toggling back and forth between depth and time domains depending of the point of departure.

Input data sets

Geological modelling of the different horizons within in the T2.1 case study area is based on a variety of different input data sets. The backbone for mapping the deeper parts of the area where downhole data are scarce and unevenly distributed are seismic surveys calibrated by reference to borehole markers of well data, input information from geological and structure maps and cross-sections, and, where available legacy models which consolidate the aforementioned baseline date in certain areas. As all faults of the central NAFB are blind faults, buried under a thick succession of younger undeformed sediments, seismic surveys are the only means for spatial modelling the structural inventory (otherwise only proved as punctual features in downhole records). However, in the shallower parts of the basin, due to their lack of hydrocarbon prospectivity and a moderate to low geothermal potential, very few seismic surveys have been carried out. Hence, where available, Bouguer gravity residual anomalies maps were utilized to accentuate the structure of the pre-Mesozoic basement.

Seismic records

Due to the extensive hydrocarbon exploration in the deeper areas of the Molasse Basin, 135 2D seismic lines with a length of 2,370 km are digitally available in Baden-Württemberg. For the Bavarian part we could hark back to overall 487 2D seismic lines totaling more than 8,800 km in length, many of them already aligned and integrated in pre-existing 3D geological models available (Figure 4.1.5). 2D seismic surveys mainly were recorded between 1970 and 1990 for hydrocarbon exploration and production. Most of them have been digitized, re-processed and harmonized following common parameters as part of the GeoMol project.

3D seismic surveys basically were carried out within recent exploration campaigns for geothermal projects, in order to gain the best information possible on the fault network at depth. 2,600 km^2 of the Molasse Basin in Bavaria (including near border areas in Upper Austria), and 136 km^2 in Baden-Württemberg are covered by 3D up to date seismic surveys.

In the shallower parts of the central Molasse Basin, due to their lack of hydrocarbon prospectivity and a moderate to low geothermal potential, seismic data are scarce; in the area of the Swabian-Franconian Alb no information from seismic surveys is available.

Borehole data

Likewise the information from seismic surveys, deep downhole data is abundant in focal areas of hydrocarbon E&P culminating in the 1970s and 1980s and recent geothermal E&P, but scares in other areas. In the Baden-Württemberg part of the case study area 3,300 borehole data sets with measured depths deeper 100 m are available. In Bavaria information on 2,360 boreholes of more than 500 m depth was already integrated in pre-existing 3D geological models (cf. Figure 4.1.5) and supplemented by 886 further boreholes from 200 to 4,700 m depth in order to close the gaps in between the legacy models. Additionally, information on the true depth of strata modelled was derived from downhole data for heat exchangers and shallow wells in the marginal areas of the basin. According to purpose of the drilling they obtain besides mandatory master data sets further information like lithological descriptions, their lithostratigraphic classification, geophysical measurements, drill stem tests, temperature data and petrophysical measurements.

Pre-existing 3D-Models

In Baden-Württemberg, various geological 3D models have been built in the vicinity of the HotLime case study area over the past 15 years. A state-wide overview model (Landesmodell Baden-Württemberg) from

2008 encompasses the principal lithostratigraphic horizons from the base of Quaternary to the top of the Crystalline Basement (RUPF & NITSCH 2008). The ISONG model provides information on the location of the main aquifers and geotechnically problematic horizons up to a depth of 400 m. Both geological 3D models were created based on borehole information and structural maps while structural information from seismic surveys were not taken into consideration. For the southern part of the T2.1 area in Baden-Württemberg a detailed and deep geological 3D model (LCA model) was available, created as part of the GeoMol project (GEOMOL TEAM 2015), based on downhole and seismic information. GeoMol's outcomes not only provide basic 3D information on certain areas of the Molasse Basin in Baden-Württemberg, Bavaria and Upper Austria (Figure 4.1.4), but also laid the foundation for methodical approaches and cross-border 3D-modeling as implemented and further specified in HotLime. The distribution of pre-existing 3D geological models in Bavarian and Upper Austrian territory available for the capture of the HotLime target horizons is depicted in figure 4.1.5.

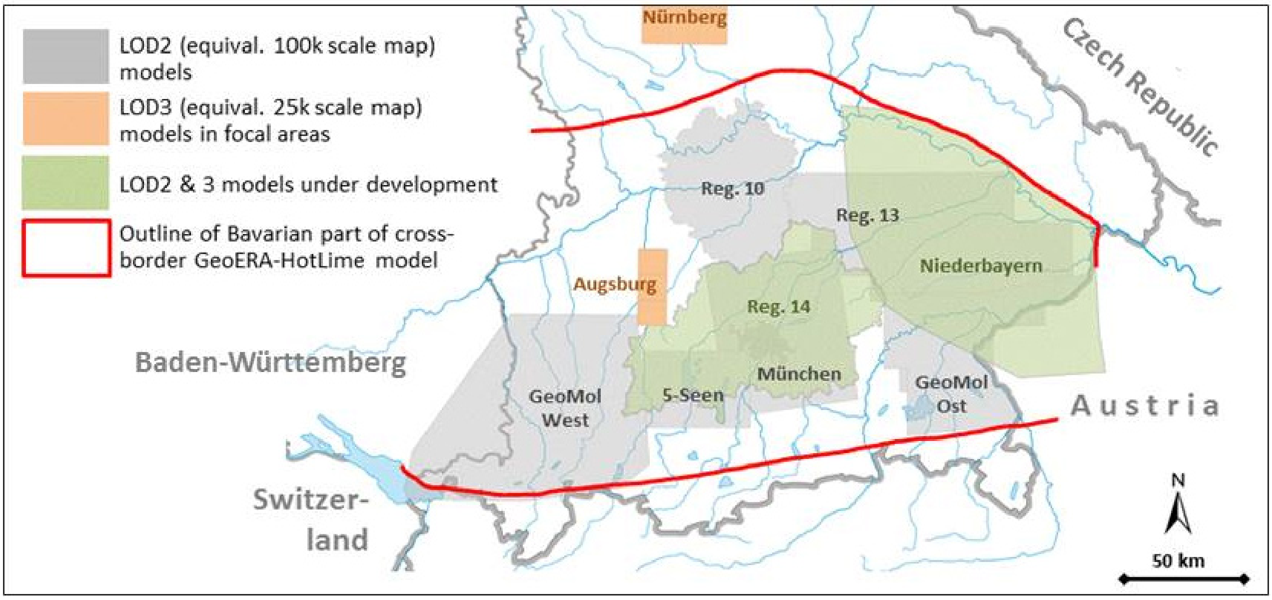

Figure 4.1.5: Sketch map of 3D geological models available for the Bavarian part of T2.1 at the beginning of HotLime implementation. Only the LOD2 models (depicted in grey) feature a suitable depth to address the issues of HotLime. "GeoMol West" marks the Bavarian share of the GeoMol "Lake Constance-Allgäu area" (LCA) Model. "Niederbayern" and "Reg. 14" (depicted in green), under preparation at the beginning of HotLime, have been refocused to the requirements of the capture of deep hydrothermal reservoirs and western Upper Austria has been included. Due to the huge size of the modelling area software limitations forced us to implement modelling by confined areas of interest using overarching cross-sections as fixed anchor lines for subsequent merger.

Additional data sets

Knowledge about thickness distribution of the modelled units is important for the derivation of horizons from previously constructed surfaces by addition or subtraction. Furthermore, such information helps to retain realistic layer thicknesses in areas with scarce or no information from downhole data. Thus, all information on layer thicknesses such as legacy contour plans or figures from literature were considered in the modelling process.

A Bouguer gravity residual anomalies map was utilized for construction of the surface of the pre-Mesozoic basement in areas with insufficient information from seismic surveys (Figure 4.1.7).

Principle modelling workflow

Modelling in all territories, Baden-Württemberg, Bavaria and Upper Austria, was implemented using the SKUA-GOCAD™ software. An established workflow was applied for the newly modelled areas apart from existing models.

1. Data preparation (construction of occurrence polygons, structural maps and facies distributions)
2. Modelling in depth domain based on outcrop and well data (entire modelling area)
3. Modelling in time domain based on seismic interpretation and well data (deeper parts of the modelling area) and time-depth conversion of the modelled objects
4. Adaptation of the 3D geological model to faults and horizons from the seismic interpretation in the depth domain
5. Consistency checks

Merger of (partial) models ensued at the very end of the modelling procedure.

Since seismic surveys for modelling horizons and faults are available in the deeper part of the case study area only, the geological 3D models initially were constructed entirely in depth domain based on borehole information, outcrop data, cross-sections and other thickness distribution information, e.g. from adjacent pre-existing 3D geo-models. Subsequently, the models converted into time domain were used to underpin the interpretation of the seismic survey information. The fault traces, derived by connecting related fault sticks picked, and horizons detected in seismic sections and 3D seismic surveys were correlated in time domain and checked for plausibility. After time-depth conversion of the objects modelled in the time domain, the geological 3D model was adapted in the southern part to the faults and horizons from the seismic interpretation.

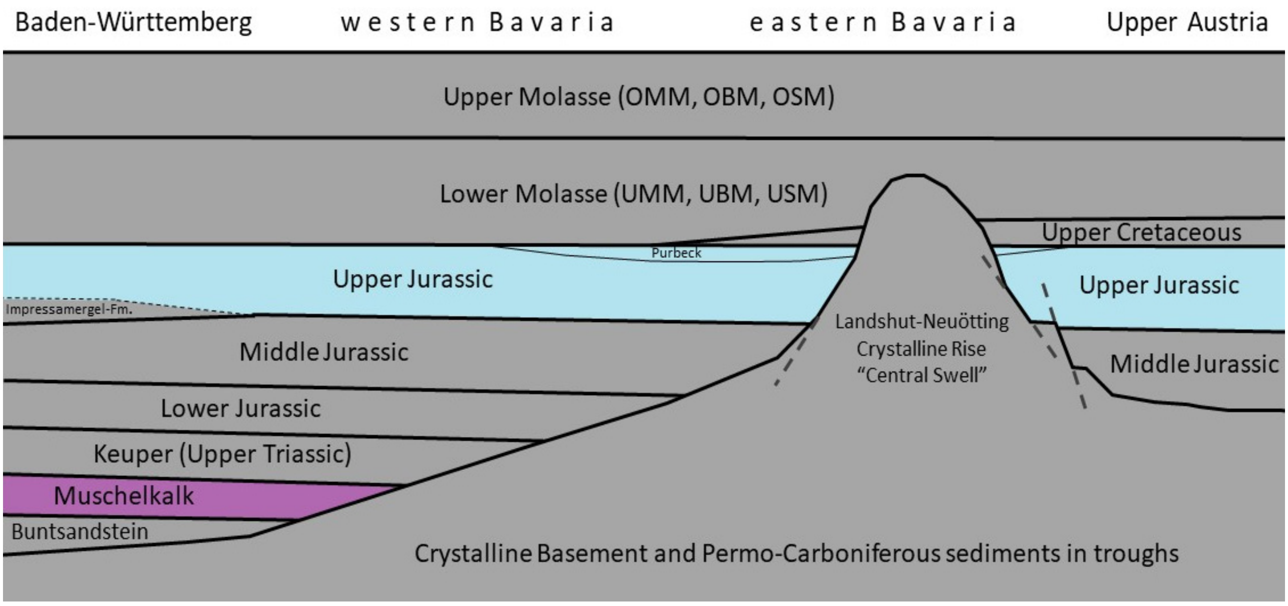

Figure 4.1.6: Lithostratigraphic scheme (schematic, not to scale) depicting the modelled horizons across the T2.1 Molasse Basin case study area from west to east highlighting the two reservoir rock suites under consideration. All boundaries shown represent a more or less pronounced unconformity but not all feature a distinct seismic reflector.

Modelling in depth domain based on outcrop and well data (entire modelling area)

Due to limited data density for the modelling region, in some areas modelling had to rely on the conceptual model of the region's structural framework. In total, up to nine lithostratigraphic horizons were modelled. For modelling the horizons in depth domain, a combined GIS and GOCAD workflow was applied using borehole information, pre-existing GOCAD model surfaces, thickness distributions, geological, structural and isopach maps.

The applied method for modelling of horizons is based on the concept of an independently modelled reference horizon (e.g. top of Impressamergel-Formation, cf. figure 4.1.6) and subsequently derived surfaces were created using pre-existing thickness distributions. A detailed description of the method can be found in RUPF & NITSCH 2008. Cross-checks of the modelled horizons and well markers ensured the correct position. In cases of deviations between well markers and horizons of more than 10 m, the borehole information had to be verified. If the well proved to be reliable, the horizon had to be locally adapted to the well marker using Discrete Smooth Interpolation Method with the drilling information as constraint.

The modelling of tectonic elements in Baden-Württemberg was based on the main fault systems of the integrated geoscientific database (GeoLa). Before importing the fault traces into GOCAD, technical revision of the given fault pattern in GIS were necessary, e.g. for closure of small gaps between adjacent fault traces.
With the help of structural maps and specifications from literature, displacements along faults within the reference horizon were modelled in GOCAD. Since there is no information about the dip of the faults in the GeoLa dataset, faults were assumed as vertical.
Finally, by cutting the modelled horizon with its occurrence polygon the final extent of the reference horizon was set.

Similarly, for the Bavarian and Upper Austrian parts of the T2.1 area starting point for the capture of horizons and the fault network has been a grid of cross-sections integrating all available information in depth domain, including legacy models. These core components for 3D modelling we utilized not only for refinement of legacy models intersected but also as fixed anchor lines to hold together the different models of modelling by areas of interest, which turned out indispensable due to the software limitations disallowing to model the entire area in one piece.
Largely based on this workflow for shallow realms of the Molasse Basin, lacking substantial seismic information thus not allowing to capture the spatial complexity of horizon surfaces in between downhole evidence, for the Lower Bavaria (Niederbayern) part of the basin additionally a Bouguer gravity residual anomalies map was used to accentuate the structure of the pre-Mesozoic.

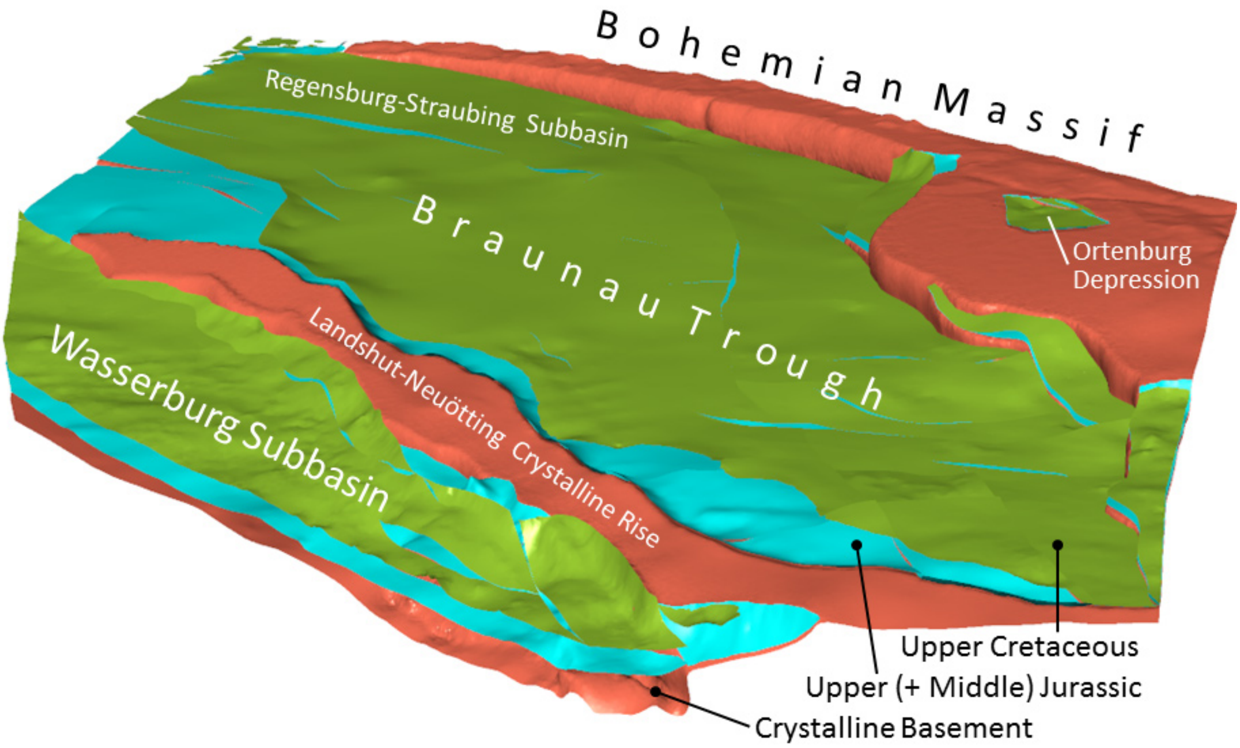

Figure 4.1.7: 3D geological model of Niederbayern and western Upper Austria, view from SW, Tertiary layers omitted for clarity. Due to the lack of hydrocarbon prospectivity and a assumedly moderate to low geothermal potential only few seismic surveys have been carried out and are limited to the southern (deeper) part of this shallow to medium-deep portion of the Molasse Basin only. Hence, a Bouguer gravity residual anomalies map was used to accentuate the structure of the pre-Mesozoic basement and the 1,000 m throw fault system along the edge of the Bohemian Massif basement complex.

Seismic interpretation in time domain (southern, deeper, modelling area)

In the southern part of the pilot area, information on the position of horizons and faults in space and time is available from seismic sections. Therefore, the well data and 3D geological models prepared in depth domain were converted into time domain using the GeoMol velocity model (GeoMol Team 2015, GeoMol LCA Project Team 2015). The well markers and horizons of the time converted 3D model underpinned the interpretation of seismic information.

Due to the small vertical offsets and the noisy seismic signature of the tertiary units, it turned out difficult to detect faults in the seismic profiles, specifically in the western part of the T2.1 area. Here, the unambiguous identification of the faults' dip and throw is only feasible in domains of strong distinct reflectors within the Mesozoic units, while the upper termination of the faults is generally difficult to determine. However, from the more intense seismic signature in the eastern part of the T2.1 area we know that the youngest horizons affected by faulting are of mid-Miocene (Badenian) age. Assuming a similar tectonic regime for the entire Central Molasse Basin it seems natural that the tectonic stress in the western T2.1 area likewise gradually ceased in during mid-Miocene

To check the interpretation, the picked horizons were triangulated to surfaces and the fault sticks on the different seismic profiles correlated. The geometry of the fault surfaces was checked for plausibility (similar dip angles, distortion-free surfaces). Afterwards, all picked horizons and faults have been converted from time to depth domain, again using the GeoMol velocity model.

Adaption of the 3D model to the results of seismic interpretation in depth domain (southern, deeper modelling area)

The horizons of the geological 3D model in the depth domain were adjusted to the information captured in seismic profiles and the faults were re-modelled. Subsequently, the spatial position of all other horizons had to be examined for intersections and plausible thicknesses, and had to be corrected where necessary.

Quality assurance

The harmonization of the input data has priority to apply consistent methods and common parameters. For the HotLime`s 3D geological model the principal input data are existing models, seismic data, boreholes, a variety of geological maps and contour line drawings. The selection and consideration of the data is based on different criteria, such as the quality of the data, the complete metadata information and the distribution within the study area. In general, the borehole data must be checked by a geological expert. This includes a consistent classification of lithostratigraphic horizons in boreholes based on geophysical well logging (mostly resistivity logging, sometimes gamma ray logging, rare sonic logging). Likewise the technical preparation and harmonization of the seismic data has to be done. Furthermore all seismic data need a common datum plane and replacement velocities.

The first step in 3D modelling is the seismic interpretation of the visible seismic reflectors and faults in time domain. After the time-depth conversion of the seismic interpretation, the 3D model was checked for fitting of the well markers. Completing the modelling of the faults and horizons in depth domain the internal consistency checks and quality assurance of the model are performed. This included an inspection for horizon crossings and, again, a test for well marker fit. Furthermore the structural inventory had to be verified by using regional geological knowledge and tectonic evolution models.

4.1.4 Rock property and temperature modelling

The most important information about the temperature distribution in the subsurface stems from borehole measurements (Bottom Hole Temperatures, Drill Stem Tests). For temperature modelling, data from archives and literature as well as specifically collected data were exploited. The quality of the temperature values depends, among others, on the measuring method of choice. Therefore, a uniform categorization with regard to the measuring methodology for the further use of the substrate temperatures was important. Another essential input data set for the temperature model included surface temperatures.

For setting up the temperature model in Baden Württemberg, the most important data source for temperature data was the geophysical information system (Fachinformationssystem Geophysik FIS-GP, KÜHNE 2006). Here, data from the subsystems "temperature" and “borehole geophysics" was used (as of 06/2013) collating all the aforementioned data. The temperature logs were compared and supplemented with analog and digital data from the LGRB data archive. Temperature logs in deflected boreholes were coupled on the drill path to assign the measurements to their respective vertical depths (TVD, true vertical depth). In addition, temperature measurements within the scope of groundwater sampling from the

laboratory database of the LGRB complement the Baden-Württemberg dataset (GEOMOL LCA-PROJEKTTEAM 2015).
The total number of wells was 350, with 131 Bottom-Hole Temperatures (BHT). There was no temperature correction method applied in the scope of the project as they were provided from the FIS-GP with correction after KÜHNE 2006 (GEOMOL TEAM 2015). The number of Drill Stem Test Temperatures (DST) totalled 65. Furthermore, 154 undisturbed temperature logs were available (GEOMOL TEAM 2015).
The input data are in the majority of good to very good quality, but are distibuted very inhomogeneously in the model area. This applies to both horizontal and vertical distribution.

After a categorization with regard to their quality according to CLAUSER et al. (2002) the measured values were transferred to an Access database. Here, filtering and a final gradient-based plausibility check of the temperatures followed where values leading to negative gradients were removed from the dataset. Next, a calculation of surface temperatures, the topography effect and the cooling influence of the Lake Constance water body was conducted. For the following temperature modelling in GOCAD the a-priori model based on regionalized geothermal gradients was applied. The calibration of the model was based on residuals. The final geostatistical temperature model is based on a regular orthogonal 3D grid.

For the Bavarian and Upper Austrian part of the T2.1 area the temperature model of AGEMAR & TRIBBENSEE (2018) was used, which collates all the aforementioned data and lately has been calibrated using the GeoMol data sets (GEOMOL TEAM 2015) and temperature measurements performed in recent geothermal developments in the Bavarian part of the Central Molasse Basin.

As a result of the increasing burial depth the temperatures at the top of the geothermal unit “Upper Jurassic” increases from fluctuating ambient temperature, with an average of about 10°C, in the northwest to approximately 160 °C in the south of the project area (Figure 4.1.8).

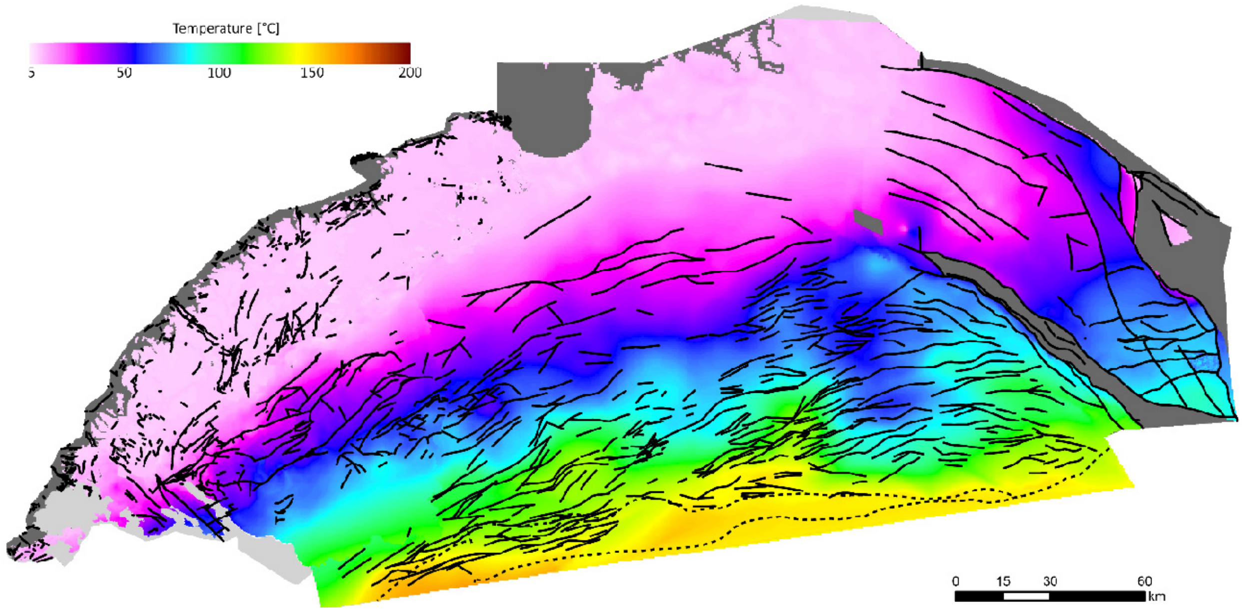

Figure 4.1.8: Temperature distribution at top of the south-dipping Upper Jurassic in the T2.1 area. The temperture ranges from ambient temperature in the northwest, with an average of about 10°C, to more than 160°C in the south. Dim grey marks areas with no Upper Jurassic carbonates present (e.g. the Bohemian Massif in the east, the Landshut-Neuötting Crystalline Rise (cf. figure 4.1.7) and the Ries Impact Crater, center north); light grey marks areas where no date have been available for temperature modelling (Swiss territory and Lake Constance in the southwest).

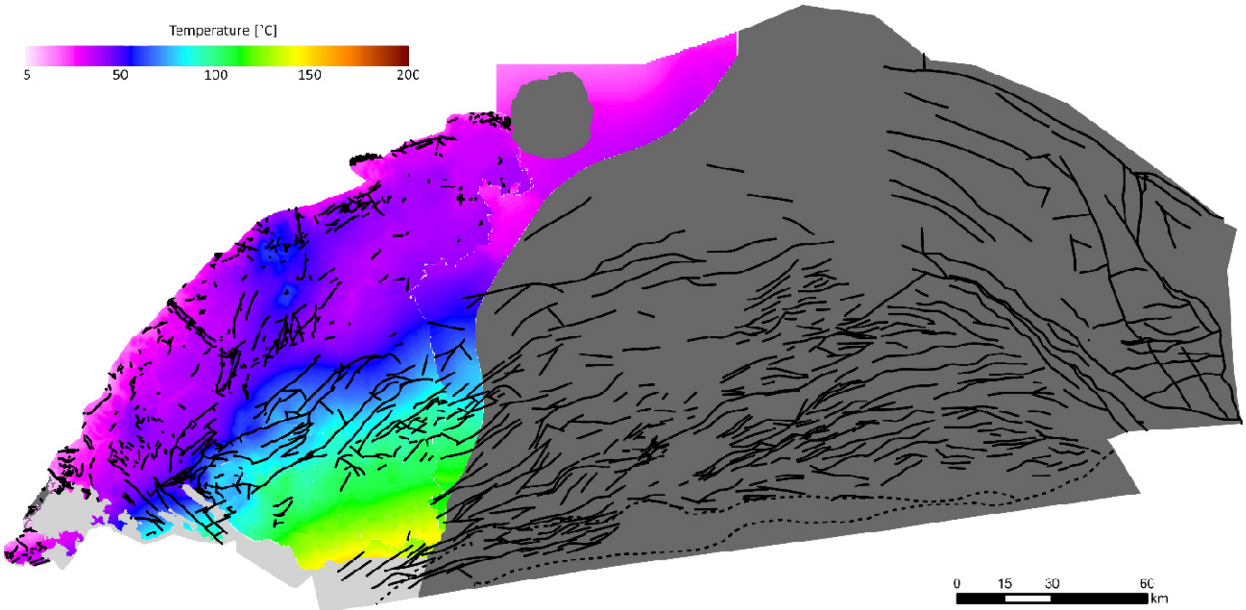

Figure 4.1.9: Temperature distribution at top of Muschelkalk carbonates in the T2.1 area. Muschelkalk pinches out to the (south)east forming a roughly 50 km wide increasingly sandy litoral facies. Dim grey marks the eastern, almost purely arenaceous areas of Muschelkalk not considered in T2.1 and westward adjoining areas with no Muschelkalk present, and accentuates the circular Ries Impact Crater in the north.

Particularly in reservoirs featuring a gross thickness of more than 200 m, the increase of temperature with depth within the target layer(s) has a significant effect on the geothermal resource base assessment as carried out in the ongoing WP3 "Play and Prospect Evaluation". Accordingly, such large-thickness reservoirs are dealt with as layered incremental intervals in the geothermal assessment using the "Heat-in-Place" method of applying fixed 'known' parameters (deterministic approach) of MUFFLER & CATALDI (1978). Pros and cons of this approach based on literature values means over certain areas/volumes are discussed in DIEPOLDER et al. (2020).

REFERENCES

AGEMAR, T. & TRIBBENSEE, K. (2018): GeotIS-Verbundmodell des Top-Malm im Bereich des Vorlandbeckens der Alpen. – *ZDGG - German Journal of Geology* **169**: 335-341. https://doi.org/10.1127/zdgg/2018/0126 [2019-12-05]

CLAUSER, C., DEETJEN, H., HÖHNE, F., RÜHAAK, W., HARTMANN, A., SCHELLSCHMIDT, R., RATH, V. & ZSCHOCKE, A. (2002): Erkennen und Quantifizieren von Strömung: Eine geothermische Rasteranalyse zur Klassifizierung des tiefen Untergrundes in Deutschland hinsichtlich seiner Eignung zur Endlagerung radioaktiver Stoffe – Endbericht zum Auftrag 9X0009- 8390-0 des Bundesamtes für Strahlenschutz (BfS). – 159 S.; Aachen (RWTH). https://www.bundestag.de/endlager-archiv/blob/388966/3ff3b8c9bf706d7de35bee49c3f733e5/kmat_12-10-data.pdf [2019-12-13]

DIEPOLDER, G.W., BOROVIĆ, S., HERMS, I. & HOTLIME TEAM (2020): HotLime – Mapping and Assessment of Geothermal Plays in Deep Carbonate Rocks. – *Proceedings,* **16040**, World Geothermal Congress, Reykjavik, Iceland. [accepted]

DIEPOLDER, G.W., PAMER, R. & GROßMANN, J. (2019): Advancements in 3D geological modelling and geo-data integration at the Bavarian State Geological Survey. – In: MACCORMACK, K.E., BERG, R.C., KESSLER, H., RUSSELL, H.A.J. & THORLEIFSON, L.H. (ed.): 2019 synopsis of current three-dimensional geological mapping and modelling in geological survey organizations. – AER/AGS Special Report **112**: 48-61; Edmonton (Alberta Energy Regulator / Alberta Geological Survey). https://static.ags.aer.ca/files/document/SPE/SPE_112.pdf [2020-01-18]

DOPPLER, G., FIEBIG, M., FREUDENBERGER, W., GLASER, S., MEYER, R.K.F., PÜRNER, T., ROHRMÜLLER, J. & SCHWERD, K. (2004): GeoBavaria – 600 Millionen Jahre Bayern. – 92 S.; München (Bayerisches Geologisches Landesamt).

FREUDENBERGER, W. (1996): Perm. – In: FREUDENBERGER W. & SCHWERD, K. (1996): Erläuterungen zur Geologischen Karte von Bayern 1 : 500 000, 4. Auflage, S. 55-64; München (Bayerisches Geologisches Landesamt).

KÜHNE, K. (2006): Das Fachinformationssystem Geophysik und seine Nutzung über das Internet. – In: MERKEL, B., SCHAEBEN, H., WOLKERSDORFER, C. & HASCHE-BERGER, A. (Hrsg.): GIS – Geowissenschaftliche Anwendungen und Entwicklungen, 57. Berg- und Hüttenmännischer Tag, 23.06.2006, Wiss. Mitteilungen des Instituts für Geologie **31**: 227–231; Freiberg.

KUHLEMANN, J. & KEMPF, O. (2002): Post-Eocene evolution of the North Alpine Foreland Basin and its response to Alpine Tectonics. – Sediment. Geol. **152**: 45–78.

GEOMOL TEAM (2015): GeoMol – Assessing subsurface potentials of the Alpine Foreland Basins for sustainable planning and use of natural resources. – Project Report, 188 S.; Augsburg (LfU)

GEOMOL LCA-PROJEKTTEAM (2015): GeoMol – Geopotenziale für die nachhaltige Nutzung des tieferen Untergrundes in den alpinen Vorlandbecken. Abschlussbericht des Pilotgebiets Bodensee - Allgäu. – LGRB-Informationen **30**: 142 S.; Freiburg i.Br.

MEYER, R.K.F. (1996): Kreide. – In: FREUDENBERGER W. & SCHWERD, K. (1996): Erläuterungen zur Geologischen Karte von Bayern 1 : 500 000, 4. Auflage, S. 112-126; München (Bayerisches Geologisches Landesamt).

MUFFLER, L.J.P. & CATALDI, R. (1978): Methods for Regional Assessment of Geothermal Resources. – Geothermics **7**: 53-89. https://doi.org/10.1016/0375-6505(78)90002-0 [2019-12-05]

PASCHEN, H., OERTEL, D. & GRÜNWALD, R. (2003): Möglichkeiten geothermischer Stromerzeugung in Deutschland – Sachstandsbericht. – Büro für Technikfolgen-Abschätzung beim Deutschen Bundestag (Hrsg.): TAB-Arbeitsbericht **84:** 124 S.; Berlin.

RUPF, I. & ARMBRUSTER, V. (2008): Das geologische Modell des Informationssystems Oberflächennahe Geothermie für Baden-Württemberg. – In: MERKEL, B., SCHAEBEN, H., WOLKERSDORFER, C. & HASCHE-BERGER, A. (Hrsg.): GIS - Geowissenschaftliche Anwendungen und Entwicklungen, 59. Berg- und Hüttenmännischer Tag, 13.06.2008, Wiss. Mitteilungen des Instituts für Geologie **37**: 179–182; Freiberg.

RUPF, I. & NITSCH, E. (2008): Das Geologische Landesmodell von Baden-Württemberg: Datengrundlagen, technische Umsetzung und erste geologische Ergebnisse. – LGRB-Informationen **21**: 81 S., 10 Beil.; Freiburg i. Br.

WELLMAN, J.F., REID, L.B., HOROWITZ, F.G. & REGENAUER-LIEB, K. (2011): Geothermal Resource Assessment: Combining Uncertainty Evaluation and Geothermal Simulation. – Conference Paper, AAPG/SPE/ SEG Hedberg Conference “Enhanced Geothermal Systems”; Napa, CA. https://www.researchgate.net/publication/237197648 [2019-11-28]

4.2 Molasse Basin-Carpathian Foredeep transition zone (AT/CZ) – T2.2

Clemens Porpazcy (GBA) and Juraj Francu (CGS)

The Pilot Area T.2.2 is located in the border region of northeastern Austria and southeastern Czechia between the Bohemian Massif in the west and the Alpine-Carpathian orogenic system in the east (Figure 4.2.1). The Upper Jurassic limestone formations under investigation within the Pilot Area are located on the southeastern dipping slopes of the Bohemian Massif, overlain by up to 2,000 m succession of Neogene sediments of the Alpine-Carpathian foreland basin.

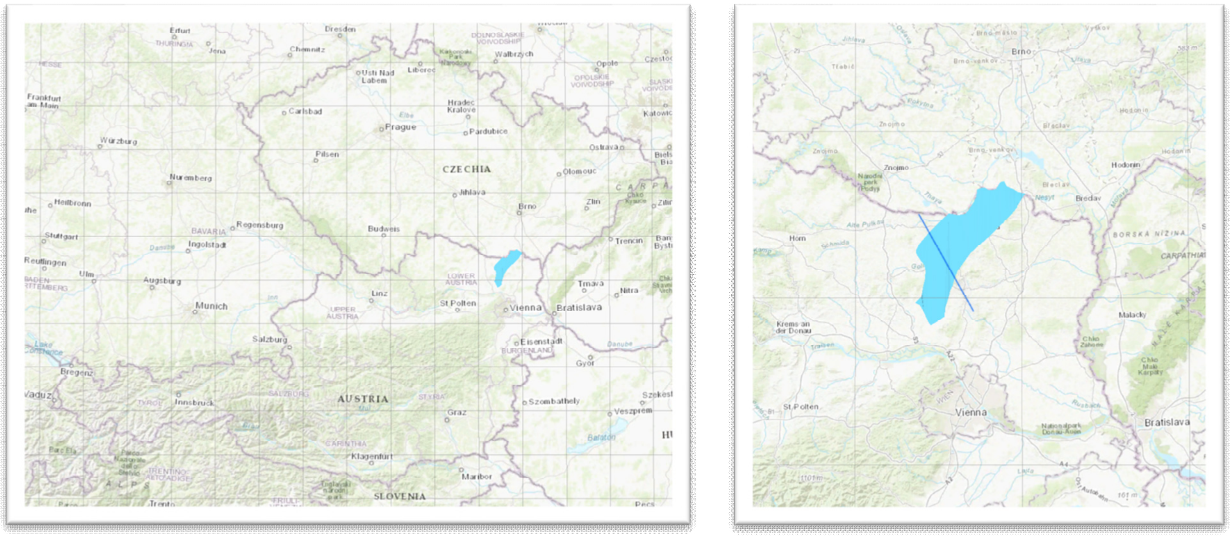

Figure 4.2.1: Hotlime Pilot Area T.2.2 between Vienna (Austria) and Brno (Czechia) indicated in light blue, showing the areal extent of the Upper Jurassic horizon covered within the 3D model. Right: Close-up view of Pilot Area and location of cross-section displayed in Figure 4.2.2.

4.2.1 Inducement and Objectives

The focus of the investigation is set on the NE-SW trending, elongated Upper Jurassic limestone body, crossing the border between Austria and Czechia beneath the Alpine-Carpathian foreland basin in a depth of 1,000 m to 3,000 m below ground level, extending further SE below the Vienna Basin. The limestone body exhibits significant yields of hydrothermal waters, which are used balneologically in the thermal spas of Laa an der Thaya (Austria) and Pasohlávky (Czechia). However, the general geothermal characteristics of this hydrothermal reservoir and the potential heat for power generation or district heating stored inside the Upper Jurassic limestone is not well understood, due to limited information about the deep subsurface. Based on all available geological subcrop data, a geological 3D model of the Upper Jurassic limestone was established for spatial characterization of the reservoir rocks and for subsequent geothermal characterization using the petrophysical data at hand. In the context of Hotlime, strong emphasis is put on the semantic harmonization of modelled formations in cross-border regions, as well as on the comparability of results between all Pilot Areas using the same methodology and toolset for the assessment of geothermal resources. The anticipated results are intended to support stakeholders and policymakers by providing a bilateral harmonized data basis in a European context for low-enthalpy, hydrothermal systems.

4.2.2 Study area and geological setting

Pilot Area T2.2. covers about 533 km² in the federal state of Lower Austria. The Austrian town of Laa an der Thaya, close to the border, represents the largest settlement within the Pilot Area, using thermal waters for balneological use in the local spa from the Upper Jurassic limestone aquifer. Thermal water is extracted from Well Laa Th Nord 1, which was drilled in 1995, reaching a depth of 1,484 m. In Czechia, 25 km northeast of Laa an der Thaya, thermal water is extracted from the Upper Jurassic via Well MU 3G Mušov, drilled in 1993 and reaching 1,455 m. These thermal waters are used for balneological purposes in the thermal spa of Aqualand Moravia near the town of Pasohlávky. So far, these are the only geothermal installations in the cross-border region using hydrothermal resources from Upper Jurassic rocks, which have been erected specifically for this purpose.

Regarding the regional geological setting, the structural framework of the subsurface exhibits half graben basins with autochthonous infill of Upper Jurassic deposits. These throughs are limited towards NW by large-scale normal faults, arranged in a NE-SW striking En-Echelon pattern with sinistral strike component, reflecting escape tectonics caused by the northward push of the Alpine-Carpathian Orogen (Figure 4.2.2). Upper Jurassic formations are located entirely in the subsurface in the southwestern, Austrian part. Towards the northern end of the Pilot Area, some Upper Jurassic formations are exposed in outcrops near Brno in Czechia.

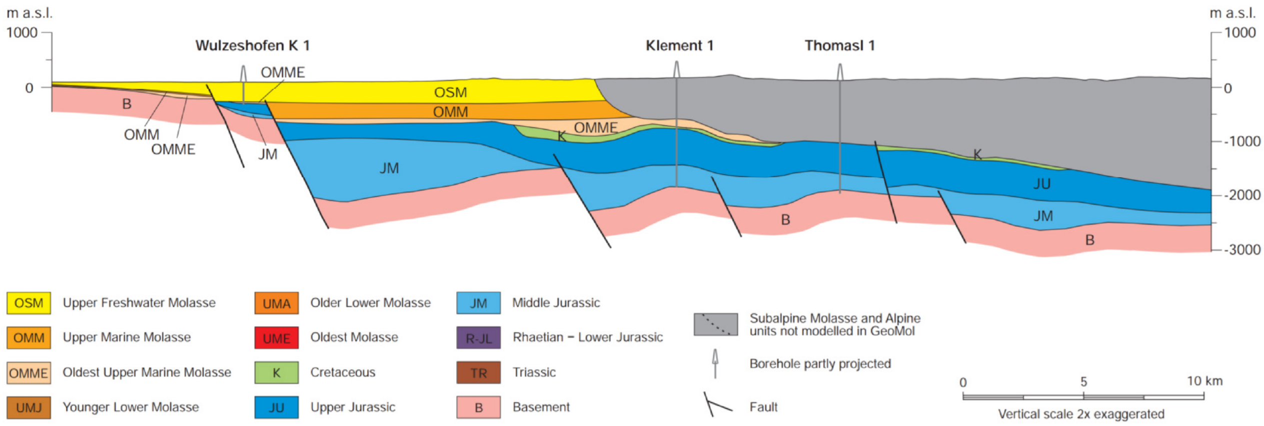

Figure 4.2.2: Schematic NW-SE cross-section, perpendicular to the striking direction of the main normal faults offsetting the half-graben basins (for location see Figure 4.2.1). Yellow, orange and light-brown units represent Neogene units of the Alpine-Carpathian foreland basin (GEOMOL TEAM 2015)

The different formations of the main carbonate platform between Austria and Czechia are grouped into two distinct depositional environments, reflecting a marginal reef carbonate facies in the west (Vranovice, Altenmarkt & Falkenstein formations), which change laterally along the NE-SW striking Mušov transition Zone towards the east into a basinal facies (Mikulov, Kurdějov & Ernstbrunn Formation, Figure 4.2.3). Deposition occurred throughout the whole Upper Jurassic, including Tithonian, Kimmeridgian and Oxfordian strata. Thickness values reach a maximum in the southern part with up to 1,000 m and gradually diminishes towards the northern, Czech part with only 200 m close to the outcrop area.

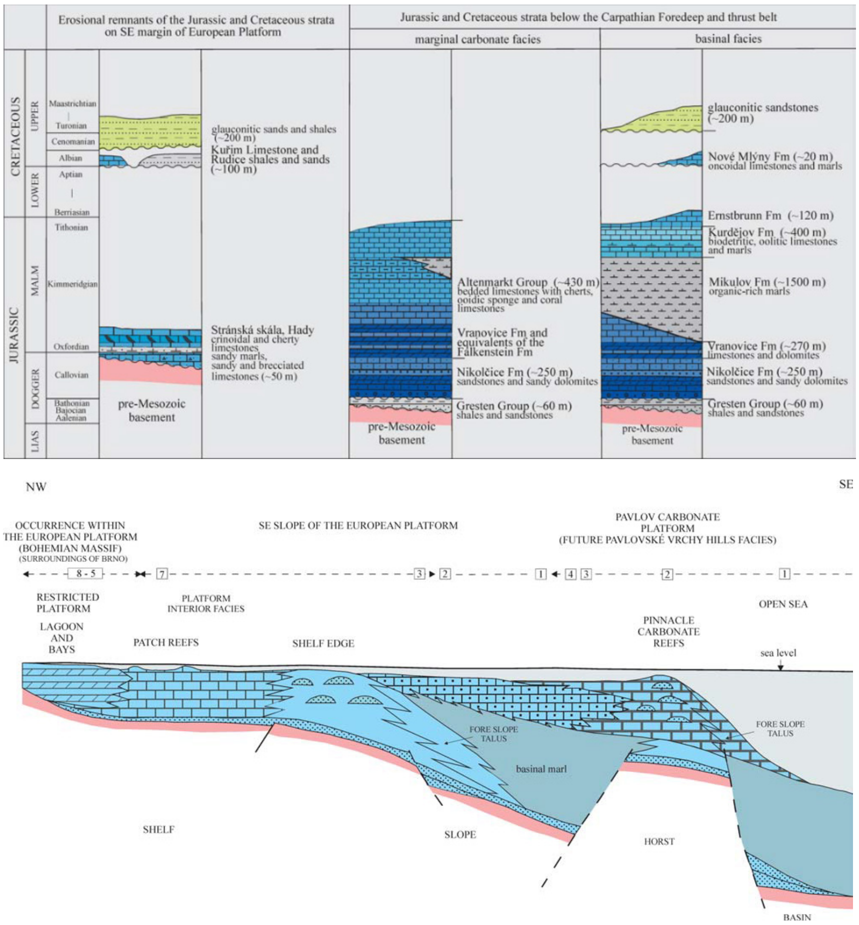

Figure 4.2.3: Lithostratigraphic units of the Mesozoic from NW to SE. Bottom: Model of depositional topography (Adamek 2005)

The overlying succession of the main carbonate reservoir constitutes Lower Miocene sediments of the Alpine-Carpathian Foreland Basin of Egerian, Eggenburgian, Ottnangian & Karpatian age (regional chronostratigraphic stages of the central Parathetys in Europe, corresponding to the international stages of Aquitanian and Burdigalian). Deposits are mostly the erosional products of older rocks from the uplifted Alpine-Carpathian Orogen and, to a small degree, of the Bohemian Massif. Gravels, sands and muds accumulated in various depositional environments, such as deltas, coastline and shelf areas, as well as in deep water marine environments on the continental slope, and in submarine canyons and deeper basinal areas. The typical sedimentary rock of this foreland basin is the "Schlier", a marly, often fine sandy siltstone. The thickness of sedimentary succession in the Foreland atop the Mesozoic units reaches up to 2000 m (Krenmayr et al. 2000).

The tectonic setting of the investigation area is characterised by three types of fault systems:

- NE-SW striking synthetic normal faults
- NE-SW striking antithetic normal faults
- NE-SW striking frontal thrusts of the Alpine-Carpathian Orogen

Upper Jurassic formations are mainly influenced by synthetic, SE-dipping normal faults with up to 700 m of vertical throw, creating depositional throughs for Mesozoic units, resulting in increased thickness close to fault zones. Antithetic, NW-dipping normal faults have only been detected in 2D seismic profiles in Czechia, exhibiting minor offsets of about 100 m. Alpine-Carpathian thrusts sheets do not affect the Upper Jurassic units in the modelling area. However, remnants of Jurassic strata from beneath the Vienna Basin further SE have been detached and transported to the surface within the frontal thrusts sheets of the Alpine-Carpathian Orogen and are now exposed in outcrops within the NE-SE striking Waschberg-Zdánice Zone.

4.2.3 3D geological modelling

The geological 3D model was established using borehole data from deep exploration and production wells from the oil and gas industry, geological cross-sections and 2D seismic profiles. Due to restrictive legal frameworks in Austria, no 2D or 3D Seismic data were available.

The model was established by the Geological Survey of Austria, using the SKUA-GOCAD™ (V.18) software suite by Emerson-Paradigm. The T2.2. Hotlime model uses WGS 1984 UTM Zone 33N.

Input data sets

<u>Borehole data</u>

35 deep wells have been available for modelling in the Pilot Area, which have been drilled by the national oil and gas company OMV of Austria. Wells have been drilled until the 1990's when production ceased, yielding information on the following geological top horizons for modelling:

Upper Jurassic:

- Top Vranovice Formation: 12 wellmarkers
- Top Altenmarkt Formation: 19 wellmarkers
- Top Falkenstein Formation: 5 wellmarkers
- Top Mikulov Formation: 12 wellmarkers
- Top Kurdejov Formation: 17 wellmarkers

Crystalline Basement (Top Paleozoic): 11 markers

<u>Contourmaps, interpreted cross sections, thickness maps</u>

Contourmaps:

- Base Karpatian (Brix & Schultz 1993)
- Base Neogene (Kröll & Wessely 2001)
- Top Upper Jurassic (Brix & Schultz 1993)
- Top Crystalline Basement (Kapounek et al. 1967)

Geological cross-sections

- 2 (Beidinger & Decker 2014)
- 2 (Brix & Götzinger 1964)

- 2 (Brix and Schultz 1993)
- 3 (Roetzel et al. 2009)
- 1 (Kapounek et al. 1965)
- 2 (Kapounek et al. 1967)
- 1 (Kröll & Wessely 2001)
- 6 (Wessely 2006)

Existing 3D models

A 3D framework model covering the Austrian part of the Pilot Area including 8 stratigraphic horizons has been created within the EU-Interreg Project GeoMol (GeoMol Team 2015). Internal Upper Jurassic strata, including the Ernstbrunn, Kurdejov and Mikulov formations were subsequently modelled in the course of the EU Project EUOGA (2016).

Principle modelling workflow

Modelling was performed using SKUA-GOCAD™. Due to limited data density for the modelling region, in some areas modelling had to rely on the general understanding of the regional structural framework. In total, five stratigraphic horizons were modelled, which include (from top to bottom):

- Top Upper Jurassic
- Base Upper Jurassic
- Top Reef Facies (Vranovice, Altenmarkt & Falkenstein formations)
- Top Basin Facies (Mikulov, Kurdejov & Ernstbrunn formations)
- Top Paleozoic (Crystalline Basement of the Bohemian Massif)

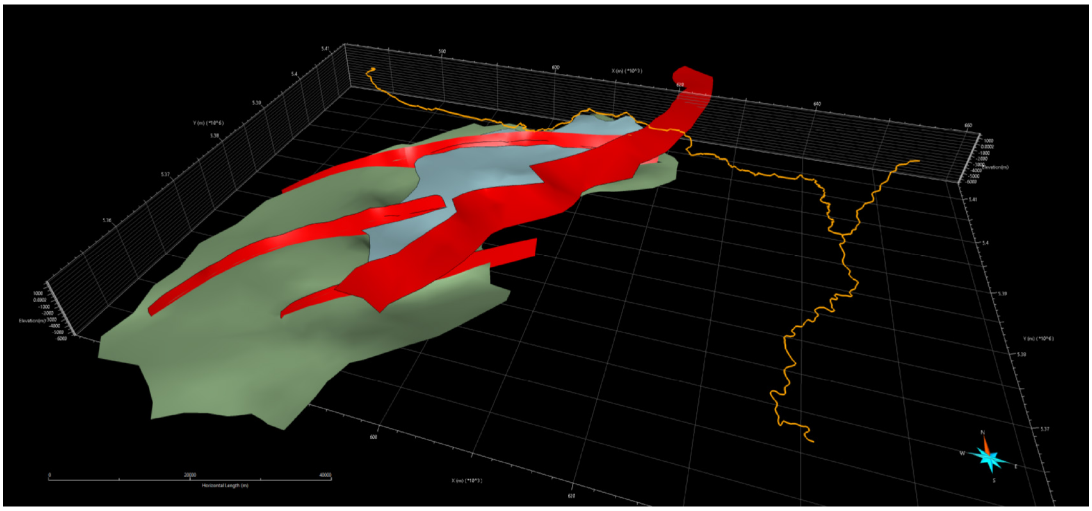

Figure 4.2.4: Overview of the geological 3D model T.2.2. (viewing direction: SE), showing fault planes and horizons Top Paleozoic (light green) and Top Upper Jurassic (light blue), colored according to color codes of the ICS International Chronostratigraphic Chart. (http://www.stratigraphy.org). Orange lines indicate Austrian and Czech borders.

The northwestern border of the modelled Upper Jurassic limestone reflects the pinch out zone between the underlying Paleozoic basement/Middle Jurassic units and the overlying Neogene strata of the Alpine-Carpathian Foreland (Figure 4.2.4). The southeastern border was set parallel to the frontal thrust line of the Alpine-Carpathian Orogen. Jurassic strata extend further towards southeast beneath the Alpine-Carpathian units and the Vienna Basin. However, limited to no well data information on the T.2.2. reservoir is available in this area as Jurassic strata is located in much greater depth. Due to seismic data being unavailable, 3D modelling in Austria was solely carried out in depth domain.

4.2.4 Rock property and Temperature modelling

In the context of HotLime, data required for the accurate determination of geothermal prospectivity of the Pilot Areas have been defined. These data include rock property data, hydrogeological data and thermo-physical parameters to in order to calculate the following reservoir qualities within WP3 (Ressource Assessment):

- The presence of a reservoir
- Permeability of that reservoir (primary or secondary)
- Gross thickness of the reservoir
- Internal and external facies distribution
- Net-to-gross ratio (ratio between the total reservoir thickness and the permeable part of the reservoir)
- Basic characteristics of groundwater flow
- Total dissolved solids (water chemistry)
- Geothermal gradient

In Austria, data for geothermal resource assessment are derived from a the OMV Thermal study in 2012 (GÖTZL et al. 2012), dealing with large-scale assessment of hydrothermal potential in northeastern part of Austria. All data are stored in a Microsoft Access Database, including multiple tables with results of measurements on hydrochemistry, permeability, porosity, rock density etc., which are assigned to the respective depth, geological unit and well.

<u>Hydrogeological parameters</u>
Hydrogeological data of the reservoir are available from chemical analyses of formation waters by the oil and gas industry, including measurements of SO_4, K, Na, Mg, Cl, CO_2, Salinity content and various other parameters.

<u>Thermo-physical parameters</u>
Rock properties from wells penetrating the Upper Jurassic carbonate reservoir, which will be used for further resource assessment include:

- 86 measurements of total Porosity in Upper Jurassic (range: 0,3-14-3%)
- 130 measurement of Effective Porosity in Upper Jurassic (range: 0,1-21,7%)
- 122 measurement of Permeability in Upper Jurassic between (range: 0,1-246 mD)

Thermo-physical parameters for the modelled formations of the Upper Jurassic like thermal conductivity and specific heat capacity were calculated for the following formations in the course of the OMV Thermal project, yielding information on parameters for respective facies (reef and basin) of the limestone reservoir:

Basin facies:
Ernstbrunn Formation: Thermal conductivity: 4,15 [W/(m.K], specific heat capacity: 888 [J/(kg.K)]

Reef facies:
Falkenstein formation: Thermal conductivity: 3,37 [W/(m.K], specific heat capacity: 993 [J/(kg.K)]
Altenmarkt Formation: Thermal conductivity: 3,7 [W/(m.K], specific heat capacity: 919 [J/(kg.K)]

Temperature modelling
Based on data obtained from the available temperature database (20 Temperature measurements for Upper Jurassic from different intervals, Temperature range: 70°-96° C), an average geothermal gradient of ~30° C/km for the investigation area was estimated. In order to calculate the temperature distribution map for the modelled horizon Top Upper Jurassic, the following formula was applied:

$$Tr = T0 + gradT * Z$$

where T0 is the mean annual surface temperature (10°C); gradT is the thermal gradient (30°C/km) and Z is the depth of the target according to the 3D model of Pilot Area T.2.2. (vertical distance between 90 m DEM and Top Upper Jurassic). The result was calculated onto a raster with cell size of 100 m (Figure 4.2.5).

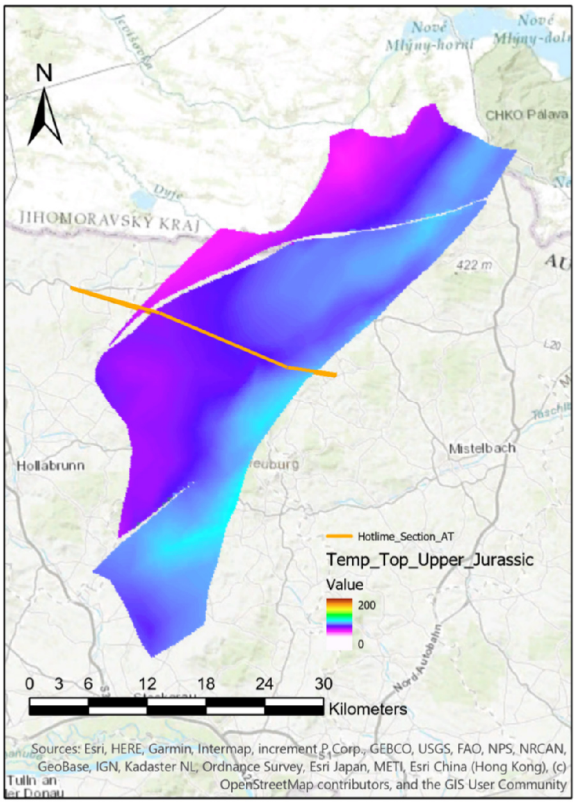

Figure 4.2.5: Temperature distribution map for top surface of the Upper Jurassic reservoir. Temperature values range from ~28°C in the northern area close to the Czech border (footwall) up to ~87°C at the southern end (hangingwall). Location of cross-section shown in Fig. 4.2.6 indicated in orange.

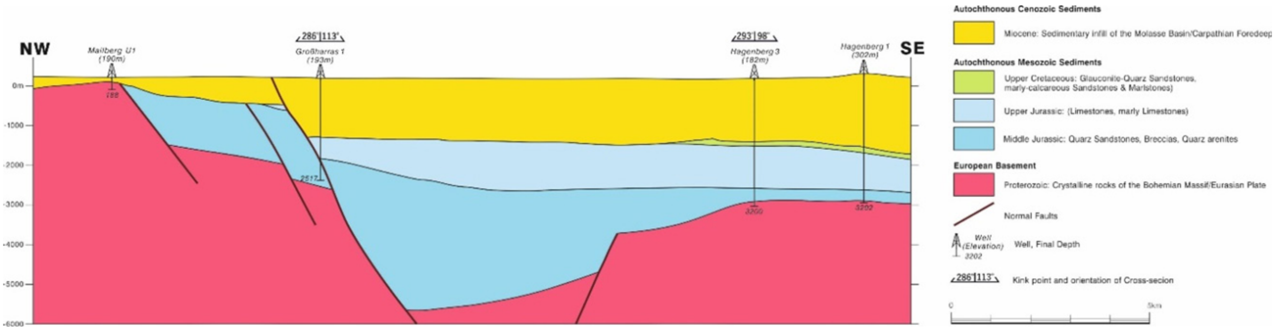

Figure 4.2.6: Cross-section showing modelled Upper Jurassic cross-border limestone reservoir in Austria, colored according to color codes of the ICS International Chronostratigraphic Chart. (http://www.stratigraphy.org).

REFERENCES

ADÁMEK, J. (2005): The Jurassic floor of the Bohemian Massif in Moravia - geology and paleogeography. – Bulletin of Geosciences **80**(4): 291-305. http://www.geology.cz/bulletin/fulltext/291_adamek.pdf

BEIDINGER, A. & DECKER, K. (2014): Quantifying Early Miocene In-Sequence and out-of-Sequence Thrusting at the Alpine-Carpathian Junction. – Tectonics **33**: 222-252. https://doi.org/10.1002/2012TC003250

BRIX, F. & SCHULTZ, O. (1993): Erdöl und Erdgas in Österreich. – Wien (Naturhistorisches Museum) und Horn (Verlag F. Berger).

BRIX, F. & GÖTZINGER, K. (1964): Die Ergebnisse der Aufschlußarbeiten der ÖMV AG in der Molassezone Niederösterreichs in den Jahren 1957-1963. – Erdöl-Erdgas-Zeitschrift **80**.

GEOMOL TEAM (2015): GeoMol – Assessing subsurface potentials of the Alpine Foreland Basins for sustainable planning and use of natural resources. – Project Report, 188 pp. Augsburg (LfU)

GÖTZL, G. et al. (2012): Nutzungsmöglichkeiten tiefer Geothermie im Wiener Becken (Tiefscholle), OMVTHERMAL.

KAPOUNEK, J., KRÖLL, A., PAPP, A. & TURNOVSKY, K. (1965): Die Verbreitung von Oligozän, Unter- und Mittelmiozän in Niederösterreich. – Erdöl-Erdgas-Zeitschrift **81**.

KAPOUNEK, J., KRÖLL, A., PAPP, A. & TURNOVSKY, K. (1967): Der Mesozoische Sedimentanteil des Festlandsockels der Böhmischen Masse. – Jahrbuch der Geologischen Bundesanstalt **110**: 73–91.

KRENMAYR, H.-G., HOFMANN, T. & PESTAL, G. (2000): Rocky Austria - An Illustrated Earth History of Austria. – Wien (GBA)

KRÖLL, A. & WESSELY, G. (2001): Molassezone Niederösterreich und Angrenzende Gebiete 1:200.000: Geologische Karte der Molassebasis.

ROETZEL, R., AHL, A., GÖTZINGER, M.A., KOCIU, A., PRISTACZ, H., SCHUBERT, G., SLAPANSKY, P. & WESSELY, G. (2009): Erläuterungen zu Blatt 23 Hadres. – Geologische Karte der Republik Österreich 1:50.000. Wien (GBA)

WESSELY, G. (2006): Geologie der Österreichischen Bundesländer – Niederösterreich. Wien (GBA).

4.3 Lough Allen Basin and Dublin Basin (IE) – T2.3

Sarah Blake, Brian McConnell, Russell Rogers & Beatriz Mozo (GSI)

This case study comprises two discrete Carboniferous basins in Ireland: the Lough Allen Basin in the northwest of the country, and the Dublin Basin on the central east coast.

4.3.1 Inducement and Objectives

Ireland has complex basement geology, created and modified by several phases of the Caledonian tectonic cycle. The resulting structural template was reactivated during Carboniferous extension to form sedimentary basins and shelves that were variable through time, resulting in complex carbonate stratigraphy. Bounding faults provided fluid pathways for mineralisation and karstification, and subsequently accommodated Variscan compression and brittle fracturing. Thus, the fault pattern defines zones of both karstic and brittle fracture high-permeability pathways for geothermal/hydrothermal fluids in these carbonate basins.

Many details of the carbonate stratigraphy, lateral and vertical facies changes, and fracture patterns within structural compartments are known from mapping and borehole drilling, but there has been very limited application of these data to the search for geothermal energy. In Ireland, there is a general coincidence of Carboniferous carbonate basins with heat demand, and potential locations for geothermal power plants (e.g., sites where old peat-burning power stations need to be replaced with renewable energy technologies).

The Lough Allen Basin has been chosen for this investigation as there is a limited legacy of hydrocarbon data including seismic and borehole data available. The Dublin Basin has been chosen as it is more closely aligned with high population densities and heat demand. These basins in Ireland are not, as yet, known to exceed 3 km in depth, so district heating will be the likely application of geothermal energy.

4.3.2 Study area and geological setting

Lough Allen Basin

The Lough Allen pilot area encompasses parts of counties Cavan, Leitrim, Roscommon and Sligo in the northwest of Ireland. The Carboniferous limestones in this region were deposited in major northeast-southwest trending synclines. The Carboniferous transgression progressed over a landscape of varied relief, and basin-forming faults of Caledonian origin (MACDERMOTT et al. 1996). The stratigraphy in the pilot area spans the Tournaisian to the Serpukhovian stages within the Carboniferous period. The target carbonate reservoir defined and characterized in this study comprises the stratigraphy above the Boyle Sandstone Fm. and below the Mullaghmore Sandstone Fm. (Figure 4.3.2), which consists of the following three formations:

<u>Kilbryan Limestone Formation</u>

Kilbryan Limestone Fm. is sparsely exposed but has been recorded in drillholes. It consists of bioturbated, nodular-bedded, limestones interbedded with calcareous, often fossiliferous shales, and strongly argillaceous limestone. The Courceyan-Chadian boundary occurs within the formation, as evidenced from Miospore assemblages (MACDERMOTT et al. 1996). The facies of this formation varies spatiallty; in the southwest of the study area in the Drumkeeran well the Fm is much thicker and more argillaceous than the typical Kilbryan Limestone elsewhere in Ireland;

Ballyshannon Limestone Formation

Ballyshannon Limestone Fm. is composed of dark grey to bluish grey crinoidal limestones, although near the top of the formation it is formed of pale grainstones (MacDermott et al. 1996). The Oakport Limestone Fm is a lateral equivalent of the Ballyshannon Limestone Fm in the south west of the study area. The Oakport Limestone Fm has a basal member of a clean fine calcarenite which contains occasional coarse crinoidal beds and argillaceous wackestones overlain by fine peloidal calcilutites and laminated calcilutites, and the top member is composed ofa uniform medium to fine calcarenites. Both formations will be treated as a single formation and referred to as the Ballyshannon Limestone Fm for the purposes of this study;

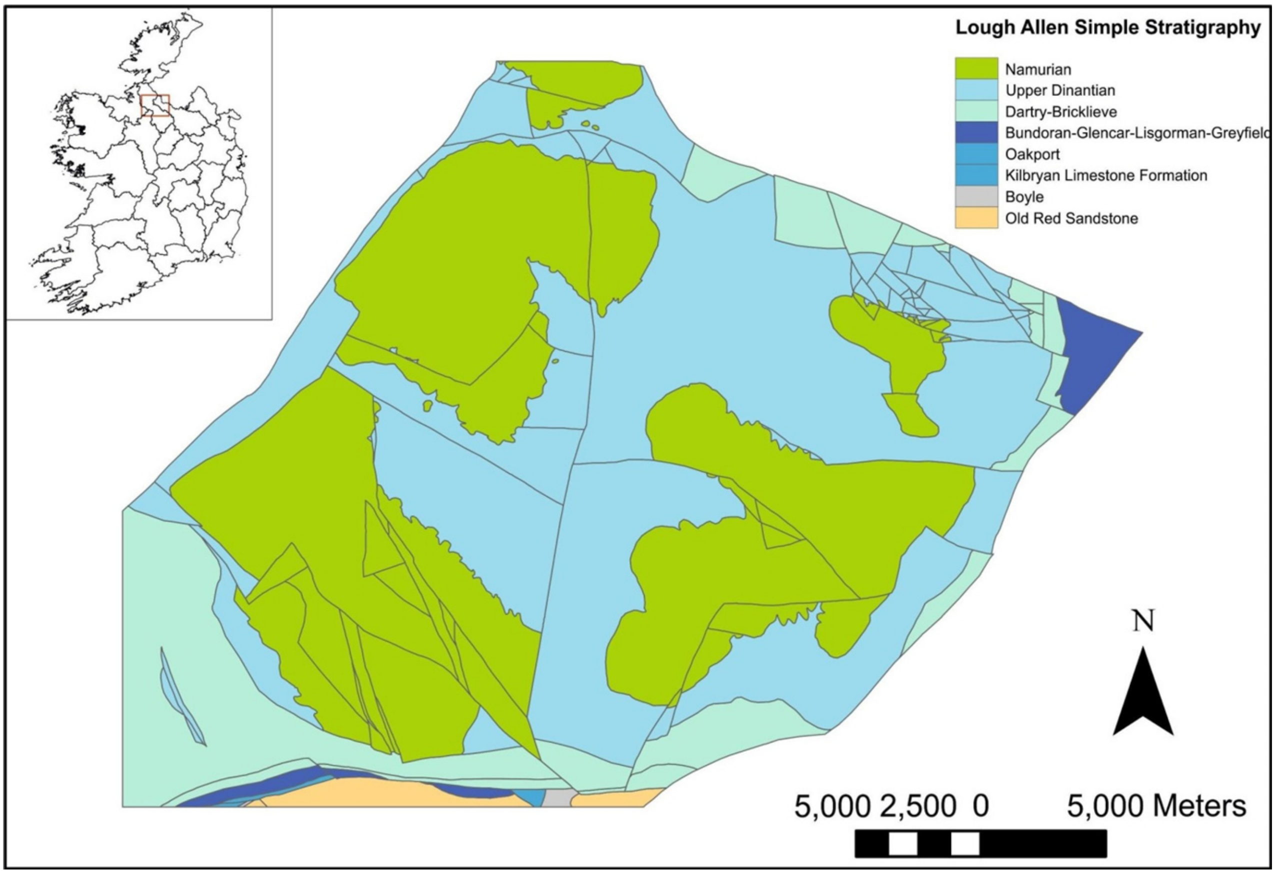

Figure 4.3.1: Geological map of the Lough Allen pilot area with the simplified stratigraphy used for 3D modelling. Inset: Location of the study area

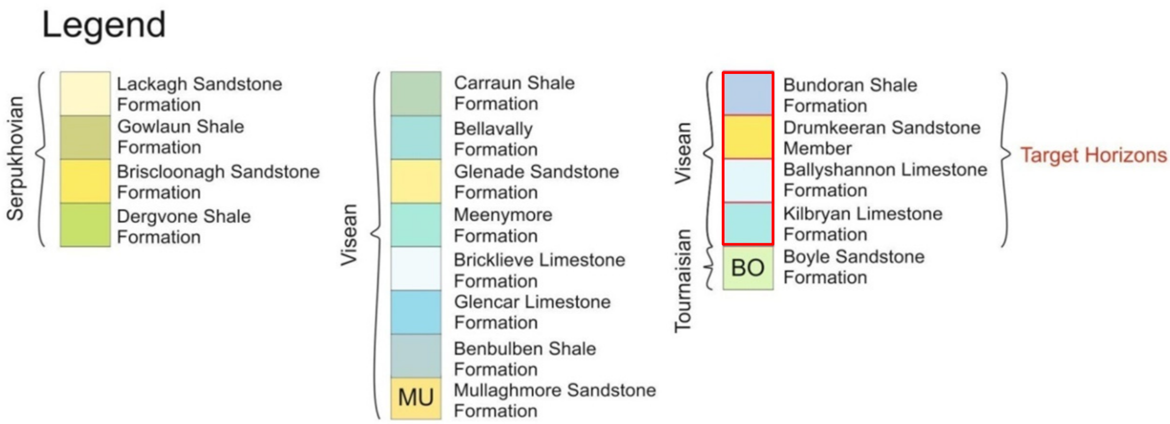

Figure 4.3.2: Detailed stratigraphy of the Lough Allen basin, with target reservoir horizons outlined in red.

<u>Bundoran Shale Formation</u>

Bundoran Shale Fm. in the Lough Allen Basin consists of laminated unfossiliferous calcareous shale and mudstone. This formation is extremely variable in facies, in some places it is dominated by calcareous shale and argillaceous very fine grained limestone. Within the study area the base of this formation is the Drumkeeran Sandstone Member, which comprises pale grey mainly fine, but locally coarse, sandstone.

The stratigraphy above the reservoir horizons extends from the Viséan into the Serpukhovian stages. The Mullaghmore Sandstone Fm. overlies the reservoir horizons and consists of a series of cyclic units of siltstones and shales, which coarsen upwards into medium- to coarse-grained sandstones. Above the Mullaghmore Sandstone Fm. is a thick sequence of limestones with minor sandstones, which extends up into the Namurian sandstone and shale units.

The Lough Allen basin is contained between major faults aligned parallel to northeast-southwest trending Caledonian terrane boundaries. The repetitive reactivation of these basin-forming faults was the subject of a research project by GUO & WALSH (2016), which has significantly informed this project. A new fault model arising from this work (Figure 4.3.3) shows that the Lough Allen basin changes its polarity from north-facing faults in the southwest to south-facing faults in the northeast. The basin-bounding Caledonian faults are observed to displace Paleogene dykes, and must have had some control over the facies distribution within the Carboniferous succession.

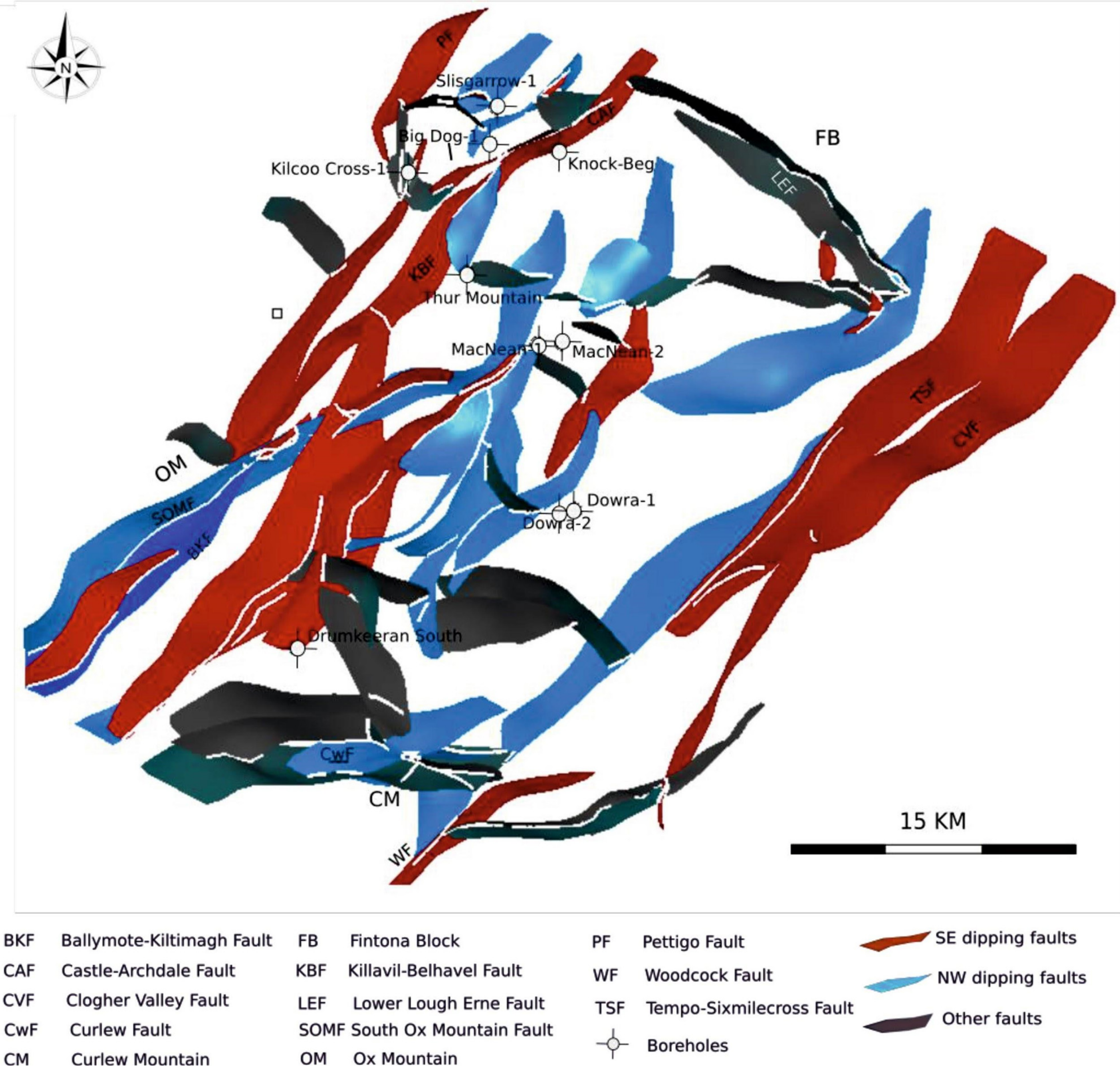

Figure 4.3.3: State-of-the-art fault model of the Lough Allen Basin, from Guo and Walsh (2016). The HotLime study area lies in the southern part of this model.

Lough Allen Basin

The Dublin pilot area comprises the eastern part of the Carboniferous Dublin Basin in the county Dublin on the eastern coast of Ireland. The Dublin basin comprises mostly Carboniferous limestones, and is both a depositional and structural basin. The stratigraphy in the pilot area encompasses the Tournaisian to the lower Viséan stages within the Carboniferous period. Most of the Carboniferous bedrock forms low-lying topography in this area, and is generally covered by a thick blanket of Quaternary sediments and peat.

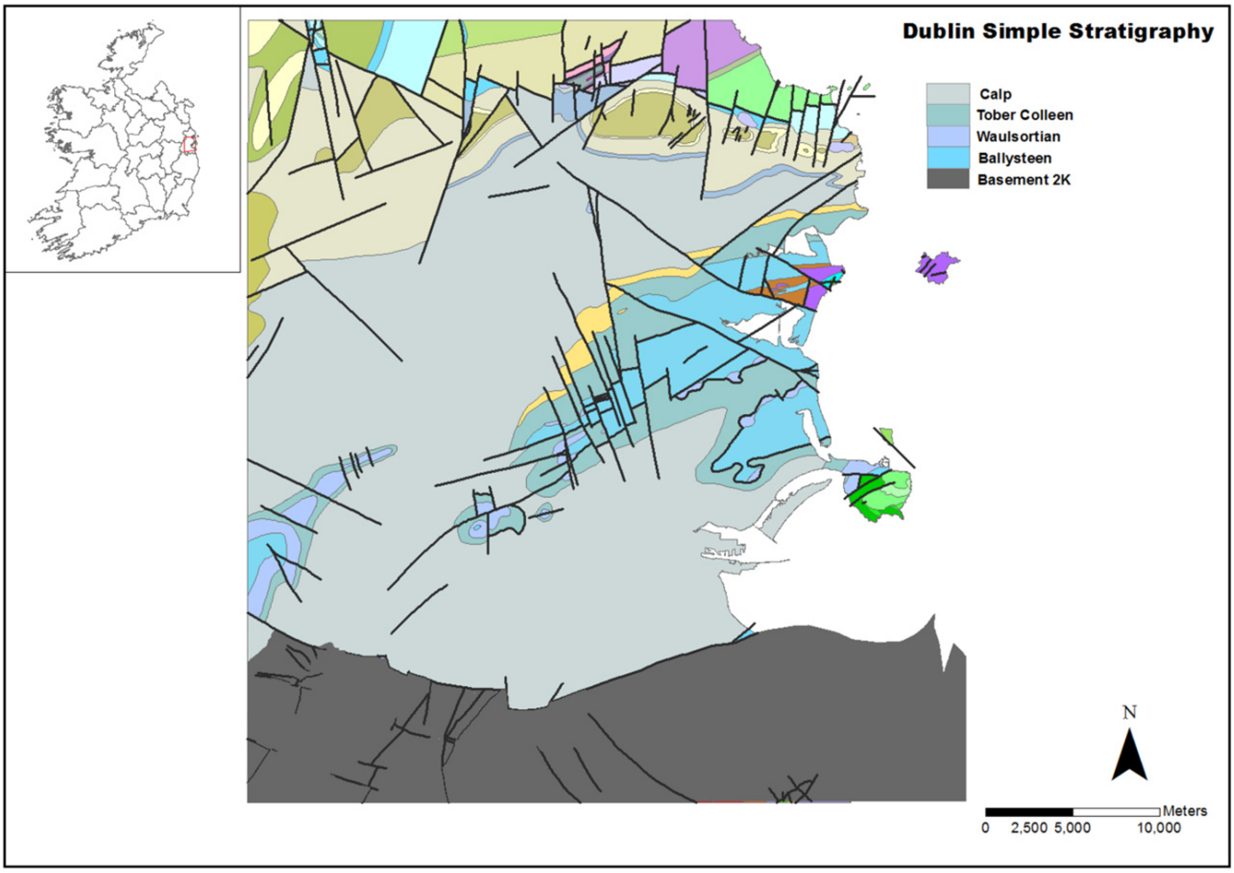

Figure 4.3.4: Location map of the Dublin pilot area with the stratigraphy that will be used for 3D modelling. Inset: location of the study area within Ireland.

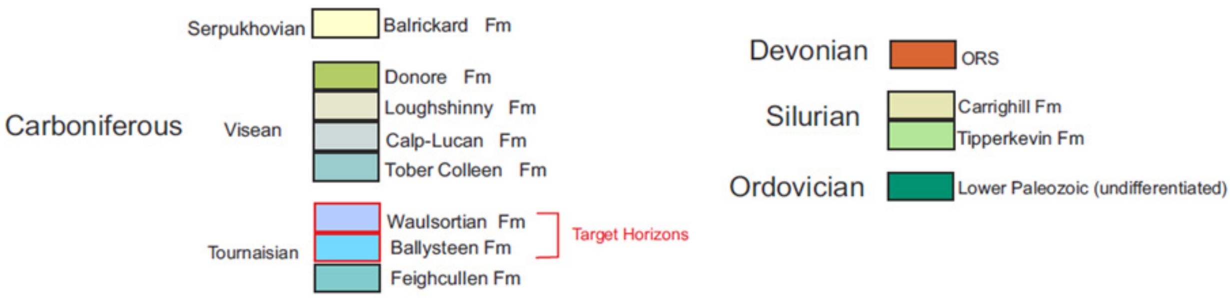

Figure 4.3.5: Detailed stratigraphy of the Dublin basin, as mapped by GSI. The target reservoir horizons for HotLime are outlined in red.

The target carbonate reservoir defined and characterized in this study comprises the stratigraphy above the Feighcullen Limestone Fm. and below the Tober Colleen Limestone Fm. (Figure 4.3.5). Within the target horizons for this part of the Dublin Basin, the Ballysteen Fm. is represented by its equivalents, the Malahide Fm. and the Boston Hill Fm. (Figure 4.3.6).

Ballysteen Limestone Formation

Ballysteen Limestone Fm. has a typical thickness of 100 – 200 m, and is sparsely exposed with only short intersections recorded in boreholes. It consists of well-bedded, relatively clean calcarenitic limestones which pass gradationally up into finer-grained and muddier limestones. Dolomitization is widespread, and oolites have been recognised in some cores (McConnell et at. 1994). The top contact is gradational into the Waulsortian Limestone Fm.

Boston Hill Limestone Formation

Boston Hill Limestone Fm. consists mainly of rather uniform thick successions of nodula and diffusely bedded, argillaceous fossiliferous limestones and subordinate thin shales. It includes major units of very distinctive, laminated fine limestone. The base of the formation is gradational by interbedding with oolites of the Feighcullen Fm. and the top passes up into the Waulsortian Limestone Fm. (where the Waulsortian is absent the boundary is problematical (Philcox 1984)). The formation is commonly divided into a number of informal units from the base. The maximum thickness of the formation is 600 m.

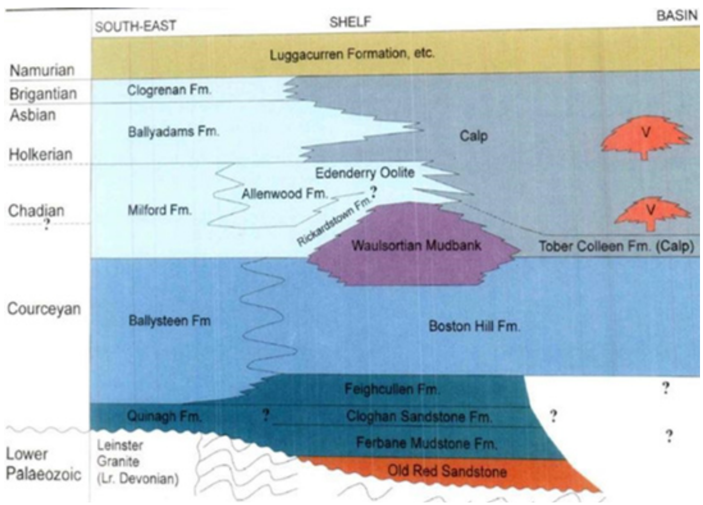

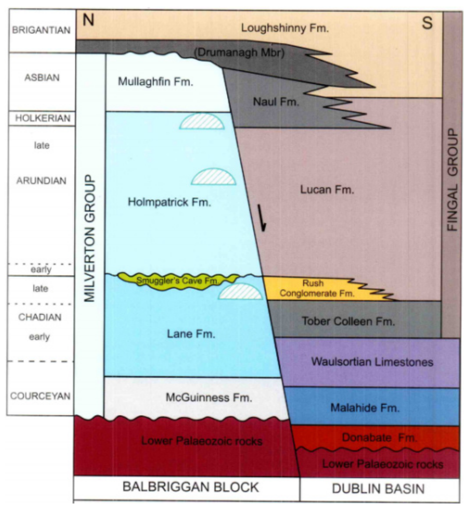

Figure 4.3.6: Stratigraphic correlation diagrams for Carboniferous Fms. in the Dublin Basin.

Malahide Formation

Malahide Fm. comprises calcareous shales, siltstones and sandstones and occasional thin limestones at its base. These are followed upwards by cyclical, peloidal and oncholitic, peritidal, occasionally nodular micrites and thick intraclastic breccia horizons, succeeded by fosiliferous limestones and shale with some oolites and sandtones, biomicrites and biosparites. The top of the formation is made up of argillaceous, less fossiliferous limestones, nodulawackestones and shales (Marchant 1978; Nolan 1986, 1989; Jones et al. 1988). The conformable upper contact with the Waulsortian Fm. is known from borehole sections. Its thickness ranges from 300 – 1,200 m.

Waulsortian Limestone Formation

Waulsortian Limestone Fm. consists mainly of pale grey biomicrite with distinctive stromatactis structures (LESS 1964). The sediments commonly form individual and coalesced mounds (or "reefs") with depositional dips of 30-40° or more and with relief typically of several tens of metres. They pass laterally into thinner time-equivalent sediments, which near the reefs are often clearly reef-related in that they include debris or consist of similar sediments ("reef' margin' and "off-reef' facies); further away there may be no indication in the sediments of reef-equivalence, other than contemporaneous faunas. The Waulsortian reaches a maximum thickness of over 400 m (SOMERVILLE et al. 1992) in the Dublin area. The thickness can change very abruptly on a local scale, even in areas of apparently continuous reef. The Waulsortian Fm. is commonly dolomitized.

The stratigraphy above the reservoir horizons extends into the Viséan stage. These formations comprise thick sequences of limestones, shales and some minor sandstones.

The southern margin of the Dublin basin is structurally well-defined with a roughly east-west orientation, which cuts obliquely across the main northeast-trending structures, although these extend well into the basin (MCCONNELL et al. 1994). The margin is apparently largely fault-controlled, for example along the line of the Rathcoole (or Blackrock-Newcastle) Fault. The northern margin of the basin is well defined by the contact with Lower Palaelozoic rocks. No distinct western boundary is identified, and the eastern boundary lies offshore.

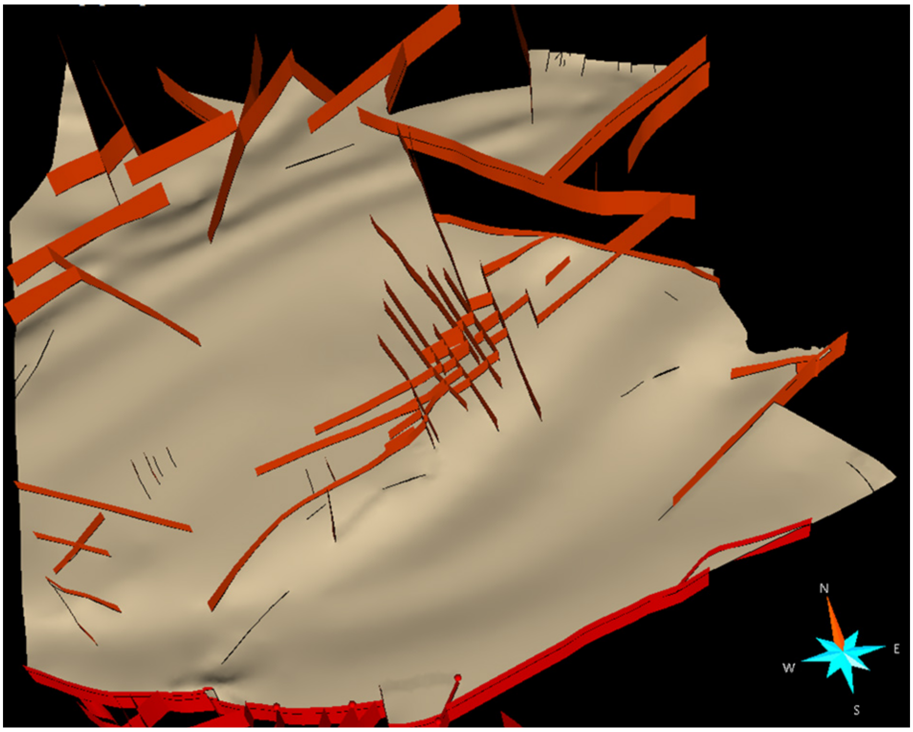

Figure 4.3.7: Latest fault model from GSI's Dublin Basin model.

4.3.3 3D geological modelling

Lough Allen Basin

Input data

The data used to create the geological model of the Lough Allen Basin are:

- GSI 1:50,000 bedrock map and cross-sections;
- Downhole borehole measurements from three deep boreholes within the study area (Dowra 1 (1969 m deep); Drumkeeran South (2,700 m deep); and MacNean 2 (1,629 m deep);
- Twenty-four 2D seismic lines, three of which have deep drillholes adjacent to them;
- Structural model of the wider Lough Allen Basin (iCRAG research group); and
- Velocity model of the wider Lough Allen basin (iCRAG).

The bedrock geology database for the area has recently been updated by the GSI and includes a full compilation of surface structural measurements, outcrop descriptions, palaeontological data and over 140 shorter drillholes with logs. Cross-sections have also been produced using these data.

The structural model produced by the iCRAG research group (GUO & WALSH, 2016) is used as the fault network for this geological model. To incorporate the structural model, the iCRAG velocity model was also used. This velocity model was derived from downhole data in the holes listed above, and additional holes in Northern Ireland that lie outside of the HotLime study area.

Modelling Workflow

For the Lough Allen basin model we have modelled 8 horizons; Base of the Boyle Formation, Base of the Kilbryan Formation, Base of the Bundoran Shale Formation, Base of the Mullaghmore Formation, Base of the Dartry-Bricklieve Unit, Base of the Upper Dinantian Unit, Base of the Namurian Unit and Base of the Overburden. The top three horizons have been modelled using only the geological, drilling and cross-section information as they were not easily distinguished from the seismics. The lower five horizons were modelled using the geological information in the three deep wells (these units are rarely seen in the shorter drillholes) and the seismic profiles.

The first step in the workflow was to interpret the seismic lines in OpendTect. This interpretation process was iterative to determine the number of horizons that could be modelled, with the 5 horizons that were modelled being the easiest to see in the seismic lines. All interpretation at this stage was in the time domain. The picks and lines interpreted in OpendTect were exported as ASCII files (X,Y,Z column files) and opened in SKUA-GOCAD. Using SKUA-GOCAD the existing structural model fault sticks and seismic horizon picks were all converted into the depth domain using the velocity model developed by iCRAG. The model itself was created using the SKUA in-built Structure&Stratigraphy workflow. This workflow constructs fault surfaces and stratigraphic surfaces concurrently and ensures that the stratigraphy is cut consistently by the structure. The workflow also ensures that all surfaces are faithful to the drillhole data.

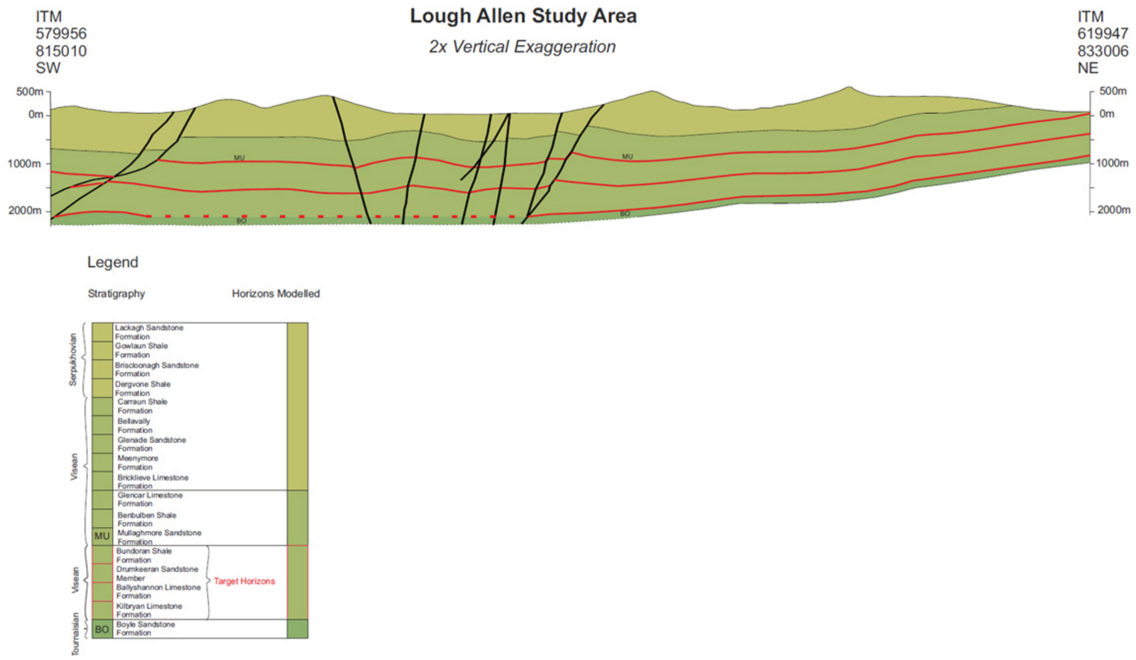

Figure 4.3.8: Lough Allen Basin cross section showing main faults and target horizons (outlined in red). The colours in the stratigraphic column are compatible with the HotLime project vocabulary.

Dublin Basin

<u>Input data</u>

The data used to create the geological model of the Dublin Basin are:

- Dublin 1:50,000 bedrock map;
- Dublin Boreholes from the National Geotechnical Borehole Database and from the Bedrock database; and
- Cross sections from the bedrock map.

Only those boreholes that were deep enough and cut more than one formation were used for the modelling.

<u>Modelling Workflow</u>

For the initial Dublin Basin model we have modelled all formations from the Cambrian to the Namurian stage of the Carboniferous. All horizons were modelled using the geological, drilling and cross-section information available to GSI. The first step in the workflow was to check all the boreholes available and to see which ones were good enough to be used. After checking the boreholes, all the data was edited, cleaned and loaded in the software SKUA-GOCAD. The model was created manually and no *Structure & Stratigraphy* workflow from SKUA was used. This is because the workflow wasn't efficient for the level of detail involved in this early version of the Dublin Basin model.

The manual model could not be used for modelling temperature due to file type restrictions in SKUA, so a simplified model was done using the *Structure & Stratigraphy* workflow from SKUA and the same data used in the creation of the previous model. Data from two new deep boreholes were made available to us from Newcastle in Co. Dublin (NGE1 and NGE2) during the project. Drill core is not available from these holes, so we must rely on the borehole log descriptions provided. Every effort was made to fit these descriptions into the stratigraphy of the model, but uncertainty remains. NGE 1 has temperature values that will be used in future HotLime activities.

This workflow constructs fault surfaces and stratigraphic surfaces concurrently and ensures that the stratigraphy is cut consistently by the structure. The workflow also ensures that all surfaces are faithful to the drillhole data. In this second iteration of the model, far fewer formations and faults were modelled. The formations modelled were:

- Ballysteen Limestone Fm.;
- Waulsortian Limestone Fm.;
- Tober Colleen Limestone Fm.; and
- Calp Limestone Fm.

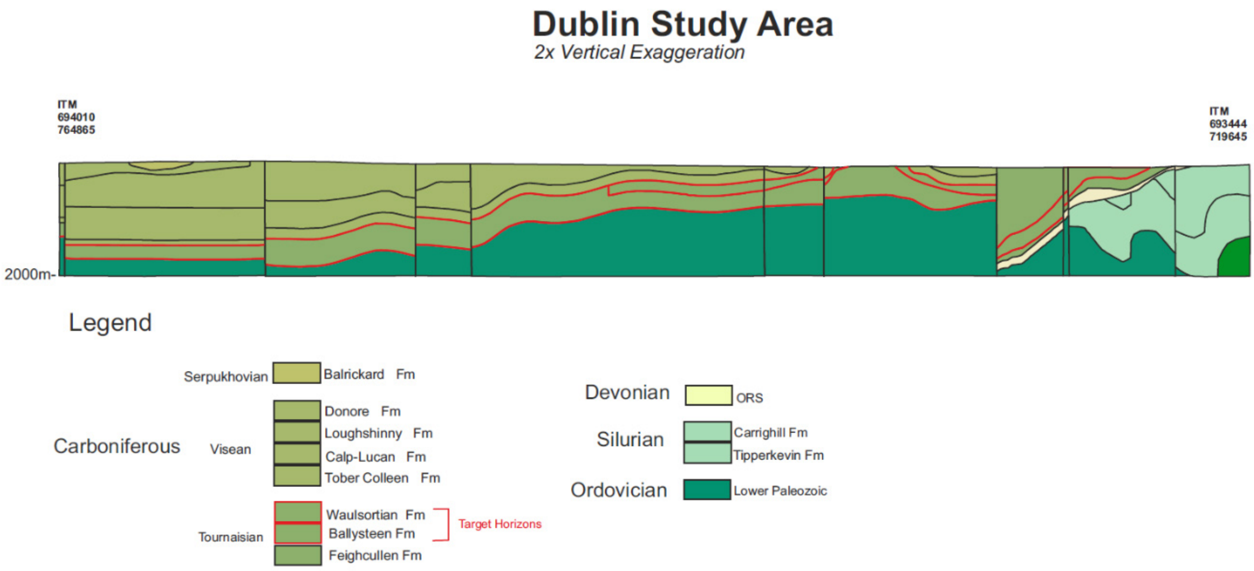

Figure 4.3.9: Dublin Basin cross section showing main (vertical) faults and target horizons (in red). The colours in the stratigraphic column are compatible with the HotLime project vocabulary.

4.3.4 Rock property and Temperature modelling

<u>Thermo-physical and hydrogeological data</u>

There is a severe lack of historical deep geological information available in the two pilot areas, and there are no deep geothermal operations or explorations in Ireland at present. Unfortunately, no new deep hydrogeological, hydrochemical, or thermo-physical data has been made available during our investigations and data collections in Lough Allen.

A small amount of thermo-physical data has been made available from two privately drilled boreholes in Newcastle, Co. Dublin, on the southern margins of the Dublin Basin, including temperature measurements with depth (to a maximum depth of 1.4 km), borehole geophysical logs and lithological descriptions. No groundwater chemistry information and no hydraulic measurements were included in the data package.

A 3D temperature model of the Irish crust has recently been published (MATHER & FULLEA 2019) and we anticipate that the results of this model will become available to us in early 2020 for incorporation into HotLime WP3 activities.

Temperature Modelling

There is a severe lack of robust subsurface temperature data for the Irish HotLime pilot areas. Therefore, temperature at the top of the target reservoirs for both the Lough Allen and Dublin Basins has been modelled simply using the depth determined in the 3D models and a geothermal gradient of 25 °Ckm^{-1} based upon an estimated average geothermal gradient for Ireland (GOODMAN et al. 2004). The surface temperature used in this model is 10 °C (based upon an average groundwater temperature for Ireland of 9.5 – 10.5 °C (ALDWELL & BURDON 1980)). We anticipate that further temperature data for our study areas will become available in the near future due to ongoing data collection and collation efforts by GSI. These data can be incorporated into this model at a future stage to improve temperature and heat estimations.

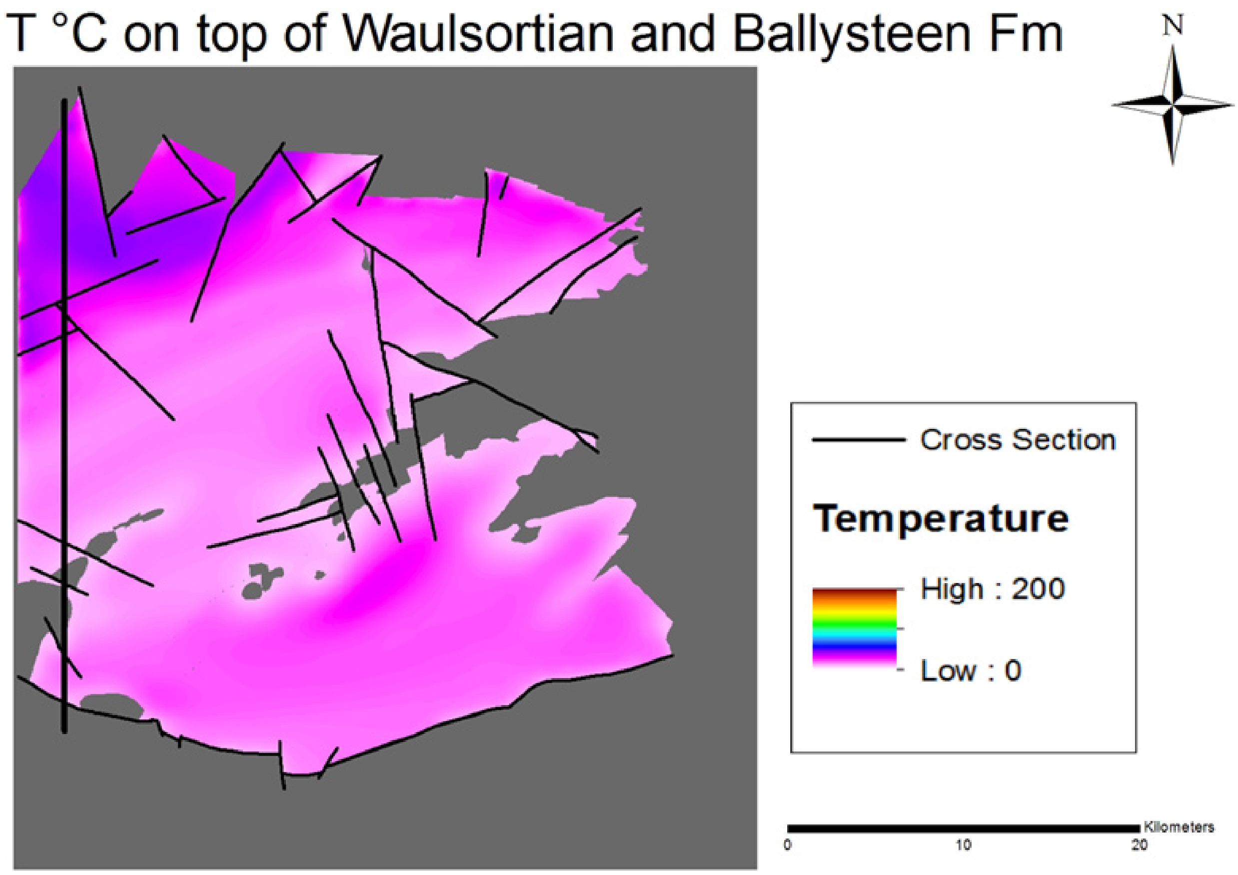

Figure 4.3.10: Temperature map of the top of target reservoir for the Dublin Basin (Waulsortian and Ballysteen Fms.). Cross-section indicated relates to Figure 4.3.9 above.

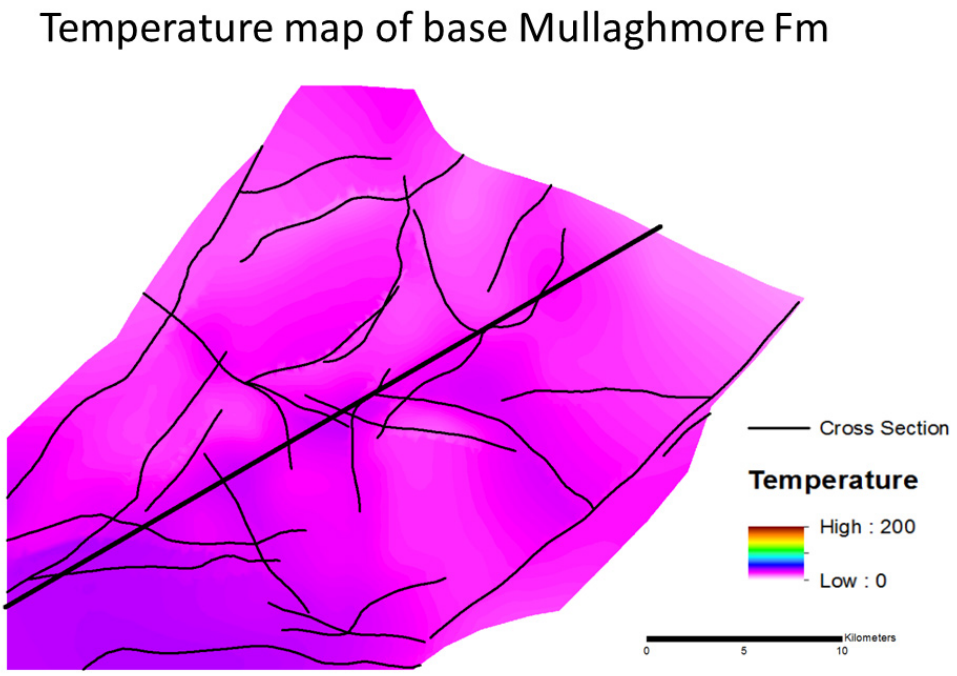

Figure 4.3.11: Temperature map of the top of target reservoir for the Lough Allen Basin (base of Mullaghmore Fm.). Cross-section indicated relates to Figure 4.3.8 above.

REFERENCES

ALDWELL, C.R. & BURDON, D.J. (1980): Hydrogeothermal Conditions in Ireland. – XXVI. International Geological Congress, Paris; Fossil Fuels Sec. 14.2; 14.0068:21.

GOODMAN, R., JONES, G., KELLY, J., SLOWEY, E. & O'NEILL, N. (2004): Geothermal Energy Resource Map of Ireland - Final Report. – Sustainable Energy Ireland (SEI), Dublin. https://www.yumpu.com/en/document/read/26170234/geothermal-energy-resource-map-of-ireland-final-iretherm

GUO, J. & WALSH, J. (2016): Structural Model of the Lough Allen Basin: highlighting the longevity of the faults and associated deformation. – iCrag (Irish centre for research in applied geosciences).

JONES, G.LL., SOMERVILE, I.D. & STROGEN, P. (1988): The Lower Carboniferous (Dinantian) of the Swords area: sedimentation and tectonics in the Dublin Basin, Ireland. – Geological Journal **23**: 221-248.

LEES, A. (1964): The structure and origin of the Waulsortian "reefs" (Lower Carboniferous) of west-central Ireland. – Phil. Trans. R. Soc. **B247**: 483-521.

MACDERMOTT, C.V., LONG, C.B. & HEARNEY, S.J. (1996): Geology of Sligo-Leitrim. A geological description of Sligo, Leitrim, and adjoining parts of Cavan, Fermanagh, Mayo and Roscommon to accompany the bedrock geology 1:100,000 scale map series sheet **7**, Sligo-Leitrim. With contributions by CLARINGBOLD, K., STANLEY, G. (Mineral Resources), DALY, D. (Groundwater Resources) and R. MEEHAN, R. (Quaternary Geology). – Geological Survey of Ireland.

MARCHANT, T.R. (1978): The stratigraphy and micropalaeontology of the Lower Carboniferous (Courceyan-Arundian) of the Dublin Basin, Ireland. – Unpublished Ph.D. Thesis, University of Dublin.

MATHER, B. & FULLEA, J. (2019): Constraining the geotherm beneath the British Isles from Bayesian inversion of Curie depth: integrated modelling of magnetic, geothermal, and seismic data. Solid Earth **10**: 839-850.

McConnell, B. & Philcox, M. (1994): Geology of Kildare. A geological description to accompany the bedrock geology 1:100,000 scale maps series sheet **16**, Kildare- Wicklow. With contributions by Sleeman, A.G., Stanley, G., Flegg, A.M., Daly, E.P. & Warren, W.P. – Geological Survey of Ireland.

McConnell, B., Philcox, M. & Geraghty, M. (2001): Geology of Meath. A geological description to accompany the bedrock geology 1:100,000 scale maps series sheet **13**, Meath. With contributions by Morris, J., Cox, W. (Minerals), Wright, G. (Groundwater) and Meehan, R. (Quaternary). – Geological Survey of Ireland.

Nolan, S.C. (1986): The Carboniferous geology of the Dublin area. – Unpublished Ph.D. Thesis, University of Dublin.

Nolan, S.C. (1989): The style and timing of Dinantian syn-sedirnentary tectonics in the eastern part of the Dublin Basin, Ireland. – In: Arthurton, R.S., Gutteridge, P. & Nolan, S.C. (eds.): The role of tectonics in Devonian and Carbonferous sedimentation in the British Isles. – Yorks. geol. Soc. Occasional Publ. **6**: 83-97

Philcox, M.E. (1984): Lower Carboniferous Lithostratigraphy of the Irish Midlands. – Jr. Assoc. Econ. Geol., 89pp

Somerville, I.D., Strogen, P. & Jones, G.Ll. (1992): Mid-Dinantian Waulsortian buildups in the Dublin Basin, Ireland. – Sedimentary Geology.

4.4 Flanks of London-Brabant Massif (NL/BE) – T2.4

Johan ten Veen & Hans Veldkamp (TNO) and Ben Laenen (VITO)

4.4.1 Inducement and Objectives

Early Carboniferous (Dinantian) platform carbonates are located along the northern flank of the London–Brabant Massif (from the UK to the Netherlands, Belgium, Germany and France). In few parts of the Netherlands the Dinantian rock formations are explored for hydrocarbons. However, as petroleum systems were never proven, the Dinantian was left relatively under-explored. Studies of Dinantian carbonates in Belgium, apart from academic interest, were mainly focused on feasibility for (gas) storage. Only limited well control exists and most of the wells are clustered around the margins of the Carboniferous basin (KOMBRINK 2008; VAN HULTEN & POTY 2008). Additionally, seismic coverage is poor because most seismic data were acquired and processed with a focus on the younger, shallower formations that are known to host significant amounts of hydrocarbon accumulations (VAN HULTEN & POTY 2008). At present these carbonates crop out at several places in France, Belgium and Germany and generally dip to the north where they are present in the subsurface down to depths of 5 km or more. Various projects within the study area focus on exploration for geothermal potential at the variables depths the carbonates reside. Valuable information to constrain future assessments include the geothermal well Merksplas–Beerse (BE), the recent Californië doublets (CWG and CLG) and the Balmatt / Mol doublet. Apart from these developments where viability of hydrothermal heat and power generation is thought to be related to enhanced aquifer performance related to secondary processes such as karstification, fautling or both, most carbonates in the area have received relatively little attention and are perceived as 'tight'.

In that respect, this study area is exemplary because it has sub-domains with different geological situations (karstification, fault- and fracture densities), data situation, and cross-domain issues (e.g. impact on groundwater, fault characterization, seismicity). Maps and models developed in past BE-NL cross-border initiatives like GEOHEAT, combined with outcrop analogues from the Namur-Dinant Basin in southern Belgium will be used to assess the geothermal potential. Combining the core material and geophysical well logs of all wells that transected the Dinantian carbonates with information from these outcrop analogues, reservoir properties will be assessed in 2 or 3 dimensions at an inter-well scale. Especially the relations between lithological units and fracture intensity (mechanical stratigraphy), and the characterization of an analogue fault damage zone, contribute to the understanding of the complex carbonate system as a geothermal reservoir.

4.4.2 Study area and geological setting

The study area in Belgium and the Netherlands only includes subsurface carbonates and is broadly defined by the sub-crop boundary in the south and southern boundary faults of the Roer-Valley Graben (Figure 4.4.1). Within this area, the distribution of the Dinantian interval was studies by using seismic- and well data. Towards this graben, the Base Dinantian horizon could not be interpreted due to its large depth (i.e. not recorded in seismic data) and structural complexity.

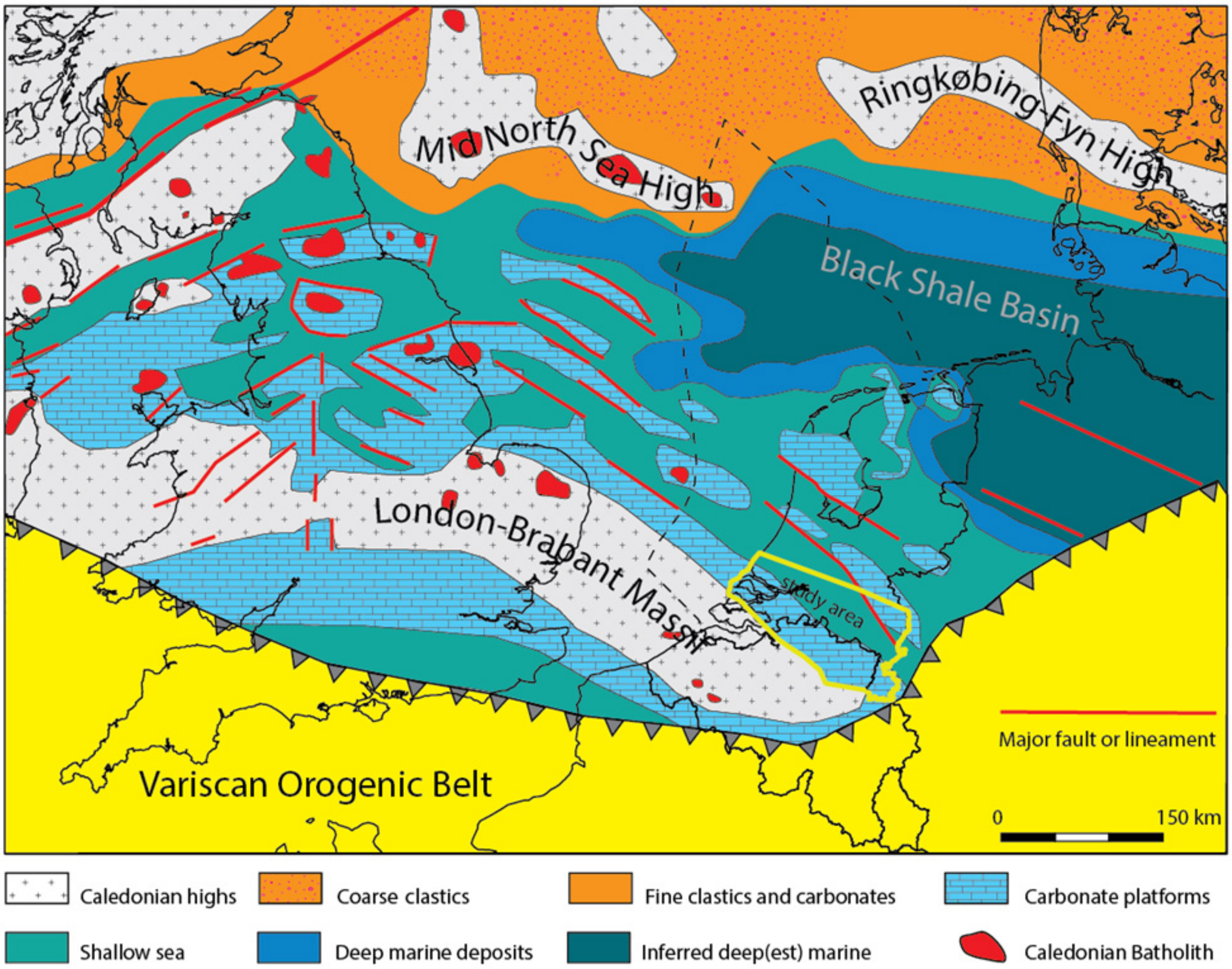

Figure 4.4.1: European map of Dinantian palaeogeography. Study area marked by yellow box. Modified after VAN HULTEN *(2012) and* REIJMER *et al (2017). Northwest European Carboniferous Basin (NWECB) roughly indicated with blue-green colours.*

Regional geological setting

The Northwest European Carboniferous Basin (NWECB; Figure 4.4.1) developed in the Devonian and Carboniferous in response to lithospheric stretching and Late Carboniferous flexural subsidence (KOMBRINK et al. 2008) in between the southern margin of the Old Red Continent to the north and the Variscan orogeny to the south, which more or less agrees with the southern margin of the Rhenohercynian Zone (ZIEGLER 1990a,b; ONCKEN et al. 1999; BURGESS & GAYER 2000; NARKIEWICZ 2007). The basin consisted of a series of WNW-trending half-grabens in the southern North Sea, in which a thick pile of Devonian and Lower Carboniferous sediments were deposited sourced from the Mid German Crystalline High in the south and the Old Red Continent in the north (Figure 4.4.3). According to FRASER & GAWTHORPE (1990), N-S extension led to the formation of the E-W trending British Graben, whereas the NW-trending structures were reactivated. The origin of the extension is either related to back-arc extension in the Rheno-hercynian Basin situated to the southeast of the Netherlands (e.g. ZIEGLER 1990b) or escape tectonics (ARETZ 1993).

The resulting horst-and-graben tectonic style steered the occurrence of isolated carbonate build-ups on intra-basinal highs. In the UK, these highs agree with the distribution of post-Caledonian granite batholiths (Figure 4.4.1), while the extension was accommodated along Caledonian structural weakness zones. This extensional style extends into the UK and Dutch offshore area (BLESS et al. 1983; VAN HULTEN & POTY 2008; KOMBRINK 2008).

Throughout the Dinantian period the London-Brabant Massif played a vital role as a relatively stable high at the southern border of the Carboniferous Basin (Figure 4.4.1; KOMBRINK et al. 2010). Due to tectonic activity, the high underwent uplift, fracturing, emersion, and karstification at several moments during the Dinantian. This resulted in a configuration with carbonate build-ups developing on the footwall block, while hanging wall blocks were filled by deeper water slope deposits (Figure 4.4.2; FRASER & GAWTHORPE 1990; BRIDGES et al. 1995; TOTAL 2007). These downthrown blocks adjacent to carbonate dominated highs were often intervening low areas, where more basinal fine-grained siliciclastic sediments, such as the Bowland Shale, were deposited.

Geological framework of the main carbonate reservoir

The carbonate deposits of the Early Carboniferous are not dominated by framework-builders, since this type of carbonate producing organism became extinct during the late Devonian 'Kellwasser' event (BUGGISCH 1991; ARETZ & CHEVALIER 2007). The main types of carbonate build-ups are microbial mud-mounds (BRIDGES et al. 1995), the product of a M-Factory type of carbonate deposition (SCHLAGER 2005). The depositional environment changed during the Dinantian in response to the main tectonic basin-forming phases and variations in sea level, which is reflected by the different types of carbonate mud-mounds that developed through time (BRIDGES et al. 1995).

The first basin-forming period documented in the UK is the Tournaisian (Late Devonian to Late Courceyan stage; Table 4.4.1), during which fluvial-deltaic deposits were derived from the basin margins. Initial carbonate deposition started in the Tournaisian to Tournaisian-Visean (Chadian stage; Table 4.4.1) and was characterized by alternations of fluvial, marginal marine and near shore siliciclastics with carbonates. The deeper basin was characterized by a carbonate ramp where Waulsortian mounds could develop (BRIDGES et al. 1995; TOTAL 2007). During the Early Visean (Late Chadian to Late Holkerian stages; Table 4.4.1) the carbonate depositional environment evolved from a carbonate ramp that developed on the exposed basement blocks to a progradational rimmed carbonate shelf (ARETZ & CHEVALIER 2007; KOMBRINK 2008). During the later Dinantian (Late Asbian to Early Brigantian stages; Table 4.4.1) the distinction between the carbonate shelf and basin areas became more pronounced. The rimmed carbonate platforms that developed on the shelf areas formed a clear topographic contrast with the basins (MUCHEZ et al. 1990). In these basins deep marine conditions prevailed with deposition of calciturbidites and siliciclastic mudstones (TOTAL 2007). Near the edges of the carbonate platforms, which became steeper during the Visean, coarse breccia's and boulder beds were deposited. In many locations the Brigantian deposits are missing and the related unconformity is widespread and associated with karst features (GALLAGHER & SOMMERVILLE 2003; TOTAL 2007). Platforms on intra-basinal highs drowned, halting carbonate deposition before the end of the Visean (WATERS et al. 2009; VAN HULTEN 2012; HOORNVELD 2013). The carbonate deposits of the Early Carboniferous are not dominated by framework-builders, since this type of carbonate producing organism became extinct during the late Devonian 'Kellwasser' event (BUGGISCH 1991; ARETZ & CHEVALIER 2007). The main types of carbonate build-ups are microbial mud-mounds (BRIDGES et al. 1995), the product of a M-Factory type of carbonate deposition (SCHLAGER 2005). The depositional environment changed during the Dinantian in response to the main tectonic basin-forming phases and variations in sea level, which is reflected by the different types of carbonate mud-mounds that developed through time (BRIDGES et al. 1995).

The first basin-forming period documented in the UK is the Tournaisian (Late Devonian to Late Courceyan stage; Table 4.4.1), during which fluvial-deltaic deposits were derived from the basin margins. Initial carbonate deposition started in the Tournaisian to Tournaisian-Visean (Chadian stage; Table 4.4.1) and was characterized by alternations of fluvial, marginal marine and near shore siliciclastics with carbonates. The deeper basin was characterized by a carbonate ramp where Waulsortian mounds could develop (BRIDGES et al. 1995; TOTAL 2007). During the Early Visean (Late Chadian to Late Holkerian stages; Table 4.4.1) the carbonate depositional environment evolved from a carbonate ramp that developed on the exposed basement blocks to a progradational rimmed carbonate shelf (ARETZ & CHEVALIER 2007; KOMBRINK 2008). During the later Dinantian (Late Asbian to Early Brigantian stages; Table 4.4.1) the distinction between the carbonate shelf and basin areas became more pronounced. The rimmed carbonate platforms that developed on the shelf areas formed a clear topographic contrast with the basins (MUCHEZ et al., 1990). In these basins deep marine conditions prevailed with deposition of calciturbidites and siliciclastic mudstones (TOTAL 2007). Near the edges of the carbonate platforms, which became steeper during the Visean, coarse breccia's and boulder beds were deposited. In many locations the Brigantian deposits are missing and the related unconformity is widespread and associated with karst features (GALLAGHER & SOMMERVILLE 2003; TOTAL 2007). Platforms on intra-basinal highs drowned, halting carbonate deposition before the end of the Visean (WATERS et al. 2009; VAN HULTEN 2012; HOORNVELD 2013).

For the Netherlands, this three-stage model was confirmed for the development of the Dinantian carbonates on the northern flank of the London-Brabant Massif (REIMER et al. 2017). Here, a Tournasian low-gradient carbonate ramp system is succeeded by a succession in which the carbonate ramp system evolved to a rimmed shelf setting. Subsidence of the northern margin of the London-Brabant Massif resulted in a landward shift of the shallow-marine facies belts, while the formation of normal faults resulted in a "staircase" shaped shallow-water platform–slope–basin profile, associated with large-scale resedimentation processes. In conjunction, the slope angles steepened and at the deeper parts of the slope and within the basin characteristic 'Kulm' shales (KOMBRINK 2008; ARETZ 2016) were deposited.After deposition, the limestone deposits were frequently exhumed and reburied. A first period of regional exhumation occurred at the end of the Dinantian, which seems to be associated with porosity enhancing meteoric karstification; possibly limited to the paleo-shelf edge. The most intense alterations seem to be present as a deep leached horizon below the Cretaceous unconformity at the top of the Dinantian sequences. In addition, clear evidence for hydrothermal fluid migration is found locally, enhancing reservoir properties at some places while occluding porosity at others. The timing of these phases of hydrothermal fluid circulation is poorly understood.

Generally, the Dinantian carbonates can be described as a slap of basinward (northward) thickening carbonates that has a thickness of 200-300 m in the south close to the exposure line and >500 m m in the north. This thickness trend is associated with the depositional geometry. To the northern limit of the study area the platform carbonates are transitional to time equivalent basinal deposits with thicknesses generally less than 100 m. Superposed on this general trend are higher-order thickness and depth variations that are determined by the local fault block geometries.

The Dinantian progressively onlap north-dipping basement rocks, which is interpreted as an episodic landward migration of marine deposits (coastal onlap) during a transgressive. In some locations the onlap seems to be defined by faults. Thickness anomalies in the Dinantian infill representing sub-basins that reside in the basement suggest the presence of a paleorelief made up by small extensional (half-graben) basins that are related to long-lived faults that have been active since at least the Devonian (MUCHEZ et al. 1987). Basinwards of the platforms, the internal structure of the Dinantian shows a downlapping geometry. The faults and sub-basins cause remarkable thickness differences in the Dinantian carbonates as shown in the thickness map of the Dinantian carbonate sequence. Thicknesses vary from 30 m near the London-Brabant Massif to over 700 m in the NW part of the study area. The carbonates pinch out towards the paleo-coastline in the southwest, which progressively onlapped the paleo-high of the London-Brabant Massif. Since carbonate deposition is restricted by sea level, more carbonates could accumulate in the deeper parts of the basin. Initial thickness differences were enhanced by subsequent uplift of the Massif, which led to erosion of the carbonate deposits.

In contrast to a general thickness increase to the north, the Dinantian sequence near the Halen well, towards the southern boundary of the Campine Basin, also showed a thick package in a half-graben structure (MUCHEZ et al. 1987). These authors also divided the Campine Basin in an eastern and western part based on well observations. The Booischot, Kessel, Poederlee, Merksplas-Beerse and Heibaart wells are located in the western part. Halen is located in the eastern Campine Basin, where the Lower Dinantian deposits attain a notable thickness (MUCHEZ et al. 1987). Seismic lines near Halen show a tilted base Dinantian while the top is near horizontal, suggesting active faulting during the early phase of carbonate deposition. Confirming tectonic basin formation since at least the Early Dinantian.

Overlying succession

In its deeper realm, the uppermost Dinantian (Visean) sequence is covered by Namurian (early Late Carboniferous) shales . The Visean-Namurian transition is characterized by a change from carbonate to clastic deposition, and in some locations a sedimentary hiatus is known to be present (HARINGS 2014). Along the margins of the London Brabant Massif, the Upper Carboniferous clastic sequence can reach a thickness up to 4 kilometres and generally showd an onlapping relationship with the carbonates In the basinal areas the Dinantian carbonates seem more or less conformably overlain by early Namurian sediments, but on topographically higher areas a sedimentary hiatus occurs that can reach into the Westphalian (RGD 1991). Thus, despite this locally comprehensive hiatus, seismic data of these basinal areas do not present obvious indications for a regionally important erosional surface. However, well data suggest Late Carboniferous erosional periods occurring along the fringes of the London-Brabant Massif. The most important surface identified in seismic data is the erosional truncation of Carboniferous strata below Cretaceous Chalk deposits (Figure 4.4.2). This erosional surface can be traced along the entire northern margin of the London-Brabant Massif, and is easily recognized as an angular unconformity below the Cretaceous and younger strata, which have a very characteristic seismic signal (VAN DER MOLEN 2004). The Base Cretaceous unconformity is widely known as a regional hiatus; in the study area Upper Cretaceous chalk deposits generally overlie Pre-Permian strat. This sedimentary hiatus spans a significant amount of geologic time; the London-Brabant Massif was exposed for long periods between the Carboniferous and Cretaceous (COWARD et al. 2003). However, this does not imply that sediments from intermediate time periods were never present in the study area. For instance, Triassic and Jurassic rocks are preserved in the the Roer-Valley Graben below the Base Cretaceous unconformity . The areas where the Dinantian carbonates are not truncated by the Base Cretaceous. In the entire study area, the Cretaceous is covered by a Cenozoic sequence that generally comprises clastic deposits (sand or clay).

Tectonic setting

Numerous faults dissect the Dinantian carbonates that can be related to several phases of tectonic disturbance. These faults are approximately trending NW-SE, i.e., paralleling the London-Brabant Massif, although the poor quality of the seismic data used does not always allow determining the exact relationship between the different faults systems. Most faults accommodate a relatively small (vertical) throw and affect the Dinantian carbonates as well as the overlying Upper Carboniferous deposits. These intra-Carboniferous faults often detach on the pre-Carboniferous basement and may be associated with the collapse of the carbonate platform, both during deposition and later reactivation. In addition to the many small-scale faults, several faults with larger offsets are present that often originate in the lower Palaeozoic. On a regional scale, the larger faults divide the sequence into discrete fault blocks that, combined, arrange the different segments into a predominant NE-dipping geometry.

Syn-depositional faulting

An early phase of basin deformation occurred before or during the Dinantian, as indicated by the presence of several 'pockets' recognized in the basement, i.e. grabens that were filled during the early Dinantian and covered by intra-Dinantian reflectors. Often fault structures are only local, however, the basement faults dividing individual fault blocks can significantly influence the thickness of the Dinantian sequence. A large extensional fault near the offshore well S02-01 has a half-graben geometry and accommodates significant throw. It displaces the 'Base Dinantian' horizon in the hanging wall block by roughly 300 ms TWT along a NW-SE oriented fault. The Dinantian deposits show a pronounced thickness change, while offset of the 'Top Dinantian' horizon seems relatively minor. The reflectors in the Devonian sequence below the 'Base Dinantian' show a wedge-shape, indicating the fault might already have been active during Devonian times. Devonian extensional movements along the Northern margin of the London-Brabant Massif were frequently reported (e.g. MUCHEZ & LANGENAEKER 1993; GELUK et al. 2007; VANDENBERGHE et al. 2014).

Additional evidence for syn-sedimentary faulting during deposition of the Dinantian carbonates is shown by northward increase in thickness of the sequence across the onshore faults. The carbonate strata wedge out towards the basin in the Northeast. It thus appears that the most important fault structures are either of Dinantian origin or inherited from the Caledonian orogeny. Distinct periods of extensional movement occurred along these faults; evidenced by thickness changes. The onshore Hoogstraaten Fault (VANDENBERGHE 1984) was also described as a long-lived Caledonian extension fault that defined the northern boundary of carbonate deposition during the Dinantian (MUCHEZ et al. 1987; VANDENBERGHE et al. 1988; MUCHEZ & LANGENAEKER 1993; LANGENAEKER 2000). The occurrence of several extensional phases during the Dinantian period was also recognized in the UK, with the occurrence of distinct fault-blocks.

Post-depositional faulting

Several instances of post-Dinantian tectonic disturbance have been recognized, however, these are not observable on the seismic data studied. There are several faults, which significantly deform the Dinantian. BÖKER et al. (2012) described two sets of fault orientations. The larger faults often cut into the basement below and divide the sequence into discrete fault-blocks. These can be traced up to the Cretaceous unconformity, occasionally offsetting even the Chalk and younger units, indicating that these faults are very long-lived and have probably been reactivated many times.

Many smaller faults seem to have only limited effect on the Dinantian sediments; often little to no offset is visible in the seismic data used, while offsets in the overlying high-reflective Westphalian strata are more evident (DOORNENBAL & STEVENSON 2010). These faults generally do not propagate above the Cretaceous unconformity; their deformation appears mostly restricted to the Upper Carboniferous strata. These are interpreted as parasitic synthetic-antithetic couples and compaction-related faults that formed in the well-layered Westphalian strata above the massive and rigid Dinantian carbonate fault blocks. Some of these faults detach onto the Dinantian or are related to distinct changes in Dinantian platform geometry.

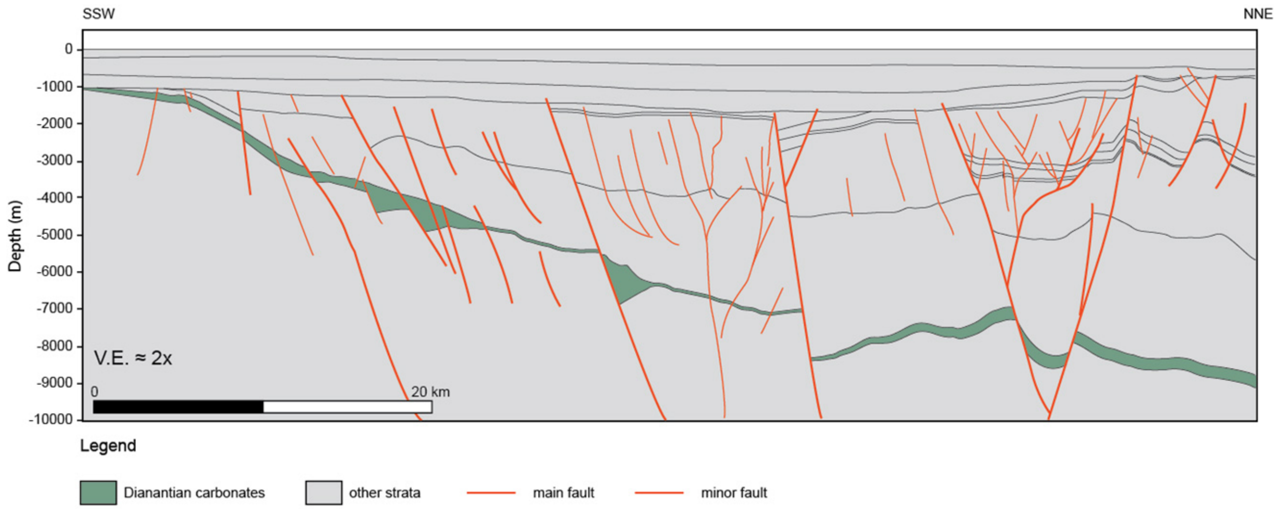

Figure 4.4.2: Representative cross section through the study area. See Figure 4.4.3 for locality.

4.4.3 3D geological modelling

Input data sets

<u>Borehole data (Figure 4.4.2)</u>

Well data covering the entire Dinantian interval are scarce. Within the study area only 8 Dutch wells and 9 Belgium wells reach the Dinantian and can be used trace the depth of the top Dinantien. Of these, only 7 wells reach the base of the Dinantian interval. and have sufficient well log data (gamma ray, sonic, lithologic and biostratigraphic logs) that can be used for correlation purposes. Two 2 wells (BHG-01, and KTG-01) were drilled for hydrocarbon exploration in the late '70's to early '80's), two for geothermal energy production (CAL-GT-01-S1 and CAL-GT-02), and one for mineral water extraction (KSL-02). Available core materials were examined and compared to previous core descriptions, thin section descriptions, carbonate depositional models and literature publicly available on the Dutch Oil and Gas Portal (nlog.nl) or in the NAM core repository. The description of the carbonate cores was done using the carbonate classification scheme of DUNHAM (1962), while the porosity of the carbonate sediments was described using the porosity classification system of CHOQUETTE & PRAY (1970). Composite logs of wells from the Belgian Campine Basin that reached the Dinantian limestones were also studied (Figure 4.4.2).

Seismic records (Figure 4.4.2)

Seismic interpretation was performed on public 2D seismic lines covering a large part of the southern Dutch subsurface, as well as part of the Campine Basin in northern Belgium (Figure 4.4.2). The seismic data set includes data with large differences in quality and often lack information on the seismic processing, which complicates the interpretation. A number of 2D lines had been digitized from paper sections, which sometimes improved the data quality and, more importantly, facilitated digital interpretation and manipulation. A limited number of wells within the study area penetrated the entire Dinantian sequence and hence only few seismic-to-well ties could be made for the entire interval.

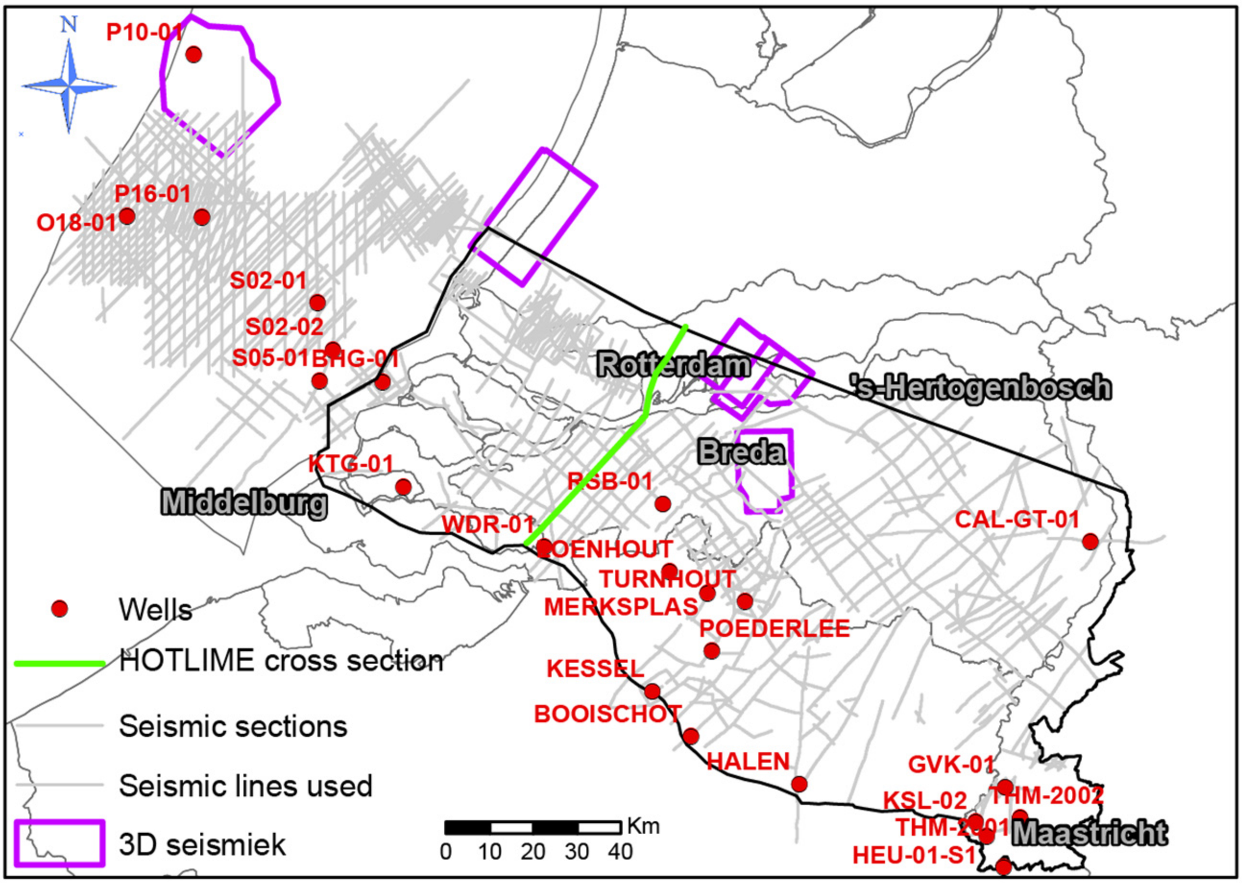

Figure 4.4.3: Data used within the BE-NL cross-border study area north of the London-Brabant-Massif.

The seismic interpretation of the Campine Basin was guided by the general structure and lithostratigraphy of the Dinantian as they were described for specific areas (LANGENAEKER 2000; LAENEN 2003). Additional well data and well logs of many Belgian wells were used to provide well control on the position of the Dinantian surface.

Table 4.4.1: Listing of wells available in the pilot area

Well name	X	Y	Top (m	Bottom	Thkn	Logs	Sonic	Check shot	Biostrat	Litholog	Core (m)	Purpose	End year
Netherlands													
KTG 01	47496	399312	937	1035	98	TRUE	TRUE	FALSE	TRUE	FALSE	51	HC exploration	1982
CAL GT 02	204164	382037	1161	1350	189	TRUE	FALSE	FALSE	FALSE	FALSE		Geothermal energy	2012
HEIBAART (LOENHOUT)	107483	378026	1115	1429	314	TRUE	FALSE	FALSE	FALSE	FALSE			
S05 01	29107	424167	1158	1967	809	TRUE	TRUE	FALSE	FALSE	FALSE	127	HC exploration	1981
CAL GT 01 S1	203631	381173	1421	2186	765	TRUE	TRUE	FALSE	FALSE	FALSE		Geothermal energy	2012
BHG 01	43983	423696.68	2009	2487	478	TRUE	TRUE	FALSE	TRUE	FALSE	25.8	HC exploration	1978
CAL GT 03	714940	5701442	1562	1966	404	TRUE	FALSE	FALSE	FALSE	FALSE		Geothermal energy	2012
GVK 01	182530	326340	885	-	-	TRUE	TRUE	FALSE	FALSE	FALSE	695	HC exploration	1986
WDR 01	79140	384600	1174	-	-	FALSE	FALSE	FALSE	FALSE	FALSE		Coal exploration	1914
HEU 01	177950	315255	67	-	-	TRUE	FALSE	FALSE	FALSE	FALSE	188	Mineral water	1981
HEU 01 S1	177950	315255	67	-	-	TRUE	FALSE	FALSE	FALSE	FALSE	193	Mineral water	1981
THERMAE – 2000	185725	319010	68	-	-	FALSE	FALSE	FALSE	FALSE	FALSE		Mineral water	1986
THERMAE – 2002	185775	319100	69	-	-	TRUE	FALSE	FALSE	FALSE	FALSE		Mineral water	1986
THERMAE – 2001	185720	318988	10	-	-	FALSE	FALSE	FALSE	FALSE	FALSE		Mineral water	1986
DB 108 MESCH	179670	308200	30	-	-	FALSE	FALSE	FALSE	FALSE	FALSE		Coal exploration	1922
DB 109 Cadier en Keer	182402	315937	62	-	-	FALSE	FALSE	FALSE	FALSE	FALSE		Coal exploration	1921
DB 105	185115	320658	111	-	-	FALSE	FALSE	FALSE	FALSE	FALSE		Coal exploration	1920
DB 123 Kastanjelaan	175570	318508	154	-	-	FALSE	FALSE	FALSE	FALSE	FALSE		Coal exploration	1929
DB 106	190419	313713	536	-	-	FALSE	FALSE	FALSE	FALSE	FALSE		Coal exploration	1921
Belgium													
BOOISCHOT	111268	340249	426	687	261	FALSE	FALSE	FALSE	FALSE	FALSE			
MOL GT 01	134720	359417	3141	-	-	FALSE	FALSE	FALSE	FALSE	FALSE			
POEDERLEE	116552	359525	1506	-	-	TRUE	FALSE	FALSE	FALSE	FALSE			
MERKSPLAS	116006	372737	1609	-	-	TRUE	TRUE	FALSE	FALSE	FALSE			
TURNHOUT	124616	370591	2132	-	-	TRUE	FALSE	FALSE	FALSE	FALSE			
KESSEL	102856	350717	565	-	-	FALSE	FALSE	FALSE	FALSE	FALSE			
HALEN	135659	328485	645	-	-	FALSE	FALSE	FALSE	FALSE	FALSE			
'S GRAVENVOEREN	181682	307932	15	-	-	FALSE	FALSE	FALSE	FALSE	FALSE			

Principle modelling workflow

The seismic interpretation mainly focused on identifying the top and base Dinantian reflectors. Only where resolution permitted, i.e., in areas where quality and coverage of seismic data were best, two intra-Dinantian reflectors were interpreted dividing the carbonates in three sections that roughly correspond to the three Dinantian depositional cycles described before. This subdivision was prominent in the Dutch offshore on the shelf area near the London-Brabant Massif. The acoustic properties of these members, which are all tight carbonates, show little variation, resulting in seismic reflectors at the transitions, that are often not very pronounced. Differences in seismic quality between different surveys also hinders a consistent interpretation. In addition, karstification also significantly influenced the seismic signature of the carbonate rocks. Consequently, this subdivision could not be pursued throughout the study area and is not presented here.

Base and top of the Dinantian were interpreted using available seismic data, which resulted into two data sets of the top and base of the Dinantian carbonate sequence, respectively. The seismic interpretation results where then converted to point data. The P-wave velocity behaviour of the Cenozoic and Mesozoic strata are well described by the velocity model VELMOD 4 made by TNO. The velocity behaviour of the Palaeozoic strata is less well-known. The availability of well-based velocity data is ample in the Westphalian (and if present the Stephanian) but is scarce for the older strata. The Namurian interval is drilled only by a few wells. Therefore an analysis was made of the velocities of both the Westphalian and Namurian strata to be able to establish a best practice approach for time-depth conversion of top Dinantian. This best practise appear to be a simple v0, k method with global (single) values for both parameters (k = 0.2524 s-1 and V0 = 3,448 ms-1). For the conversion of the top Dinantian, the base Rotliegend (RO) from TNO's DGM-deep v5.0 model was chosen as reference. The depth of this surface was obtained using layer-cake velocity modelling using Velmod 4. Using the (where available) TWT thickness of the Dinantian the depth of the base Dinantian point sets can be straightforwardly calculated using an interval velocity of 6,000 ms-1 for the Dinantian carbonates. After obtaining the interpretations points in depth (TDV), surfaces where generated using Petrel's convergent gridding algorithm. The surfaces are tied to the respective data at well location (using a 3 km influence radius) to produce well-tied maps. Gridding was only performed within the limits of the interpretation. For this purpose, polygons were created for both top and base of the Dinantian. Note that thickness can only be calculated there where the base Dinantian was interpreted. Consequently, the thickness map has the same coverage as that of the Base Dinantian.

The seismic interpretation of the Belgian data was executed at an earlier stage and resulted in mapping products for the NL-BE crossoborder project GeoHEAT (LAGROU et al. 2014). Both top and base depth maps of the Dinantian were merged with corresponding depths maps for the Dutch part of the pilot area.

Quality assurance

Quality assurance measures during the preparation of the input data

Polygons were constructed that are based on the experience of the seismic interpreter and serve to indicate data-poor areas or areas where the image of the Dinantian is poor. These polygons were only created for the top Dinantian but logically apply also to deeper levels and can be used to blank the maps inside the interpretation area.

Quality assurance measures during 3D Modelling

By applying a regional V0, k method for time-depth conversion, the calculated depth (Z) may deviate from the True Vertical Depth (TVD) observed in wells. This mis-tie is indicative for the goodness of the applied TD conversion. Table 4.4.2 lists the mis-ties between wells and the non well-tied grid of top Dinantian. Mis-ties are both positive and negative and the average mis-tie is 60 m. The use of one single velocity function, knowing that there is considerable spread in velocity information, importantly contributes to the mis-tie at well location. With a ~1,000 m thickness of the overlying Upper Carboniferous Limburg Group (DC), 1 SD of the velocity data corresponds to +/-150 m depth variation for the top of the Dinantian (Table 4.4.3). This value is in general agreement with the calculated mis-tie values, however it will increase with increasing Upper Carboniferous thickness. Moreover, mis-ties might be related to inaccuracies in the seismic interpretation as well.

Subsequently, the generated maps for the base, top and thickness of the Dinantian interval were well-tied to the corresponding information in the wells. In other words, the well information was considered dominant over the TD conversion and the mis-tie at well location becomes zero.

Table 4.4.2: Mistie analysis of the top Dinantian grid versus well depth

well	Z_{well} (m)	non-well tied top Dinantian (m)	Difference (m)
KTG-01	-937	-805	-132
BHG-01	-2009	-2009	0
GVK-01	-885	-884	-1
CAL-GT-02	-1161	-1320	159
CAL-GT-01	-1422	-1694	272
Average			**60**
Stdev			**157**

4.4.4 Rock property and Temperature modelling

A 3D temperature model of the Netherlands was generated using JAVA-coded in-house software. The code is a forward steady state temperature **model** that is calibrated to temperature observations ("**data**") using Ensemble Smoother Multiple Data Assimilation (ES-MDA) (BONTÉ et al. 2012; BÉKÉSI et al., in prep.).

Input data sets

- a geological layer cake model of the subsurface. For the current update, the Digital Geological Model (DGM-Deep v5) of the Netherlands was used (www.nlog.nl). This model contains depth grids of 13 main horizons from surface level down to the base of the Dinantian (Table4.4.3).
- Depths of the base of the Upper and Lower Crust using data from LIMBERGER & VAN WEES (2014); LIMBERGER et al. (2015).
- For all layers, a bulk lithological composition was estimated. Using the lithological composition, the prior authigenic heat production (A, µW/m³) and vertical thermal conductivity (KV, mW/mK) were calculated using the property values (per lithology) and methodology suggested by HANTSCHEL & KAUERAUF (2009), which takes porosity-depth relationships for different lithologies and the temperature dependence of thermal conductivity into account. For the Dinantian and overlying Namurian / Westphalian, adapted values were used based on literature study.
- Temperature data was collected from public sources available on www.nlog.nl and collected into a database. Currently, the temperature measurements database contains about 1800 data points. The data is spread heterogeneously over the country, with emphasis on the Western and Northern parts at depths between 1500 and 3000 meters (Figure 4.4.5). Various measurement types are contained in the database:
  1. Geothermal operations
  2. Well tests (DST) and repeat formation tests (RFT)
  3. Bottomhole temperatures (BHT) collected over longer periods, long after drilling.
  4. Distributed Temperature Sensing (DTS) using fibre optic cable
  5. Bottomhole temperatures (BHT) collected during or shortly after drilling

Data types 1 through 4 are the most reliable (when measured and collected cautiously). Data type 5 is by far the most abundant type, and is usually measured in boreholes that are not in temperature equilibrium due to the circulation of cold drilling mud. Various methods are available for correcting those measurements (e.g. BLACKWELL & RICHARDS 2004; GOUTORBE et al. 2007), but the resulting temperatures have a high uncertainty and tend to be biased towards lower temperatures. For our database, either the Horner correction was used when sufficient supporting data were available, or the Instantaneous Cylindrical Source method (ICS) (GOUTORBE et al. 2007). If no supporting data were available, a statistical bulk correction was applied following BLACKWELL & RICHARDS (2004).

*Table 4.4.**3**: Layers in the geological model, based on DGM-Deep v4 (www.nlog.nl).*

model layer number	Unit	DGM-Deep code	age
1	Upper North Sea Group	NU	Paleogene
2	Lower and Middle North Sea Group	NLNM	Paleogene
3	Chalk Group	CK	Cretaceous
4	Vlieland Group	KN	Cretaceous
5	Schieland Group	S	Jurassic
6	Altena Group	AT	Jurassic
7	Triassic Group	RBRN	Triassic
8	Zechstein Group	ZE	Permian
9	Rotliegend Group	RO	Permian
10	Caumer/Dinkel/Hunze Subgroups (Westfalian)	DCC/DCD/DCH	Carboniferous
11	Geul Subgroup (Namurian)	DCG	Carboniferous
12	Carboniferous Limestone (platform)	CL	Carboniferous
13	Carboniferous Limestone (non-platform)	CL	Carboniferous
14	Base Paleozoic (Zeeland area)		Paleozoic
-1	Upper Crust		
-2	Lower Crust		
-3	Mantle	-	

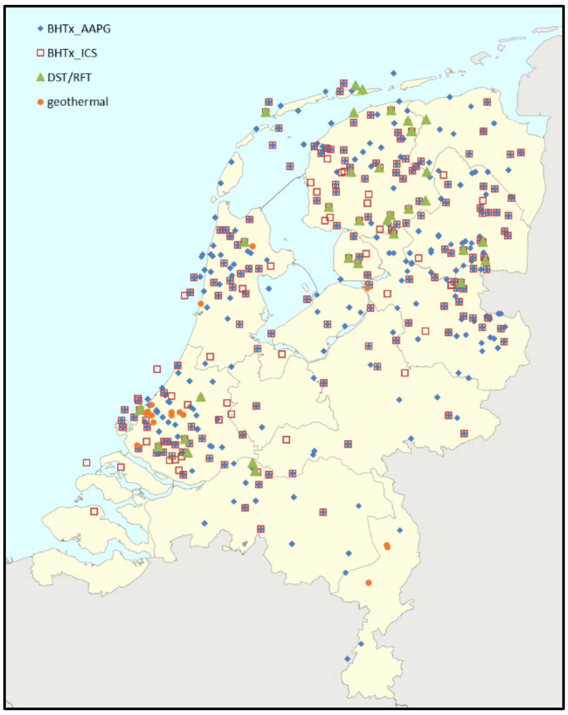

Figure 4.4.4: Distribution of temperature measurements. At a single XY location (well) usually multiple measurements are available.

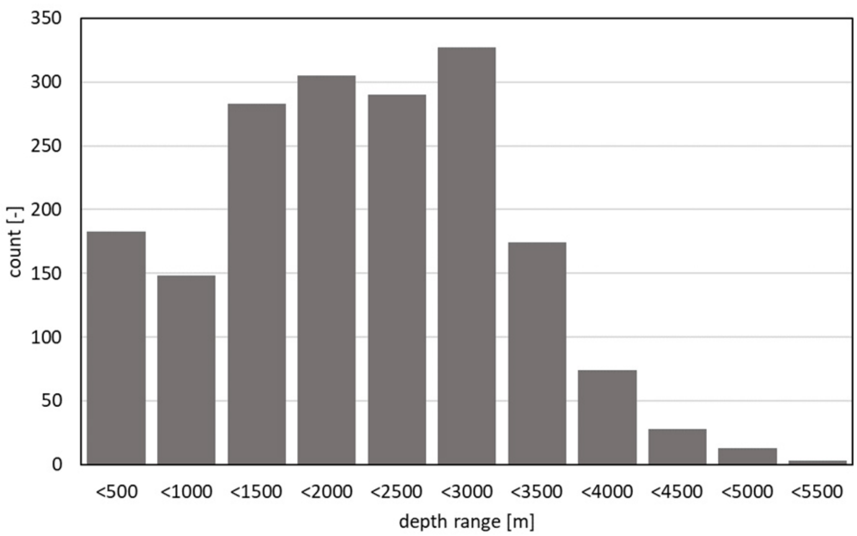

Figure 4.4.5: Depth distribution of temperature measurements.

Temperature Model

A first 3D temperature model of the Netherlands was published by BONTÉ et al. (2012). It has been updated several times since 2012. The latest revision is from 2018 and was prepared by BÉKÉSI et al. (in prep.). The generation of a 3D, high resolution temperature model is very calculation and computer memory intensive. Therefore, the modelling is split in multiple steps (Figure 4.4.6).

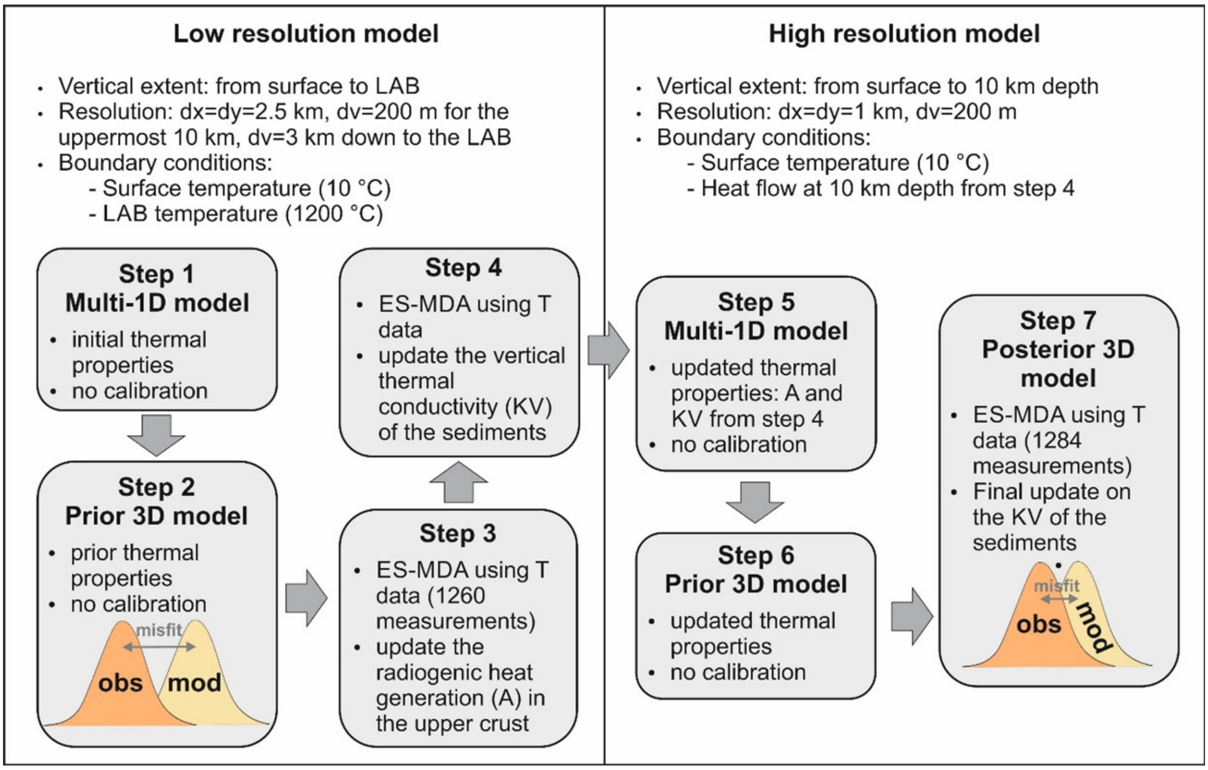

Figure 4.4.6: Temperature model steps.

1. A coarse scale 3D grid model is built. The spatial resolution of this model is 3,000 by 3,000 meters in the horizontal plane, and 200 meters vertically down to a depth of 10 kilometers. Deeper than 10 kilometers the vertical resolution is 3000 meters down to a depth of 100 kilometers. The subsurface multi-layer model includes layers defined in the DGM-Deep v5 model, the lower crust and the upper crust and the lithospheric mantle (Table 4.4.3). Prior thermal conductivity and authigenic heat production values are assigned to all layers. The bulk thermal conductivity of a heterogenous volume of rock is a function of the contributing rock types, and pore water, at given temperature and pressure. Rock thermal conductivities relevant to the Dutch subsurface typically lie within a range from ~0.8 to ~6.5 W/mK (Figure 4.4.7). The thermal conductivity depends on temperature and pressure (KUKKONEN et al. 1999). An increase in temperature reduces the thermal conductivity. Increasing pressure, due to burial, reduces the porosity (compaction) which replaces water by rock in the bulk rock volume, thereby increasing the bulk thermal conductivity1. The initial thermal conductivities are corrected for burial using porosity-depth relationships (Athy's law).The heat equation is then solved for each X,Y location in this grid ('multi-1D') using the layer model and the rock thermal properties. The boundary conditions are a temperature of 8 °C at surface level2, and 1,200 °C at 100 kilometers depth (LIMBERGER

[1] The effect of pressure alone on thermal conductivity is very limited
[2] Bonté et al., (2012) proposed a surface temperature of 10 °C, which is in agreement with the current average surface temperature of the Netherlands. Because the subsurface temperature is currently not in equilibrium with the surface temperature as a result of the various age ages in the last ~150,000 years and the Holocene warm period since ~10,000 years, a better fit with measured temperatures in the shallow subsurface up to ~2 kilometers is obtained using a surface temperature of 8 °C.

& VAN WEES (2014), TESAURO et al. (2009)). This yields initial values at each grid cell for the temperature, the thermal conductivity and the authigenic heat production that agree with first order estimates.

2. Based on these default properties a starting 3D thermal model is calculated. In this step, the model is not yet fitted to any temperature measurements so there is a misfit between observed and modelled temperature. An important difference with step 1 is that this step is 3D instead of multi-1D.

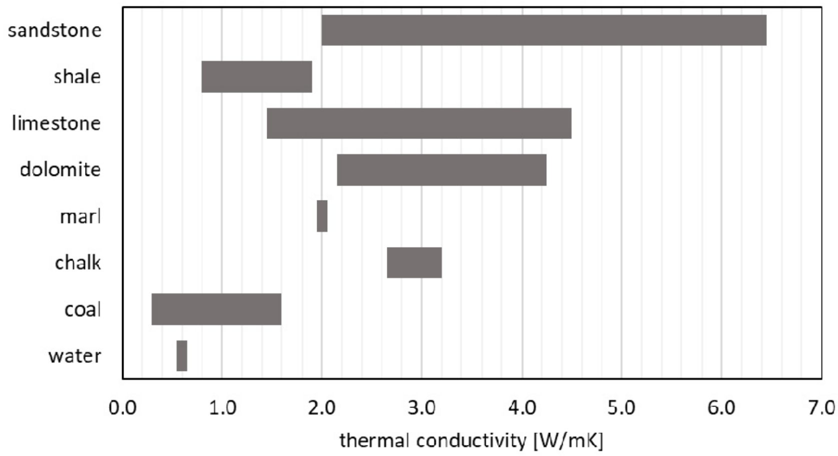

Figure 4.4.7: Typical rock thermal conductivity ranges from Hantschel & Kauerauf (2009) and water, at ambient conditions.

3. Next, the prior low-resolution forward model is fitted to the temperature measurements in two further steps:
4. The prior estimate of radiogenic heat production (A) in the upper crust is updated using an inversion procedure with an Ensemble Smoother with Multiple Data Assimilation (ES-MDA, EMERICK & REYNOLDS (2013)) which uses subsurface temperature measurements as observation points.
5. The prior estimate of the vertical thermal conductivity (KV) in the sedimentary layers is updated using ES-MDA. In the assimilation the temperature calculated by the model is compared to the temperature observations. The latter are measurements that are taken in boreholes during or after drilling.
6. Next, the resulting 3D grid of the first four steps is used to calculate a high-resolution model:
7. A multi-1D model is calculated using the updated thermal properties authigenic heat production (A) and vertical thermal conductivity (KV) obtained from step 4. The horizontal resolution is 1000 meters, and the vertical resolution 200 meters, down to a depth of 10 kilometers. The (lower) boundary condition is the heat flow at 10 kilometers depth, derived from step 4, and a constant surface temperature of 8 °C. The temperature measurements are not used in this step.
8. A prior high-resolution 3D model is calculated from the result of step 5, without using the temperature measurements as calibration.

9. The cooling effect of the glaciations that occurred between 150,000 years (150 ky) ago and present is introduced using estimates of the paleo-surface temperature. The cooling is mimicked by lowering the authigenic heat production.

10. The final model step updates the vertical thermal conductivity (KV) of the sediments using ES-MDA, using the temperature observations as calibration.

During the modelling steps that involve ES-MDA, key rock properties (thermal conductivity and authigenic heat production) and heat flow are modified in order to obtain a better match between the modelled and the observed (measured) temperatures. The rock properties are allowed to change within user specified limits, using a uniform or triangular distribution, or a shift. It is important to allow the model to vary the rock properties in a sufficiently wide range. If the range is too restricted, a good fit between observed and modelled temperatures cannot be obtained. If the range is set too wide on the other hand, unrealistic rock property values may result. The range can be applied on a national scale, or using a range of influence.

- Both the depth and thickness of the reservoir are poorly constrained in a large part of the Dutch subsurface;
- Few reliable temperature measurements exist at the depth of the reservoir. Some of the available data suggest increased temperatures in the Dinantian with respect to the average gradient published by BONTÉ et al. (2012) but the underlying mechanism is not fully understood;
- The facies, and therefore the rock type and the relevant rock thermal properties, are not well known;

The permeability is not well known over the entire reservoir– this property is important because it determines, among other factors, what the dominant heat transport mechanism is (conduction or convection). Currently, the evidence from sparse cores, production data and petrophysical logs shows that the permeability is too low to enable convective heat transport.

As a result, the modelled temperature of the Dinantian rocks is uncertain. A more accurate knowledge of the above-mentioned parameters is key for an improved understanding the temperature distribution.

REFERENCES

ARETZ, M. & CHEVALIER, E. (2007): After the collapse of stromatoporid-coral reefs-the Famennian and Dinantian reefs of Belgium: much more than Waulsortian mounds. – In: ÁLVARO, J.J., ARETZ, M., BOULVAIN, F., MUNNECKE, A., VACHARD, D. & VENNIN, E. (eds): Palaeozoic Reefs and Bioaccumulations: Climatic and Evolutionary Controls. Special Publication. Geological Society (London): 143-168.

ARETZ, M. (2016): The Kulm Facies of the Montagne Noire (Mississippian, southern France). – In: DENAYER, J. & ARETZ, M. (eds.): Devonian and Carboniferous research: homage to Professor Edouard Poty. Geologica Belgica **19** (1-2). http://dx.doi.org/10.20341/gb.2015.018

BÉKÉSI, E., STRUIJK, M., BONTÉ, D., VELDKAMP, J. G., LIMBERGER, J., FOKKER, P. A., VRIJLANDT, M. & VAN WEES, J. D.: An updated geothermal model of the Dutch subsurface based on inversion of temperature data. (in prep.)

BLACKWELL, D. D. & RICHARDS, M. (2004): Calibration of the AAPG Geothermal Survey of North America BHT Data Base. – AAPG Annual Meeting

BLESS, M.J.M., BOUCKAERT, J. & PAPROTH, E. (1983): Recent exploration in Pre-Permian rocks around the Brabant Massif in Belgium. The Netherlands and the Federal Republic of Germany. – In: KAASSCHIETER, J.P.H. & REIJERS, T.J.A. (eds): Petroleum geology of the southeastern North Sea and the adjacent onshore areas. – Geologie en Mijnbouw (The Hague): 51-62.

BÖKER, U., DIJKSMAN, B. & VAN DEN GRAAFF, E. (2012): Winterton Area Dinantian Prospectivity Review, Technical Summary and Concepts for Reservoir Models. – Project G977, PanTerra Geoconsultants, Leiderdorp.

BONTÉ, D., VAN WEES, J. D. & VERWEIJ, H. (2012): Subsurface temperature of the onshore Netherlands: new temperature dataset and modelling. – Netherlands Journal of Geosciences **91**(4): 491-515.

BRIDGES, P.H., GUTTERIDGE, P. & PICKARD, N.A.H. (1995): The environmental setting of Early Carboniferous mud-mounds. – In: MONTY, C.L.V., BOSENCE, D.W.J., BRIDGES, P.H. & PRATT, B.R. (eds): Carbonate Mud-Mounds: Their Origin and Evolution. Special Publication of the International Association of Sedimentologists: 171-190.

BUGGISCH, W. (1991): The global Frasnian-Famennian » Kellwasser Event «. – Geologische Rundschau **80**: 49-72.

BURGESS, P. M. & GAYER, R. A. (2000): Late Carboniferous tectonic subsidence in South Wales: implications for Variscan basin evolution and tectonic history in SW Britain. – Journal of the Geological Society **157**(1): 93-104.

CAMERON, T.D.J. (1993): Chapter 5, Carboniferous and Devonian of the Southern North Sea. In: KNOX, R.W.O.B. & CORDEY, W.G. (eds): Lithostratigraphic Nomenclature of the UK North Sea. – British Geological Survey.

CHOQUETTE, P. W. & PRAY, L.C. (1970): Geologic nomenclature and classification of porosity in sedimentary carbonates, AAPG Bulletin **54**(2): 207-250.

COWARD, M.P. (1993): The effect of Late Caledonian and Variscan continental escape tectonics on basement structure, Paleozoic basin kinematics and subsequent Mesozoic basin development in NW Europe. – In: PARKER, J.R. (ed): Petroleum Geology of Northwest Europe: Proceedings of the 4th Conference. Geological Society, London, 1095–1108.

COWARD, M.P., DEWEY, J., HEMPTON, M. & HOLROYD, J. (2003): Tectonic evolution. In: Evans, D.J., Graham, C., Armour, A. & Bathust, P. (eds): The Millennium Atlas: Petroleum Geology of the Central and Northern North Sea. The Geological Society (London): 17-33.

DOORNENBAL, H. & STEVENSON, A. (2010): Petroleum geological atlas of the southern Permian Basin Area. – EAGE Publications (Houten): 1-352

DUNHAM, R.J. (1962): Classification of carbonate rocks according to depositional texture. – In: HAM, W.E. (ed): Classification of carbonate rocks. – American Association of Petroleum Geologists Memoir **1**: 108–121.

FRASER, A.J. & GAWTHORPE, R.L. (1990):. Tectono-stratigraphic development and hydrocarbon habitat of the Carboniferous in northern England. – In: HARDMAN, R.F.P. & BROOKS, J. (eds): Tectonic Events Responsible for Britains Oil and Gas Reserves. Geological Society Special Publications. Geological Society (London): 49-86.

GALLAGHER, S.J. & SOMERVILLE, I. (2003): Lower Carboniferous (Late Visean) platform development and cyclicity in southern Ireland: foraminiferal biofacies and lithofacies evidence. Rivista Italiana di Paleontologiae Stratigrafia **109**(2): 159-171.

GELUK, M.C., DUSAR, M. & DE VOS, W. (2007): Pre-Silesian. – In: WONG, T.E., BATJES, D.A.J. & DE JAGER, J. (eds): Geology of the Netherlands. Royal Netherlands Academy of Arts and Sciences (KNAW), (Amsterdam): 27-42.

GOUTORBE, B., LUCAZEAU, F. & BONNEVILLE, A. (2007): Comparison of several BHT correction methods: a case study on an Australian data set. Geophysical Journal International **170**(2): 913-922.

HANTSCHEL, T. & KAUERAUF, A. I. (2009): Fundamentals of basin and petroleum systems modeling Springer Science & Business Media.

HARINGS, M.J. (2014): CAL-GT-01-Implications for the Distribution of the Early Namurian Geverik Member in the Netherlands, 76th EAGE Conference & Exhibition 2014. EAGE, Amsterdam: 1-4.

HOORNVELD, N. (2013): Dinantian carbonate development and related prospectivity of the onshore Northern Netherlands, Vrije Universiteit Amsterdam (Amsterdam): 1-142.

KOMBRINK, H. (2008): The Carboniferous of the Netherlands and surrounding areas; a basin analysis. GEOLOGICA ULTRAIECTINA, Mededelingen van de Faculteit Geowetenschappen. Universiteit Utrecht (Utrecht): 294: 1-184.

KOMBRINK, H., BESLY, B. M., COLLINSON, J. D., DEN HARTOG JAGER, D. G., DROZDZEWSKI, G., DUSAR, M., HOTH, P., PAGNIER, H. J. M., STEMMERIK, L., WAKSMUNDZKA, M. I. & WREDE, V. (2010): Carboniferous. – In: DOORNENBAL, J. C. & STEVENSON, A. G. (eds): Petroleum Geological Atlas of the Southern Permian Basin Area. AEGE Publications b.v. (Houten): 81-99.

KOMBRINK, H., LEEVER, K.A., VAN WEES, J.-D., VAN BERGEN, F., DAVID, P. & WONG, T.E. (2008): Late Carboniferous foreland basin formation and Early Carboniferous stretching in Northwestern Europe: inferences from quantitative subsidence analyses in the Netherlands. Basin Research **20**(3): 377-396.

LAENEN B. (2003): Lithostratigrafie van het pre-Tertiair in Vlaanderen, Deel II Dinantiaan.

LAGROU, D. LOVELESS, S., LAENEN, B., HARCOUËT-MENOU, V., ROMBAUT, B., LANCKACKER, T., DE BOEVER, E., KLEINEGRIS, L., ROELSE, B., DOORNENBAL, J.C., PLUYMAEKERS, M.P.D., TEN VEEN, J. & KRAMERS, L. (2014): GEOHEAT-APP. – Report from Departement Omgeving. Afdeling Vlaams Planbureau voor Omgeving (in Dutch).

LANGENAEKER, V. (2000): The Campine Basin. Stratigraphy, structural geology, coalification and hydrocarbon potential for the Devonian to Jurassic. Aardkundige Mededelingen, Leuven University Press **10**.

LIMBERGER, J. & VAN WEES, J. D. (2014): 3D subsurface temperature model of Europe for geothermal exploration. – 76th EAGE Conference and Exhibition 2014

LIMBERGER, J., VAN WEES, J. D., TESAURO, M., BONTÉ, D., LIPSEY, L., BEEKMAN, F. & CLOETINGH, S. (2015): Thermo-mechanical models of the European lithosphere for geothermal exploration. – Abstracts, EGU General Assembly 2015.

MUCHEZ, P. & LANGENAEKER, V. (1993): Middle Devonian to Dinantian Sedimentation in the Campine Basin (Northern Belgium): Its Relation to Variscan Tectonism. – In: FROSTICK, L. E. & STEEL, R. J. (eds): Tectonic Controls and Signatures in Sedimentary Successions. Blackwell Publishing Ltd. (Oxford): 171-181.

MUCHEZ, P., VIAENE, W., BOUCKAERT, J., CONIL, R., DUSAR, M., POTY, E., SOILLE, P. & VANDENBERGHE, N. (1990): The occurrence of a microbial buildup at Poederlee (Campine Basin, Belgium); biostratigraphy, sedimentology, early diagenesis and significance for early Warnantian paleogeography. – Annales de la Societe Geologique de Belgique **113**(2): 329-339.

MUCHEZ, P., VIAENE, W., WOLF, M. & BOUCKAERT, J. (1987): Sedimentology, coalification pattern and paleo-geography of the Campine-Brabant Basin during the Visean. – Geologie en Mijnbouw **66**: 313-326.

NARKIEWICZ, M. (2007): Development and inversion of Devonian and Carboniferous basins in the eastern part of the Variscan foreland (Poland). – Geological Quarterly **51**(3): 231-265.

ONCKEN, O., VON WINTERFELD, C. & DITTMAR, U. (1999): Accretion of a rifted passive margin; the late Paleozoic Rhenohercynian fold and thrust belt (middle European Variscides). – Tectonics **18**(1): 75-91.

REIJMER, J., TEN VEEN, J.H., JAARSMA, B. & BOOTS., R. (2017): Seismic stratigraphy of the Dinantian carbonates in the Southern Netherlands. – Netherlands Journal of Geosciences. (under revision)

RGD (Rijks Geologische Dienst) (1978): Het Paleozoïcum van de Diepboring Brouwerhavensegat-1 (N.A.M.) tussen 1398 en 2906.8 m. Retrieved from www.nlog.nl

TOTAL E&P UK (2007): A regional review of the Dinantian carbonate play: Southern North Sea & onshore UK, Total E&P UK.

VAN DER MOLEN, A. S. (2004): Sedimentary development, seismic stratigraphy and burial compaction of the Chalk Group in the Netherlands North Sea area. GEOLOGICA ULTRAIECTINA, Mededelingen van de Faculteit Geowetenschappen. Universiteit Utrecht (Utrecht): 248: 1-180.

VAN HULTEN, F.F.N. & POTY, E. (2009): Dinantian Reefs underneath the Netherlands. EAGE 71th Conference and Technical Exhibition. EAGE, Amsterdam. W039: 1-5.

VANDENBERGHE, N., DE CRAEN, N. & BEERTEN, K. (2014): Geological framework of the Campine Basin Geological setting, tectonics, sedimentary sequences. – Studiecentrum voor Kernenergie. External Report **262**: 1-113.

VANDENBERGHE, N., DUSAR, M., LAGA, P.G. & BOUCKAERT, J. (1988): The Meer well in North Belgium. – Memoirs of the Geological Survey of Belgium **25**. Ministère des Affaires économiques, Administration des Mines, Service géologique de Belgique (Brussels).

WATERS, C.N. & DAVIES, S.J. (2006): Carboniferous: extensional basins, advancing deltas and coal swamps. – In: BRENCHLEY, P.J. & RAWSON, P.F. (eds): The Geology of England and Wales. Geological Society (London): 173-223.

ZIEGLER, P.A. (1990a): Geological atlas of Western and Central Europe. – Shell International Petroleum Maatschappij B.V., 237 pp.

ZIEGLER, P.A. (1990b): Tectonic and palaeogeographic development of the North Sea Rift system. – In: BLUNDELL, D.J. & GIBBS A.D. (eds): Tectonic Evolution of the North Sea Rifts. Oxford Science Publications (Oxford): 1-36.

4.5 Po Basin (IT) – T2.5

Chiara d'Ambrogi & Maurizio Marino (ISPRA), Michele Morelli (ARPAP), and Fabio Carlo Molinari (SGSS)

4.5.1 Inducement and Objectives

The case study focuses on the geothermal resources of the Late Triassic - Middle Eocene carbonate succession of the Po Basin. The main objective is the regional assessment of the temperature at the top of the carbonate succession and, where possible, of specific carbonate targets. The well stratified Jurassic and Cretaceous sediments, from carbonate platform to basin environment, possibly contain layers with geothermal potential for balneological use, direct heating, and electricity production.

The characterization of fault systems (Mesozoic inherited faults, active buried thrusts and their relationships), will be addressed together with facies changes and properties of prospective units.

4.5.2 Study area and geological setting

The study area, located in the Northern Italy, covers an extension of > 21,000 km^2 from Piemonte Region (to the west) to Emilia Romagna Region - Adriatic coast line (to the east), with its western-central portion belonging to the Lombardia Region. The city of Torino is located in the western corner, Bologna and Ferrara near the eastern boundary.

It is an almost completely plain area, with a mean elevation < 100 meters, crossed by the east-west elongated Po river valley, with the frontal part of the Ivrea moraine amphitheater located in the western sector, and the moraine hills south of the Garda Lake, in the north-central sector.

Regional geological setting

The Po Basin is the foreland of two oppositely-verging fold-and-thrust belts: the Southern Alps, to the north, and the Northern Apennines, to the south.

It consists of late Triassic - Eocene evaporitic–siliciclastic and carbonate succession deposited on the Adria paleomargin and covering the Variscan basement, followed by a thick pile of Oligocene to Pliocene foredeep deposits, locally up to 8,000 meters, and by Quaternary shallow marine and continental sediments deposited in a generally regressive sequence.

The architecture of the Po Basin is the result of the Mesozoic (mainly Late Triassic-Early Jurassic) extensional phases, that fragmented the Adria paleomargin, followed by Alpine (Late Eocene?-Miocene) and Apennine compressional phases (Late Oligocene-Pleistocene). The compressional phases produced several thrust systems, buried and even blind, and the formation of the two chains, the south-verging Southern Alps, and the north-verging Northern Apennines. In the area between Crema and Cremona, the Alpine and Apennines thrust systems, west-east elongated in this sector, face very closely one to another.

The Mesozoic extensional phases produced a pattern of faults mainly NNW-SSE or NW-SE trend, with minor N-S and E-W trend, that controlled an articulated paleogeography, with the Jurassic–Cretaceous Lombardian, Belluno (out of the study area), and Adriatic carbonate basins (100-km wide), and

i) intrapelagic ridges, in the western sector, ii) Trento plateau, in the central-eastern sector, and iii) long lasting carbonate platform (i.e. Bagnolo) in the south-central sector (Figure 4.5.1).

The Mesozoic paleogeographic domains controlled the distribution, geometries and thickness of the carbonate units that are characterized by the transition from condensed successions, on the top of structural highs, to thick successions, within troughs.

The overlying succession is constituted by a very thick pile of clastic terrigenous units including the syntectonic clastic wedge of the Gonfolite at the Southern Alps margin, related to Oligocene-Miocene tectonic phases, and the Plio-Pleistocene clastic sequence filling the Apennines foredeep.

Geological framework of the main carbonate reservoir

The carbonate reservoir of the Po Basin is constituted by a Late Triassic-Middle Eocene carbonate succession that has been subdivided into three main units bounded by horizons (unconformity or top surface) (Figure 4.5.2). The base of the carbonate reservoir is the **TEu** horizon, known as the Carnian unconformity; it is the base of the Norian-Rhaetian succession documenting a regionally extended carbonate platform. The top of the reservoir is the **SCA** horizon that corresponds to the end of the sedimentation of the basinal calcareous deposits (Middle Eocene). In-between, two further horizons have been considered: i) **E-J**, representing the drowning unconformity at the top of the Lower Jurassic carbonate platform; ii) **MAI**, that is the top of the basinal calpionellid-mudstone, Early Cretaceous (Barremian) in age. All the horizons correspond to lithological changes observed throughout the study area and they bound the following three units (Figure 4.5.2).

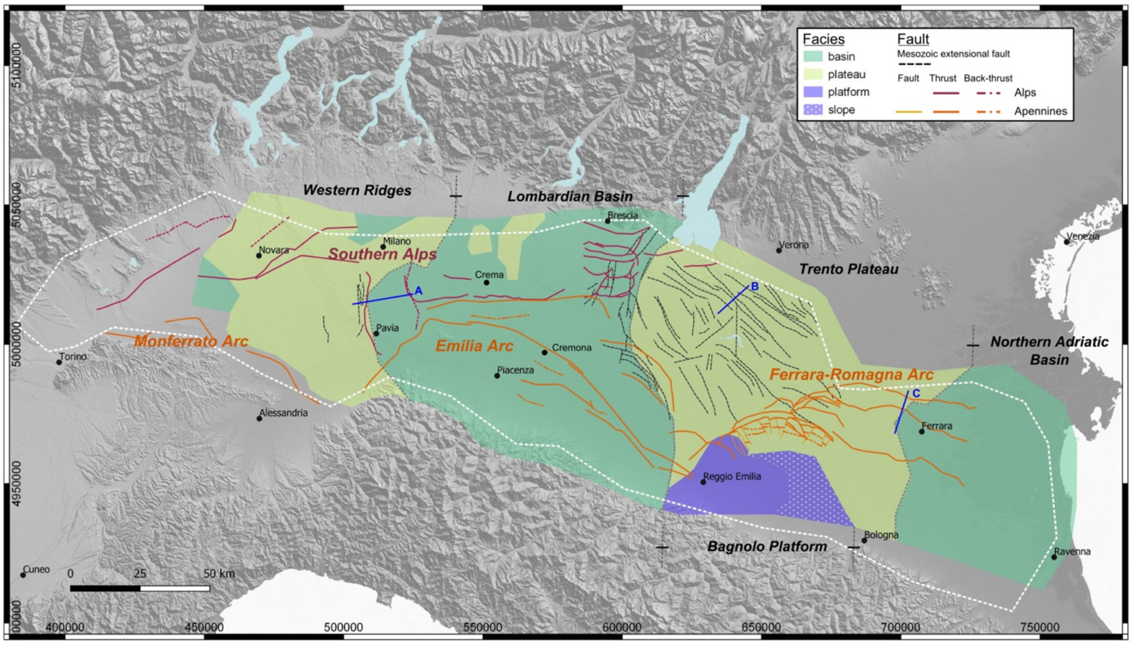

Figure 4.5.1: Paleogeographic domains and carbonate facies of the Po Basin; the mapped faults include Mesozoic extensional faults, and Alpine and Apennines thrusts with associated structures. The white dashed line is the boundary of the HotLime case study area. The blue lines are the cross-sections in Fig. 4.5.3.

Unit TR-J (Late Triassic-Early Jurassic p.p.) includes: i) Norian-Raethian dolostone and calcareous dolostone, dolomitized mudstone, and wackestone, with local anhydrite intercalated mainly in the eastern areas, and ii) Lower Jurassic intraclastic, oolitic, onkolitic, and fossiliferous grainstone-to-mudstone, sometimes dolomitized (mainly at the base), calcareous dolostone, dolomitic limestone, dolostone, stromatolitic grain-to-wackestone and mudstone, with local paleokarst. The deposits sedimented in shallow-water carbonate platform environments. Horizon TEu at the base and E-J at the top.

Unit J-K (Early Jurassic p.p.-Barremian): alternating mud-to-packstone, even intraclastic and fossiliferous, marl, with common cherty nodules and thin beds, nodular limestone and marl, cherty limestone, silicified limestone, radiolarites, radiolarians mudstones, with locally clay and sandstone intercalated; dolostone, calcareous dolostone and dolomitized limestone (mostly in the lower portion). These deposits sedimented in pelagic environments including deep basin (thicker successions), (intrabasinal) morpho-structural highs (plateau and ridges; thinner successions) and slopes. It is bounded by E-J, at the base, and MAI, at the top.

Unit K-PAL (Aptian-Early/Middle p.p. Eocene): the lower part (Aptian-Albian) is composed of grey to black and varicolored marl and clay, fossiliferous clayey mud-packstone and marl, intraclastic packstone, with cherty nodules and locally silicified, with rare quarts sandstone intercalated. The upper part is composed of fossiliferous mudstone-wackestone, often argillaceous, marl, with cherty nodules and thin-bedded chert. Locally clay and (quartz) sandstone intercalated occur in the western sectors. These deposits sedimented in a quite homogeneous, temporally euxinic (Aptian-Albian), basin environments (locally slopes). Horizon MAI at the base, and SCA at the top.

These units recorded (i.e. thickness, multiple unconformities with different ranges, lateral variability) the changes in the topography of the area resulting after the Late Triassic-Early Jurassic rifting. According to this, the area is subdivided into five paleogeographic domain characterized by the following differences, thickness, and depth of the carbonate units, from west to east (Figures 4.5.1 and 4.5.2):

Western Ridges evolved from carbonate platform (Late Triassic) to basin, with a non-depositional phase (emersion) in the Lower Jurassic, or locally longer. The maximum thickness of the carbonate units is about 1,400 meters. The depth of the top of the reservoir ranges from up to 7,000 meters, in the most-western portion, to 3,000 meters in the eastern portion, where a structural high is controlled by the inversion structure of Lacchiarella (Fig. 4.5.3b), at the boundary with the Lombardian Basin. Noteworthy, to the southwest, the top of the reservoir is not continuous due to the occurrence of a Cenozoic volcanic complex, with a dome-like morphology, that crosses the reservoir and whose top is 5,000 to 8,000 m in depth.

Lombardian Basin evolved from carbonate platform (Late Triassic, and locally Early Jurassic p.p.) to basin, with deeper areas and intrabasinal structural highs. The maximum thickness of the carbonate units can exceed 4,000 meters. In this area, the top of the reservoir deepens toward W-SW, and its depth ranges from 2,000 meters up to 10,000 meters.

Trento Plateau evolved from a carbonate platform (Late Triassic-Early Jurassic) to a pelagic plateau. The maximum thickness of the carbonate units is up to 2,000 meters. In this area, the top of the reservoir is very shallow in the NE portion (less than 1,000 meters) and deepens toward the south, beneath the Apennines thrusts. This monocline trend is controlled by a dense network of extensional faults (Figure 4.5.3b).

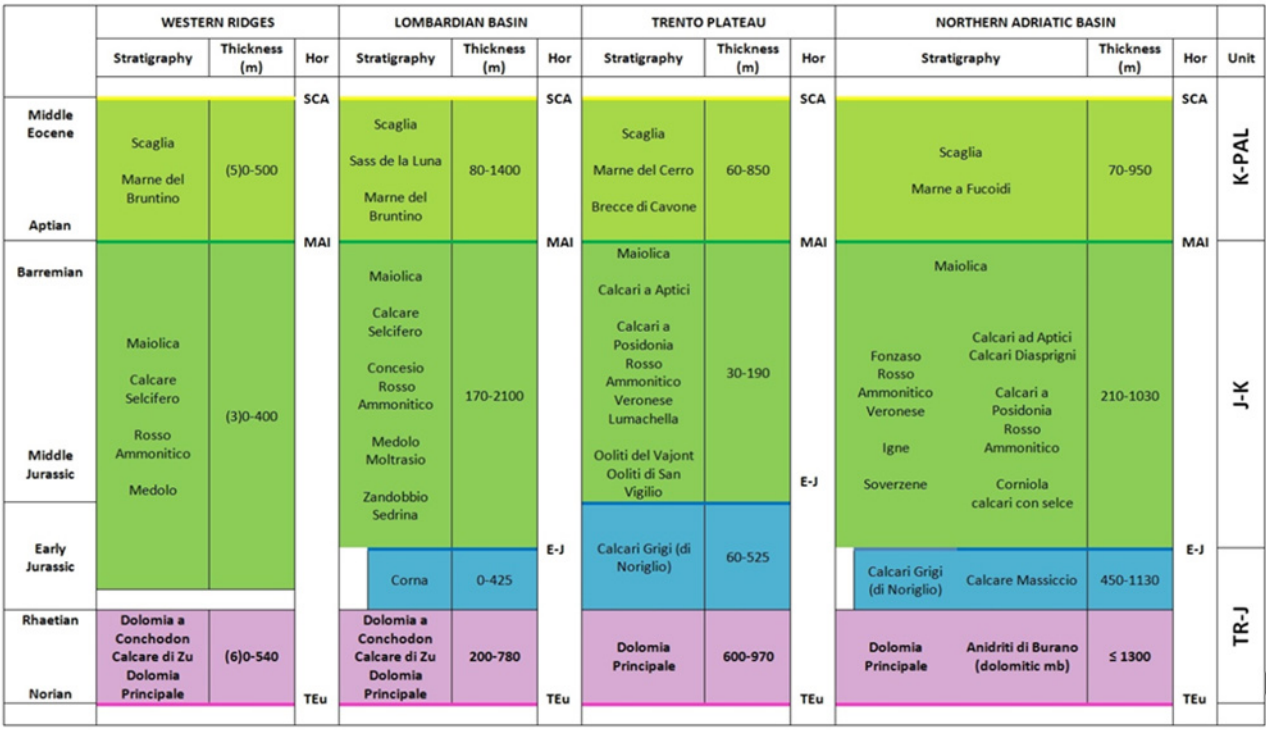

Figure 4.5.2: Stratigraphic scheme of the carbonate units in the Po Basin area. The range of thickness is reported for the main units, in each paleogeographic domain.

Northern Adriatic Basin evolved from carbonate platform (Late Triassic-Early Jurassic p.p.; locally sabkha environments in the Late Triassic) to pelagic basin. As in the Lombardian Basin, the maximum thickness of the carbonate units can exceed 4,000 meters. However, in this area, the activity of the Apennines thrusts strongly control the depth of the top of the reservoir, which ranges from a few hundred up to 8,000 meters.

Bagnolo Platform was a long-lasting carbonate platform active at least in the Late Jurassic-Oligocene interval. It is unconformably sealed by Upper Miocene terrigenous deposits. The reservoir is represented by the carbonate platform succession, mostly composed by fossiliferous and intraclastic mud-to-grainstone, partly dolomitized, with marls intercalated and breccias in the Cretaceous beds. The previously described horizons cannot be separated in this domain, and only the top of the carbonate succession is reported (mean depth 4,000 meters).

Overlying succession

The succession overlying the carbonate reservoir is Upper Eocene-Quaternary in age. During this time interval, the depositional architecture was affected by the Tertiary Southern-Alps deformation, and then, since the Pliocene, by the Northern Apennines deformation.

The base is represented by the SCA horizon, separating the mostly calcareous deposits from the marly-argillaceous ones marking the top of the *Scaglia*. Within this succession two horizons are distinguished: i) **PLu**, that represents the base of the Pliocene deposits and corresponding to the post-Messinian unconformity; ii) **QMu** that corresponds to the (post-Gelasian) unconformity, at the base of the Pleistocene *Quaternario marino* sequence. The entire succession thickness ranges from a few hundred meters near the Po Basin margins and at the top of more recent thrusts, locally up of 8,000 in the Pliocene foredeep depocenter.

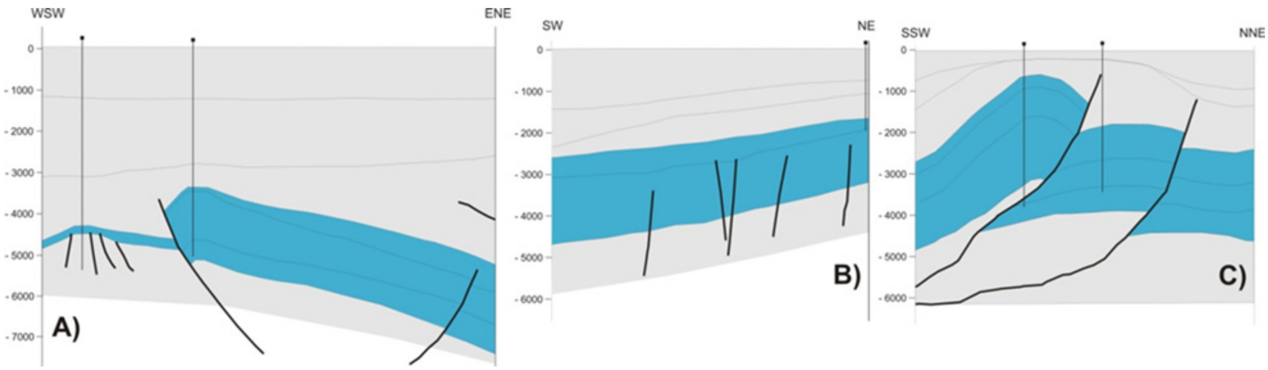

Figure 4.5.3: Cross-section derived from the 3D geological model of the case study area, representative of the different stratigraphic-structural architecture (see fig. 4.5.1 for location). A) Western ridges-Lombardian Basin: Lacchiarella; B) Trento Plateau; C) Trento Plateau-Northern Adriatic Basin: Casaglia. The blue color represents the carbonate reservoir units.

The **SCA-PLu** interval is represented in the lower part (Upper Eocene-Middle/Upper Miocene) by deep marine (bathyal to lower neritic) deposits, and in the upper part (Upper Miocene) restricted marine, brackish lagoon and evaporitic, to littoral-continental deposits.

In the lower part, main lithologies are: alternating clay, silty clay, marl, polygenic conglomerate, breccias, sandstone, quartz sandstone, limestone and calcarenite (mainly at the base); in the upper part clay and silty clay alternate with sandstone, quartz sandstone, anhydrite, gypsum, rare salt and conglomerate. Its thickness ranges between 600 and 4,000 meters in the western and north-western sectors, with maximum thickness due to the occurrence of the *Gonfolite* clastic wedge (Southern Alps foredeep). Eastward the thickness ranges from 200 up to 4,000 meters to the southeast, where Miocene Apennines foredeep turbidites (*Marnoso-Arenacea* Fm) occur. To the southwest, a Cenozoic volcanic complex, with a dome-like morphology, is intercalated within the sedimentary succession. Where drilled its radiometric age resulted between 16,1±1,5 Ma (Langhian) and 20,9 ±0,8 Ma (Aquitanian), and it is sealed by lower Miocene deposits.

The **PLu-QMu** interval is represented by littoral-neritic to epi-bathyal deposits, locally including turbidites; it is constituted by clay, silty and sandy clay, alternating clay and quartz sand, with locally intercalated conglomerate and glauconitic sand. The top interval, lying on the **QMu** horizon, is mostly represented by clastic neritic, littoral, deltaic, locally epi-bathyal and alluvial deposits. It is composed of sand, quartz and micaceous sand, clayey sand, with intercalating clay, silt, polygenic pebbly and gravel levels, clay with intercalated sand, gravel, peat, and lignite beds.

Tectonic setting

The present-day structural architecture of the Po Basin area is the result of Mesozoic rifting, acting on the Adria continental paleomargin, and subsequent Alpine/Apennines compressional phases.

The normal faults mapped in the area are mainly related to the syn- and post-rift extensional phases (Carnian – Early Cretaceous) that dismembered the Adria paleomargin and produced the maximum basin widening and deepening. They are very well documented at the boundary between the Trento Plateau and Lombardian Basin and poorly defined in the western sector (Fig. 4.5.1). The extensional faults have mainly NW-SE and NNW-SSE trend; they cut the Mesozoic carbonate succession, with upper tips overall not exceeding the SCA horizon. They are grouped in major fault systems, according to their orientation and history.

The convergence between the European and Adria plates since the Late Cretaceous is responsible for the thrusting. Several thrust systems of the Southern Alps and Northern Apennines are mapped, buried and even blind, related, the first, to the post-collisional phase of the Alpine orogeny (Late Eocene?-Miocene) and, the second, to the Apennine compressional phases (Late Oligocene-Pleistocene), both acting on the previously deformed continental margin (Figure 4.5.1).

The main Northern Apennines thrust systems are, from west to east: the Monferrato Arc, the Emilia Arc, and the Ferrara-Romagna Arc. Additional information is derived from the position where thrust ramps are rooted in the sedimentary pile, and by the deformed horizon and growth strata. On these bases the thrusts are distinguished in: i) L1, for thrust ramp rooted at ≈TEu detachment level, and L2, for thrust ramp rooted at the top of the carbonate succession detachment level (e.g. Oligocene marls); ii) age of the youngest deformed horizon.

Finally, on the one hand, the normal faults controlled the distribution and thickness of the reservoir, on the other hand, the thrusts controlled the position and depth of the top of the carbonate units (Figure 4.5.3c).

4.5.3 3D geological modelling

Input data sets

Geological 3D modelling of the Po Basin area is based on a huge input dataset, mostly provided by ENI SpA under a confidentiality agreement.

The input dataset is constituted by 305 well data (see Table below) and by 799 2D seismic profiles, together with existing 3D geological models covering portions of the studied area, deriving from previous EU-funded projects (i.e GeoMol) or from modelling activities of Regione Emilia Romagna.

Literature depth contour maps of the base of Pliocene succession and of the top of Mesozoic carbonate succession of the entire area, together with structural maps and geological cross-sections covering portions of the Po Basin area, and highlighting different structural domains (e.g. Mesozoic rifting, Cenozoic compression), are used as comparison data.

The maximum depth reached by the wells is 7,329 meters, with a mean depth of 2,700 meters. The wells are distributed homogeneously along the area, with a poor distribution only in the central portion.

	N. total	Carbonates
Log (public)	268	75
Log (ENI confidential data)	37	17
Time-Depth table (ENI confidential data)	81	32

The seismic data are represented by 2D seismic profiles mostly acquired between ’70 and ’90, with very good coverage of the entire area (mean spacing of ≈ 5 km).

Principle modelling workflow

According to the geological complexity of the Po Basin and the HotLime objective, five key horizons have been modeled. They subdivided the carbonate Triassic-Middle Eocene succession into three units, as the overlying Upper Eocene-Pleistocene succession.

The horizons are TEu (Carnian unconformity), MAI (top of Maiolica formation), SCA (top of Scaglia formation) that represents overall the top of carbonate succession, PLu (Pliocene unconformity – Zanclean), QMu (*Quaternario marino* unconformity – lower Pleistocene, 1.5 Ma).

The 3D modelling software used for the Po Basin area is Move^{TM} but the input dataset has been managed also with Leapfrog, and with common GIS software to extract specific information (including Vel-IO 3D tool).

The 3D modelling workflow (Figure 4.5.4) can be summarized in the following main steps:

- interpretation of seismic profiles, according to the defined stratigraphic scheme, and 3D modelling in time domain derived from picked horizons (>1.500.000 points) and fault sticks (> 2,000 fault sticks for 150 faults);
- elaboration of Time-Depth tables to derive velocity parameters, the building of the 3D velocity model and Time-Depth conversion (using Vel-IO 3D tool);
- elaboration of well data to derive depth constraints (used in Vel-IO 3D) and for analysis of carbonate facies;
- refinement, in depth domain, of the modeled horizons, according to additional constraints, and check of the fault displacements consistency.

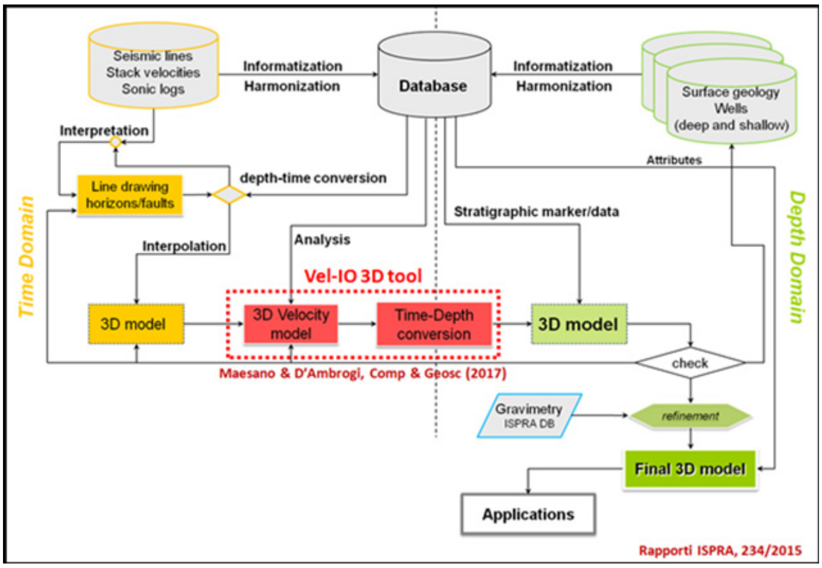

Figure 4.5.4: Scheme of the 3D modelling workflow.

Quality assurance

The huge amount of input data, the different vintages, and the large area (> 21,000 km^2) impose the adoption of quality assurance measures, here summarized:

- harmonization according to the project stratigraphic scheme;
- for seismic profiles: consistency check of the datum plane and, eventually, the datum shift;
- for the well data and surface geology: the harmonization of geological horizons;
- for the structural/isobath maps: the check of depth consistency with well data constraints.
- check of the geometric consistency of the 3D modeled horizons and faults (e.g. displacements along faults).

The 3D geological model is used as base elaboration for the automated production of the depth and thickness maps of the main units, both of the carbonate reservoir (Figure 4.5.5) and the overlying succession.

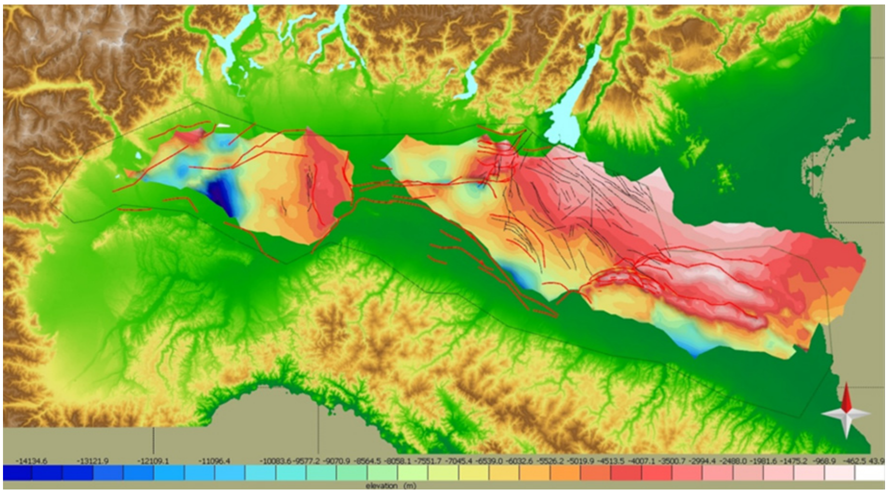

Figure 4.5.5: Depth of the top of the carbonate reservoir from 3D model. Red lines represent thrust, black lines represent extensional faults.

4.5.4 Rock property and Temperature modelling

The collection and evaluation of the hydrogeological and thermo-physical parameters are not yet completed; despite a large number of hydrocarbon wells, only very few of them include such parameters.

The groundwater chemistry, rock porosity, thermal conductivity could be derived from some well but it is not yet defined, from a methodological point of view, the representativeness of these data if applied into the very large case study area. On the other hand, literature data will be applied at a regional level.

Temperature Modelling

<u>Conceptual model and input data sets</u>

The main objective is the collection and investigation of subsurface temperatures and development of 3D Temperature model and delineation of promising geothermal plays, and data preparation for subsequent HotLime WP. The Temperature model will be able to estimate temperature prediction at various depth levels which can be applied to the local situations.

The geothermal gradient domain has been subdivided into two different geothermal gradients; the boundaries of these gradients are geological horizons recognized in the seismic interpretation and modeled in the 3D.

1. **K0**, from ground level to the **SCA** horizon (siliciclastic sequence).
2. **K1**, from the **SCA** horizon, the top of the reservoir, to the **TEu** horizon, the base of the reservoir (carbonate succession).

Modelling workflow

The temperature modelling workflow is summarized in Figure 4.5.6. After the first data validation phase, the two geothermal gradients were interpolated over the whole study area using a geostatistical tool in ArcGis (IDW); the results are two different grids related to K0 (Figure 4.5.7) and K1. The trend of geothermal gradients is a function of the structural architecture and geodynamic evolution.

Looking at the geothermal gradient map (Fig. 4.5.7), we can divide the study area into the following sectors:

1. **Southern Alps/Structural highs**: ~2,7 / 2,8 (°C/100 m);
2. **Lombardian basin**: ~2,2 / 2,3 (°C/100 m);
3. **Northern Apennines Foredeep**: ~2,0 / 2,1 (°C/100 m);
4. **Ferrara Folds**: ~3,2 / 8,0 (°C/100 m);
5. **Ovest (West) monocline**: ~2,1 / 2,2 (°C/100 m);
6. **Est (East) monocline**: ~3,0 / 4,5 (°C/100 m).

Some positive geothermal anomalies are located in the Ferrara folds sector, probably due to recent structural evolution, and controlled by the geothermal gradients and the position of the top of carbonate succession.

Subsequently, in the GIS environment, the shapes (X, Y, Z) related to the depths of the **SCA** and **TEu** horizons were imported, and all X Y Z points were linked to K0 and K1 grid data.

The shapefiles (X, Y, Z, *K*) allow the calculation of the first geothermal outputs:

1. Isotherm Map at the top of carbonate succession (Figure 4.5.8);
2. Isotherm Map at the base of carbonate succession.

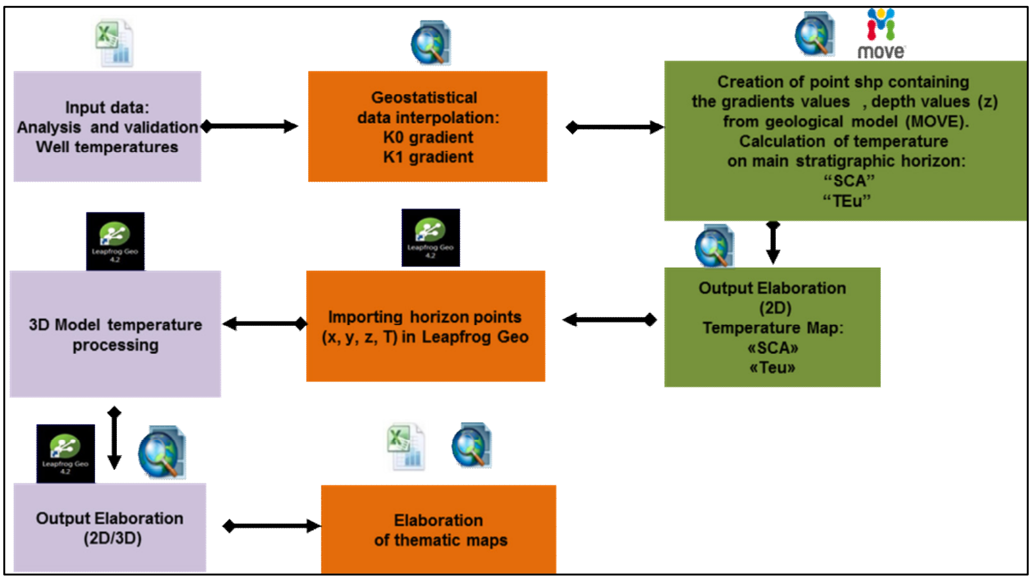

Figure 4.5.6: Temperature modelling workflow.

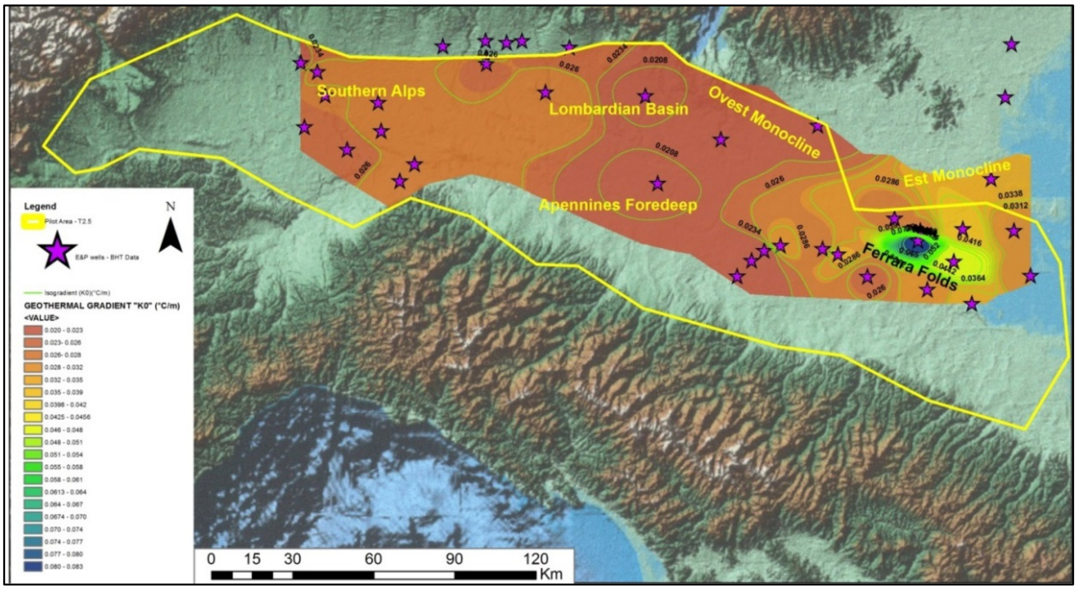

Figure 4.5.7: K0 Geothermal Gradient Map.

The map of the temperatures at the top of the carbonate succession (Figure 4.5.8) allows to identify two distinct sectors, strongly related to the overall structural architecture of the case study area:

1. the western part of the Southern Alps structural highs: in this sector the highest temperatures have been calculated as the result of both a relatively high geothermal gradient and the position of the top of the carbonate succession, at a depth of 4,000-5,000 meters;
2. the Lombardian Basin, Apennines Foredeep, Monocline, and Ferrara Folds: in this sector, except for the Ferrara Folds, the temperatures never exceed 150°C even when the top of the carbonate succession is at a depth of 6,500-7,000 meters. In the structural high of Ferrara Folds, the maximum temperatures at the top of the carbonate succession are around 70-75 °C, despite being the top of the carbonate succession is at a depth of 800-1,000 meters.

Once the structural maps relative to the depth of the top and the base of the carbonate succession have been definitively validated it will be possible to start the next phase related to the elaboration of the 3D temperature model.

The shapefiles of temperature (T) and depth (Z) data will be downloaded in Leapfrog Geo to obtain a pure conductive 3D temperature model. This 3D model, based on pure conductive heat transport, will be processed using geo-statistical interpolation of subsurface temperature values.

In the final phase it will be possible to elaborate the 3D Temperature Model Output within GIS and Excel to obtain different thematic maps:

- Depth-serialized: temperatures at predefined depths (e.g. 500 m, 1,000 m, 1,500 m, 2 km, 3 km and 4 km below surface);
- Temperature-serialized: depths of predefined isotherms (e.g. 60 °C, 100 °C and 150 °C);
- Horizon-serialized: temperatures at the top and the bottom of carbonate succession or the main geothermal reservoirs identified for potential geothermal use;
- Heat in Place Map.

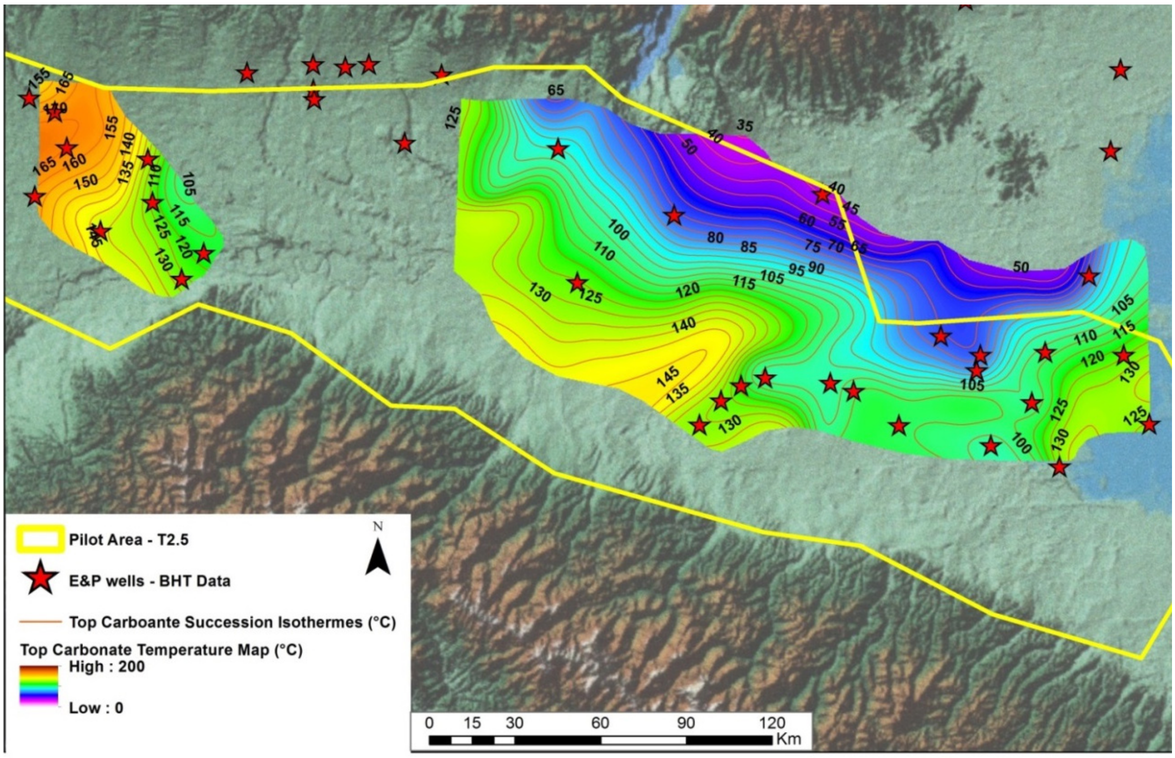

Figure 4.5.8: Map of temperature distribution on top of carbonate succession (SCA horizon).

4.6 Krško-Brežice sub-basin, SI – T2.6

Dejan Šram, Jure Atanackov & Dušan Rajver (GeoZS)

4.6.1 Inducement and Objectives

This sub-basin of SE Slovenia belongs to the SW part of the Pannonian basin. The basement geothermal reservoir is formed in fractured and karstified Triassic carbonates. A large thermal water convection cell formed, resulting in a natural thermal spring which ceased due to exploitation of thermal water at three sites. Production of water is extensive, causing a possible regional depletion of the reservoir. In such non-porous systems, a large risk of cooled water breakthrough exists. Therefore to evaluate a possible interference to existing production sites, a structural 3D geological model was created and implemented to 2D thermal numerical model to identify where pathways for thermal ground flow could be identified.

4.6.2 Study area and geological setting

The study area spans the southern half of the Krško basin and northeastern slopes of the Gorjanci mountains, located in southeastern Slovenia and covers an area of 281 km^2 (Figure 4.6.1).

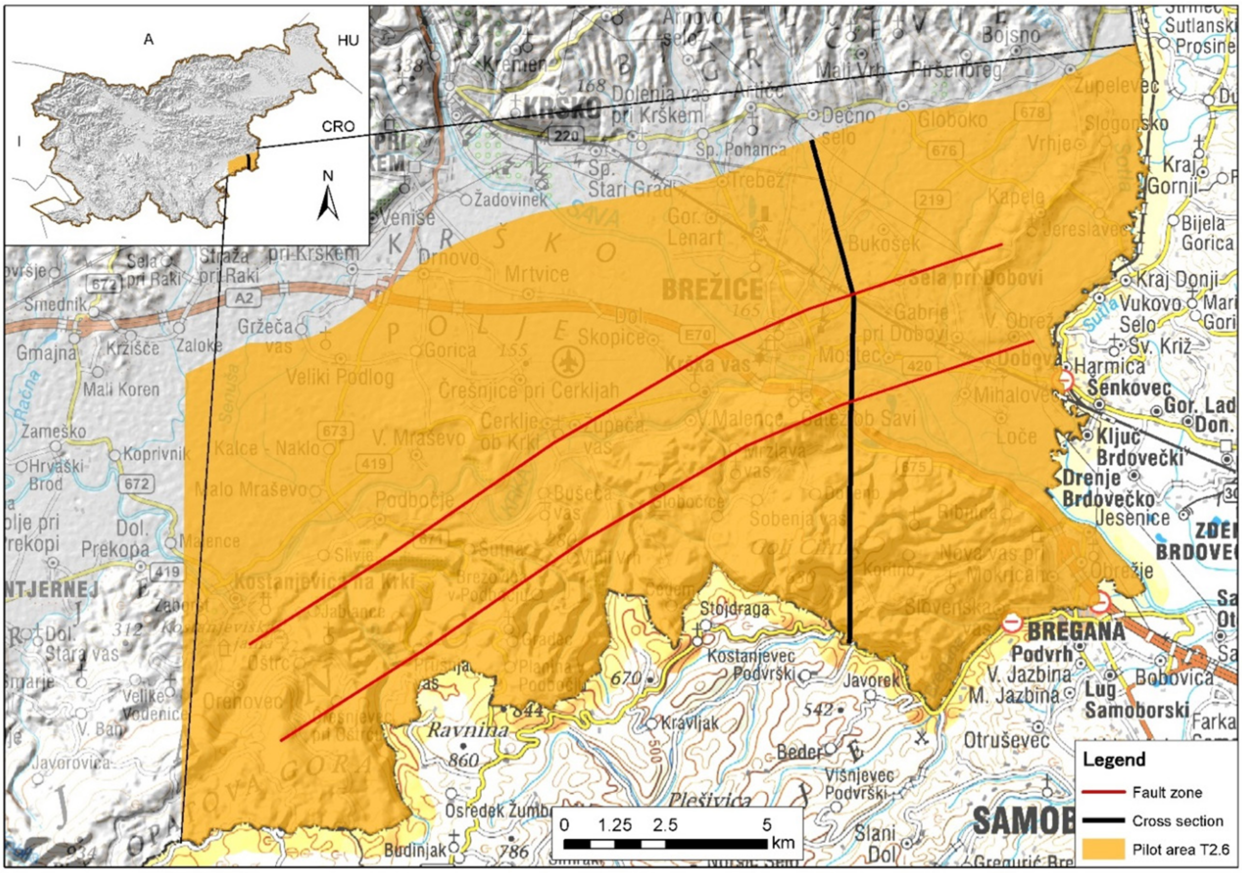

Figure 4.6.1: Study area for T2.6 with cross-section and fault zone.

Regional geological setting

The study area is part of the Sava folds, in the transition area between the Sava Compressive Wedge and the Mid-Hungarian Zone (PLACER 1998). The region has seen extensive tectonic development. Mesozoic tectonic development was mainly influenced by the opening and closing of the Meliata and Vardar oceans, while the current tectonic setting is mostly the result of Paleogene, Neogene and Quaternary tectonics. In the Paleogene the region experienced large-scale NE-SW folding and overthrusting as part of the formation of the Dinaric thrust and fold belt (PLACER 2008).

In the Neogene the region experienced a complex tectonic development, characterized predominantly by E-W extension, with dominant ~N-S normal faulting and formation of horst, graben and half-graben and formation of locally very deep (>2 km) sedimentary basins, filled with deep to shallow marine sediments of the Paratethys ocean (TOMLJENOVIĆ et al. 2001). In more detail, the first Neogene tectonic phase was Eggenburgian-Ottnangian (~20-18 Ma) extension, producing NNW-ESE normal faulting. It was followed by a short inversion, with ~N-S shortening and WSW-ENE reverse faulting. This phase was short, spanning only the Late Ottnangian (18 Ma). It was followed by a longer and extensional phase, lasting through Karpatian – Badenian – Sarmatian (17-12 Ma), producing new NE-SW normal faults and reactivating NNW-ESE normal faults. It was in turn followed by a short inversion with NNW-SSE shortening in the Late Sarmatian (12-11 Ma).

The penultimate tectonic phase lasted through all Pannonian into early Pontian (11-7 Ma), with ~E-W extension producing horst, graben and half graben structures along ~N-S normal faults. It was followed by the ultimate tectonic phase, with ~N-S shortening producing E-W reverse faulting and folding and associated strike slip faults and forming the Sava Folds. Most noteworthy, the ultimate and penultimate tectonic phases produced by far the most pronounced signature and structures in the study area. In the study area the penultimate tectonic phase produced the Globoko basin, the deep eastern part of the Krško syncline. The depth of Neogene sediments in the Globoko basin exceeds 2 km. The amount of vertical displacement due to compression in the ultimate tectonic phase exceeds 2 km.

The study area is characterized by the Globoko basin, part of the Krško syncline to the north, the Čatež fault zone in the central part and the Gorjanci mountains (or the Gorjanci antiform) in the south. The Čatež fault zone is a 2.4 km wide zone of reverse faulting and folding along the northern foot of the Gorjanci antiform, at the transition into the Globoko basin (Figure 4.6.1). The zone is not uniform, single fault, rather a complex zone of relatively short reverse fault segments and folds. The exact tectonic history of the Čatež fault zone is currently not constrained, however, it is assumed to be post-Ottnangian (18 Ma) and with the ultimate tectonic phase likely producing the largest contribution. Recent activity of the Čatež fault zone has not been demonstrated.

Geological framework of the main carbonate reservoir

Main carbonate reservoir (Figures 4.1.2 and 4.1.3) bearing thermal water (HotLime target layer) is composed of Mesozoic carbonates, overlain by a thick succession of Mesozoic deep water marine sediments, mainly flysch and thick Neogene and Quaternary marine and fluvial sediments. It includes the Triassic Main dolomite (Hauptdolomit) and the Jurassic Dachstein limestone, in a total thickness of approximately 1,400 m. Both were deposited over the clastics of the Slovenian basin, indicating again a shallower environment.

- **Main dolomite (Hauptdolomit)**: well-bedded Upper Triassic dolomite, deposited in inter- and supratidal environments. Total thickness: 1,000 m.
- **Dachstein limestone**: thick-bedded to massive limestone with occasional lenses of dolomite. Upper Triassic to Lower Jurassic. Total thickness: 400 m.

Formation thickness is assumed from mapped outcrops in the Gorjanci mountains and the near region of the study area. Lacking any data on thickness in the study area, the thickness is assumed to be constant.

Overlying succession

The overlying succession is mainly composed of approximately 1 km of Cretaceous deepwater sediments and flysch and about 2 km of Neogene sediments. The overlying succession begins with the Lower Jurassic **Izvir formation**, composed of basal breccias and platy, highly silicified limestones, in a total thickness of 50 m. It is overlain by Upper Jurassic and Lower Cretaceous **Biancone limestone,** deep water, pelagic platy limestone in a total thickness of 100 m. The sedimentation then transitions into flysch. This includes the Lower Cretaceous **Gora formation**, composed of breccias, conglomerates in basal part, upper part typical turbidite succession, with calcarenites with chert, siltstones, claystones and intercalations of conglomerates. The total thickness of the Gora formation is up to 300 m. It is overlain by the hemipelagic Upper Cretaceous **Krško formation**, composed of red platy limestone with chert and interbeds of shale in a total thickness of 250 m. The uppermost part of the deep water succession is represented by the **Veliki Trn formation**. It is composed of breccias and conglomerates, transitioning upwards into well-bedded calcarenites and further upwards into marly limestone and marlstone.

There is a long erosional hiatus, spanning much of the Paleogene with only local Paleogene and Eocene outcrops, which have little importance for our model. The hiatus is followed by a thick succession of fluvial and marine sediments of the Neogene Paratethys sea. It begins with the terrestrial sediments of the Ottnangian **Govce formation,** consisting of gravel, sand, clay and coal in a total thickness of 300 m. There is an erosional hiatus until the marine Badenian and brackish Sarmatian sediments, represented by up to 70 m of (clastic and bioclastic) lithotamnium limestone and marls. It is followed by up to 350 m thick succession of mostly very uniform Pannonian marls. The Neogene succession ends with a 1,100 m of Pontian (upper Pannonian) delta sediments, mostly sands with marls, gravels and coal. Another erosional hiatus follows, and the final up to 150 m of Plio-Quaternary and Quaternary fluvial gravels, including recent (Holocene) Sava alluvial sediments.

In the absence of direct structural data on the succession below the Neogene (e.g. no available geophysical data), we assume the formations within the study area to be of uniform thickness and homogenous in lithology. There is, highly likely, present faulting from the successive phases of normal faulting / rifting in Mesozoic. Additionally, there are likely thrusts and folds present, associated with the Paleogene formation of the Dinarides thrust and fold belt. Structures from this phase do appear to be present in the Gorjanci mountains, however, at this time there is insufficient data to properly ascertain thrust and/or fold geometry. We therefore assumed no significant influence of Paleogene tectonics on the thickness of formations.

4.6.3 3D geological modelling

3D modelling was done in ArcMap 10.6 and JewelSiute2018. To create 3D model we have used 1 seismic line which was used directly and 2 seismic lines were used indirectly. Layers from 3D model from the Northern part of the pilot area from project DARLINGe were used for help to construct the Northern part of the area. The structural profile was made in part along the seismic line.

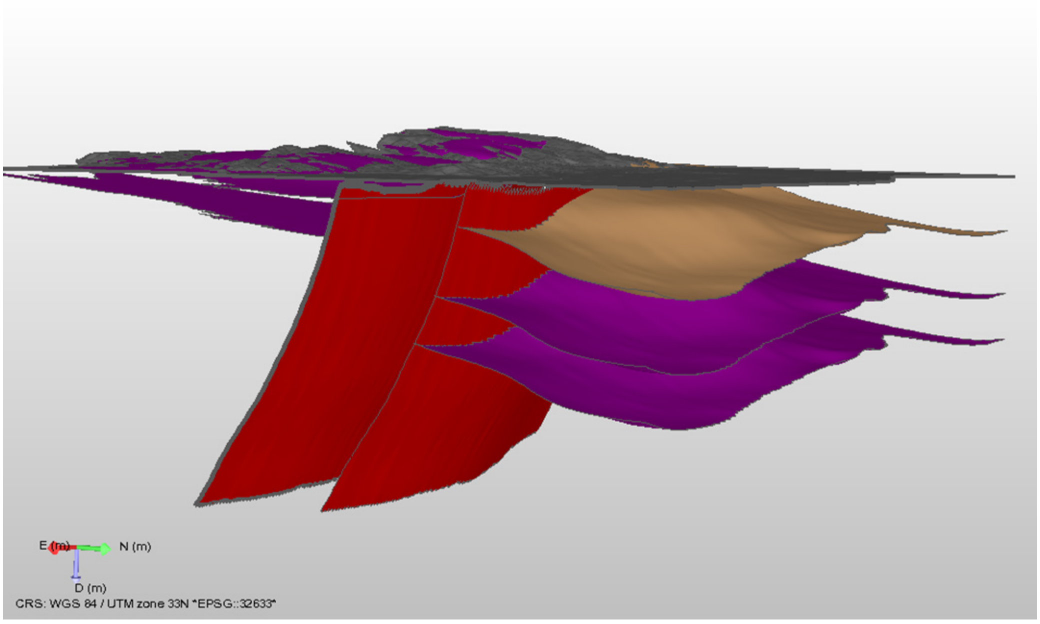

Figure 4.6.2: 3D geological model (view from SE to NW) (Red – fault zone, violet – HotLime target layer).

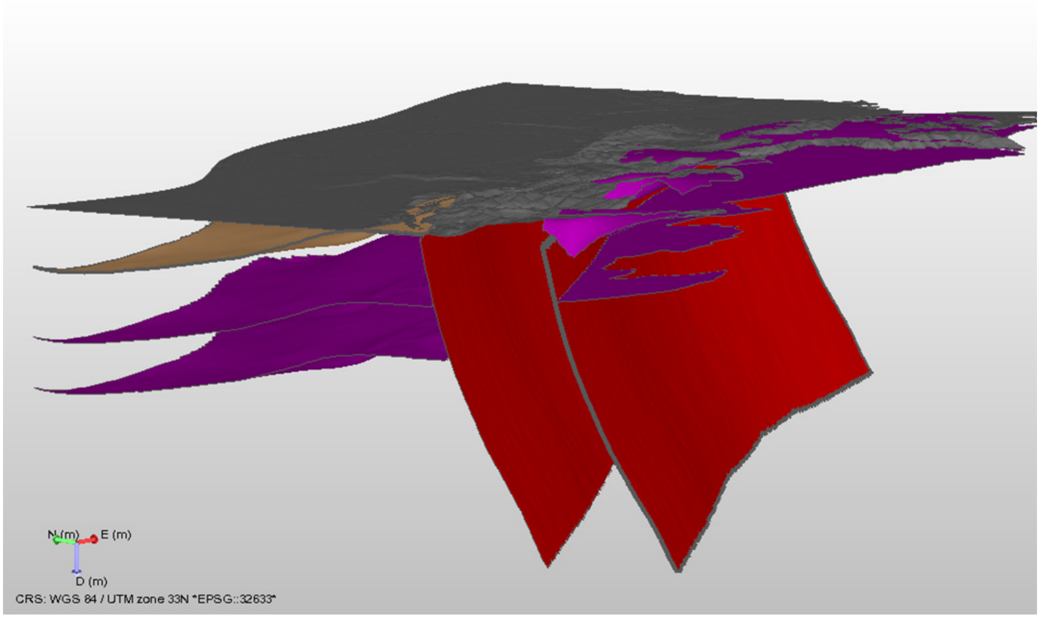

Figure 4.6.3: 3D geological model (view from SW to NE). (Red – fault zone, violet – HotLime target layer).

4.6.4 Rock property and Temperature modelling

Temperature has been measured in 34 boreholes with thermally stable condition what we always strive for (Figure 4.6.4). Temperature was usually measured point by point at intervals of 5 to 10 m, depending on variations in the lithology. In the deepest borehole DRN-1 (depth of 1,252 m) it was measured in stable condition only down to a depth of 640 m. In the most significant geothermal anomaly (Čatež field) geothermal measurements have been done in 10 deep boreholes and in one at Dobova (which is also a part of the Čatež field).

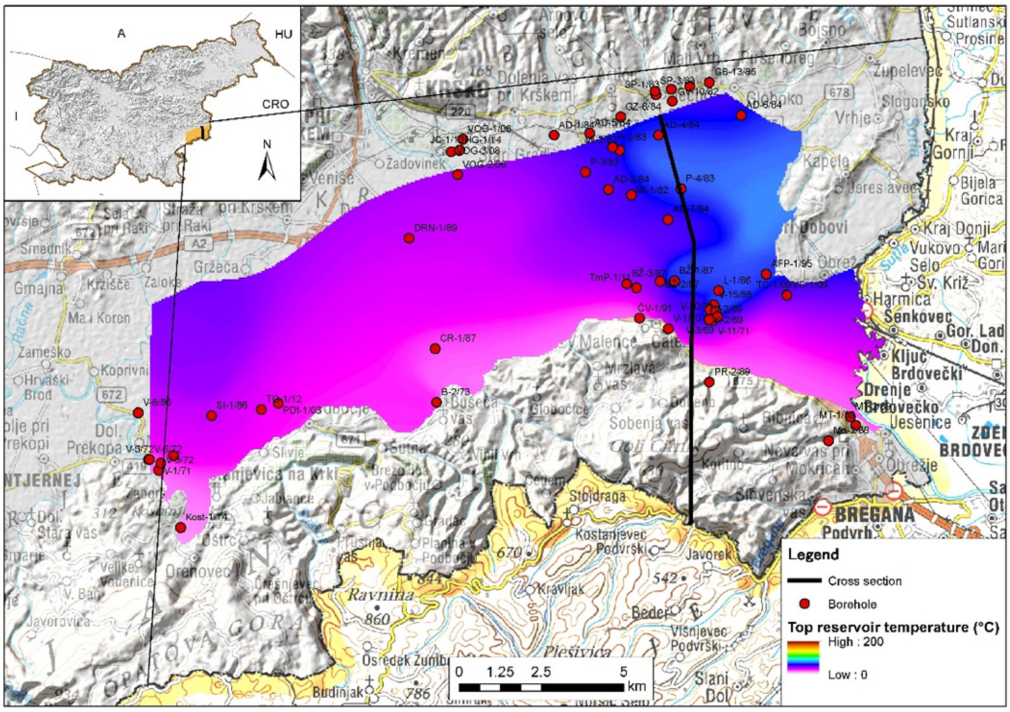

Figure 4.6.4: Temperature on the top of the HotLime target horizont (Upper Triassic)

We have distributed geotherms according to the relation between increasing temperatures in Tertiary beds and much higher and constant ones in Mesozoic complex. The increasing ($dT/dz > 0$) and the isothermal ($dT/dz = 0$) types of geotherm have been obtained in many boreholes. At the contact between Tertiary and Mesozoic sediments the isothermal type predominates, especially in the Čatež field area. Its main characteristic is high temperature, which is maybe a sign that a borehole is situated at top of the fractured convection-dominated area. An example of such geotherm is represented from the AFP-1/95 borehole at Dobova (Figure 4.6.5) that has reached a thermal aquifer with 63°C. An example of completely isothermal geotherm is from the V-2/69 borehole at Čatež Spa (Figure 4.6.5). Geothermal gradient there is almost zero due to measurements in artesian condition.

High temperatures are calculated also north of the main anomaly of the Čatež field that are even higher than those measured in boreholes of the Čatež field owing to the rapidly deepening of the Triassic base towards north.

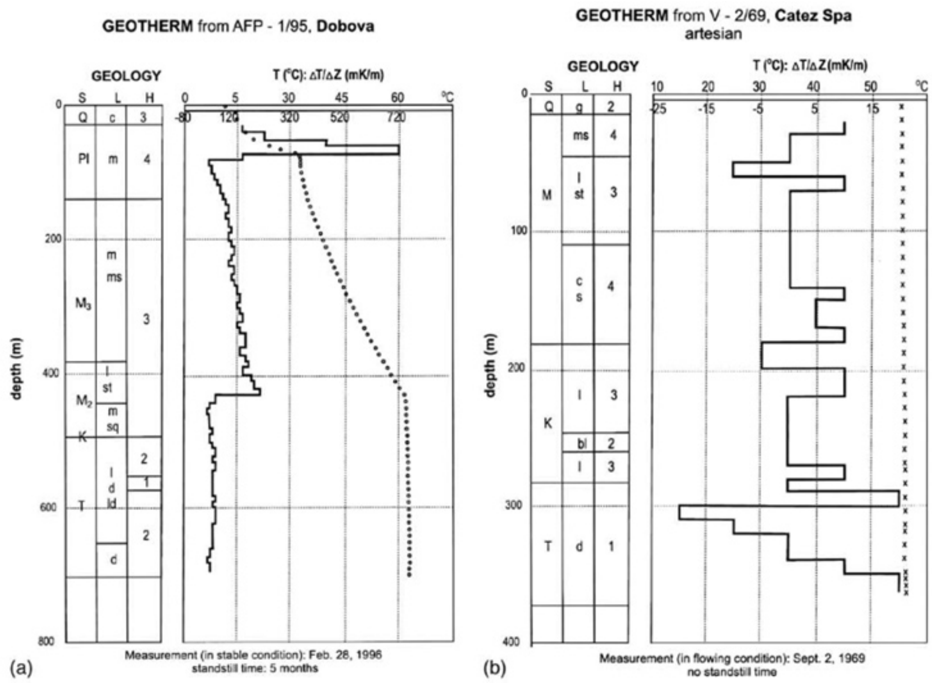

Figure 4.6.5: Measured temperatures in APF-1/95 and V-2/69.

The results, especially from the Čatež field, show the temperature increase of thermal water from south to north. A similar situation, although with lower temperatures, is determined north of Kostanjevica. Below Tertiary sediments Mesozoic carbonates (mostly dolomites) form primary aquifers with thermal water. Within them there is up to 100 m thick sequence of mostly low permeable Upper Cretaceous beds (»scaglia«).

The highest temperature (64°C) was recorded in a borehole in the middle of the Čatež field within Čatež Spa. There is at least one deep water flow from the Gorjanci Mountains below the Čatež field area further to the north that is heated in depth and somewhere at fault zones it partly turns and flows southward immediately below the Tertiary (Cretaceous) low permeable cover. This flow must be quite intense what is proved by high porosity that is a consequence of chemical solution of rocks by thermal water at the Tertiary – Mesozoic contact (VERBOVŠEK et al. 1986).

Maximum temperature and circulation depth

Surface meteoric waters flow into depth and get warmer due to elevated or just average geothermal gradient. If they are heated enough, they flow, as becoming lighter, to the surface through open fractures or through fissured permeable zones and emerge as thermal springs on the surface. Such circulation can be created also due to forced convection without the need for very heated water. Ordinarily it is possible to get water of higher temperature than the one at thermal spring if it is captured with a borehole below the zone of mixing with colder groundwater. Even if the influence of subsurface water cooling is isolated, it is questionable whether we have attained the maximum possible temperature.

The necessary circulation depth for meteoric water to reach temperatures of 55 to 80°C in the Čatež field may be estimated from the geothermal gradient. In the boreholes around the Čatež field anomaly gradients are in the range 17 – 27 mK/m and almost on the border of geothermal anomaly they are about

37 mK/m. Assuming temperature T0 to be 11°C, such gradients would place the circulation depth of the Čatež thermal water with at least 60°C in the range of 2 to 3 km.

The most important geothermal anomaly is the broader Čatež field area where geological, hydrogeological and geothermal research has been predominantly concentrated. The boreholes there have reached temperatures of 50 to 64^{0}C.

Deeper boreholes with acquired thermal data are concentrated in the Čatež field. The highest temperatures, say over 50ºC, at certain depths (i.e. 300 m) after data acquired to date are found in the Čatež field and further to the ENE towards Dobova.

REFERENCES

PLACER, L. (1998): Strukturni pomen Posavskih gub. – Geologija **41**: 191-221.

PLACER, L. (2008): Principles of the tectonic subdivision of Slovenia. = Osnove tektonske razčlenitve Slovenije. – Geologija **51**(2): 205–217.

TOMLJENOVIĆ, B. & Csontos, L. (2001): Neogene–Quaternary structures in the border zone between Alps, Dinarides and Pannonian Basin (Hrvatsko zagorje and Karlovac Basins, Croatia). - International Journal of Earth Sciences **90**(3): 560–578. https://doi.org/10.1007/s005310000176

VERBOVŠEK, R., LOČNIŠKAR, A. & NOSAN, A. (1986): Thermal water research in the Čatež field. – Unpublished Report, Geological Survey Ljubljana, 20 pp (in Slovene).

4.7 Zagreb geothermal field (HR) – T2.7

Staša Borović & Marco Pola (HGI-CGS)

4.7.1 Inducement and Objectives

Zagreb is the capital of the Republic of Croatia and by far the largest urban agglomeration in the country with 800,000 inhabitants (DZS, 2018), meaning, among other, that it has a high energy demand, around half of it being for thermal energy, with an average of 220 heating days annually.

Zagreb geothermal field (GTP ZG) was discovered in 1964 by hydrodynamic (HD) measurements on a negative hydrocarbon well. Since the testing yielded significant amounts of thermal water, the area was developed as geothermal field, which included drilling additional 26 wells until 1988. The measurements indicated a sustainable pumping capacity of 77 l/s using geothermal doublets while in 2018 only 9 l/s on average were utilized (only one doublet system is in operation).

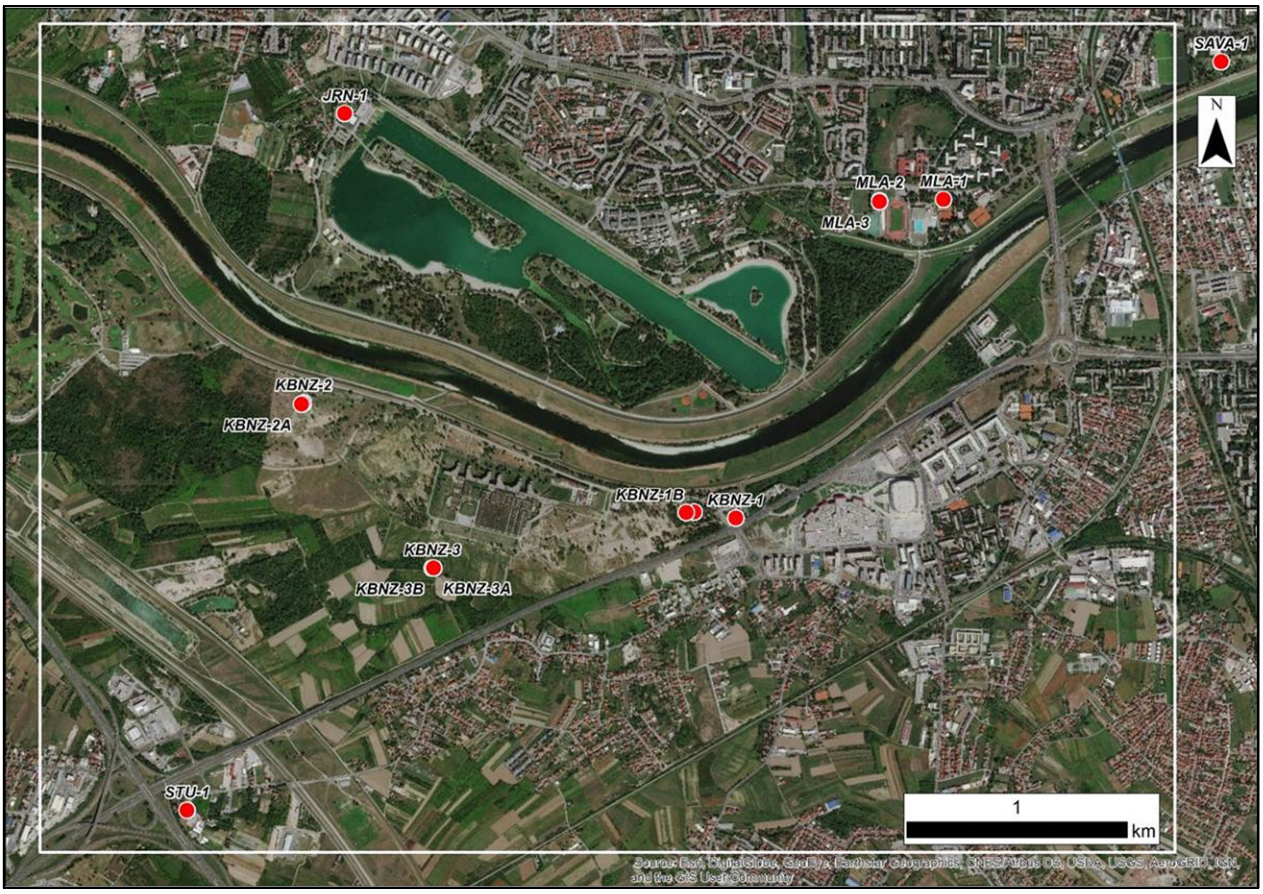

Figure 4.7.1: Central part of the Zagreb geothermal field (satellite imagery in the background by Google Earth).

Despite significant quantity of previously acquired geological and geophysical data, contemporary scientific researches of GTP ZG are lacking because of two principal reasons: (i) extremely low level of resource utilization did not warrant funding of detailed (hydro)geological and reservoir engineering research by the user and (ii) data (although acquired by national petroleum company - INA - using public funds) was not available to researchers. Data used and interpreted in WP2 was obtained by the

Hydrocarbon agency of the Republic of Croatia (AZU) on 22 October 2018 for use in this project for scientific purposes only.

In the area of GTP ZG a total of 27 boreholes were drilled, 30 seismic reflection profiles were measured, as well as 589 points of gravimetric measurements (i.e. 11 points/km^2) and 389 magnetometric measurements (i.e. 7 points/km^2) (ZELIĆ et al. 1995). In communication with the AZU borehole and seismic data were obtained, while the gravimetric and magnetometric data seem to be missing. Inquiries were also made toward INA, but they are also unaware of these data.

4.7.2 Study area and geological setting

GTP ZG extends below the Croatian capital itself (Figure 4.7.1), comprising the area of 54 km^2, according to conducted researches (ZELIĆ et al. 1995). The area is situated in the NW part of the Sava Basin in the SW part of the Pannonian Basin System (PBS) (Figure 4.7.2). Formation of the PBS started during Early Miocene by continental collision of and subduction of Eurasian plate beneath Pannonian crustal fragment. The back-arc extensional tectonic regime in the PBS formed four elongated sub-basins that represented main depocentres: Drava Basin, Bjelovar Basin, the Sava Basin, and Eastern Slavonian Basin (PAVELIĆ & KOVAČIĆ 2018). Due to extensional tectonic setting, the majority of faults display normal character.

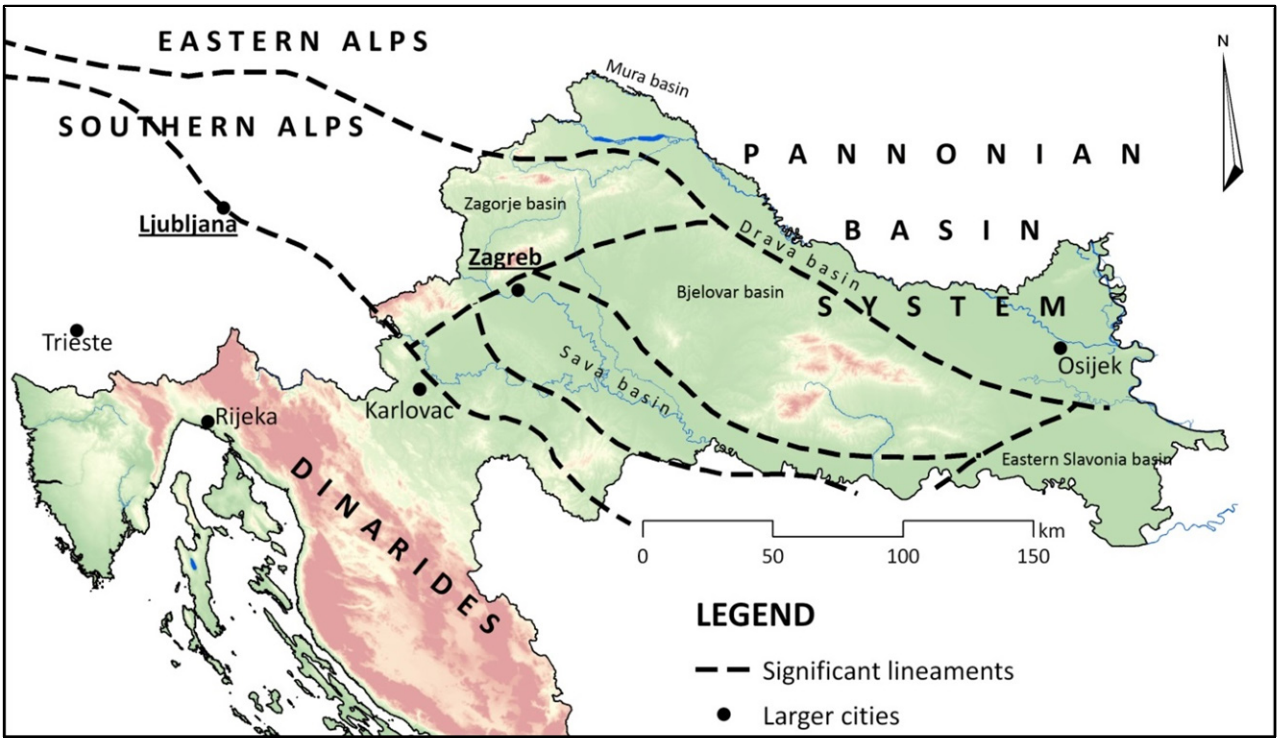

Figure 4.7.2: Position of Croatia in relation to major European tectonic units (according to TARI & PAMIĆ 1998; LUČIĆ et al. 2001; VELIĆ et al. 2012). Adopted from (BOROVIĆ et al. 2016).

GTP ZG includes two distinctive but connected carbonate thermal aquifers: Triassic dolostones, limestones and dolomitic limestones and Lower and Middle Miocene bioclastic (*Lithotamnium*) limestones.

Triassic aquifer is very fractured and can predominantly be classified as dolomite breccias with high secondary porosity and good permeability. The thickness of the aquifer varies from 5 to 357 m.

Miocene aquifer has good primary porosity due to bioclastic composition, but also good secondary porosity, appearing as breccia or breccia-conglomerate in some boreholes. Owing to that, it has excellent permeability.

The whole formation has thickness from 35 to 1,016+x m, however, it also includes marly sections of lower permeability and cannot be considered an aquifer in total thickness.

Geothermal aquifers are overlain by a thick succession of Tertiary and Quaternary sedimentary rocks and sediments: M_6^1 Prkos Fm (clayey limestones, M_6^2 Ivanić Grad Fm (marl, sand, sandstone, gravel, conglomerate), M_7^1 Kloštar Ivanić Fm (marl, sand, clay), M_7^1 and M_7^2 Široko Polje Fm (sand, marl, clay), PlQ Lonja Fm (gravel, sand, silt, clay).

4.7.3 3D geological modelling

Due to lacking digitalized materials of any kind, the collaborators working on T.2.7 have not committed to 3D modelling in this phase of the research, as foreseen also during project application. The main cause is the expected (and indeed confirmed) status of the data gathered by the national petroleum company decades ago. Fig. 4.7.3 exemplifies the problems encountered in that sense.

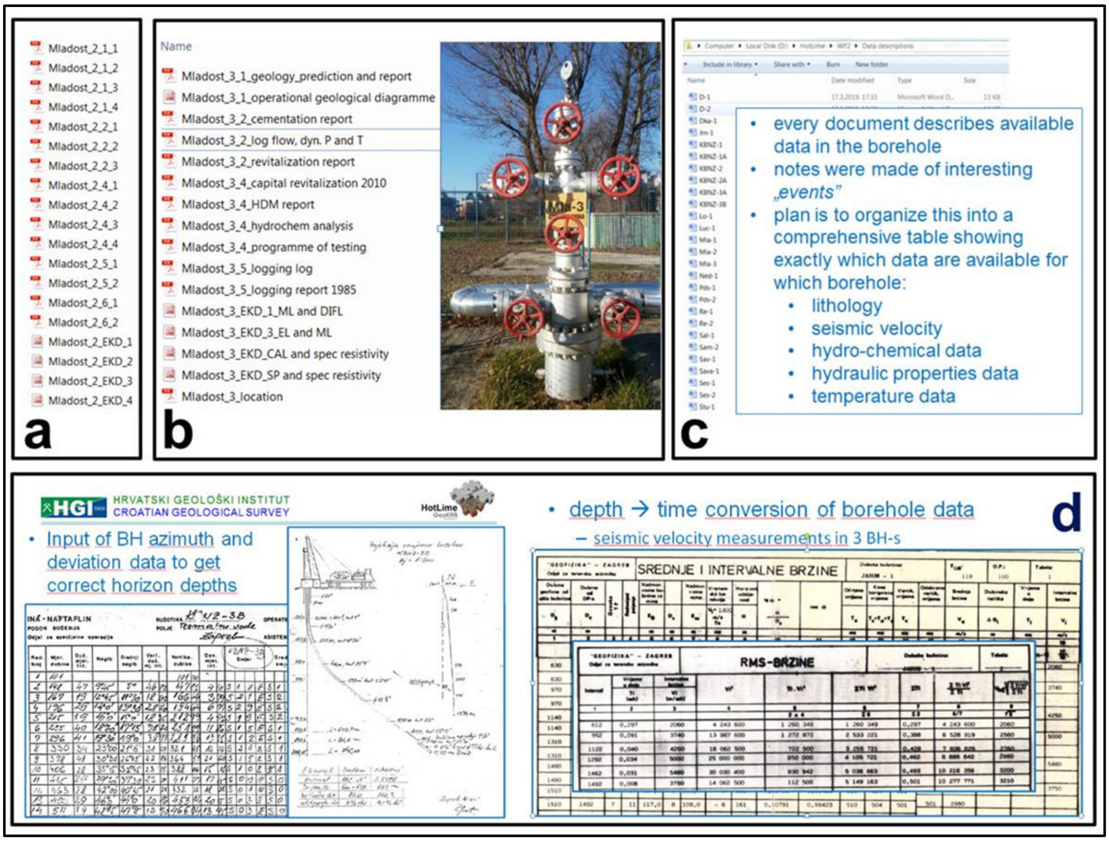

Figure 4.7.3: (a) original data and file names; (b) renamed files; (c) created data descriptions; (d) examples of the scanned PDF documents.

In this phase of research the geometry of the described aquifers was defined by analyzing existing bibliography about this area and by visual analysis of seismic sections. More detail interpretation of seismic section was not possible due to lack of digitalized borehole data. The oldest determined rocks are Mesozoic and Paleozoic crystalline basement which represent footwall to the Triassic geothermal aquifer. Triassic geothermal aquifer is composed of dolstones, dolomites and dolomitic limestons with thickness between 50 and 350 m (Figure 4.7.4). Triassic aquifer is overlain by thick sequence of Miocene sediments of the Sava Basin. Boundary between Triassic aquifer and Neogene sediments is transgressive in character. Lowermost unit of Miocene are Badenian transgressive bioclastic breccias and biogenetic *Lithotamnium* limestones. This unit represents second geothermal aquifer. Cover of the Badenian aquifer is composed of vertical and lateral interchanges of marls, sandstones, clayey sandstones and sandy marls with thickness over 1 km. Two aquifers have an overall thickness of over 500 m in some places. Main structural features are normal faults, moderately dipping towards NW and SE. Faults are probably of lower to middle Miocene age since they do not reach the surface (Figure 4.7.4).

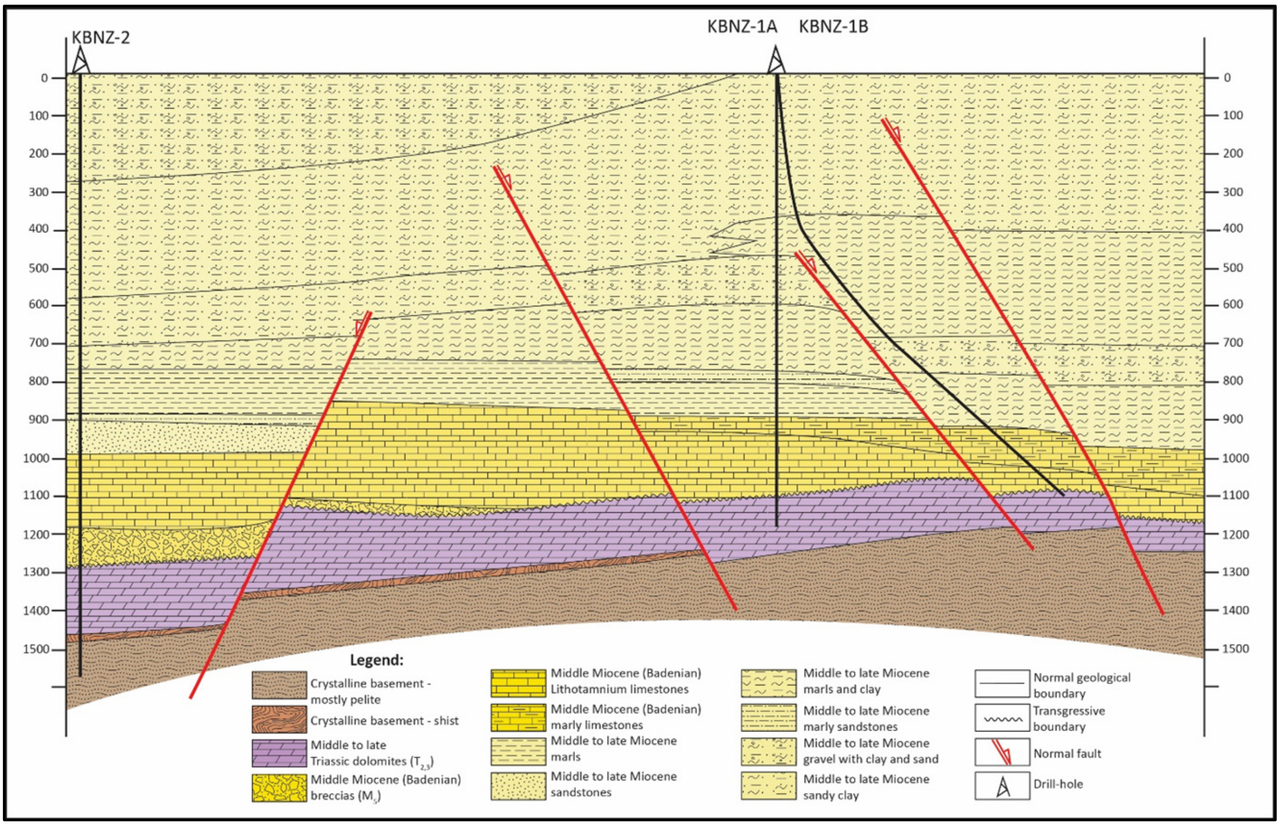

Figure 4.7.4: Characteristic geological cross-section in the productive part of the GTP ZG.

4.7.4 Rock property and Temperature modelling

Hydrogeological parameters

HD measurements were conducted at the following boreholes:

- KBNZ-1A - calculated permeability 4.32 - 4.53 E-13 m^2, sustainable pumping rate 8 l/s;
- KBNZ-3B - measurements in *Lithotamnium* limestones (1,245-1,347 m) did not yield especially good results: airlift gave only 0.25 l/s of water, temp 33-35 °C;
- Lo-1 - DST at two different depths in *Lithotamnium* limestones: hydrodynamic characteristics at 1737-1759 m were determined as not favourable; at 1700-1936 m favourable, water T = 93 °C; laboratory measurements show porosity of 17.5 % and permeability of 0.3 mD;
- Luč-1 - filter section in *Lithotamnium* limestones: outflow of 10 - 6.2 l/s, water temperatures 55-58 °C;
- Mladost system HD measurements: filter sections in *Lithotamnium* limestones (950-1,050 m), Mla-1 17 days of test production, ca. const. 290 m^3/day (3.4 l/s) with T = 68 °C; Mla-2 3,600 m^3/day (41.7 l/s) with T = 64 °C; Mla-3 4,200 m^3/day (48.6 l/s) with T = 79 °C. Permeability was calculated from interference measurements of Mla-1 and Mla-2 (5,874 mD) and Mla-1 and Mla-3 (6,977 mD). Mla-3 is logically chosen for production, and Mla-2 for reinjection, and that is the only active doublet system of GTP ZG until present day;
- N-1 - filter section in both Miocene and Triassic aquifer; after well development, the outflow is almost const. 9.5 l/s of 64-65 °C water;
- Sava-1 - laboratory measurements on *Lithotamnium* limestone (1,032-1,040 m) show porosity of 5.6 % and permeability of 0.02 mD;
- Stu-1 - permeability was calculated from interference measurements of Stu-1 and KBNZ-3A (213 E-9 m^2).

Due to spatial constraints of this report, data cannot be presented. However, it can be stated that at the majority of the 27 wells at least some kind of production testing was performed - ranging from filling in test pools to serious DSTs. Laboratory poro/perm measurements are quite rare and show lower permeabilities than natural-scale reservoir tests, accentuating the importance of fault and fracture systems for the geothermal aquifers in GTP ZG. An interesting and detailed approach of interference testing (which was the basis for the determination of geothermal field size) may be useful in the future as calibration data for models.

Hydrochemical parameters

Laboratory analyses of water samples from six wells in GTP ZG were done between the years of 1984 and 1992. These data were also found in the borehole documentation. Principal anion and cation composition is shown numerically and graphically in Fig. 4.7.5. It is visible from the Fig. 4.7.5.a that the total mineralization is not especially high (around 2 mg/l). The only exception is the water from KBNZ-3A borehole, which has much lower mineralization (0.6 mg/l) - not even considered mineral water (the limit is set at 1 g/l in Croatia (MARKOVIĆ et al. 2015)). KBNZ-3A well punctured the geothermal aquifer at shallower depth, so that could be the cause of lower TDS - a hypothesis to be tested via future data analyses. Also, the majority of hydrothermal systems in the Republic of Croatia are fed by fractured carbonate (predominantly dolostone) aquifers (BOROVIĆ et al. 2016), and they exhibit mineralization lower than 1 g/l, i.e., they are more alike to cold and potable groundwaters from carbonate aquifers (BOROVIĆ 2015; MARKOVIĆ et al. 2015; ŠIMUNIĆ 2008). Although it is absolutely proven during drilling operations that the water resides in dolostone and limestone aquifers, the water chemistry does not immediately reflect it: the waters display Na-HCO_3 hydrochemical facies, and adding to that, also high chloride anion content. Even though counterintuitive, such water composition and hydrochemical stratification is known in other carbonate aquifers in the PBS and indicates long residence time of groundwater (SZŐCS et al. 2013). That is a consequence of cation exchange of Ca^{2+} and Mg^{2+} cations with Na^{+} cations during longer time periods (HEM 1989).

a

	Mla-1	Mla-2	Mla-3	KBNZ-1A	KBNZ-1B	KBNZ-3A
Ca^{2+}	65	56	20	43	46	36
Mg^{2+}	12	9	8	28	16	11
Na^{+}	576	550	495	516	525	125
K^{+}	23	30	27	28	25	15
HCO_3^-	991	926	732	973	814	247
Cl^-	252	255	234	248	294	50
SO_4^{2-}	322	290	296	239	284	158
TDS	2248	2122	1822	2083	2013	645

b

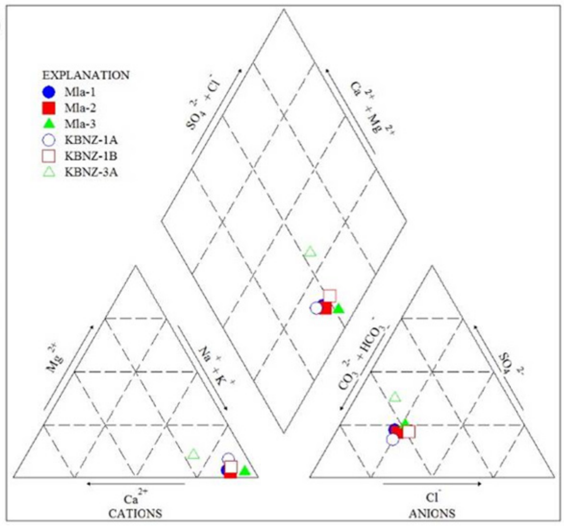

Figure 4.7.5: Major ion composition (a) and Piper diagram (b) of the waters from GTP ZG boreholes in Mladost and KBNZ technological systems.

New data concerning water and gas geochemistry are expected over the course of the next months because a sampling campaign was conducted in November 2019 in collaboration with DeepCarbonObservatory project (https://deepcarbon.net/). The data will encompass:

- *in situ* measurements of physico-chemical parameters and alkalinity;
- laboratory analyses of water: principal anions and cations (Ca^{2+}, Mg^{2+}, Na^{+}, K^{+}, HCO_3^-, SO_4^{2-}, Cl^-), isotope composition of hydrogen and oxygen in the water, trace elements, strontium isotopes, total dissolved inorganic carbon (TDIC), dissolved hydrogen-sulphide (H_2S) and ammonia (NH_4), isotope composition of sulphur and oxygen from sulphates (SO_4^{2-}), dissolved gas composition;
- laboratory analyses of gas: gas composition, ^{13}C from CO_2, ^{2}H from CH_4, noble gas analyses.

The sampling was done in both most productive localities of GTP ZG: Mladost (production well Mla-3) and KBNZ (production well KBNZ-1B) (Figure 4.7.6). Analyses will be conducted in different specialized laboratories. They should give an insight into the connection of identified geothermal aquifers to deeper sources of analysed compounds (if such connection exist, e.g. in the fault zones).

Figure 4.7.6: Sampling at KBNZ-1B well of GTP ZG (30/11/2019): (a) gas sampling; (b) water sample conservation; (c) an example of full set of water and gas samples for different analyses. Photo: V. Cazin.

Thermophysical parameters

Thermal conductivities of rocks and sediments in the area of GTP ZG were measured on a total of 43 samples by Kovačić (2002) and 26 samples by Borović (Soldo et al. 2016). Average thermal conductivities range from 1.8 W/(m·K) for sediments at shallow depths (up to 150 m), 2.7-3.3 W/(m·K) for Miocene *Lithotamnium* limestones and up to 4.4-5.3 W/(m·K) for Triassic carbonate rocks. Samples were outcrop analogues and borehole core samples in similar proportion.

In the borehole data obtained by the AZU no data on thermal properties measurements were found.

Temperature Modelling

Available temperature data include BHT from the majority of the boreholes, while temperature logs are available from 15 boreholes. Temperature logging data was used in order to make a uniform overview of the temperatures at 500 m and 1,000 m depths.

Unfortunately, no time-since-circulation info, mud consistency and temperatures are recorded, so attempts of correction would be dubious. There are reports of such situation being resolved by simply increasing temperature by some amount, e.g. by 18 °C (Corrigan, 1997) or by 10% (Joyner 1975). In this report the temperatures interpolated from raw thermal logging data at (a) 500 m and (b) 1000 m depth-sections are presented (Figure 4.7.7). The interpolation was done using ESRI ArcGIS software, Spatial Analyst Tool, Natural Neighbor interpolation. The interpolation was used with default parameters. Previously all other interpolation methodologies available in the software were tried out with different settings, and the interpolation method with the lowest RMS error was selected. These depths were selected because those are the depths currently utilized and expected to be utilized in foreseeable future.

It is visible that at both depth sections the temperatures are the highest in the productive areas of Mladost and KBNZ systems in the central part of GTP ZG. Temperatures range from 27 to 52 °C at 500 m, and from 38 to 81 °C at 1,000 m depths.

Although the temperature data has not been subjected to corrections, we have reason to consider them realistic because in all the wells which had Drill Stem Test data the temperatures were corresponding to thermal log data. Our assumption is that it is because of the shallow depth of the geothermal aquifer, as well as because of its high permeability.

(a)

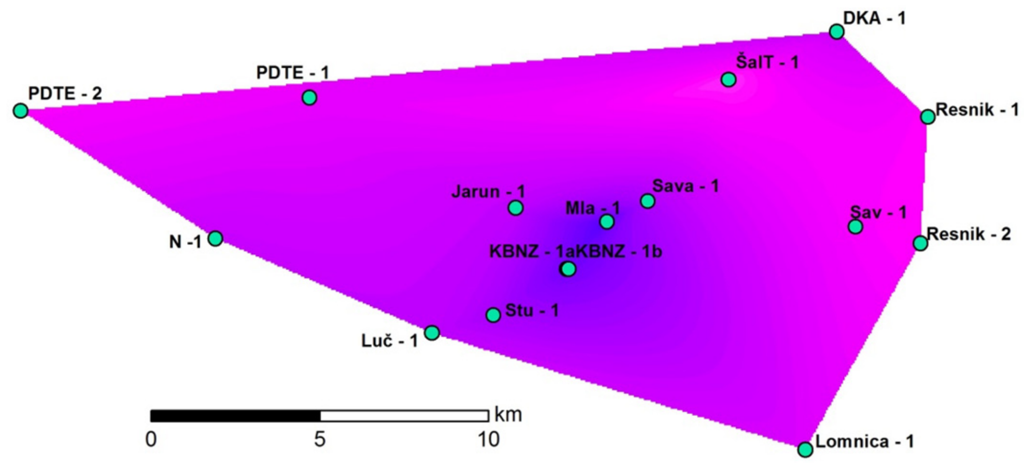

(b)

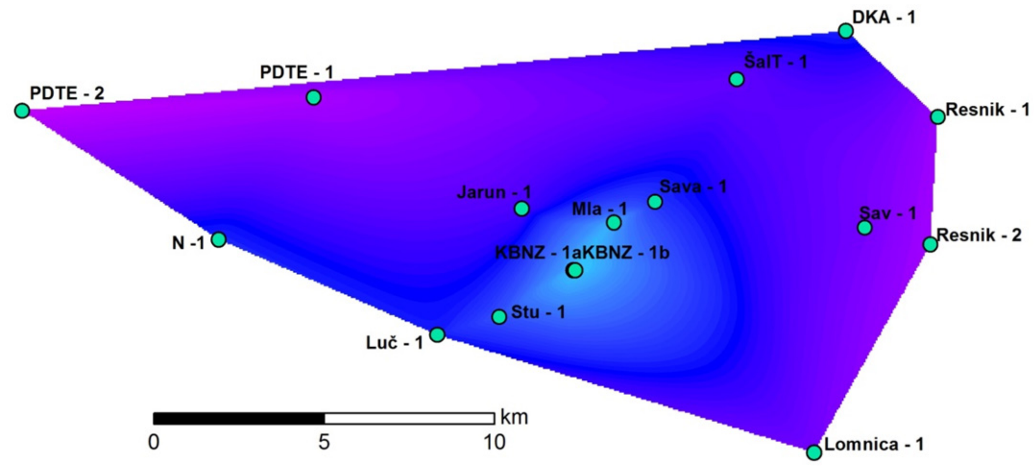

Figure 4.7.7: Interpolated temperatures at (a) 500 m and (b) 1,000 m.

REFERENCES

BOROVIĆ, S. (2015): Integrated hydrogeological-hydrogeochemical model of Daruvar geothermal aquifer. – Unpublished PhD thesis, University of Zagreb - Faculty of Mining, Geology and Petroleum Engineering, Zagreb, 148 p. (in Croatian)

BOROVIĆ, S., MARKOVIĆ, T., LARVA, O., BRKIĆ, Ž., & MRAZ, V. (2016): Mineral and thermal waters in the Croatian part of the Pannonian basin. – In: PAPIĆ, P. (ed.): Mineral and Thermal Waters of Southeastern Europe. Springer, Cham, 31-45.

CORRIGAN, J. (1997): Correcting bottom-hole temperature data. – AAEPT Research Memo **97-007**.

CROATIAN BUREAU OF STATISTICS (DZS): Results of the 2011 population census, https://www.dzs.hr/ [2019-07-30]

LUČIĆ, D., SAFTIĆ, B., KRIZMANIĆ, K., PRELOGOVIĆ, E., BRITVIĆ, V., MESIĆ, I. & TADEJ, J. (2001): The Neogene evolution and hydrocarbon potential of the Pannonian Basin in Croatia. – Marine and Petroleum Geology **18**: 133-147.

HEM, J. D. (1989): Study and Interpretation of Chemical Characteristics of Natural Water 3rd edition. – USGS, Menlo Park, California.

JOYNER, H. D. (1975): A correlation of electric-log-indicated temperature with actual reservoir temperature - Southwest Louisiana. – Journal of Petroleum Technology **27**: 181-182.

KOVAČIĆ, M. (2002): Causes of a positive geothermal anomaly in the Zagreb area. – Unpublished PhD thesis, University of Zagreb - Faculty of Mining, Geology and Petroleum Engineering, 102 p. (in Croatian)

MARKOVIĆ, T., BOROVIĆ, S. & LARVA, O. (2015): Geochemical characteristics of thermal waters of Hrvatsko zagorje. – Geologia Croatica **58**(1): 67-77.

PAVELIĆ, D. & KOVAČIĆ, M. (2018): Sedimentology and stratigraphy of the Neogene rift-type North Croatian Basin (Pannonian Basin System, Croatia): A review. – Marine and Petroleum Geology **91**: 455-469.

SOLDO, V., BOBAN, L. & BOROVIĆ, S. (2016): Vertical distribution of shallow ground thermal properties in different geological settings in Croatia. – Renewable Energy **99**: 1202-1212.

SZOCS, T., RMAN, N., SÜVEGES, M., PALCSU, L., TÓTH, G. & LAPANJE, A. (2013): The application of isotope and chemical analyses in managing transboundary groundwater resources. – Applied Geochemistry **32**: 95-107.

ŠIMUNIĆ, A. (2008): Influence of geological structure to the emergence of thermal and mineral waters. – In: ŠIMUNIĆ, A. (ed.): Geothermal and mineral waters of the Republic of Croatia. – Croatian Geological Survey, Zagreb, 5-36. (in Croatian)

TARI, V. & PAMIĆ, J. (1998): Geodynamic evolution of the northern Dinarides and the southern part of the Pannonian Basin. – Tectonophysics **297**: 269-281.

VELIĆ, J., MALVIĆ, T., CVETKOVIĆ, M. & VRBANAC, B. (2012): Reservoir geology, hydrocarbon reserves and production in the Croatian part of the Pannonian Basin System. – Geologia Croatica **65**(1): 91-101.

ZELIĆ, M., ČUBRIĆ, S., KULENOVIĆ, I., KUŠEK, M., MARČAN, B. et al.: Main mining design of the Zagreb Geothermal Field. – INA plc., Zagreb, (1995), 268 p. (in Croatian)

4.8 Pantelleria - Linosa - Malta Rift Complex (MT) – T2.8

Charles Galea (OPM)

4.8.1 Inducement and Objectives

The main objective of case study T2.8 was to carry out a preliminary investigation of the geothermal potential of a study area in Malta.

Malta can easily be overlooked as a location for geothermal energy exploitation as there are no manifest surface expressions of geothermal sources such as hot springs, geysers or hot aquifers. Although the Maltese Islands are located on an extensive and thick carbonate platform and thus not situated in an ideal geological setting for geothermal energy exploitation, a pronounced rift complex located southwest of the Islands partly within the study area, could provide such conditions. This complex is called the Pantelleria - Linosa - Malta Rift Complex (PLMRC), a zone of pronounced crustal extension, lithospheric thinning, magma intrusion, volcanism and thermal subsidence. The volcanic islands of Pantelleria and Linosa form part of this fault complex through which lava was extruded and along which the islands have elongated.

This case study aims to assess the geothermal potential of deeply buried carbonates in the study area.

4.8.2 Study area and geological setting

T2.8 covers a surface area of 6,850 km^2. It includes the Maltese Islands (an area of 316 km^2) and the surrounding marine waters. Water depths in the study area vary from very shallow (<50 m) to very deep (>1,000 m).

Regional geological setting

The Maltese Islands are located on the Pelagian Block of the Central Mediterranean. This block is attached to the African plate and constitutes part of the African foreland area. It is bounded on its sides by four major structural elements:

- The Calabrian fore-arc scraping zone in the north, marking the collision zone between Africa and Europe;
- The Sicily - Malta Escarpment in the east, a passive Neotethyan margin separating the Pelagian Block from the Ionian Basin;
- The Gafsa-Djeffara fault system in the south, running parallel to the Tunisian and Libyan coasts;
- The North-South axis of Tunisia in the west, a geomorphic and structural feature separating the Sahel (the onshore portion of the Pelagian Block) from the Atlasic folds.

The Pelagian Block is made up of a thick (>8 km) sedimentary sequence underlain by continuous crystalline basement. It is extensively faulted in places as a result of several extensional phases since the Late Paleozoic. A pronounced rifting phase occurred in the Late Triassic - Early Jurassic when the Pelagian Block was extended as a result of the opening of the Neotethys in the east resulting in the formation of several rift basins.

The most recent and significant tectonic event from the point of view of geothermal dynamics in Malta is the formation of the PLMRC which formed in the Late Miocene - Early Pliocene and is still active today. This rift complex divides the Maltese Islands and the surrounding areas into two main tectono-stratigraphic domains: (i) a platform domain north of the Islands and (ii) a rift domain in the southwest.

The platform domain includes the Maltese Islands and consists of a very thick Mesozoic - Tertiary sequence consisting mainly of limestones and dolomites and occasional evaporites and marls. The sequence is also characterized by Jurassic and Cretaceous volcanic occurrences drilled in deep oil exploration wells. Red marls of continental - sabkhaic origin have been encountered in the Late Triassic.

The rift domain lies immediately to the southwest of Malta along a structurally complex elongated belt defined by bounding faults trending predominantly NW-SE. The complex is characterized by numerous horsts and grabens, volcanic occurrences and magmatic intrusions. The process of rifting produced three pronounced bathymetric features namely the Pantelleria, Linosa and Malta Troughs having maximum water depths of 1,300 m, 1,600 m and 1,700 m respectively. The troughs are filled with Lower Pliocene - Pleistocene turbidites with thicknesses of about 1,000 m, 2,000 m and 1,500 m respectively. The origin of the PLMRC is debatable. Some authors consider the troughs as an expression of large pull-apart basins developed along a principal dextral wrench zone connecting the plate collision in northwest Africa and northern Sicily with that occurring at the Aegean plate boundary, south of Greece. Others consider the crustal stretching and subsequent rifting and fault development as being controlled by slab-pull forces of the subducted African slab beneath the Tyrrhenian basin, causing trench retreat and roll-back of the African plate in the collision between Africa and Europe.

The rift area is highly significant for geothermal energy potential as demonstrated by ongoing commercial exploration activities onshore Pantelleria. Although temperature gradients measured in wells are relatively low in the Malta platform domain, they demonstrate appreciably higher values in the rift domain.

Geological framework of the main carbonate reservoir

The sedimentary sequences onshore and offshore Malta consists mostly of carbonates with interbedded marls and evaporites. Although there are several carbonate formations that can act as potential thermal reservoirs in the Cretaceous-Jurassic interval, this case study will focus on the upper member of the Late Triassic Kercem Formation.

The upper member of the Kercem Formation is of Norian-Rhaetian age. It consists predominantly of interbeddings of carbonate mudstone, packstone and grainstone. These lithofacies are characteristic of shallow water carbonates deposited in a shelf environment.

The Kercem Formation has only been encountered in the MTZ well, a deep stratigraphic well drilled in the study area (see figure 4.8.2 for location) onshore Gozo in 1999. The well penetrated nearly 1,300 m of the upper member of the Kercem Formation at a depth of 6,055 m below sea level.

Although the top of the Kercem Formation was mapped from 2D seismic data in the study area, the bottom of this interval could not be mapped with sufficient confidence and thus there is not enough well and seismic data to map the thickness of this potential reservoir in the study area. However, given the paleo-depositional environment in which the formation was deposited and in the absence of other data, the thickness of the member encountered in the onshore well was considered as a representative thickness in the area of interest.

The depth of the Kercem Formation is around 6,000 m in the study area, going down to over 7000 m in the deepest part of the Malta Graben. The formation is located at shallower depths along the uplifted flanks of the Malta Graben.

Overlying succession

The Kercem Formation is overlain by the Rhaetian Red Shale Formation, consisting of grey/green and red shales with layers of anhydrite and fine dolomite deposited in a continental to sabkha environment. The Red Shale Formation acts as thermal barrier separating the Kercem Formation from overlying cooler sediments. The overlying succession is characterized by a sequence of latest Triassic limestones and dolomites overlain by Jurassic – Cretaceous - Tertiary limestone and occasional marls.

Within the PLMRC, the sedimentary sequence is capped by thick deposits of pre- and post-rift Plio-Quaternary sediments having thickness which vary from less than 1,000 m on some structural highs to over 2,000 m within the grabens. The sediments consist mostly of carbonate muds, marls and a thick sand-shale sequence.

Several magmatic bodies intrude the sedimentary succession especially in the Pantelleria and Linosa Grabens. These are important in determining the heat flow distribution in the rift complex and surrounding areas.

Tectonic setting

The prevalent faulting system affecting the study area is an extensional NW-SE complex forming part of the PLMRC. One of these bounding faults extends onshore Malta (Maghlaq Fault) along the south coast of the island. Recent activity of this fault is demonstrated by slickensides on the fault scarps and displacement of recent sediments. This fault extends for a considerable distance offshore. The late Miocene – early Pliocene uplift as a result of tectonic activity in the PLMRC caused the emergence and subsequent tilting of the Maltese Islands towards the NNE.

An older fault system of early Mesozoic age trends ENE-WSW. This is evident onshore the Maltese Islands (Victoria Lines Fault in Malta and the Qala Fault in Gozo). The area between these two faults has been tectonically active since the early Miocene resulting in the development of a series of horsts and grabens which manifest at the surface as a series of valleys and ridges.

Although the predominant faults in the PLMRC are normal, strike-slip faults and are also known in the offshore. Indeed, some authors attribute the origin of the complex as a pull-apart basin which developed along a right-lateral wrench zone.

4.8.3 3D geological modelling

Input data sets

In order to create the subsurface maps, data from five wells located in the study area was used to calibrate the formation tops with available seismic data. Two wells are located onshore (NAX and MTZ) and three wells offshore (LAM, GOZ and AQ). The depths of the wells vary from shallow (AQ, 1,781 m) to very deep (MTZ, 8,012 m). Final geological reports, wireline logs and check-shot/VSP from these wells were available for this study.

Over 1,800 line km of offshore 2D time-migrated seismic data was used for the interpretation and mapping. The study area is not covered by any 3D or onshore seismic surveys. The available seismic data was acquired in marine surveys conducted in 1988, 1991, 2001 and 2014 and data consists of migrated stack for the two older surveys and pre-stack time migration for the more recent ones. Data coverage density across the study area is not uniform with maximum debsity north of the Maltese Islands.

The quality of the seismic data varies from good to fair. Data quality is very good in the Pliocene - Pleistocene and Tertiary intervals and but degrades appreciably in the Mesozoic section. In the structurally complex Malta Graben, data quality is affected by out-of-plane reflections from faults that cut to the sea-bed.

Principle modelling workflow

The following seismic horizons were interpreted and mapped in time and depth:

- Sea-bed
- Top of Miocene
- Top of Cretaceous and
- Top of Kercem Formation.

Seismic and well data were loaded and interpreted using Kingdom® software from IHS Markit. As the seismic datasets originated from various vintages, data was by checked for misties and phase reversals. Adjustments were necessary to the input data.

Interpretation was carried out in the time domain and then converted to depth. Interpreted lines were converted to depth using generalized mean interval velocities calculated from wells in Malta. The first two horizons can be interpreted with excellent confidence. These are high amplitude continuous events easily correlated across faults. The Top of the Cretaceous marks a prominent unconformity surface across the entire study area. At shallow intervals, pick continuity was often extremely poor. Evidence of discontinuities in the shallow section, possibly caused by erosion features makes interpretation away from well control more difficult. The quality of this horizon improves in sections having a thick overlying Plio-Quaternary sequence.

The Top of the Kercem Formation is identified as a low amplitude pick. Away from well control, the confidence in picking this horizon identification is fair to low.

4.8.4 Rock property and Temperature modelling

Hydrogeological and Thermo-physical parameters

Limited rock property data is available from MTZ, the only well in the study area that penetrated the Kercem Formation.

Porosity values of between 1% and 2% have been determined from bottom cores in the formation. Although primary porosity is low, interpretation of formation micro-scanner logs indicates that the upper member of this formation is extensively fractured in places becoming less so with depth. In addition, the predominant strike of the fractures is oriented favorably with respect to the horizontal stress direction so the fractures should remain open. This was collaborated by mud losses during the drilling of MTZ which indicate that the fractures are open. Evidence of water flow is evident from changes in mud salinity where increases in mud salinity were observed.

Salinity data is available from a single fluid measurement within the upper member of the Kercem Formation which yielded a sodium chloride content of 86 gr/l.

Temperature Data

Temperature profiles and gradients measured during logging were available for 13 wells. All wells in Malta show a generally linear temperature gradient with depth. This linearity is typical of low temperature environments and a lithology predominantly composed of low permeability carbonates for which heat transfer is by conduction only. The temperature gradient values vary from as little to 5^{o}C/km to about 19^{o}/km. Interestingly, the highest value of 28^{o}C/km has been recorded at AQ, one of the offshore wells in the study area located at the southern extent of the Malta Graben.

MTZ demonstrates two linear temperature gradients: the gradient above the Red Shale Formation is 13^{o}C/km and the gradient below reaches 27^{o}C/km.

Temperatures measured during logging are generally lower that the true formation temperature due to loss of thermal equilibrium during drilling operations and consequently the temperatures are negatively biased. The impact of this bias on heat flow estimation was validated for MTZ and found to have an associated bias of -2.5% (DEBONO 2014).

DEBONO (2014) constructed a preliminary heat flow map for the Maltese Islands and surrounding areas on the basis of temperatures recorded in deep oil exploration wells in Malta and on published information in the region. As thermal conductivity measurements for the Maltese rock formations are not known, published values for similar lithologies were used to extract the heat flows. The thermal conductivity of carbonates is relatively high for dense limestone and dolomite (3 $Wm^{-1}K^{-1}$ and 4.7 $Wm^{-1}K^{-1}$ respectively) and as a result heat flow is relatively fast and the geothermal gradient generally low. Other sediments like shale have thermal conductivities in the order of 1.5 to 2.3 $Wm^{-1}K^{-1}$ and consequently the geothermal gradient is twice as great for the same heat flow.

The lithology for the Malta wells is largely composed of limestone, dolomitic limestone and dolomite. Marls and anhydrite are also present in minor quantities as well as volcanics in some wells. An average thermal conductivity of 3.7 $Wm^{-1}K^{-1}$ was used for the wells except for GOZ for which an average value of 3.0 $Wm^{-1}K^{-1}$ was used due to the more marly carbonates encountered in the well.

A heat flow map was generated from the well data using the interval and Bullard methods. The heat flow is calculated from the product of the thermal conductivity and the thermal gradient in the interval method or from the slope of the temperature against thermal depth using the Bullard method.

The heat flow map (Fig. 4.8.2) defines two distinct provinces offshore Malta:

- A north province covering the platform domain characterised by low heat flow (<65 mWm^{-2}) and low average thermal gradients (<18 °C/km).
- A south province covering the rift area characterized by medium-to-high heat flows (>65 mWm^{-2}) and geothermal gradients (>18 °C/km).

Based on the above map, the upper member of the Kercem Formation in the rift domain area southwest of the Maltese Islands is expected to be at temperatures of >130°C. Although this area is offshore, the technology for the exploitation of offshore geothermal resources exists and could possibly be applied in the future.

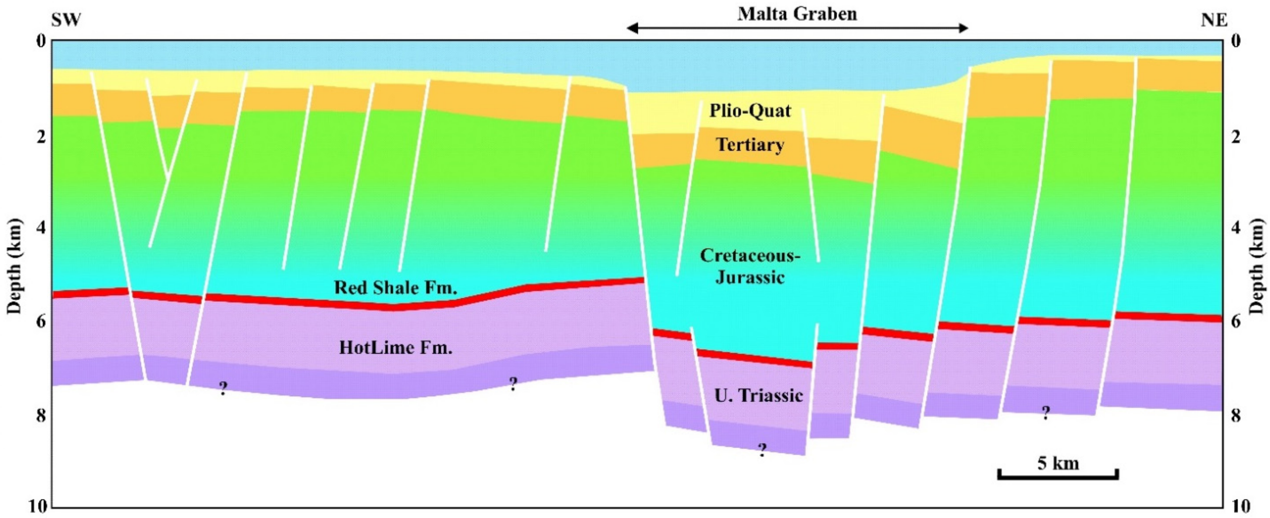

Figure 4.8.1: NE-SW depth section across the study area showing the HotLime Formation at about 6,000 m close to the Maltese Islands (VE = 2x)

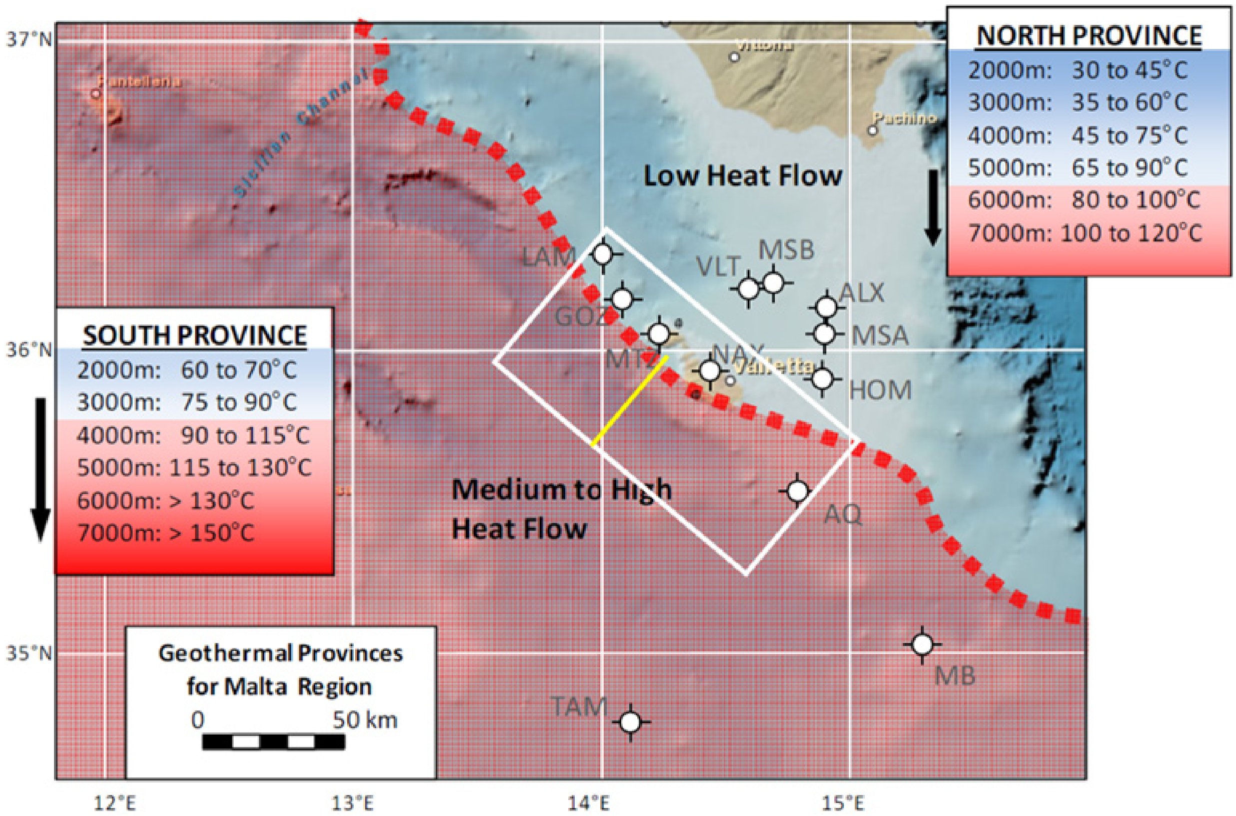

Figure 4.8.2: Map showing geothermal provinces in the Malta region (study area in white, depth section location in yellow)

REFERENCES

ARGNANI, A. (1990): The Strait of Sicily rift zone: Foreland deformation related to the evolution of a back-arc basin. – Journal of Geodynamics **12**: 311-331.

ARGNANI, A. (1993): Neogene Basins in the Strait of Sicily (Central Mediterranean): Tectonic Settings and Geodynamic Implications. – In: BOSCHI, E., MANTOVANI, E., MORELLI ,A. (eds): Recent Evolution and Seismicity of the Mediterranean Region. – NATO ASI Series (Series C: Mathematical and Physical Sciences), **402**. Springer, Dordrecht.

DEBONO, G. (2014): A preliminary assessment of the geothermal potential of Malta. (unpublished)

CIVILE, D., LODOLO, E., ACCETTELLA, D., GELETTI, R., BEN-AVHRAHAM, Z., DEPONTE, M., FACCHIN, L., RAMELLA, R. & ROMEO, R. (2010): The Pantelleria graben (Sicily Channel, Central Mediterranean): An example of intraplate 'passive' rift. – Tectonophysics **490**: 173-183.

JONGSMA, D., VAN HINTE, J.E. & WOODSIDE, J. M. (1985): Geologic structure and neotectonics of the north African continental margin south of Sicily. – Marine and Petroleum Geology **2**: 156-179.

LODOLO, E., CIVILE, D., ZANOLLA, E. & GALETTI, R. (2012): Magnetic signature of the Sicily Channel volcanism. – Marine Geophysical Research **33**: 33-44.

STOBER, I., FRITZER, T., OBST, K., AGEMAR, T. & SCHULTZ, R. (2017): Deep Geothermal Energy – Principles and Applications in Germany. – Leibniz Institute of Applied Geophysics , 88p. https://www.geotis.de/homepage/sitecontent/info/publication_data/public_relations/public_relations_data/LIAG_Deep_Geothermal_Energy.pdf

4.9 Empordà Basin (ES) – T2.9

Montse Colomer Casas & Ignasi Herms Canellas (ICGC)

4.9.1 Inducement and Objectives

The Catalan Case study focuses in Empordà Basin (EB) (NE Catalonia, Spain) where a potential hot deep aquifer exists in a Lower Tertiary Eocene carbonate reservoir according to geothermal evidences from old deep wells (gas/oil). Thus, there is no hydrothermal evidence on the surface – such as springs in the boundary basin – and the first evidence was found in the old Girona-2 gas well drilled in the 60's when cutting this horizon and producing, at artesian rate, geothermal fluid at temperatures around 50ºC. Some years after, another well of 968 m deep was drilled nearby (Jafre well). This well was also artesian and geothermal fluid still flows in our days at temperature of around 50ºC.

Nowadays, EB is in its early-stage of exploration phase as far as geothermal resources assessment. Therefore, the main aim for this pilot area is mapping and characterizing the study area to make a first assessment of geothermal resources, as a previous step to help taking future decisions in new exploration investments (e.g. 3D seismic geophysical / drilling new slim-hole wells, etc).

4.9.2 Study area and geological setting

Study area is properly located in the South of the Empordà Basin (EB), so-called 'Baix Empordà'. Currently this basin is comprised into the Girona province and, in fact, the study area comprises a zone limited by structural boundaries with an area of 750km^2 from the East of the Girona city until the coastline.

The EB is a Neogene basin closed to the Pyrenees ranges. Therefore, it presents a complex geological development, which it already started with the deformation of Paleozoic basement due to Variscan orogeny. Later, the collision between Iberian and Eurasian plates during the Alpine orogeny produced the Pyrenees mountain range from late Cretaceous until Miocene (VERGÉS et al. 2002).

After that, the EB was generated in the eastern margin of the Pyrenees and the Ebro Depression during the opening of the 'Solc de València' (Late Oligocene – Middle Miocene) as the propagation of the European Cenozoic Rift System. Due to extensional tectonics, EB was formed as a tectonic graben by a NW-SE-trending faults system, which overlaps the contractive structures of Alpine period (SAULA et al. 1996).

EB is internally structured by normal faults with listric geometry. The main faults – those ones with measured dip slips of about 1,000 meters – in the study area are Camós-Celrà fault (a major fault with a dip slip > 1,300 metres, defining the southern boundary of the study area), Riuràs fault and Juià fault (SAULA et al. 1996). The minor faults are in the hanging walls of the main ones and they present a dip slips at least, lesser in one order of magnitude. The hanging walls of the main faults hold half graben basins, with a sedimentary infill mainly Neogene in age. This rift process was also characterized by the occurrence of some volcanic emission centres.

The regional lithostratigraphic succession in the area is formed by Paleozoic and Paleogene bedrock. Paleozoic bedrock consists of slates with interlayered quarzites and volcanic rocks of Cambro-Ordovician, all of them affected by the Variscian orogeny and intruded by granitoids of this period. The Paleogene bedrock overlies unconformily the Paleozoic series and it only outcrops in the southern boundary of the EB basin, closed to the Camós-Celrà fault. It is constituted mainly by marine sediments from Paleocene to

Priabonian period which describe 4 tectonostratigraphic sequences (SERRA-KIEL et al. 2003a; MUÑOZ et al. 2010). This sedimentary sequence is represented by clays, sandstones and conglomerates of the of Pontils Formation.; Girona limestones and marls Formation (GLF); Beuda evaporites Formation.; Banyoles marls Formation; Bracons limestones Formation; and sandstones of Bartonian age. The thickness of the Paleogene succession varies from few metres in the South boundary until more than 3,000 m in the north.

The EB infill consists on Neogene and Quaternary sediments. Neogene detrital sediments are associated with alluvial fans formed by erosion of the surrounding areas. Geophysical studies revealed that the Neogene sedimentary basin achieves more than 1,500 m of depth near the Camós-Celrà fault (ACA 2008). The only relevant Quaternary sediments of the study area are the fluvio-deltaic deposits of Ter and Fluvià rivers with a decametric thickness (maximum 50 m of thickness in delta plain next to the coastline).

The main carbonate reservoir in the study area is the Girona Limestone Formation (GLF). It is a carbonate formation in the Lower Eocene part of the sequence. Specifically, a Low-Lutetian to Middle Lutetian age was stablished by the benthonic association SBZ13 and SBZ14 (SERRA-KIEL et al. 2003a). From the studied outcrops in the South boundary of EB, the GLF presents a variation of thickness from 22m, at Easternmost sector, until 170m, at Westernmost part of the study area, showing an increase of thickness towards to the W. Towards to the N and in depth, the unit thickness increases until achieving 270 m, according to interpreted cross-sections. The maximum depth reaches the 2650 m in the study area (Figure 4.9.1). Although it cannot be ruled out that the presence of faults have altered the actual values of thickness of the formation, these values are congruent with the bibliographic values (PALLÍ 1972).

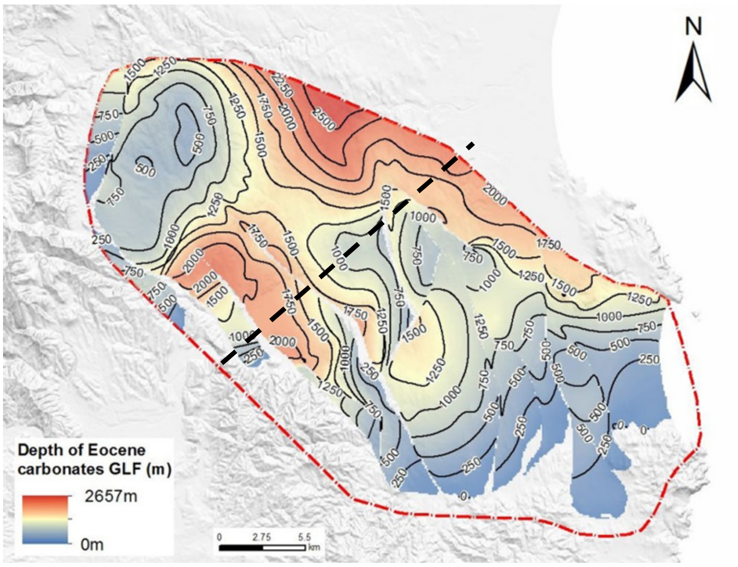

Figure 4.9.1: Preliminary depth distribution to the top of the Eocene carbonates (GLF) of the Empordà Basin (EB). Dashed dark line indicates the position of the cross section shown in figure 4.9.2.

The GLF can be divided into four sedimentary cycles constituted by several transgressive and regressive systems represented by different depositional environments and containing abundant larger foraminifera, mainly *Alveolina* and *Nummulites* (SERRA-KIEL et al. 2003a,b). But, in general terms, it registers a general transgressive trend, in accordance with a retrogradation of the carbonate platform system to the south due to basin deepening. Thus, facies of shallow marine environments (lagoon and shoal) are characteristic in the lower part of GLF progressing toward middle and external ramp to the top of the sequence. This means globally the packstones, grainstones and rudstones are predominant in the studied outcrops while mudstones and wackestones only are well-developed locally. Despite of the heterogeneity of facies – until eight different facies have been detected –, the most abundant ones are rudstones and floatstones of *Nummulites* (66%), followed by facies of packstones and grainstones of foraminifera (17%), mudstones and sandstones (3%) and finally oolitic grainstones and packstone-grainstones of *Nummulites* and *Alveolina* (1%).

In depth, the only available registers of GLF are found in old oil-wells – located in a Northern of the EB and >1,000 m of depth – which indicate the presence of proximal internal platform (probably packstones and grainstones of miliolids, alveolines and oolits). This distribution is likely due to the retrogadation of carbonated platform to the South from which the proximal facies are moved to the final sedimentary register.

A preliminary diagenetic study mainly indicates an early cementation and practically sinsedimentary. The main cement is calcite and only silification and dolomitization were detected in few samples. On the other hand, all the outcrops show an intense stylolitization of compaction, indicative of the existence of burial previous to the current aerial exposition.

Furthermore, the Lutetian marine rocks are highly affected by faulting, mostly normal faults with metric displacements related to the Neogene extension. These structures, with the presence of marls between limestone beds, can produce a potential compartmentalization of the carbonate unit from a reservoir point of view in the subsurface.

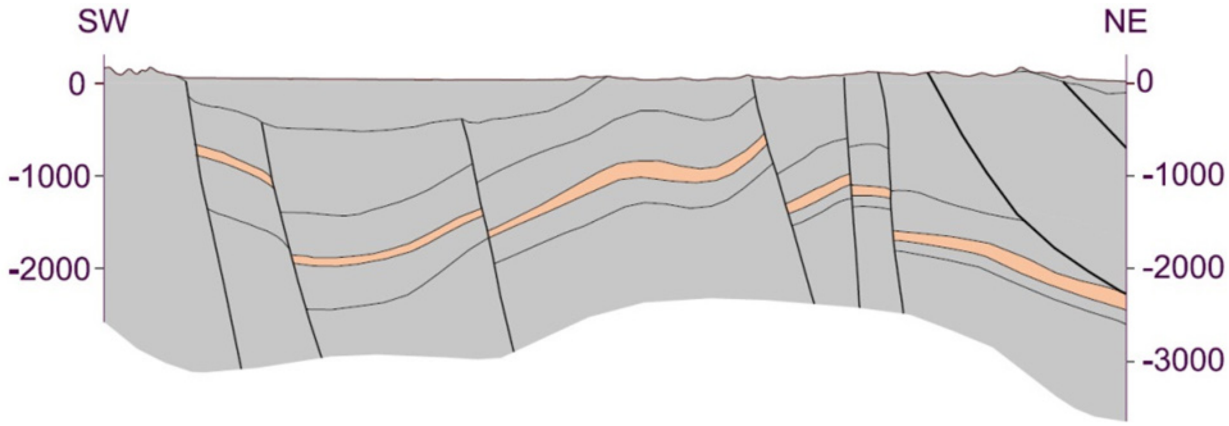

Figure 4.9.2: Representative cross-section across the Empordà Basin hosting the HotLime reservoir, the Girona Limestones Formation (GLF). Cross section location is indicated in figure 4.9.1.

4.9.3 3D geological modelling

Input data sets

The input data sets for 3D Geological modelling have been collected from different sources:

- 5 well data sets from old oil–gas deep wells (Geot–2 of 749 m deep, Girona–1 of 1,680 m deep, Girona–2 of 3325 m deep, Fallinas–1 of 401 m deep and La Bisbal– 1 of 564 m deep) and 1 slim-hole geothermal well (Jafre well of 968 m deep). They were drilled in the 60's and 80's on the last century

- Structural maps:
    - Geological and structural map 1:250,000 of Catalunya (ICGC, 2017), only for supportive use.
    - Geological and structural map 1:25,000 of Catalunya (ICGC, 2003).
- Previous surfaces from the surface-based 3D Geological Model of Catalonia v.1.1.2015: 9 available sets of previous surfaces (ICGC & UB, 2015).
- Interpreted cross sections: 18 deep geological cross-sections and 7 shallow geological cross-sections (last ones only for supportive use)
- 2D seismic lines: discarded by no information or in border of the study area.
- Additional data sets:
    - ca. 1400 field structural data (dip/azimuth)
    - new field gravity data (365 new gravity stations), produced in new geophysical survey, from December 2018 to April 2019 + old gravity data (95 reviewed gravity stations from the geophysical database)
    - additional information based on old gravity survey: gravity anomaly maps (ACA 2008) and gravity profiles (RIVERO et al. 2001)
    - depth map of the Neogene base provided from a hydrogeological report (ACA 2008)

Principle modelling workflow

In order to build up the 3D geological model, all the input data has been integrated in a first preliminary 3D Geological Model after its processing (homogenization, format adaptation etc.). The 3D modelling software used was 3DMOVE (by Midland Valley), to get the first generated surfaces, and GOCAD (by Paradigm) to obtain more accurate and constrained surfaces. Because of the lack of seismic lines to integrate, the modelling workflow has been in depth domain.

Then, the 3D model has been validated according to available geophysical potential-field data (gravity) by means of forward modelling and geophysical inversion. Thus, we used GeoModeller3D software (by Intrepid Geophysics) for the geophysical inversion with a full gravity litho-constrained stochastic approach. For the modelling process, petrophysical properties (rock density) have to be considered for each rock formation. Figure 4.9.2 shows density data (average and standard deviation) from a new thermo-physical survey (January – June 2019) mainly focused in the GLF and which was completed with bibliographic references (AYALA et al. 2015; HUSSON et al., 2018; ICGC (2012); IGME-DPA (2014); RIVERO et al. 2001; SCHÖN 1995). The 3D inversion modelling approach is applied to fit the most probable 3D model through a stochastic approach. The result is a 3D Probabilistic Geological Model, which honours all the data and from which we can perform the first surfaces until obtaining the final and definitive ones.

In the study area five geological horizons have been modelled (Figure 4.9.3): a) base of Neogene and Quaternary deposits, b) top of Lutetian sediments, c) top of Girona Limestone Formation (GLF), d) top of continental Paleocene and e) top of Paleozoic. Although Cretacic formations are considered in the EB modelling as a lithology unit, its basal horizon corresponds to the Montgrí thrust and the top is the topographic surface.

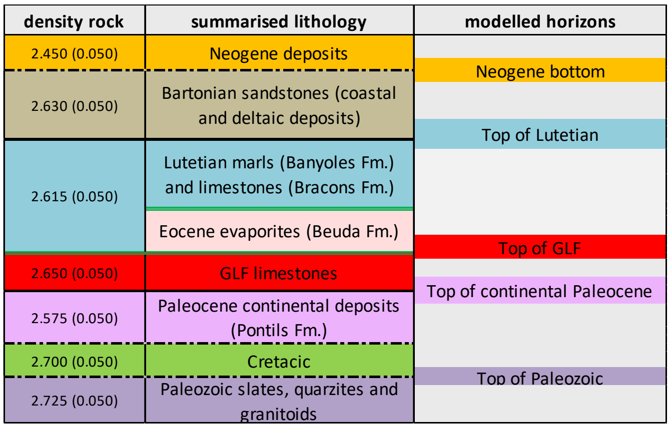

Figure 4.9.3: Summarized lithology in the study area, final modelled horizons in the 3D geological model and density rock (average value and standard deviation) for each formation.

Qualitiy assurance

<u>Quality assurance measures during the preparation of the input data</u>

- Checking the reliability of punctual data due to measurement errors, positioning, incorrect interpretation, etc. and transferring its weight to the model.
- Accuracy and precision in georeferencing raster data until the image is in the right position (using visual controls).
- Accuracy in picking the information as vector features in previous 2D software or in the 3D model. It must be according to the DEM resolution (not too many points) but honouring the original geometry.
- Being methodical and taking note of the adopted decisions (interpretations…) in each step throughout the input process.

<u>Quality assurance measures during 3D Modelling</u>

- Reducing ambiguity of structure in accordance to recognized structural theories.
- Using the high reliable data (for instance, boreholes) to check the lowest ones and declining them if necessary.
- Ensuring that the 3D model is compliant and realistic with the conceptual geological model: surfaces obey the macro-topology according to the previous hypotheses (relationship between layers, hierarchy of faults, etc.) and the geometric constraints (thickness constraints, etc.).
- During the surface construction, being accurate in the selection of the interpolation method, the constraints adopted, the additional data included and the refinement processes.
- Being methodical and taking note of the adopted decisions in each step throughout the modelling process.
- Geophysical modelling is in itself a quality control of previous geological 3D model and, in particular, the inversion process has the potential to improve greatly the geological interpretation of geophysical data. In this case, it is essential to choose a suitable data misfit (difference between results of the inversion data and observed data) taking into account the rest of the constraints. On the one hand, the misfit data depends on the quality of geophysical data. On the other hand, a good knowledge of the geology, geophysics and appropriate modelling workflow are the key points to define the right constraints.

4.9.4 Rock property and Temperature modelling

Hydrogeological and Thermo-physical parameters

For reservoir predictions and modelling, hydro-geothermal parameters such as permeability, thermal conductivity, and specific heat capacity have to be quantified. In the early stage of the hydrothermal reservoir exploration of the case 2.9, this characterization is restricted to the evaluation of few pre-existing downhole data from old oil-gas wells but also from a new field survey purposely carried out for this project.

In order to obtain thermo-physical parameters, a new survey was made from January to June 2019. Equipment used for the thermal properties measurements was a QuicklineTM-30 d'Anter Corporation combined with an ISOMET 2114 measuring device. Thus, thermal conductivity, diffusivity and the product of density per specific heat capacity are directly calculated. Therefore, having the density value will be enough to obtain the specific heat capacity.

The measures obtained show that **thermal conductivity** of the GLF ranges between 1.76-3.34 W/mK in saturated conditions with an average value of 2.82 W/mK. However, this parameter is controlled by depositional textures: the highest values correspond to grainstones, packstone-grainstones and wackestones (2.78-3.34 W/mK) – the most predominant facies among the EB – and the lowest ones to packstones, rudstones and floatstones (2.34-2.88 W/mK). From the same samples, the **specific heat capacity** in saturated conditions for the reservoir GLF takes values between 625.5 – 1011.2 J/kgK with an average value of 858.4 J/kgK.

On the contrary, the bulk permeability and porosity of the reservoir are not controlled by facies and there is not a relationship among them. Firstly, the recent measured samples from GLF present a high variability of **primary porosity**. With this purpose a helium porosimeter Jones S/N 9501 is used at atmospheric conditions. The range value is from 1.6% up to 15.7%, which confirms the few available literature data (IMPROGESA 2003). However, and according to interpretation of sonic porosity from ancient downhole data of Girona-2 (ACA 2008), the register shows that porosity is quite irregular with punctual values up to 30-40% and is assumed that it is caused by fracturing.

From the same measured samples, we obtained an average value of 2.626 g/cm^3 of the reservoir **bulk density** with a value range from 2.301 to 2.702 g/cm^3.

Regarding the **matrix permeability of the reservoir rock**, all samples have very low values which range between below the detection limit (ca. 0.0101mD) and 0.254 mD, in measures taken with a nitrogen permeameter Jones S/N 9501 at atmospheric. These extremely low values are due to early cementation and chemical compaction (stylolitization) and only increase – until one order of magnitude – when microfractures are present or when stylolites appear open. Additionally, the matrix permeability of some of these samples have been measured at reservoir conditions (at two different reservoir depths: P=10MPa and T=40ºC; and P=20MPa and T=80ºC) with a thermo-triaxial-cell obtaining results which indicate that it is practically impermeable.

Regarding the **reservoir hydraulic permeability** of (considering both primary porosity and secondary porosity), a well pumping test in Jafre well has been interpreted (IMPROGESA 2003). Available data indicates a value of the reservoir transmissivity of 150 m^2/d. This would suggest a hydraulic conductivity of 6 m/d ($7\cdot10^{-5}$ m/s), considering a 25 m of aquifer thickness. In the EB, these data point out that the differences between the hydraulic permeability of the matrix and the hydraulic permeability of the reservoir is mainly controlled by the existence of a fracture network related to the Neogene extension, although karstification cannot be ruled out.

Taking into account the productive layers considered in several bibliographic references (ACA 2008; IMPROGESA 2003), the **net-to-gross ratio** – considered as the ratio between the total reservoir thickness and the permeable part of the reservoir – of reservoir unit GLF ranges from 0.24 to 0.58.

Hydrochemistry

From pre-existing data, groundwater chemistry is characterized by a calcium-sodium sulphate facies with a high conductivity (4450 to 4896 microS/cm), high carbonate hardness (Ca and Ca-Mg saturated and SO_4Ca subsaturated) and a TDS close to 5g/kg (IMPROGESA 2003).

Several available bottom hole temperature data (BHT) indicate a corrected geothermal gradient of 47º/km for Girona-2 well. According to GESSAL (1986), the silica and Na-K-Ca chemical geothermometers show results of 62º and 68º C respectively.

During the drilling phase of Girona-2, it was detected free CO_2 in a volumetric ratio of 4:1 (IGME 1982). Available data of gas geothermometer based on CH_4-H_2 and CH_4-H_2-CO_2 indicate a temperature of 140 and 159ºC respectively close to that measured in the bottom of the Girona-2 well by means of corrected BHT (145ºC at 3231m depth) (GESSAL 1986). Also C^{13} test results show a volcanic origin (GESSAL 1986). Thus, it is assumed an endogenetic origin for the gas with an ascending flow (IMPROGESA 2003).

Temperature Modelling

The available ground-temperature data inside the EB are scarce. For the Girona-2 well, GESSAL (1986) indicates about 5 corrected BHTs data and 10 drill-stem tests (DSTs) and a calculated thermal gradient for these data of 47˚C/km. Moreover, a thermal gradient of 39.6˚C/km has been calculated for the Jafre well (IMPROGESA 2003). Thus, a representative regional geothermal gradient of 40ºC/km has been considered for the whole basin to obtain a first draft of the reservoir temperature distribution at the top of the GLF, by applying the following basic equation:

$$Tr = T_0 + gradT * Z$$

where T_0 is the mean annual air temperature; *gradT* is the thermal gradient and *Z* is the depth of the target according to the preliminary 3D model. Figure 4.9.4 shows the average reservoir temperature at the top of the target unit (GLF).

To assess the deep geothermal potential for any target, the volumetric Heat in Place (HIP) method (MUFFLER & CATALDI 1978), also referred to as 'stored heat', is used. The HIP approach is based on the simple concept of evaluating the thermal energy *Q* stored in a homogenous volume *V* of a rock, calculated as:

$$Q_{Total} = V \cdot [\emptyset \rho_W C_W + (1-\emptyset)\rho_R C_R] \cdot (T_R - T_r)$$

where *V* is the reservoir volume (m^3), Ø is the porosity (dimensionless), ρ is the density (Kg/m^3) and *C* is the specific heat capacity (KJ/kg·ºC) - the subindex W or R indicate water or the rock grains respectively. The T_R is the average reservoir temperature (ºC) and T_r is the reinjection or reference temperature (ºC).

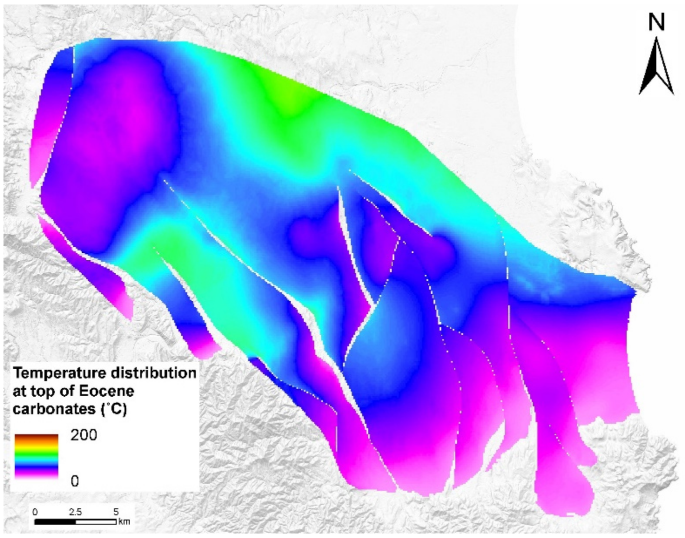

Figure 4.9.4: Preliminary temperature distribution calculated for the top of the Eocene carbonates (GLF) of the Empordà Basin (EB) considering a representative geothermal gradient of 40ºC/km.

This evaluation depends on the volume of the reservoir (inherence from the 3D model), the thermal rock properties, the temperature of the reservoir and the reference temperature. Despite of the uncertainty that implies the lack of knowledge of the parametric distribution in the whole study area, a first roughly approach is possible considering the deterministic method. That is using fixed values for the rock properties (porosity and specific heat capacity) and considering several maps of distribution for bulk density (Figure 4.9.5) and the temperature parameters. The obtained temperature at the top of reservoir map is used as the average reservoir temperature (T_R). About the reference temperature (T_r), it is used the assumption of LIMBERGER et al. (2018) for a global geothermal source assessment. This means considering a minimum reinjection temperature by unitarily adding 10 °C to the mean air temperature at the surface.

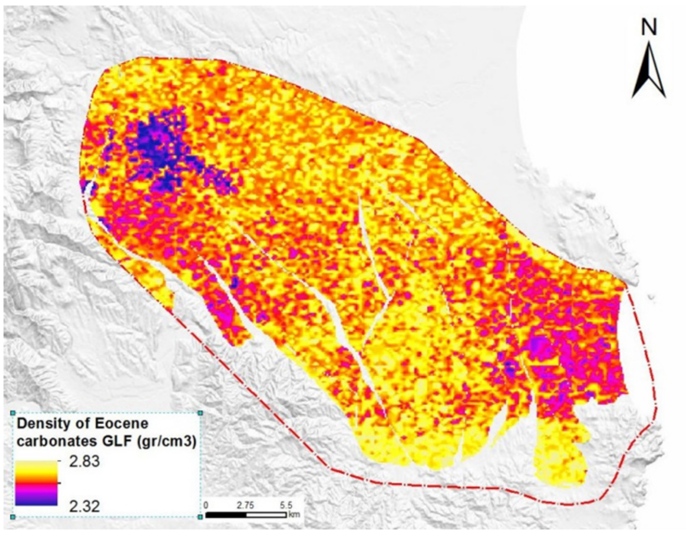

Figure 4.9.5: Preliminary density distribution for the top of the Eocene carbonates (GLF) of the Empordà Basin (EB). The map has been generated from the final voxel model obtained from the geophysical inversion with a full gravity litho-constrained using a stochastic approach. The results are consistent with the laboratory measured samples.

Considering V as the volume of each voxel (*V=H·a* where *H* is the vertical reservoir thickness for each voxel location and '*a*' the area of voxel, here 100x100m), the HIP method was been applied to the 3D voxel-based model as the Figure 4.9.6 shows:

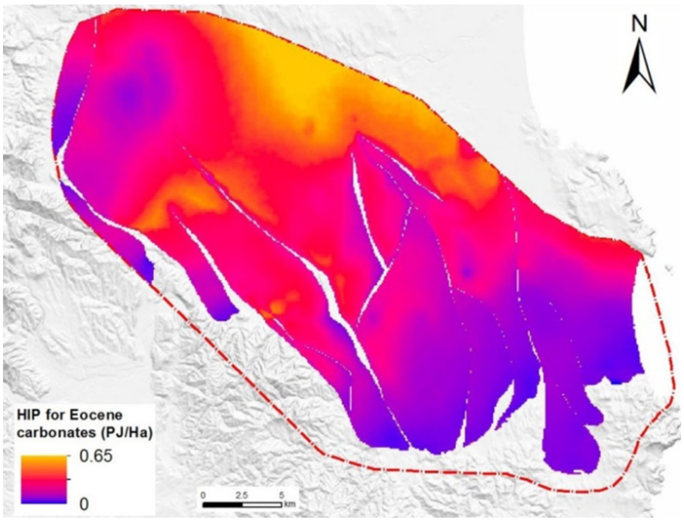

Figure 4.9.6: Map of preliminary "Heat-in-Place" assessment for target unit GLF.

The values obtained range between 0 and 0.6 PJ/Ha. Considering the whole volum of the GLF, the total amount of stored heat in the study area is 10436 PJ (10.4 EJ*). 1 EJ = 10^3 PJ = 10^{18} J.

REFERENCES

ACA (2008): Investigació dels recursos hídrics als aqüífers profunds presents al sector de l'Empordà. – Barcelona, 102 pp.

AYALA, C., IZQUIERDO-LLAVALL, E., RUBIO, F., PUEYO, E., CASAS, A., OLIVA-URCIA, B., RODRÍGUEZ-PINTÓ, A., REY-MORAL, C. & MEDIATO, J.F. (2015): Basement characterization and cover deformation of the Linking Zone (NE Spain) from 2.5D and 3D geological and geophysical modelling. – Presentation 8th EUREGEO 2015, ICGC, Barcelona, Spain.

GESSAL (1986): Proyecto de recuperación del sondeo petrolero Gerona-2 para utilización geotèrmica, Madrid, 18pp.

HUSSON, E., GUILLEN, A., SÉRANNE, M., COURRIOUX, G. & COUËFFÉ, R. (2018): 3D Geological modelling and gravity inversion of a structurally complex carbonate area: application for karstified massif localization. – Basin Research **30**: 766-782. https://doi.org/10.1111/bre.12279

ICGC (2003): Mapa geològic de Catalunya 1:25.000 (Geotreball I). Institut Cartogràfic i Geològic de Catalunya (ICGC), Barcelona. http://www.icgc.cat/

ICGC (2012): Geothermal Atlas of Catalonia: Geoindex-Deep-geothermal. http://www.icgc.cat/

ICGC (2017): Mapa de les unitats estructurals majors 1:250.000. Institut Cartogràfic i Geològic de Catalunya (ICGC), Barcelona. http://www.icgc.cat/

ICGC & UB (2015): Model geològic 3D de Catalunya v1.1. 2015. ICGC, Barcelona. http://www.icgc.cat/

IGME (1982): Estudio geotérmico preliminar de la Depresión del Ampurdán (Gerona). – Instituto Geológico y minero de España. Ministerio de Industria y Energia, Madrid, 319pp.

IGME-DPA (2014): Desarrollos metodológicos en geología del subsuelo para la caracterización de recursos hidrogeológicos profundos de la provincial de Alicante (HIDROPROAL). Resumen metodológico y de resultados. – Instituto Geológico y Minero de España y Diputación Provincial de Alicante, 89 pp.

IMPROGESA (2003): Proyecto General de aprovechamiento de un manantial de agua termal y mineromedicinal, situado en el término municipal de Jafre (Girona). – Investigacions i prospeccions geotèrmiques, 197 pp.

LIMBERGER, J., BOXEM, T., PLUYMAEKERS, M., BRUHN, D., MANZELLA, A., CALCAGNO, P., BEEKMAN, F., CLOETINGH, S., & VAN WEES, J.-D. (2018): Geothermal energy in deep aquifers: A global assessment of the resource base for direct heat utilization. – Renewable and Sustainable Energy Reviews **82**: 961–975. http://dx.doi.org/10.1016/j.rser.2017.09.084

MUFFLER, L.J.P. & CATALDI, R. (1978): Methods for Regional Assessment of Geothermal Resources, Geothermics **7**: 53-89. https://doi.org/10.1016/0375-6505(78)90002-0

MUÑOZ, J.A., GARCÍA-SENZ, J., BERÁSTEGUI, X., CABRERA, L., SERRA, J. (2010): El registre geològic. 270-75 milions d'anys: el cicle Alpí. A: ICGC, Atles Geològic de Catalunya. ICGC, Barcelona.

PALLÍ, L. (1972): Estratigrafía del Paleógeno del Empordà y zonas limítrofes. – Publicaciones de Geología, Universidad Autónoma de Barcelona, pp. 338.

RIVERO, L., VILAS, M., PINTO, V. & CASAS, A. (2001): Modelización gravimétrica 2D de la fosa de l'Empordà (NE de la Península Ibérica). – Acta Geologica Hispanica **36**: 97-113. https://www.raco.cat/index.php/ActaGeologica/article/view/75633

SAULA, E., PICART, J., MATÓ, E., LLENAS, M., LOSANTOS, M., BERÁSTEGUI, X. & AGUSTÍ, J. (1996): Evolución geo-dinámica de la fosa del Empordà y las Sierras Transversales. – Acta geológica hispánica **29**: 55-75. https://www.raco.cat/index.php/ActaGeologica/article/view/75472/98282

SERRA-KIEL, J., TRAVÉ, A., MATÓ, E., SAULA, E., FERRÀNDEZ-CAÑADELL, C., BUSQUETS, P., TOSQUELLA, J. & VERGÉS, J. (2003a): Marine and Transitional Middle/Upper Eocene Units of the Southeastern Pyrenean Foreland Basin (NE Spain). – Geologica Acta **1**: 177-200. https://doi.org/10.1344/105.000001609

SERRA-KIEL, J., MATÓ, E., SAULA, E., TRAVÉ, A., FERRÀNDEZ-CAÑADELL, C., BUSQUETS, P., SAMSÓ, J.M. TOSQUELLA, BARNOLAS, A., ÀLVAREZ-PÉREZ, G., FRANQUÈS, J. & ROMERO, J. (2003b): An inventory of the marine and transitional Middle/Upper Eocene deposits of the Southeastern Pyrenean Foreland basin (NE Spain). – Geologica Acta **1**: 201-229. https://doi.org/10.1344/105.000001610

SCHÖN, J. H. (1995): Physical properties of rocks. – Pergamon, 575pp.

VERGÉS, J., FERNANDEZ, M. & MARTINEZ, A. (2002): The Pyrenean orogen: pre-, syn-, and postcollisional evolution. – In: ROSENBAUM, G. & LISTER, G. (eds.): Reconstruction of the Evolution of the Alpine-Himalayan Orogen. – Journal of the Virtual Explorer **8**: 1441-8142. https://doi.org/10.3809/jvirtex.2002.00058

4.10 Umbria Trough (IT) – T2.10

Andrea Motti, Norman Natali & Sonia Mariuccini (Regione Umbria)

4.10.1 Inducement and Objectives

The discovery of the Torre Alfina and Castelviscardo geothermal field during the research carried out by ENEL in the late 1970s-1980s to define the structural setting of the potential reservoir the possible temperatures at the top of it. To date, 10 wells have been drilled, 5 of which have excellent permeability characteristics and high 3 that are initially permeable but unusable and 2 are dry. The majority of them are deep between 600/800 m and 2,368 m. The well Alfina 15 has reached the depth of 4,826 m. The well reports include water composition, temperature, velocity and resistivity. The ITWLKW Geotermia Italia S.p.A. is, to date, the only company in Italy to receive the authorization for the exploitation of geothermal resources of medium-high entalpy (about 150°) for electricity generation, and this is why we have decided to consider this work in HotLime Project.

4.10.2 Study area and geological setting

Pilot area is located in the in central Italy (see figure 4.10.1), inside Umbria Region territory, covering 240 km^2 and partly contained in northern Lazio.

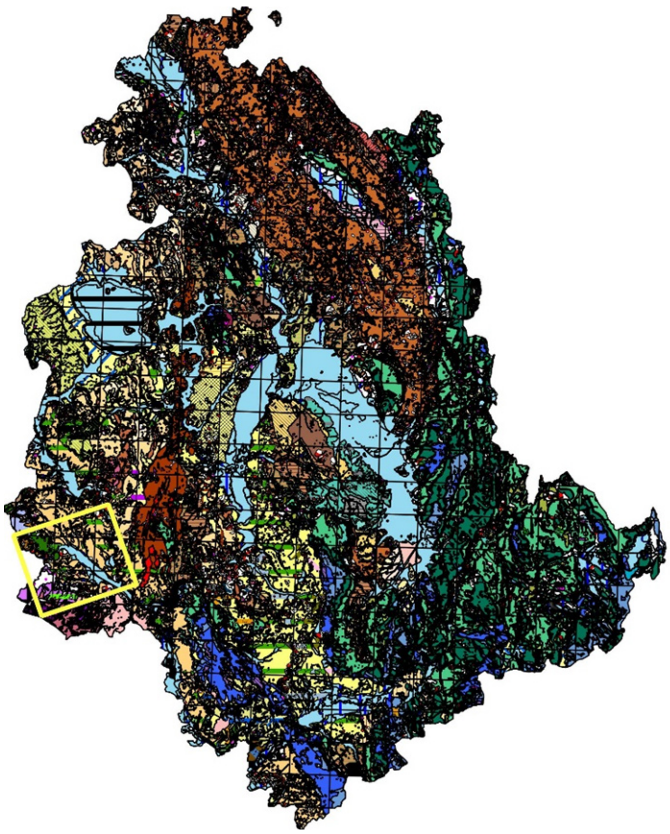

Figure 4.10.1: Overview of the case study area and Umbria Region.

The area, showed in the geological map of figure 4.10.2, is divided in two parts: the first, in the northern and eastern parts, is occupied by sedimentary soils from Quaternary continental deposits, miocene-pleistocene succession and by the Tuscan Domain; the second part, in the south-west of the area includes quaternary magmatic products of the volcanic apparatus of Torre Alfina and Vulsini Mountains and the Ligurian Domain.

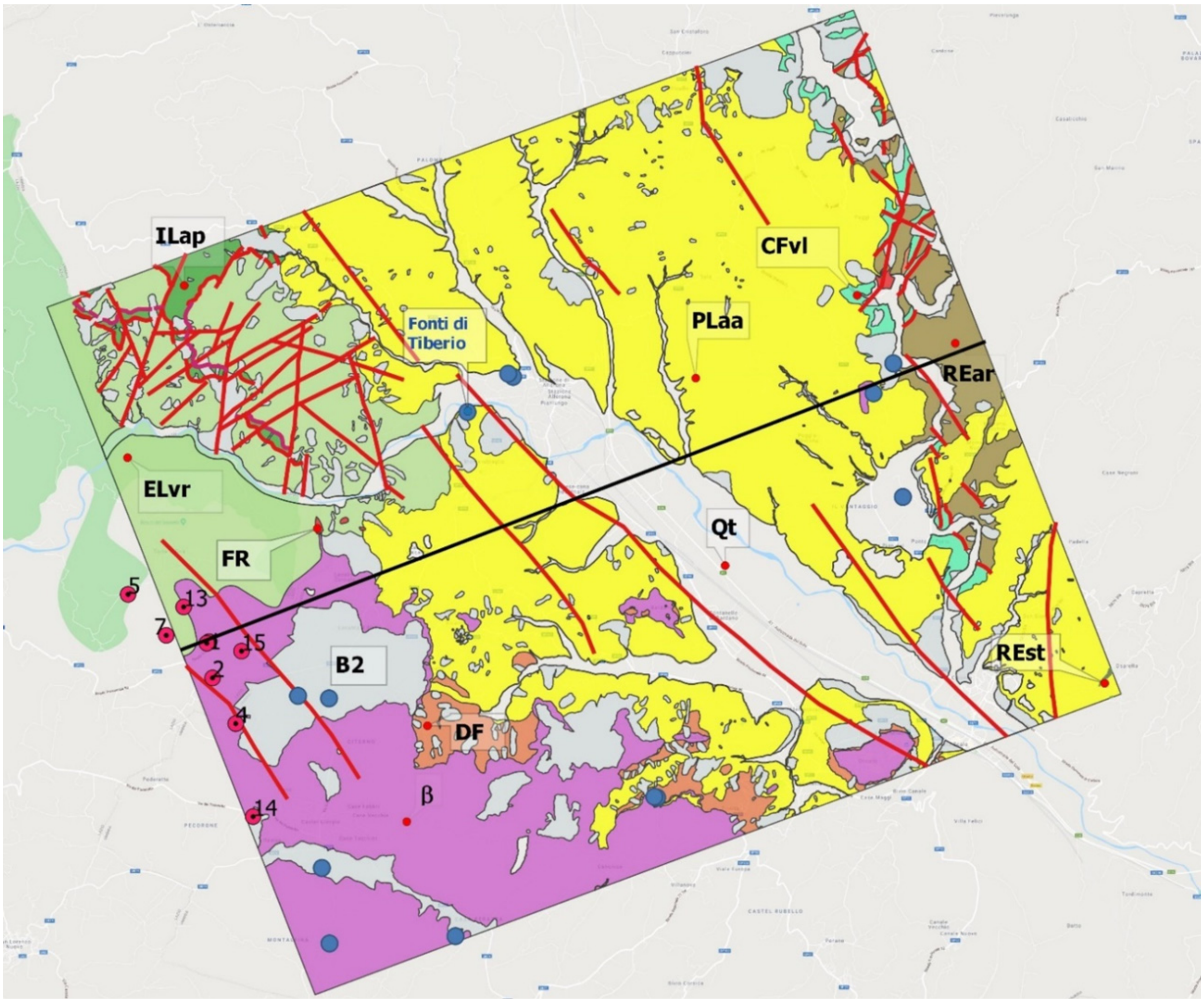

Figure 4.10.2: Geologic Map of the case study area with deep geothermal wells, and springs location.

In outcrop we can find the Quaternary continental and coastal deposits (Qt), indicated with light grey color on the map, of Holocenic age: they are formed by alluvial plain, deltaic and littoral deposits, that are sands, gravels and muds.
The Ligurian Domain consists of sedimentary successions that represent the remnants of the Piemont-Ligurian ocean. It is divided in two parts: the Internal and the External Ligurian Domain. The Internal is represented by successions deposited in the Piemont-Ligurian oceanic basin, now dismembered and outcropping in different tectonic units. In our area we find in outcrop marlstones and limestones (ILap Calpionella Limestones and Palombini Shales), indicated in dark green color on the map, that derive from distal carbonate and mied silicoclastic-carbonate turbidites and pelagites that grades upward in a thick turbiditic succession of mainly silicoclastic composition. The whole succession is mainly early Cretaceous in age.

The External succession (ELvr), indicated in light green on the map, is represented by different successions at the base of which is represented by thick varicolored shales alternating with siltstones, siliceous limestones, calcareous marls and carbonate sandstones.
The Tuscan Domain is represented by Rentella Unit that outcrops in the south-eastern part of the area of interest. It is a succession with characters intermediate stratigraphy between the Tuscan Succession and the Umbrian-Marche succession. Tectonically the Rentella Unit is interposed between the Tuscan units and the underlying Umbrian units. The basal part of this sequence (REst), indicated in yellow color on the map, is represented by varicolored marl, marly limestone and siltstone of Rupelian-Aquitanian age. Above follow sandstones, turbiditic marls and siltite marls with age-rich silica levels Aquitaniano-Burdigaliano,(REar), indicated in dark brown on the map; the presence of lithic fragments rich in clasts of sedimentary origin allows tom differentiate this succession from the adjacent turbidite silicoclastic sequences of Tuscan Domain.
In the same period in which the basal part of the Rentella unit was formed, we can find in outcrop the Marne of Civago and the Marne of Villore (CFvl), indicated in dark yellow on the map, that are variegated marl and clayey marl, of variable color from light gray to greenish, sometimes reddish that testify to sedimentation pelagic and hemipelagic that precedes the establishment of forefossa with turbiditic sedimentation.
Tuscan Scaglia (CFvl) is made up of polychrome schists of the Tuscan series: sit of argillite rich in manganese red-brown and gray-green with rare calcareous layers (Cretaceo-Miocene inf.).
The Pliocene-Pleistocene Marine Deposits are part of the Miocene-Pleistocene succession of the Tyrrhenian margin and Inner basins; they are composited and strongly heterogeneous, mainly clastic and with very subordinate carbonates and evaporites, linked with the post-orogenic depositional phases that took place the Northern Appennines back-arc, since the Middle-Late Miocene.
The Pliocene I Unit marine deposits (PLaa), indicated in dark yellow color on the map, extend both west and east of the Middle Tuscan Ridge, mainly formed by fossiliferous clays, silt and sand interbeds of outer shelf environment.
Volcanic Deposits: after the compressive tectonic phases which led to the implementation of the various units tectonic an important magmatic activity is imposed in the Tyrrhenian margin of the northern Appennines, contemporary to the extensional tectonic phases that characterize this area during the Neogene. This magmatic activity originates effusive magmatic rocks and pyroclastic (β) indicated on the map in pink color.
These paleogeographic domains include the litostratigraphic units with references to the main tectonic units. In the area of interest we can find four different tectonic units, which were stacked during the Miocene compression phase. Proceeding from the highest and originally most western, they are: the Ligurian Units, the Tuscan Units, the Tuscan-Umbrian Units and the Umbrian-Marche Units.
Figure 4.10.6 shows two types of main faults in red: inverse faults linked to the miocene, low-angle and vergence NW-SE compression tectonics which testify to the overthrusting of the Tuscan Dominion units on the Scaglia Tuscan formation and of the Tuscan carbonate sequence which , in turn it is overridden on the Rentella Unit which has set itself on the Umbrian-Marche calcareous series in the same way. All this sedimentary complex determined at the end of the Miocene, was subsequently dismembered by the plio-Pleistocene distension tectonics through faults directed at high angle with vergence towards NE or towards SE.

Geological framework of the main carbonate reservoir

In the section of figure 4.10.3 geothermal cross-section with the light blue color the two main carbonate present on our site are indicated.

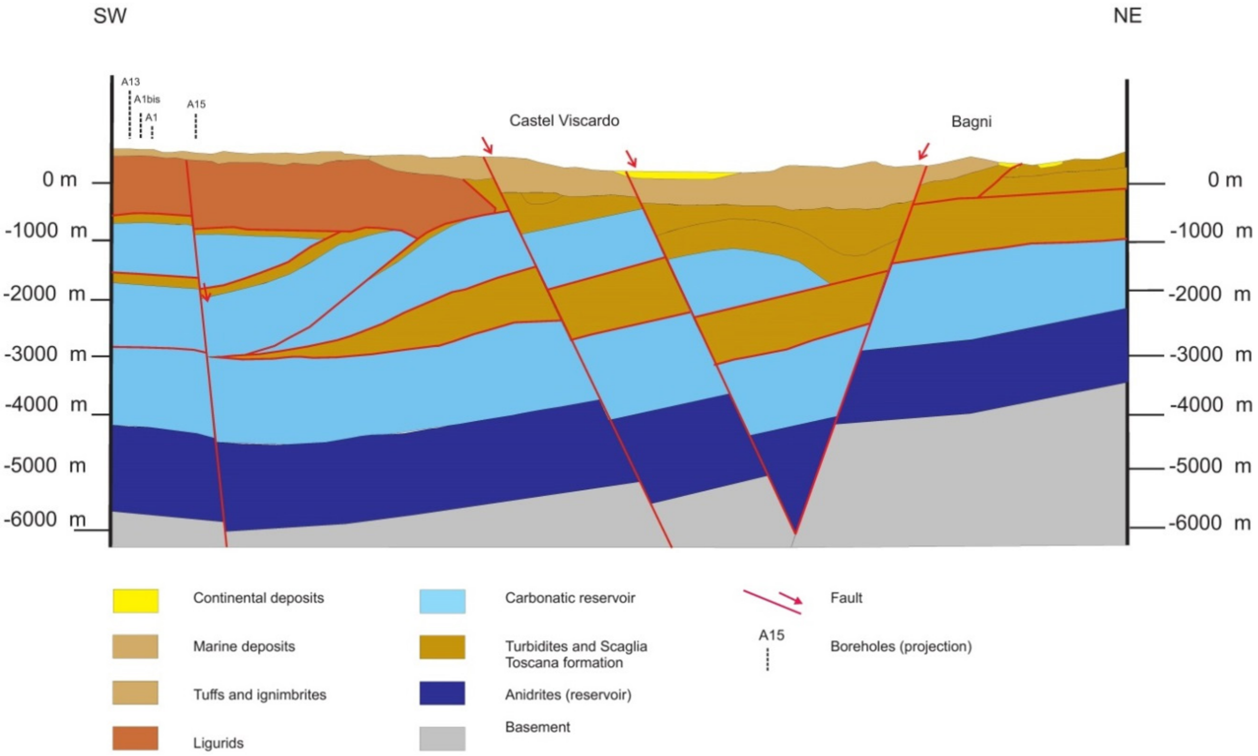

Figure 4.10.3: Geothermal cross-section.

The tectonic history of the area tells us that, during the miocenic compression phase, the carbonatic succession and the Tuscan scale that covered it, overlapped the Umbrian carbonatic sequence including the Rentella Unit to the top, characterized by varicolored marl and marly limestone. In this way two carbonate tanks overlapped and limited to the top by the waterproof units of the Scaglia Toscana and the Unit of Rentella were created.

The most superficial carbonate reservoir consists of the Tuscan limestone sequence that has an age between the Trias and the lower Miocene; the stratigraphy of the Tuscan sequence (see figure 4.10.4) testifies to a carbonate sedimentation of a continental shelf from the Noricum to the Lower Jurassic (Hettangian). Starting from the Sinemurian, a relaxing tectonics linked to the opening of the central Atlantic, leads to the fragmentation and drowning of the carbonate platform and to the establishment of a pelagic sedimentation below the CCD that persists throughout the Jurassic and up to the Paleogene. The sedimentation is interrupted in the lower Miocene (Aquitanian) due to the overthrusting and placement of the Ligurian Units above the Tuscan aquifer.

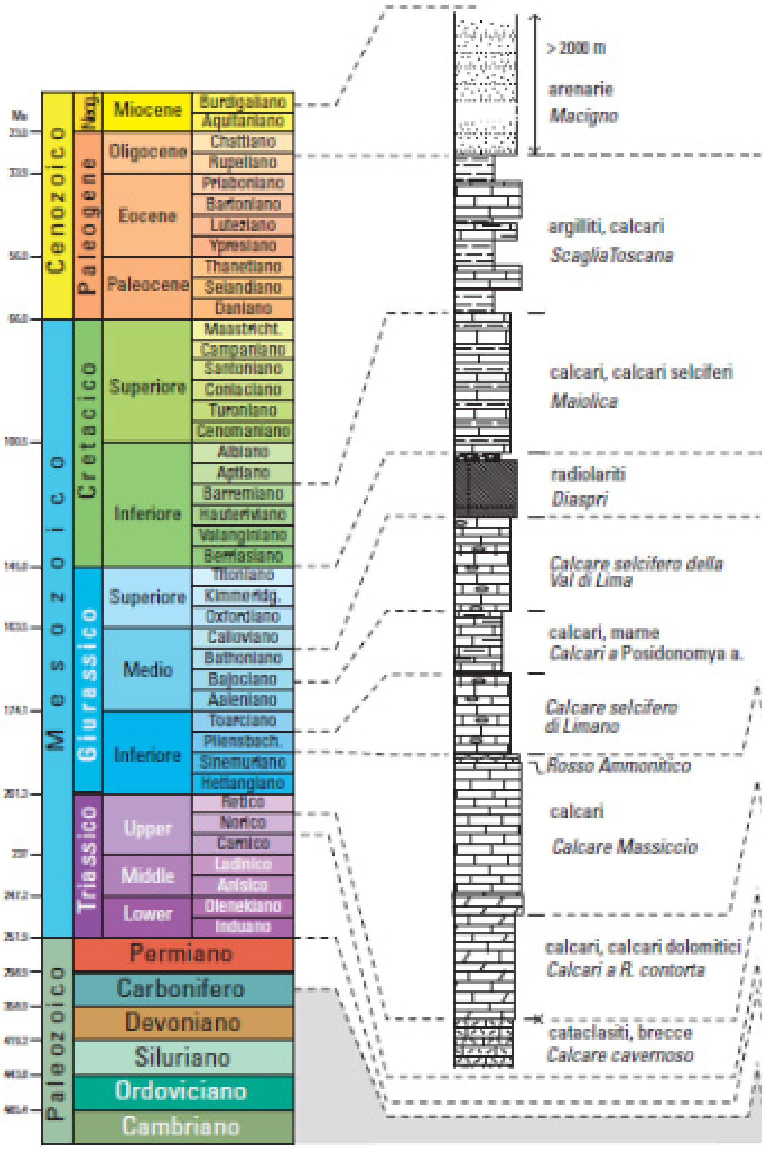

Figure 4.10.4: Stratigraphy of the Tuscan Succession.

The basis of the succession (Calcare cavernoso-Norico) consists of an alternation of dolomites and anhydrites which represent the deposition in a carbonate platform environment with evaporitic episodes. Towards the top we pass to calcareous and calcareous marl deposits well stratified with the typical dark gray and blackish color (Calcari a Rhaetavicula contorta). Follow the carbonate platform deposits of the massive limestone. The succession continues with hemipelagic and condensed deposits of the Rosso Ammonitico represented by marly limestone of reddish color to which marl and argillite are intercalated. There are also limestones with flint and slumping nodules, witnesses of a synsedimentary tectonic activity. Towards the top there is a thick basin succession with turbiditic carbonatic sedimentation (Limano's limestone) and again a pelagic formation (Posydonia alpina limestones and marls) with marl and marly limestone. Deep sedimentation below the carbonate compensation limit (CCD) continues with the deposition of the Diaspri, the Rosso a Aptici and the Maiolica, of a predominantly calcarenitic nature.

In total, the thickness of the carbonate reservoir relative to the Tuscan aquifer is about 2000 m in the south-western area, ie where there is a doubling of the water table by the compressive tectonics. Moving towards the northeast, the total thickness of the reservoir is halved and reaches 1,000 m of power.

The second important reservoir is contained within the Umbrian-Marche carbonatic series which is intercepted starting from about 2900 m of depth in the south-western area and at about 1000 m of depth in the north-eastern area.
The Umbrian carbonatic series of the Marche region (see figure 4.10.5) begins with the rocks of the pre-Triassic age that never outcrop in this part of the Apennines, but have only been found through deep surveys, and are made up of Permian sandstones and phyllites.

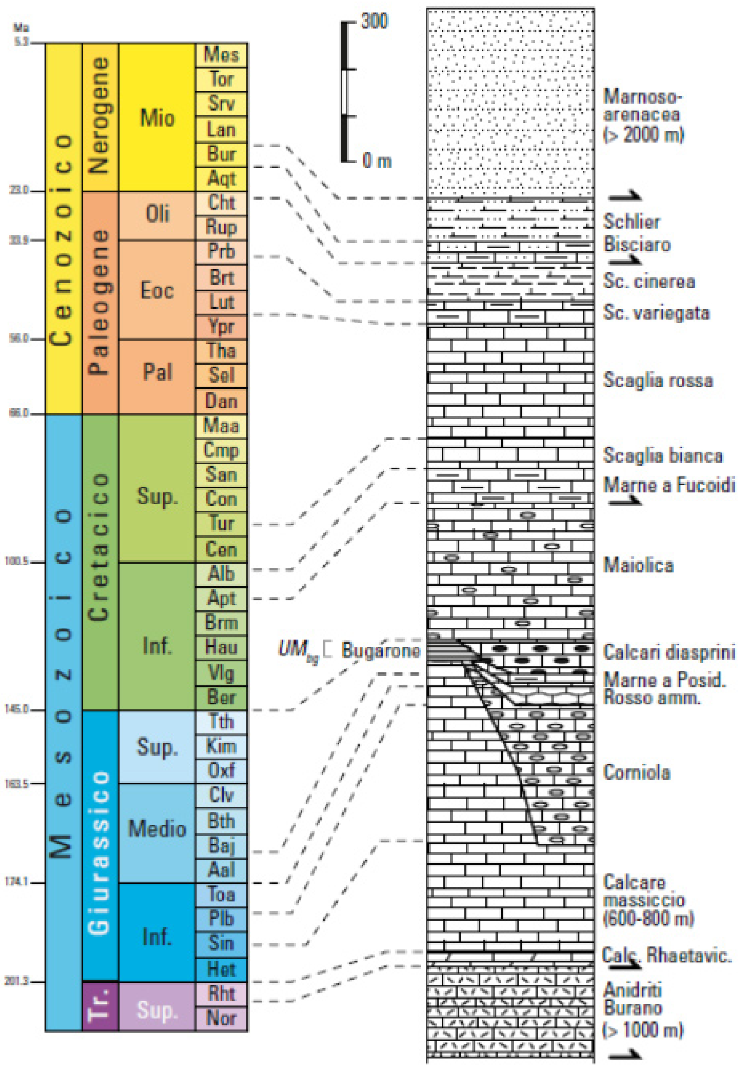

Figure 4.10.5: Stratigraphy of the succession of the Umbria-Marche Domain.

The Triassic is represented by an alternation of anhydrites, dolomites and calcareous dolomites; the action of exogenous agents on the Anhydrites of Burano, according to many authors, would have caused the dissolution of the sulphates and the de-dolomitization of the carbonates, producing the characteristic cellular structure of the "Calcare Cavernoso". These characteristics, which are accompanied by intense tectonic deformations, have determined, in this Unit, a good mixed permeability for porosity and fracturing. The thickness of the Anhydrites of Burano is very variable from a few hundred meters up to a maximum of about 2500 m, for reasons of a tectonic nature. This evaporitic succession passes upwards to an alternation of black limestone and marl (Calcari and Marne a Rhaetavicula Contorta), while starting from the lower Jurassic a carbonate platform develops in which the Massive Limestone is formed. Above these the sedimentation continues with the deposition of micritic limestones of pelagic environment (Corniola) and upwards we pass to limestones, marly limestone and marl (Rosso Ammonitico and Marne a Posidonia) followed by sedimentation of an even deeper environment represented by micritic limestone, limestone and calcarenite (limestone diasprigni). The deposition of the Majolica testifies to the end of the extensional events that have affected the carbonate platform during the Jurassic and establishes homogeneous sedimentation conditions on a regional scale throughout the domain. With the deposition of the Marne a Fucoidi it passes into the Umbrian-Marche domain, from a mainly calcareous-siliceous sedimentation to a marly-calcareous and marly-clayey sedimentation. Pelagic sedimentation continues with the deposition of micritic limestones and limestone with flint (Scaglia Bianca, Scaglia Rossa and Scaglia Variegata). In the area of our interest, above the Umbrian-Marche carbonate succession, the Rentella Succession was formed which has intermediate stratigraphic characters between the Tuscan succession and the Umbrian-Marche succession; these are sandstones, turbiditic marls and siltite marls with levels rich in silica that represent the waterproof top of the Umbria-Marche carbonate reservoir. The thickness of the carbonate reservoir relative to the Umbrian-Marche series is about 1500 m, as shown in figure 4.10.3 (geothermal section) and figure n 4.10.6. (geological section) although, in our opinion, given the already described characteristics of permeability of the Formation of the Anhydrites of Burano, they too can be considered a possible reservoir of geothermal energy.

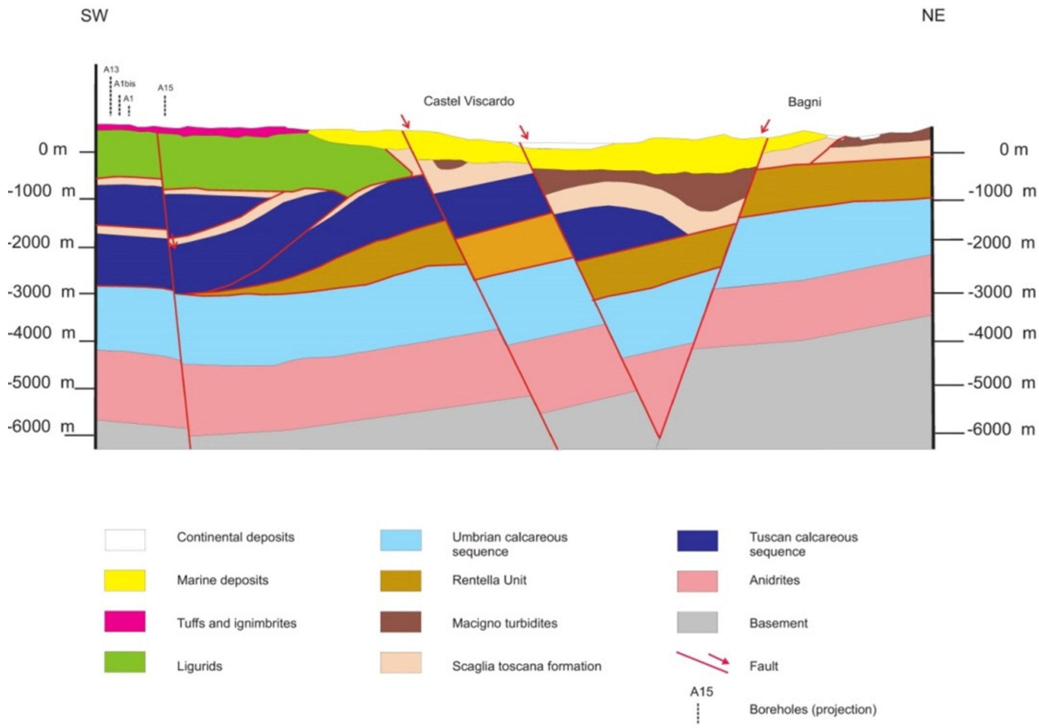

Figure 4.10.6: Geological cross-section.

Description of overlying succession

The carbonate reservoir relative to the Tuscan aquifer is limited to the top, as already mentioned, by the Scaglia Toscana Formation which was formed in a wide sea basin from the lower Cretaceous (Aptian) to the upper Oligocene and consists of a thick succession of argillites , siliceous shales and reddish marls with intercalated calcilutites and turbiditic calcarenites for a total thickness of about 500 m. Starting from the upper Oligocene, the Tuscan domain represents the foredeep basin of the Apennine range, with the sedimentation of the Macigno Formation, consisting of a thick succession of turbidite and silitite sandstones (> 200m).

In correspondence with the westernmost part of our study area, the Tuscan carbonatic succession is covered instead by sediments belonging to the Ligurian Dominion which, during the Miocene compressive tectonic phase, overlapped the Tuscan carbonatic series. It consists of sedimentary successions that represent the remnants of the Piedmont-Ligurian ocean. It is divided into two parts: the Internal and the External Ligurian Domain. The Internal is represented by successions deposited in the Piedmontese-Ligurian oceanic basin, now dismembered and outcropping in different tectonic units. In our area we find in outcrop marlstones and limestones (ILap Calpionella Limestones and Palombini Shales) that derives from distal carbonate and mied silicoclastic-carbonate turbidites and pelagites that grades upward in a thick turbiditic succession of mainly silicoclastic composition.

After the Miocenic compressive tectonic phases, an important magmatic activity is established in the Tyrrhenian margin of the northern Apennines, simultaneously with the extensional tectonic phases that characterize this area during the Neogene. In the westernmost part of our area of interest, volcanic rocks deriving from lava with mainly mafic chemistry and pyroclastic rocks cover the sediments of the Ligurian Dominion.

Further east and with heteropic contact the volcanic rocks are replaced by marine deposits

As is evident from figure 4.10.6 the average thickness of the waterproof sediments covering the carbonate reservoir of the Tuscan series is approximately 800 m.

The carbonate reservoir of the Umbrian-Marche series closes at the top with the sediments of the Rentella Unit: it is a succession with intermediate stratigraphic characters between the succession Toscana and the Umbrian-Marche succession. Tectonically it is interposed between the Tuscan units and the underlying Umbrian units. The basal part of this succession is represented by varicolored marl, marly limestone and siltstone of Rupelian-Aquitanian age that testify a progressive lowering of the sea level. Above they follow sandstones, turbiditic marl and siltite marls with silica-rich levels of Aquitanian-Burdigalian age. The thickness of the Rentella Unit is around 1,000 m.

4.10.3 3D geological modelling

For our case study we have preliminary considerd the Gravity Map of Italy (see in bibl. ISPRA) and the Heat Flow Map (see in bibl. Regione Umbria 2014) as a valuable tool for identifying the generic geological conditions and the distribution of potential resources.

Input data sets

The list of the available input datasets consists of a specific study on the geothermal potential financed by Regione Umbria (Studio delle potenzialità geotermiche del territorio regionale umbro [2012]), the geological maps realized by regional geological surveys, gravimetric information, deep wells logs together with a catalogue of the main thermal springs and all previous scientific literature.The G.I.S. version of the

Regione Umbria Geological Map at 1:10.000 scale consists of a subset of 6 different layers including geology, geomorphology and faults information.

We also considered the Geologic Database of Regione Toscana and the Geological map of Regione Lazio for the re-interpretation of the case study western border.
Gravimetric data are synthesised in the 1:250.000 national gravimetric map by ISPRA (2005).

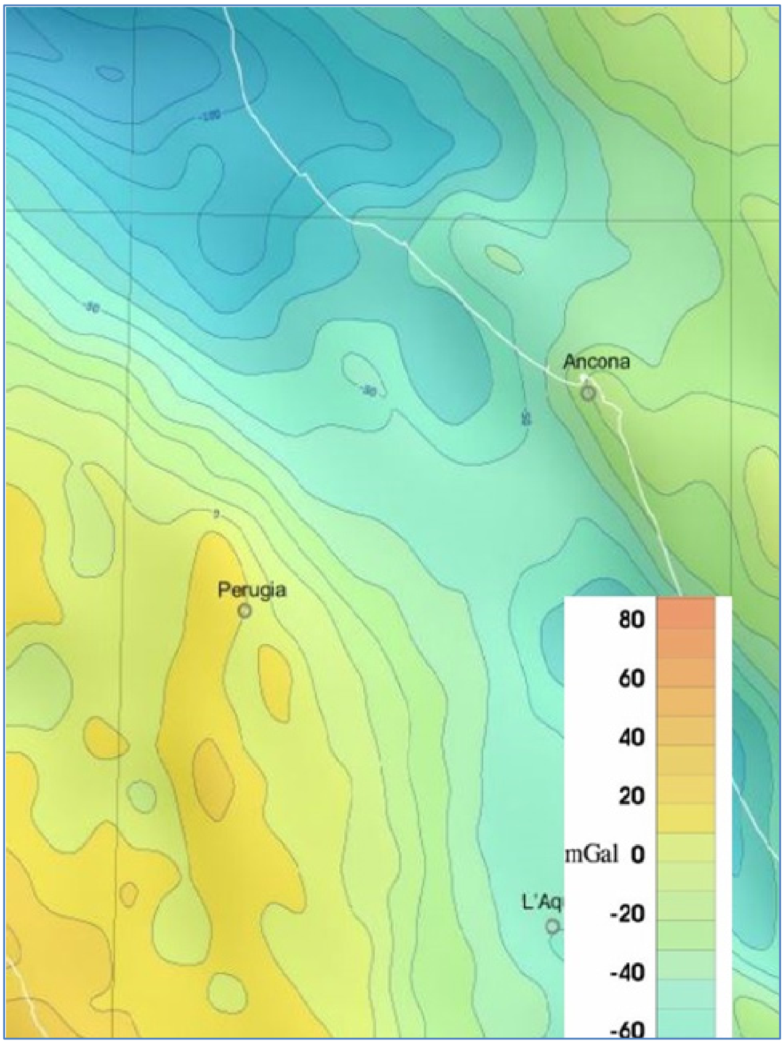

Figure 4.10.7: Screenshot from the National gravimetric map of Italy and case study area (see in bibl. ISPRA).

Other Regional vector topography maps (see in bibl., Regione Umbria Umbriageo) and a (20x20 m) DEM terrain model are available (see in bibl., ISPRA) as basic input datasets used for GIS analysis.

Principle modelling workflow

In this study we were taking advantage of joint interpretation of the available multiple datasets to reconstruct the subsurface geological setting of the case study area and then transferred it to the reservoir model which allowed for assessment of the reservoir behavior. Reconstruction of the geological setting of the area started taking into account the study of geothermal potential of Regione Umbria which contains also useful information about the complex geological history of the area. Tectonic overview and

structural trends were evaluated through interpreted cross sections, fault distribution and pre-existing seismic reflection profiles throughout central Italy and Umbria territory. Using these data and information we produced a set of brand new geological, geothematic maps and sections through the study area.
The generation of the final geologic map of the case study area was performed through the GIS analysis and merge tools on the existing geologic database (see figure 4.10.2).
In the elaboration of the 2D analytical modelling we referred to the logs of the 9 deep geothermal wells drilled during the late 70's exploration led by ENEL private company.
Well logs show stratigraphy , water composition, temperature variation, velocity and resistivity data from 500 to 4,800 m below sea level.
The significant geological section was traced with geologist's expertise in correspondence of the most relevant density of data, where depth and thickness of the reservoir rock modelled are shown as a result of both the interpretation of the geology information available and the borehole data logs.
Finally we generated through ESRI ArcGIS 3D Analyst tool the raster map of the top of the reservoir along the transect interpolating at the vertices of multiple grids of 2 X 1 Km along the section the depth values of the top of the karst reservoir obtained from wells data interpretation.

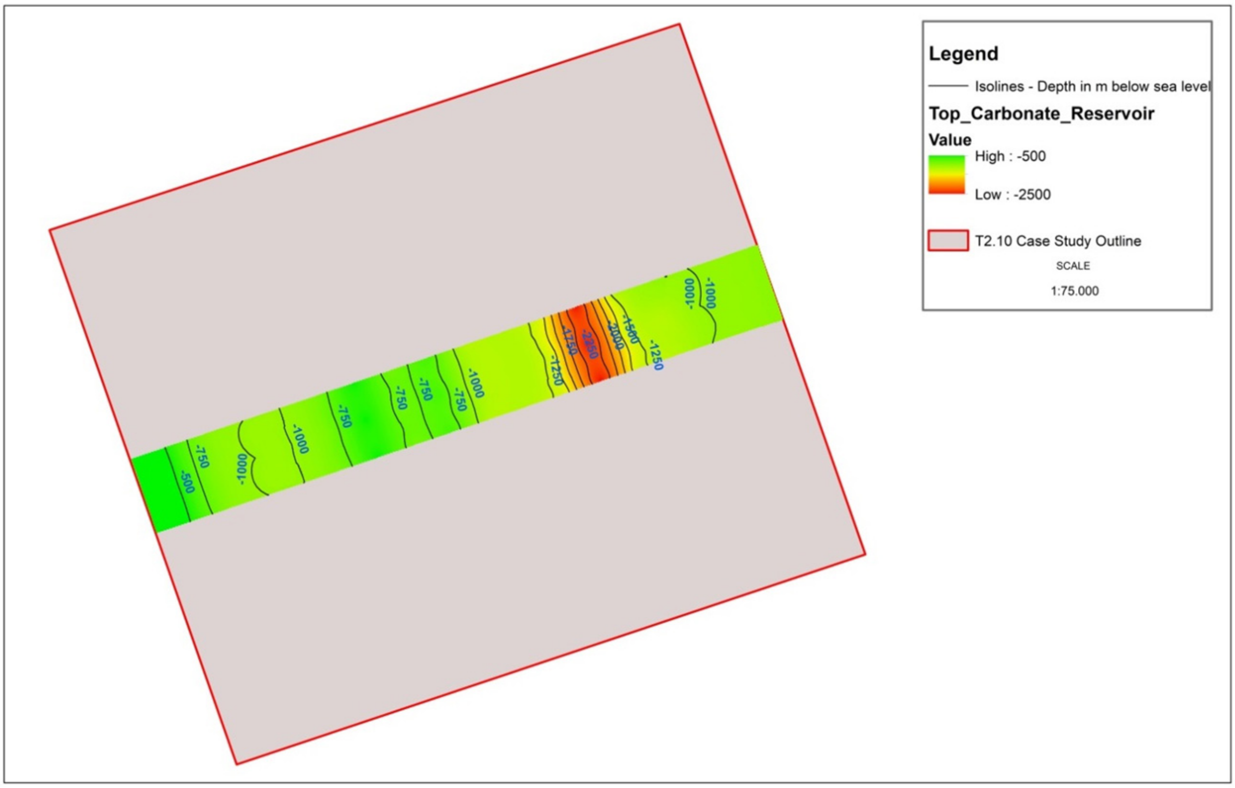

Figure 4.10.8: Top of carbonate reservoir.

The map shows that in the SW part of the area the top of carbonate reservoirs starts at about 500 m below sea level, reaching its greatest depth at 2,500 m in the central part of the transect.

4.10.4 Rock property and Temperature modelling

Hydrogeological and Thermo-physical parameters

The wells drilled by ENEL are distributed in a small area near Castelgiorgio; farther east, in close proximity to Monte Rubiaglio, some small depth surveys were carried out privately. As is evident from Figure 4.10.2, the Fonti di Tiberio are very close and, through chemical analyzes, it has been shown that its waters have similar characteristics to those of the wells of our study.
The samples of spring waters and gases were collected according to the methods used in the geothermal exploration of the 1970s. In particular, the emergency water temperature, that of the environment, the pH with an indicator map and the flow rate were determined. The water collected from the wells was taken by the Kuster sampler.

The analytical techniques adopted in the water laboratory are respectively the following: potentiometric pH;

Na^+, K^+	for atomic absorption;
Ca^{++}, Mg^{++}	volumetrically with EDTA or atomic absorption;
Total Fe	by atomic absorption;
Cl^-	volumetrically according to Mohr;
SO_4^{--}	by gravimetric method;
NH_4^+	by volume after NH_3 development after performing the Nessler test;
Total B	by alkaline or colorimetric route;
SiO_2	by atomic absorption or colorimetry;
Total H_2S	by iodimetric route;
HCO_3^{--}	via alkaline and calculus.

Table 4.4.2: Chemical composition of the waters of geothermal wells

n° camp.	data camp.	T°C	pH	Na^+ mg/l	K^+ mg/l	Ca^{2+} mg/l	Mg^{2+} mg/l	Fe_{tot} mg/l	NH_4^+ mg/l	Cl^- mg/l	HCO_3 mg/l	HSO_4^{2+} mg/l	B_{tot} mg/l	SiO_{2tot} mg/l	H_2S_{tot} mg/l
PP1 A1bis	09/09/74	102	7.20	2020	144	158	20.0	n.d.	20.7	2480	1280	439	22.7	439	as.te
PP2 2) A1bis	29/11/74	116	7.70	1970	171	137	20.0	n.d.	38.7	2110	1800	374	32.2	101	as.te
PP3 3) A1bis	29/11/74	117	7.70	1940	171	131	14.0	n.d.	43.4	2100	1670	426	38.5	128	as.te
PP4 A4	01/09/74	119	8.70	1800	2000	10	11.0	n.d.	25.0	2630	59	405	28.7	176	tracce
PP5 A4	03/09/74	119	8.60	2030	225	8	12.0	n.d.	9.5	2950	87	427	30.5	204	as.te
PP6 4) A4	03/09/74	119	8.40	2000	205	22	12.0	n.d.	19.0	2660	550	419	28.4	190	as.te
PP7 A7	04/02/74	90	7.30	2160	117	147	14.0	0.87	21.4	2460	n.d.	543	21.7	96	as.te
PP8 5) A7	11/02/76	90	7.35	2300	144	139	19.0	0.52	18.6	2640	2110	70	22.7	103	as.te
PP9 5) A7	16/02/76	90	7.30	2330	153	134	16.0	0.42	12.0	2660	2090	79	23.4	106	as.te
PP10 A7	05/07/75	80	6.90	2250	165	148	20.0	1.40	19.2	2700	1440	511	25.0	117	as.te
PP11 A7	07/07/75	81	7.40	2250	149	71	24.0	0.20	19.0	2610	1320	505	24.8	117	as.te

The water chemistry of the PS1 sample of Monte Rubiaglio (Fonti di Tiberio) is of the sodium chloride type and all the waters of the ENEL wells cluster in the area ofinterest the Piper diagram with chlorinated-sodium chemistry. This homogeneity of the chemical composition of the water is an indication of the continuity of the geothermal reservoir in which there would be a practically non-differentiated fluid from one area to another.

Temperature modelling

Local scale thermal model has been realized along the transect where the geological cross-section was drawn, assigning temperature values one for each of the 4 vertex of the 2 km^2 wide.

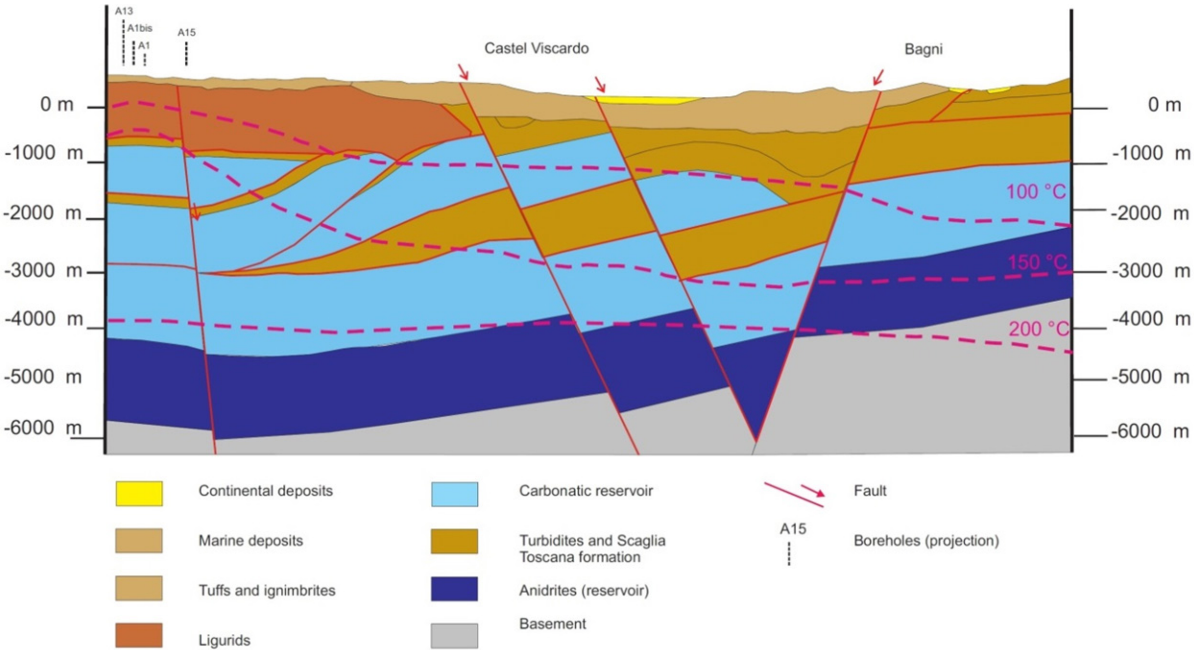

Figure 4.10.9: Cross section reservoir with isotherms (T in °C).

Assessment of temperature (T) values for each vertex was performed through the interpretation of the BHT, and the information from the thermal springs and wells in the area.

Hydraulic conductivity of the reservoir due to fractures, karst and dissolution supplemented by (primary/secondary) porosity and permeability data, where available and meaningful also was considered in temperature prediction at various depth levels.

The map of temperature distribution on the top of the reservoir was created through GIS geostatistical modelling applying the ordinary Kriging method on the T calculated for the vertex of every grid of the transect.

Temperature map on top of carbonate reservoir show moderate-to-high temperature resources (about 100°C) at 500 m below sea level in the SW part of the transect.

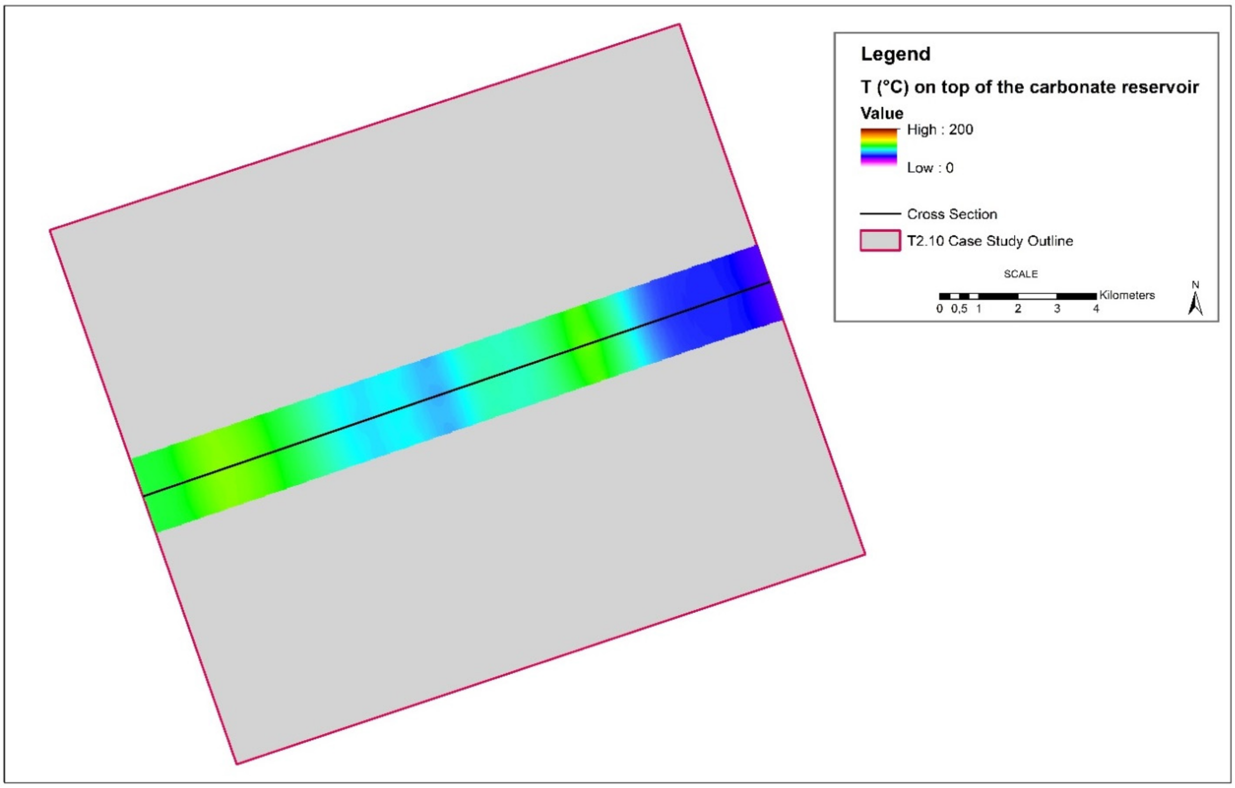

Figure 4.10.10: Temperature (°C) on top of the carbonate reservoir along the cross-section shown in figure 4.10.9.

Conclusions

This study has allowed us to achieve some results including:

- geological maps from thousands of data from different and recent geological databases;
- revision of drilling data;
- geological profiles concerning potential reservoirs and temperatures;
- geostatistical analysis and cross that identified the depth and temperature of the top of carbonatic reservoir(s).

The study needs further data to confirm the geothermal resources that can be exploited in quantitative detail in the area of southwestern Umbria.

REFERENCES

BARSELLA, M., BOSCHERINI, A., BOTTI, F., MARRONI, M., MENEGHINI, F., MOTTI, A., CALANDRI, S. & PANDOLFI, L. (2009): Oligo-Miocene fordeep deposits in the Trasimeno Lake area (Central Italy): insights into the evolution of the Northern Apennine. – It. Journal of Geosciences **128**(2): 341-352. https://doi.org/10.3301/IJG.2009.128.2.341

BOSCHERINI, A., BARCHI, M. & MOTTI A. (2009): 20 anni di cartographia geologica e geotematica. – Mem. Desc. Carta Geol. D'Italia **LXXXVIII**: 78-78.

BOSCHERINI, A., MOTTI, A. NATALI, N. & SIMONE, G. (2010): Geothematic cartography applicationas in Regione Umbria. - 85° Congesso della Societ`a Geologica Italiana, Pisa, Settembre 2010.

BUONASORTE, G. FIORDELISI, A. & PANDELI, E. (1991): The Alfina well 15: Deep geological data from northern Latium. – Boll. Soc. Geol. It. **110**: 823-831.

BUONASORTE, G., CATALDI, R., CECCARELLI, A., COSTANTINI, A., D'OFFIZI, S., LAZZAROTTO, A., RIDOLFI, A., BALDI, P., BARELLI, A., BERTINI, G., BERTRAMI, R., CALAMAI, A., CAMELI, G., CORSI, R., DACQUINO, C., FIORDELISI, A., GHEZZO, A. & LOVARI, F. (1988): Ricerca ed esplorazione nell' area geotermica di Torre Alfina. – Boll. Soc. Geol. It. **107**: 265-337.

ISPRA: DEM http://www.sinanet.isprambiente.it/IT/SIA-ISPRA/DOWNLOAD-MAIS/DEM20/VIEW/

ISPRA (2005): Carta Gravimetrica d'Italia. http://www.isprambiente.gov.it/MEDIA/MILIONE_GRAV/MILIONEGRAV_2004/MILIONE.HTM

REGIONE UMBRIA – SERVICIO GEOLOGICO (2013): Cartografia Geologica Informatizzata a vettorale della Regione Umbria. In: http://www.regione.umbria.it/, http://dati.umbria.it/, http://www.umbriageo.regione.umbria.it/

REGIONE UMBRIA – SERVICIO GEOLOGICO (2013): Cartografia Geologica della Regione Umbria per Google Earth http://www.territorio.regione.umbria.it/STATIC/GEOLOGIAKMZ/GEOLOGIAKMZ/INDEX_KMZ.HTM , http://dati.umbria.it/

REGIONE UMBRIA (2014): Studio delle Potenzialità geothermiche del territorio regionale Umbro.

REGIONE UMBRIA, REGIONE EMILIA-ROMAGNA, REGIONE MARCHE, REGIONE TOSCANA, UNIVERSITÀ SIENA CGT (2019): Geologic Map of the Northern Apennines, in print.

REGIONE UMBRIA: UmbriaGeo http://www.umbriageo.regione.umbria.it/